

# **University of Southampton**

Faculty of Engineering and Physical Sciences

Centre for Doctoral Training in Sustainable Infrastructure Systems

## **Drivers of Negative Phonotaxis for Common carp (*Cyprinus carpio*) in Response to Resonant Insonified Bubble Curtains**

DOI: [10.5258/SOTON/D2013](https://doi.org/10.5258/SOTON/D2013)

By

**Nicholas Flores Martin**

ORCID ID [0000-0003-1131-2934](https://orcid.org/0000-0003-1131-2934)

Thesis for the degree of Doctor of Philosophy

January 2021



# University of Southampton

## Abstract

Faculty of Engineering and Physical Sciences

Centre for Doctoral Training in Sustainable Infrastructure Systems

Doctor of Philosophy

Drivers of Negative Phonotaxis for Common carp (*Cyprinus carpio*) in Response to  
Resonant Insonified Bubble Curtains

by

Nicholas Flores Martin

This thesis investigates the potential for insonified bubble curtains that use the resonant properties of bubbles to be used as behavioural deterrents for fish. This can help mitigate the ecological impacts of river and estuarine infrastructure such as hydropower technologies. To this end, in a series of four flume experiments, the following was tested: (1) the reactions of fish to a low air flow bubble curtain; (2) the effect of deconvoluting visual cues from stimuli generated by the bubble curtain; (3) the effectiveness of resonant versus non-resonant insonified bubble curtains to deter passage, determining the stimuli responsible for eliciting deterrence; (4) the question of whether regions with different levels of particle motion or acoustic pressure influence fish behaviour. Models of the extinction cross-section for each bubble population were used to explain the acoustical effects, confirming bubble resonance. Results of this fundamental study showed that bubble clouds with a higher proportion of resonant bubbles were better at deterring fish passage and this was likely influenced by multimodal cues, specifically, particle displacement, and sound pressure within a body length of the fish. All insonified bubble curtains were less effective in the presence of visual cues, likely because when available these are given greater importance by fish over mechanosensory cues. The benefits of energy-efficient, resonance-based acoustic behavioural deterrents examined by this thesis may be explored further for field-based applications. Finally, the importance of avoiding certain historical pitfalls when characterising acoustically active bubble curtains is discussed.

Key words: *Bubble resonance, bubble coalescence, particle motion, fish screening, fish passage*



**Dedication:**

To the Unity, Dancing Man, Rochefort, Het Anker, De Dolle, Van Steenberge, Surly, Theakstons, Black Sheep, and Northern Monk breweries. And also to my favourite locals: The Guide Dog, Beards and Boards, Bitter Virtue, and the Bookshop Alehouse, without whose never-failing sympathy and liquid encouragement this lengthy tome would have been finished in half the time.

(with apologies to PG Wodehouse)



**Actual Dedication:**

To my parents, Mr Martin Elliott, Dr Lenicker, Dr Hallidie-Smith, and the staff at Great Ormond Street Children's Hospital. Without whom all of this would quite literally have not been possible.





## **Table of Contents**

<b>List of Figures</b>	<b>V</b>
<b>List of Tables</b>	<b>XII</b>
<b>List of Equations</b>	<b>XIV</b>
<b>List of Additional Materials</b>	<b>XIII</b>
<b>Declaration of Authorship</b>	<b>XV</b>
<b>Acknowledgements</b>	<b>XVI</b>
<b>Definitions and Abbreviations</b>	<b>XVIII</b>
A. Fish families	XVIII
B. Fish species	XIX
C. General terms	XXII
D. Symbols and abbreviations	XXIV
<b>Structure of the thesis</b>	<b>XXX</b>
<b>Chapter 1: Research Background –A Narrative Literature Review</b>	<b>1</b>
1.1 Introduction	1
1.2 Behavioural Deterrents	3
1.3 Bubble Screens and Combination Screens	6
1.4 Underwater Bubbles	11
1.5 Absorption by Bubble Clouds	32
1.6 The Mechanics of Hearing in Fish	34
1.7 Directionality in Fish Hearing	40
1.8 Measuring Auditory Sensitivity	43

1.9	Underwater Sound and the Near and Far-Fields	45
1.10	Thresholds and criteria for injury and behavioural effects on fishes	47
1.11	The relationship between the lateral line system and the ear	48
1.12	Response to stimuli in fish	49
1.13	Common Carp ( <i>Cyprinus carpio</i> ) as a Study Species	51
<b>Chapter 2: Aims and Objectives</b>		<b>55</b>
2.1	Rationale	55
2.2	Aim	56
2.3	Research Objectives	56
<b>Chapter 3: Reactions of juvenile common carp (<i>Cyprinus carpio</i>) to a bubble curtain with low air flow</b>		<b>57</b>
3.1	Abstract	57
3.2	Introduction	57
3.3	Methodology	60
	3.3.1 <i>Experimental Set-up</i>	60
	3.3.2 <i>Subject Fish</i>	61
	3.3.3 <i>Experimental Trials</i>	61
	3.3.3 <i>Behavioural Analysis</i>	62
	3.3.4 <i>Statistical Analysis</i>	63
3.4	Results	64
	3.4.1 <i>Coarse Scale Results</i>	64
	3.4.2 <i>Modelling in GAMS</i>	65

3.5	Discussion	66
3.6	Conclusions	68
3.7	Ethics	68
<b>Chapter 4: Common carp (<i>Cyprinus carpio</i>) response to insonified bubbles with different size distributions, and influence of visual cues</b>		<b>69</b>
4.1	Abstract	69
4.2	Introduction	69
4.3	Methodology	73
	4.3.1 <i>Experimental Set-up</i>	73
	4.3.2 <i>Air Flow Rate Selection and Bubble Sizing</i>	75
	4.3.3 <i>Determination of Extinction Cross-Sections</i>	76
	4.3.4 <i>Mapping of Stimuli</i>	78
	4.3.5 <i>Subject Fish</i>	83
	4.3.6 <i>Experiments</i>	86
	4.3.7 <i>Behavioural and Statistical Analysis</i>	87
4.4	Results	89
	4.4.1 <i>Influence of Visual Cues on Fish Response to an Insonified Bubble Curtain</i>	89
	4.4.2 <i>Comparing Fish Response to Resonant and Non-Resonant Bubble curtains</i>	91
4.5	Discussion	95
4.6	Conclusion	101
4.7	Ethics	101

<b>Chapter 5: Reactions of common carp to regions of sound with high acoustic pressure, or high particle displacement</b>	<b>103</b>
5.1 Abstract	103
5.2 Introduction	103
5.3 Methodology	106
5.3.1 <i>Experimental Set-up</i>	106
5.3.2 <i>Experimental Trials</i>	108
5.3.3 <i>Experimental Fish</i>	109
5.3.2 <i>Mapping</i>	109
5.3.5 <i>Statistical Analysis</i>	112
5.4 Results	115
5.4.1 <i>Coarse Rejection Counts</i>	115
5.4.2 <i>Analysis of Fish Movement and Orientation</i>	115
5.4.3 <i>Fish Response to Speaker Stimuli</i>	117
5.4.3 <i>Analysis of Group Behaviours</i>	118
5.5 Discussion	120
5.6 Conclusion	125
5.7 Ethics	125
<b>Chapter 6: Thesis Discussion</b>	<b>127</b>
6.1 Conclusions	135
6.2 Contributions to existing knowledge and thinking	137
<b>References</b>	<b>141</b>
<b>List of Appendices</b>	<b>181</b>

## List of Figures

- Fig. 1.1:** Selected frames from a high-speed photographic sequence, showing a single bubble released from a metal nozzle, depicting the “*needle shape*” (frames 2 and 12), and “*pancake shape*” (frames 7 and 17) [from Leighton *et al.*, 1991]. 29
- Fig. 1.2:** Frames showing a bubble being released from a metal nozzle, excited by contact with and absorption of successor bubbles (Flow rate: 0.2 ml/s) [from Leighton *et al.*, 1991]. 30
- Fig. 1.3** - Frames showing a characteristic multiple-bubble complex showing A: superior, B: intermediate, C: successor, D: replacement of successor, E: fragmentation. (Flow rate: 15 ml/s) [from Leighton *et al.*, 1991]. 31
- Fig. 1.4** – Schematic of a whale insonifying a bubble-net. According to Huygens’ principle, the position of a wavefront (locally normal to the rays) can be found from the envelope of small Huygens wavelets propagating out from the original position of the wavefront. [Leighton *et al.*, 2004]. 33
- Fig. 1.5:** Inner ear of a perch [from Ladich & Popper, 2004]. Medial view on the left and lateral view on the right. **AC**, **HC**, **PC** - anterior, horizontal, and posterior semicircular canals; **L** - lagena; **LO** - lagena otolith; **MN** - macula (papilla) neglecta; **MU** - utricular epithelium; **MS** - saccular epithelium; **N** - eighth cranial nerve; **S** - saccule; **SO** - saccular otolith; **UO** - utricular otolith. 35
- Fig. 1.6:** The otolithic hearing mechanism. The dense otolith lags behind the sensory epithelium, which tends to move with the fluid. The cell output is proportional to the pivot angle:  $\alpha = \delta / L$ . The sensor is a dipole [from Rogers & Zeddies, 2008]. 37

**Fig. 1.7:** Saccular hair cell orientation patterns from different fish. Anterior is to the right and dorsal to the left. The dotted lines are the areas of what is generally an abrupt transition in orientation between directions. Arrowheads indicate the direction of the kinocilia on the hair cells in each region of the epithelium. The “Standard” pattern is typically found in fishes that are hearing generalists. Other patterns are most often found in hearing specialists. The same basic pattern can be found in taxonomically diverse fishes [from Popper & Schilt, 2008]. 39

**Fig. 1.8:** An illustration of how the difference angles of the fish’s bearing relative to the sound source and to the local particle motion vectors can be determined [from Zeddies *et al.*, 2010]. 43

**Fig. 1.9:** Auditory thresholds from a select group of teleost fish [from Fay, 1988]. 44

**Fig. 1.10:** Comparison of audiograms of carp obtained by a classical behavioural method, electrocardiogram (ECG), and auditory brainstem response (ABR) methods [from Kojima *et al.*, 2005; behavioural audiogram from Popper, 1972]. 46

**Fig. 3.1** – Schematic of the experimental set-up. There was a 7.5 cm gap between the sides of the bubbler and the flume. The asterisk indicates the release point for fish at the start of each trial. Greyed out section indicates area of flume not used during the experiment (drawing dimensions not to scale). 61

**Fig. 3.2** Box plots of *Number of passes* and *Passage efficiency* for all treatments for the 60 L min<sup>-1</sup> bubble curtain during test and post-treatment periods. Pairs with significant difference are denoted by an asterisk. 65

**Fig 3.3:** Count of *Passes* by location along the bubbler for fish during different treatments. *L* = left, *LC* = left centre, *C* = centre, *CR* = centre right, *R* = right.

65

**Fig. 4.1 a)** Schematic of the bubble curtain and air supply system used for Experiments 1 and 2 of a study to investigate the response of common carp to insonified bubble curtains in the presence and absence of visual cues. A single needle is shown for simplification; **b)** plan of the experimental set-up used in Experiments 2 and 3. The asterisk indicates the release point for fish at the start of each trial. Grey areas indicate section of flume not used in experiment, dark grey blocks indicate mesh barriers. The asterisk indicates the release point for fish at the start of each trial.

74

**Fig. 4.2 – Left:** External view of one of the two bubblers used for this study. For health and safety reasons, injection needles were fitted into place once bubbler was positioned inside the flume. **Right:** Close-up of the 3D-printed cylindrical housing and vibrating motor.

75

**Fig. 4.3 –** Distribution of bubble diameters ( $\mu\text{m}$ ) at: **a)**  $6 \text{ L min}^{-1}$  ( $3 \text{ L min}^{-1} \text{ m}^{-1}$ ) with standard injection, and vibration at 3 V, **b)**  $10 \text{ L min}^{-1}$  ( $5 \text{ L min}^{-1} \text{ m}^{-1}$ ) with standard injection and vibration at 2.2 V. When the vibrating motors are activated, the general increase in bubble counts for the same volume gas flux is because the gas is distributed in more smaller bubbles. Note that the volume of gas in the largest non-vibrating bubble peaks (diameters  $>10^{3.5}$  microns for (a) and  $>10^6$  microns for (b) disappear when vibration (3 V) is activated, and these peaks contain the bulk of the gas.

77

**Fig. 4.4 –** Original frames of the two bubble populations equivalent to a flux of  $6 \text{ L min}^{-1}$  ( $3 \text{ L min}^{-1} \text{ m}^{-1}$ ), **left:** without vibration, **right:** with vibration at 3 V.

78

**Fig. 4.5. –** Modelled extinction cross sections for bubble distributions determined for Experiments 1 and 2: **a)** an air flow of  $6 \text{ L min}^{-1}$  ( $3 \text{ L min}^{-1}$

m<sup>-1</sup>) insonified at either 1750 Hz or 4000 Hz, with either standard injection or vibration at 3 V, and **b**) an air flow of 10 L min<sup>-1</sup> (5 L min<sup>-1</sup> m<sup>-1</sup>) insonified at 1000 Hz with standard injection or vibration at 2.2 V.  $\sigma_{90}^e$  signifies the range of bubble diameters at which the central 90% of the attenuation occurs. The populations with a higher proportion of bubbles at resonance with the sound field are: 1750 Hz standard injection, 4000 Hz vibrated injection, 1000 Hz standard injection.

79

**Fig. 4.6** - Acoustic spectra for Experiment 1: a) background and vibrating motors (at 2.2V), b) both populations of bubbles, injected with standard injection, and vibrated injection, c) spectrum produced by the underwater speaker emitting a 1000 Hz tone, d) spectra for both bubble populations insonified by a 1000 Hz signal.

80

**Fig. 4.7** - Acoustic spectra for Experiment 2: a) background and vibrating motors (at 3V), b) both populations of bubbles, injected with standard injection (bubbles), and vibrated injection (small bubbles), c) spectra for both bubble populations insonified by a 1750 Hz signal, d) spectra for both bubble populations insonified by a 4000 Hz signal

81

**Fig. 4.8** – Acoustic maps at 15, 30, and 45 cm depths for: *Top* - 1750 Hz bubble set-ups; *Bottom* - 4000 Hz bubble set-ups. Resonant treatments are marked by a dagger (Experiment 2). B = standard injection, VB = vibrated injection. On this scale the nearest edge of the loudspeaker is at horizontal position -17 cm, and the centre of the speaker at horizontal position -26 cm.

82

**Fig. 4.9** – Assembly drawing tetrahedral frame used to make particle velocity measurements. Material used was 6061-T6 aluminium, all measurements in mm.

83

**Fig. 4.10** – Particle displacement in the: (a) xyz direction, and (b) maps at 20 cm depth. Resonant treatments are marked with a dagger (Experiment 2). B = standard injection, VB = vibrated injection.

84



- Fig. 4.11** – Turbulence intensity for treatments in Experiment 2. 85
- Fig. 4.12** – Standard deviation of the flow ( $\text{ms}^{-1}$ ) for treatments in Experiment 2 85
- Fig. 4.13** The median, interquartile range and minimum/maximum whiskers of *Number of passes* and *Passage efficiency* for all treatments in Experiment 1 ( $10 \text{ L min}^{-1} / 5 \text{ L min}^{-1} \text{ m}^{-1}$  bubble curtain). Significant differences are denoted by an asterisk. Treatments with a greater number of bubbles at resonance with the sound field are marked by a dagger. 90
- Fig. 4.14** - The median, interquartile range and minimum/maximum whiskers of mean sinuosity indices per trial for passes ( $10 \text{ L min}^{-1} / 5 \text{ L min}^{-1} \text{ m}^{-1}$  bubble curtain). Pairs with significant differences are denoted by an asterisk. Treatments with a greater number of bubbles at resonance with the sound field are marked by a dagger. 91
- Fig. 4.15** – Scatterplots of *Angular dispersion* for rejected attempts from Experiment 3 ( $10 \text{ L min}^{-1} / 5 \text{ L min}^{-1} \text{ m}^{-1}$  bubble curtain). Values nearer to 1.0 indicate greater directionality. Negative x-axis values indicate motion towards the barrier, positive x-axis values indicate motion away from the barrier. 93
- Fig. 4.16** – The median, interquartile range and minimum/maximum whiskers of *Number of passes* and *Passage efficiency* for Experiment 2 ( $6 \text{ L min}^{-1}$  bubble curtain) during pre-treatment and test periods. Pairs with significant difference are denoted by an asterisk. Resonant treatments are marked by a dagger. B = standard injection, VB = vibrated injection. 94
- Fig. 4.17** – Scatter plots of rejection counts against gradients (averaged for 5 cm bins) of all three stimuli generated by the bubble curtains. 94

**Fig. 4.18** - The median, interquartile range and minimum/maximum whiskers of mean sinuosity indices per trial for passes during Experiment 3 ( $6 \text{ L min}^{-1} / 3 \text{ L min}^{-1} \text{ m}^{-1}$  bubble curtain). Pairs with significant difference are denoted by an asterisk. Resonant treatments are marked by a dagger. B = standard injection, VB = vibrated injection.

95

**Fig. 5.1** - Schematic of the experimental setup. Area marked with grey vertical lines indicates the “reaction zone”, and asterisks mark the three randomly selected fish release points. Due to the location of the cameras, for tracking purposes, the left-most speaker (Speaker A) in the diagram was considered to be  $Y = 0$ , the right-most speaker (Speaker B) was  $Y = -1$ . The virtual “centreline” running between both speakers was considered to be  $X = 0$ , with the limits of the reaction zone at  $X = 0.5$  and  $X = -0.5$ . The dark grey boxes indicate location of the mesh barriers, and light grey sections indicate areas of the flume not used in the experiment.

107

**Fig. 5.2** - Acoustic spectra : a) background; b) 1750 Hz signal (146 dB re  $1 \mu\text{Pa}$  at 1 m); c) 0-0 speaker treatment (145 dB re  $1 \mu\text{Pa}$  at 1 m); d) 0-270 speaker treatment (154 dB re  $1 \mu\text{Pa}$  at 1 m). All measurements taken at 20 cm depth, in the centre of the flume, 90 cm away from the virtual centreline between the speakers.

110

**Fig. 5.3** - Acoustic pressure maps for 0-0 and 0-270 treatments at 10 and 20 cm depth. Location of speaker A is at  $x = 0$ ,  $y = 100$ , Speaker B is at  $x = 0$ ,  $y = 0$ . Location of acoustic pressure minima was due to one speaker being underpowered.

111

**Fig. 5.4** – Particle displacement maps for 0-0 and 0-270 treatments at 10 and 20 cm depth. Location of speaker A is at  $x = 0$ ,  $y = 100$ , Speaker B is at  $x = 0$ ,  $y = 0$ .

111

**Fig. 5.5** – Maps showing the ratio of acoustic pressure : particle motion for 0-0 and 0-270 treatments at 10 and 20 cm depth. Location of speaker A is at  $x = 0$ ,  $y = 100$ , Speaker B is at  $x = 0$ ,  $y = 0$ . 112

**Fig. 5.6** – The median, interquartile range and minimum/maximum whiskers of *Number of rejections* for both experimental treatments and the control. Asterisks mark significance at a  $p < 0.05$  level. 116

**Fig. 5.7** – The median, interquartile range and minimum/maximum whiskers for the indices of *Straightness* and *Sinuosity*. Asterisks mark significance at a  $p < 0.05$  level. 116

**Fig. 5.8** – *Straightness* index plotted against the Y axis: *Mean Y* - mean location of the fish on the Y axis throughout the *Crossing attempt*; *Initial Y* - location of the fish on the Y axis at the start of the Crossing attempt; and *Y<sub>0.1</sub>* - mean location of the fish on the Y axis when the fish was within  $\pm 0.1$  m of the centreline. Red circles indicate pre-test experimental phase, blue circles indicate test experimental phase. 119

**Fig 5.9** - Binned *Number of rejections* for the 0-0 and 0-270 acoustic treatments against stimuli generated by the speakers. The solid red line indicates density. SPL = Sound pressure level; PD = Particle displacement. 120

**Fig 5.10** - Locally estimated scatterplot smooth (smooth parameter = 0.05) of group *Distance* plotted against time. Phase refers to Experimental phase, PT = Pre-test, T = Test. 122

**Fig 5.11** - Locally estimated scatterplot smooth (smooth parameter = 0.05) of group *Swimming speed* plotted against time. Phase refers to Experimental phase, PT = Pre-test, T= Test. 123

## List of Tables

- Table 1.1** Effectiveness of bubble barrier and combination bubble barriers used in previous studies. Flow refers to water flow, and air flow refers to the quantity of air used to generate the bubble curtain.. *Note:* Rey *et al.*, [1976] contains several (pers. communications) not included as references. 13
- Table 3.1:** The deviance explained relative to null (%), estimated degrees of freedom (edf) and significance (p value) of variables within the minimum adequate models fitted to Number of passes, and Passage efficiency. 67
- Table 4.1:** Mean length, weight, and holding tank temperature for common carp used in the two experiments to investigate their response to insonified bubble curtains. 86
- Table 4.2:** Results obtained for the modelled effects of the stimuli generated by an insonified bubble curtain on fish swimming velocity (Experiment 2). The deviance explained relative to null (%), estimated degrees of freedom (edf) and significance (p-value) of the terms in the minimum adequate model fitted to swimming velocity are listed. Brackets indicate smoothed terms. 96
- Table 5.1 -** Results obtained for the modelled effects of the terms affecting the Straightness index of fish trajectories. The deviance explained relative to null (%), estimated degrees of freedom (edf) and significance (p value) of variables within the minimum adequate model (MAM) are listed. Exp. Phase refers to the experimental phase of the trial (i.e. pre-test / test). Brackets indicate smoothed terms. 117
- Table 5.2 -** Results obtained for the modelled effects of the terms affecting the inverse *Swimming speed* of fish. The deviance explained relative to null (%), estimated degrees of freedom (edf) and significance

(p value) of variables within the MAM are listed. Exp. Phase refers to the experimental phase of the trial. Brackets indicate smoothed terms. 118

**Table 5.3** - Results obtained for the modelled effects of the terms affecting the Number of rejections. The deviance explained relative to null (%), estimated degrees of freedom (edf) and significance (p value) of variables within the MAM fitted for each of the four datasets ((a) to (d)) are listed. Exp. Phase refers to the experimental phase of the trial. Brackets indicate smoothed terms. 121

**Table 5.4** - Results obtained for the modelled effects of the terms affecting the Group distance, and log of Swimming speed. The deviance explained relative to null (%), estimated degrees of freedom (edf) and significance (p value) of variables within the MAM are listed. Exp. Phase refers to the experimental phase of the trial. Brackets indicate smoothed terms. 122

## List of Equations

<b>Eq. 1.1</b> - The acoustic output of a freely oscillating bubble	12
<b>Eq. 1.2</b> - Resonance frequency of a bubble driven to oscillation by a sound field	27
<b>Eq. 1.3</b> - Internal pressure of a bubble as a result of the gas and vapour pressure of the liquid medium	27
<b>Eq. 1.4</b> - Internal pressure of a bubble as a result of liquid pressure and excess pressure	27
<b>Eq. 1.5</b> - Surface tension on a bubble annulus	28
<b>Eq. 1.6</b> – The excess pressure, or Laplace pressure, inside a bubble	28
<b>Eq. 4.1</b> - Equation for determining particle velocity	81
<b>Eq. 5.1</b> - Equation for particle acceleration	104
<b>Eq. 5.2</b> - Equation for particle displacement	104

## List of Additional Materials

N/A

## Research Thesis: Declaration of Authorship

Print name: NICHOLAS FLORES MARTIN

Title of thesis: Drivers of negative phonotaxis for Common carp (*Cyprinus carpio*) in response to resonant insonified bubble curtains.

I declare that this thesis and the work presented in it is my own and has been generated by me as the result of my own original research. I confirm that:

1. This work was done wholly or mainly while in candidature for a research degree at this University;
2. Where any part of this thesis has previously been submitted for a degree or any other qualification at this University or any other institution, this has been clearly stated;
3. Where I have consulted the published work of others, this is always clearly attributed;
4. Where I have quoted from the work of others, the source is always given. With the exception of such quotations, this thesis is entirely my own work;
5. I have acknowledged all main sources of help;
6. Where the thesis is based on work done by myself jointly with others, I have made clear exactly what was done by others and what I have contributed myself;
7. Parts of this work will be submitted for publication as:

Flores Martin, N., Leighton, T.G., White, P.R., Kemp, P.S. (in prep) "The response of common carp (*Cyprinus carpio*) to insonified bubble curtains," *Journal of the Acoustical Society of America*.

Signature:

Date:

## Acknowledgements

Over the course of this PhD I received help and support from a number of people. Firstly, I would like to thank my supervisor, Prof. Paul Kemp, for his guidance, knowledge and enthusiasm, without which this research would not have been possible. I'm particularly indebted for his (exacting!) guidance on how best to prepare my research for submission to research journals. I would also like to thank my two co-supervisors for their support. Prof. Tim Leighton for first linking me to his “vibrating bubbles” video thus kicking off the idea for my thesis, his incredibly supportive comments were a huge confidence boost. Prof. Paul White for patiently walking me through various equations, code, and guidance on statistics and taking acoustic readings. His quips on my “masonry” skills and in my drafts were a source of infinite amusement.

To the members of ICER (aka “Team Fish”), I'm extremely grateful for the feedback you gave me when planning my experiments and writing drafts, and your help with running my experiments. In order of seniority / PhD start date: Toru, Andy (Vowles), Jim, Jasper, Matty, Daniella, Helen, James, Nick, Andy (Johnson), Mhairi, Andrew, Amelia, Jack, and Lewis. Andy (Johnson) thank you for suggesting I christen each and every experimental fish with a punny name as a means to keep myself awake during my first experiment; “Genghis Carp”, “Rosa Karpis”, “Carp2D2”, “Mary Wollestonecarp” and “Ghetto Trout”, are still firm favourites. I'm also very grateful to my non-fishy office and Chilworth colleagues Aminu, Jack, Francisco, and Ash for being workout pals, providing help and cover, and time to chat.

A big thank you to my closest friends strewn all over the globe; Luke, Amanda, Pedro, Jonathan, Sebastian, Daria, and Chris, for listening to my moping and griping and providing me with the occasional wedding to attend to. To the residents of 60 Padwell Road (feat. Krzysztof), my home during my final year, I wish we'd met earlier and being on lockdown with you was a pleasure. I never knew that the human capacity for putting away craft and cask ale could be so frighteningly and unashamedly bottomless. To the members of the Hillwalking society, thank you for keeping me sane with expeditions to Scotland, and introducing me to the joys of roaring down the M6 in a minibus at 3 a.m or rallying through narrow tracks in the Dales or Lakes. I have rather enjoyed being the “wise” and grumpy elder of the club and assume the average age should now drop off considerably (buoyed only by Simon).



Finally to my family, my two sisters Ilaria and Nadine, and to my Mum and Dad. Thank you for your support, particularly during my final year, and thank you for providing me with the grit and resilience to see this to the end. For the record, I still don't know whether this was a good idea.

Funding for this research was provided by an EPSRC Doctoral Training Centre grant.

## Definitions and Abbreviations

### A. Fish families

COMMON NAME	LATIN NAME
Anchovies	<i>Engraulidae</i>
Carp	<i>Cyprinidae</i>
Catfish	<i>Ictaluridae</i>
Cichlids	<i>Cichlidae</i>
Cods	<i>Gadidae</i>
Croakers	<i>Sciaenidae</i>
Damselfish	<i>Pomacentridae</i>
Eel	<i>Anguillidae</i>
Righteye Flounders	<i>Pleuronectidae</i>
Gobies	<i>Gobiidae</i>
Herring	<i>Clupeidae</i>
Lamprey	<i>Petromyzontidae</i>
Paddlefish	<i>Polyodontidae</i>
Perch	<i>Percidae</i>
Salmon	<i>Salmonidae</i>
Smelt	<i>Osmeridae</i>
Squirellfish	<i>Holocentrinae</i>

Sunfish	<i>Centrarchidae</i>
Suckers	<i>Catostomidae</i>
Temperate basses	<i>Moronidae</i>
Tuna	<i>Scombrinae</i>

## B. Fish species

COMMON NAME	LATIN NAME
Alewife	<i>Alosa pseudoharengus</i>
American shad	<i>Alosa sapidissima</i>
Atlantic cod	<i>Gadus morhua</i>
Atlantic herring	<i>Clupea harengus</i>
Atlantic menhaden	<i>Brevoortia tyrannus</i>
Atlantic salmon	<i>Salmo salar</i>
Atlantic tomcod	<i>Microgadus tomcod</i>
Ballan wrasse	<i>Labris bergylta</i>
Bay anchovy	<i>Anchoa mitchilli</i>
Black carp	<i>Mylopharyngodon piceus</i>
Black crappie	<i>Pomoxis nigromaculatu</i>
Blueback herring	<i>Alosa aestivalis</i>
Bighead carp	<i>Hypothalmichthys nobilis</i>

Brown trout	<i>Salmo trutta</i>
Bullhead	<i>Ameiurus melas</i>
Chinook salmon	<i>Oncorhynchus tshawytscha</i>
Common carp	<i>Cyprinus carpio</i>
Common dab	<i>Limanda limanda</i>
Common roach	<i>Rutilus rutilus</i>
Cutthroat trout	<i>Oncorhynchus clarkia</i>
Crappie	<i>Pomoxis spp.</i>
Cuckoo wrasse	<i>Labrus mixtus</i>
Emerald shiner	<i>Notropis atherinoides</i>
Eurasian ruffe	<i>Gymnocephalus cernuus</i>
European eel	<i>Anguilla anguilla</i>
Freshwater drum	<i>Aplodinotus grunniens</i>
Gizzard shad	<i>Dorosoma cepedianum</i>
Goldfish	<i>Carassius auratus</i>
Grass carp	<i>Ctenopharyngodon idella</i>
Japanese horse mackerel	<i>Trachurus japonicas</i>
Largemouth bass	<i>Micropterus salmoides</i>
Lemon sole	<i>Microstomus kitt</i>
Logperch	<i>Percina caprodes</i>

Muskellunge	<i>Esox masquinongy</i>
Northern pike	<i>Astronotus ocellatus</i>
Oscar	<i>Astronotus ocellatus</i>
Oyster toadfish	<i>Opsonus tau</i>
Paddlefish	<i>Polydon spathula</i>
Plainfin midshipman	<i>Porichthys notatus</i>
Plaice	<i>Pleuronectes platessa</i>
Pollack	<i>Pollachius pollachius</i>
Rainbow smelt	<i>Osmerus mordax</i>
Rainbow trout	<i>Oncorhynchus mykiss</i>
River lamprey	<i>Lampetra fluviatilis</i>
Roundfish	<i>Pollachius spp</i>
Saithe	<i>Pollachius virens</i>
Sea lamprey	<i>Petromyzon marinus</i>
Silver carp	<i>Hypothalmichthys molitrix</i>
Silver chub	<i>Macrhybopsis storeriana</i>
Smallmouth bass	<i>Micropterus dolomieu</i>
Sockeye salmon	<i>Oncorhynchus nerka</i>
Striped bass	<i>Morone saxatilis</i>
Spot	<i>Leiostomus xanthurus</i>

Topmouth gudgeon	<i>Pseudorasbora parva</i>
Walleye	<i>Sander vitreus</i>
White perch	<i>Morone Americana</i>
White sucker	<i>Catostomus commersonii</i>
Yellow perch	<i>Perca flavescens</i>

### C. General terms

Adiabatic:	A process that occurs with no transfer of heat or mass between an object and its surroundings.
Clupeid:	A family of small pelagic fish, including herrings, sardines, and shad.
Dipole-quadrupole sensor:	The result of combining a dipole and quadrupole sensor, to create a unidirectional sensor, with a response chart that resembles a “heart” shape.
Dipole sensor:	A sensor that responds proportionally to the pressure gradient.
Evanescent field:	In this thesis, a sound wave that does not propagate, but decays exponentially due to the water depth being $< \frac{1}{4}$ of the wavelength of the sound wave.
Fourier transform:	An analytical method which converts a signal (a function of time) into the frequencies that make up the signal.
Infrasound:	Sound with a lower frequency than 20 Hz.
Isothermal:	A process in which the temperature does not change.
Kinocilium:	One of two types of microscopic hair-like structures found on the surface of acoustic hair cells in fish as part of a

	ciliary bundle. A single kinocilium is present on each hair cell, in contrast with many, shorter, stereocilia.
Macula neglecta:	Sensory epithelium found within the utricle, does not have an otolith associated with it, and it is unknown whether it can act as a transducer for sound.
Monopole sensor:	A sensor that responds proportionally to acoustic pressure.
Monopole-dipole cardioid:	The result of combining a monopole and dipole sensor, creating a unidirectional sensor, with a heart-shaped response chart.
Multipole:	A sensor composed of monopoles, dipoles, or quadrupoles, and combinations of monopoles, dipoles, and quadrupoles.
Otolith Organ:	Three organs within the inner ear; the Sacculle, Utricle, and Lagena, which house calcareous structures known as otoliths. Enable fish to detect particle acceleration.
Quadrupole sensor:	A sensor that responds to the second derivative of the pressure.
r-selected species:	A species which exhibits rapid growth rates, short generation times, and high reproductive output in the early stages of its life cycle.
Semicircular canal:	Three pairs of fluid filled calcareous structures in the inner ear, oriented in different planes, which allow a fish to detect motion in different directions.
Sensory epithelium:	An epithelium that lines the otolith organ, covered by sensory hair cells. Hair cell stimulation results from the relative motion between the sensory epithelium and the otolith, enabling detection of particle acceleration.

Stereocilia:	One of the two types of microscopic hair-like structures found on the surface of acoustic hair cells in fish as part of a ciliary bundle. Several stereocilia are found in a ciliary bundle.
Ultrasound:	Sound with a frequency higher than 20 kHz.
Weberian ossicles:	An anatomical structure composed of four pairs of bones that connect the swimbladder to the inner ear, allowing fish to detect acoustic pressure. Found in otophysian fish such as carp and goldfish.

#### D. Symbols and Abbreviations

##### *Symbols:*

$A$	zero-to-peak amplitude of a wave
$A_{max}$	maximum amplitude of a wave
$b$	coefficient of variation of step length
$c$	speed of sound in water ( $1500 \text{ ms}^{-1}$ )
$\bar{c}$	mean cosine of turning angles
cm	centimetre
$d$	distance
dB	decibel
$dE$	Euclidean (or shortest) distance between two points
$D_p$	the gas diffusivity ( $D_p = k/(\rho_a c_p)$ ) where $k$ is the thermal conductivity of gas and $c_p$ is the specific heat of gas at constant pressure
$F_0$	the frequency of a freely-oscillating bubble of radius, $R_0$
$f$	frequency of a wave
g	gram
GW	giga watt
$I$	intensity of an acoustic beam



$I_0$	intensity of an acoustic beam at the point of origin
$K$	polytropic index
kHz	kilohertz
km	kilometre
Hz	hertz
L	litre
lx	lux
m	metre
min	minute
mL	millilitre
mm	millimetre
ms	millisecond
n	sample size
$n_b$	number of bubbles per unit volume
$n_b^{gr}(R_0)$	number of bubbles of a given radius per unit volume
$n_b^{gr}(R_0)d(R_0)$	number of bubbles with radius between $R_0$ and $dR_0$ per unit volume
$P$	acoustic pressure
$p$	mean step length
$P_0$	hydrostatic liquid pressure outside a bubble
$P_a$	pascal, unit of pressure
$P_i$	the internal pressure within a bubble
$P_g$	pressure of the gas within a bubble
$P_\sigma$	surface tension pressure within a bubble, or Laplace pressure
$P_v$	vapour pressure
ppm	parts per million
$Q_{rad}$	radiative damping factor
$Q_{th}$	thermal damping factor
$Q_{vis}$	viscous damping factor

$R$	radius of a bubble
$R_0$	equilibrium radius of a bubble
$r$	mean vector, or angular dispersion
$s$	second
$\bar{s}$	mean sin of turning angles
$t$	time
$u$	particle velocity between two points
$V$	volt
$v$	circular standard deviation
$W$	watt
$\langle \dot{W} \rangle$	time-averaged power loss per bubble
$X$	X co-ordinate of the rectangular mean coordinates
$\bar{x}$	mean
$Y$	Y co-ordinate of the rectangular mean coordinates
$z$	distance travelled by an acoustic beam through a bubble population
$\beta_{vis}$	viscous damping factor [from Baik, 2013]
$\gamma$	the specific heat ratio of gas at constant pressure and volume
$\phi$	phase angle
$\sigma$	surface tension
$\sigma_a$	absorption cross-section
$\sigma_{b-s}^b$	backscatter cross-section of a bubble
$\sigma_{b-s}^{cv}$	backscatter cross-section of a bubble cloud with population described by $n_b^{gr}(R_0)$
$\sigma_e$	extinction cross-section
$\sigma_e^{90}$	range of bubble radii which account for 90 % of the extinction cross-section
$\sigma_e^b$	extinction cross-section of a bubble

$\sigma_e^c$	extinction cross-section of a bubble cloud with population described by $n_b^{gr}(R_0)$
$\sigma_s$	scattering cross-section
$\sigma_s^b$	scattering cross-section of a bubble
$\lambda$	wavelength
$\mu$	shear modulus
$\mu^*$	complex shear modulus
$\mu_i$	imaginary part of a complex shear modulus
$\eta$	shear viscosity
$\eta_e$	shear viscosity
$\eta_{fs}$	shear viscosity of the viscous shell
$\eta_{ws}$	shear viscosity of surrounding liquid
$\theta$	turning angle
$\theta_r$	mean angle
$\xi$	particle displacement
$\pi$	pi $\approx 3.14159$
$\rho$	density
$\delta_{Weston}$	weston damping factor
$\omega$	angular frequency
$\omega_{res}$	angular frequency at resonance
$\epsilon$	thickness ratio of the viscous shell

**Abbreviations:**

3D	Three dimensional
ABR	Auditory Brain Response
AIC	Akaike Information Criterion
atm	Atmospheric pressure (unit of)
CGS	Clean Growth Strategy

COM	European Commission
CWA	Clean Water Act
DC	Direct Current
df	Degrees of freedom
EA	Environmental Authority
EC	European Council
ECG	Electrocardiogram
edf	Estimated degrees of freedom
EIA	Environmental Impact Assessment
EU	European Union
FAO	Food and Agriculture Organisation of the United Nations
FPS	Frames Per Second
GAM	Generalised Additive Model
GES	Good Ecological Status
GEP	Good Ecological Potential
GCV	Generalised Cross-Validation Score
HP	Horse Power
HSD	Honestly Significant Difference
IAS	Invasive Alien Species
ICER	International Centre for Ecohydraulics Research
ID	Internal Diameter
IHA	International Hydropower Association
IR	Infra-red
MAM	Minimum Adequate Model
MSFD	Marine Strategy Framework Directive
NERC	Natural Environment and Rural Communities
PD	Particle Displacement
PRV	Pressure Reducing Valve
PVC	Polyvinyl Chloride

SAFFA	Salmon and Freshwater Fisheries Act
SD	Standard Deviation
SE	Standard Error
SEA	Strategic Environmental Assessment
SI	Statutory Instrument
SL	Standard Length
SNI	Sinuosity Index
SPL	Sound Pressure Level
ST	Straightness Index
UK	United Kingdom
UKBAP	United Kingdom Biodiversity Action Plan
WCA	Wildlife and Countryside Act
WFD	Water Framework Directive
WRA	Water Resources Act

## Structure of the thesis

This research project was undertaken to assess the potential of a novel insonified bubble curtain which uses the resonant properties of bubbles as a behavioural deterrent.

Research also focused on how the stimuli generated by this deterrent, as well as the presence or absence of visual cues affected fish behaviour. The individual chapters of this thesis are intrinsically linked. Chapter 1 provides a broad narrative overview of the challenges faced by fisheries managers due to infrastructure in rivers, and detailed explanations of the mechanisms of fish hearing, as well as the properties of bubbles. It also provides detailed background literature on behavioural deterrents, summarising and discussing research trends, biases and gaps in knowledge. Information from this chapter, and in particular insight on the properties of bubbles, guided the development of comprehensive research aims and objectives (Chapter 2).

Chapters 3-5 present the results of four flume experiments on common carp. The first of these tested the ability of a bubble barrier with an air flow at least three times lower than what is recommended by the industry to serve as a behavioural deterrent for fish. In Chapter 4, the differences in resonant versus non-resonant insonified bubble curtains and the effects of visual cues were tested. Despite the use of bubble curtains to contain sound fields in particular regions dating back to the late 1940s, investigations for their use as behavioural deterrents have met with a lack of cumulative progress. Worryingly, due to the lack of sufficient details provided when reporting results, previous studies are often not comparable or replicable, and the concepts of bubble coalescence and bubble resonance have remained largely unexplored.

The final experiment chapter (Chapter 5), advanced our understanding of how fish react to the different components of a sound field; acoustic pressure and particle motion. Chapter 6 provides an overall discussion and conclusions from the research contained within this thesis, mentions pitfalls to avoid for future researchers working with bubble barriers, in addition to recommendations for management and future research. It also provides some overall remarks on the shift towards standardisation in the field of bioacoustics, the upcoming challenges being faced as a result of climate change, the expected rise in hydropower capacity worldwide, and how cheap and

energy efficient behavioural barriers can be used as a tool to help slow the spread of invasive species.

## Chapter 1

### Research Background – A Narrative Literature Review

*"The Cossacks of the Ural have a singular way of catching sturgeon," observed my companion, "and it is a method, I believe, unknown in any other part of Europe. At certain times in the winter, the men assemble in large numbers by the side of the river, and, dismounting from their horses, cut a deep trench across the stream from one of its banks to the other. They lower their nets into the water, and arrange them so as to block up the entire channel, when, getting on their horses, they will ride for seven or eight miles along the banks. They then form a line of horsemen reaching from shore to shore, and gallop down in the direction of the nets. The fish, hearing the clatter of a thousand hooves, swim away from the sound and dart like lightening in the opposite direction. Here their course is at once arrested, and they become entangled in the trammels." "*

Extract from 'A ride to Khiva' by Fred Burnaby [1874]

#### 1.1 Introduction

Humans have actively altered fluvial and marine ecosystems for centuries, as part of efforts to exploit water as a resource for energy, flood defence, food, and transport. River, estuarine and coastal infrastructure development (in particular the construction of dams and weirs) have consequently impacted flows, modified water chemistry, altered geomorphology, and disconnected ecosystems. Human presence, construction, and resource use has also given rise to effects such as the creation of underwater sound and the accidental introduction of invasive species, which have further consequences on the behaviour and physiology of fish, as well as on community structure and ecosystem function.

Engineered structures are known to interfere with fish migrations [Dadswell *et al.*, 1987; Fu *et al.*, 2003; Chen *et al.*, 2004] that may be a requisite for the fish's life cycles [Dadswell *et al.*, 1987; Zhang *et al.*, 2012] and cause habitat fragmentation and loss of gene flow [Louzada, 2017]. Mortality rates of migratory fish species at large dams, and hydropower facilities are assessed by the tonnage [Baxter, 1977;



Baumgartner *et al.*, 2006; Brown *et al.*, 2014], but even small overflow dams can impede or stop fish migration [Beasley & Hightower, 2000]. Death or injury may occur directly as a result of mechanical blade strike, or indirectly via shear stresses, elevated total dissolved gas, or rapid pressure fluctuations [Cada *et al.*, 2006; Brown *et al.*, 2009]. Injured fish may incur delayed mortality, or loss of mobility through disorientation or injury preventing control of movement within the water column, inhibiting successful feeding and increasing susceptibility to predators [Carr, 2000]. Elevated predation risk occurs because migratory species aggregate at dams and weirs, causing stress and increased energy costs [Lucas *et al.*, 2009]. Juvenile fish may lack the swimming capability to escape once impinged [Moser *et al.*, 2014], and tend to encounter many dams in their migration to the sea which means cumulative stresses should also be considered [Budy *et al.*, 2002].

The search for effective and economical means to influence fish movement without direct physical intervention is one of the great challenges of fisheries management [Popper and Carlson, 1998]. Guidance technologies have long been used in fisheries management to direct fish movement in the vicinity of structures such as hydropower dams [Noatch and Suski, 2012]. Mitigation efforts have included fish "friendly" turbines [Brown *et al.*, 2012], fish ladders, runs, lifts, and pumps [Odeh, 2000], trap and transport techniques [Rosell *et al.*, 2005], dam removal [American Rivers *et al.*, 1999], and mechanical screens [Hocutt, 1981; Popper & Carlson, 1998]. When designed and operated correctly, commonly found physical or mechanical barriers can be >90% effective against certain species [Turnpenny and O'Keefe, 2005].

As a consequence of species diversity, complexities in life cycle stages and geographical variation, it has proven difficult to develop standardised mitigation practices [e.g. Sheridan, 2014]. Passage success of a particular species in a specific life-cycle state does not necessarily guarantee success for all fish. There has been a historic focus on the preservation of commercially important species (e.g. adult salmonids) without considering the entirety of an ecosystem [Lucas & Baras, 2001]. This has resulted in a reduction in species diversity, the greater plasticity of some species allowing for their adaptation and survival due to less competition [Dudgeon, 1992].

Key to the development of successful fish passage structures for downstream migrants requires knowledge of matters such as behavioural response to flow [Enders *et*

*al.*, 2009], and preferred position in the water column. There are several examples of successful bypass systems that have taken account of fish behaviour in their design. For downstream migrating juvenile salmonids, spill from the water surface is more effective than spill from the seabed because juvenile salmonids are surface-orientated [Johnson & Dauble, 2006]. Silver eels (*Anguilla anguilla*), on the other hand, would gain more from downstream-migrating facilities being located near the riverbed, because they are bottom-orientated during their migration [Jonsson, 1991; Tesch, 1999, Brown *et al.*, 2009]. Problems associated with poor attraction efficiencies for Atlantic salmon (*Salmo salar*) and brown trout (*Salmo trutta*) have been related to insufficient attraction flows [Aarestrup *et al.*, 2003; Thorstad *et al.*, 2003], lights at exits [Carr & Whoriskey, 2008], and to inappropriate design or location of the entrances of the fishways [Gowans *et al.*, 1999].

The intrinsic variability of fish behaviour [Huntingford, 1993; Knudsen *et al.*, 1997; Schilt, 2007] can compromise the effectiveness of mechanical screens and fish passes, but can also be manipulated to improve it. Consequently, this has led to an interest in developing non-physical methods of deterrence which manipulate the behaviour of fish to improve the efficiency of physical screens [Kemp *et al.*, 2012].

## **1.2 Behavioural Deterrents**

A behavioural deterrent (or guidance system) can be defined as “*any stimulus or non-solid obstruction that discourages or prevents a selected species from passing through a target region*” [Noatch & Suski, 2012]. Guidance systems have been used to direct the movements of commercially or recreationally valuable fish around facilities such as hydropower dams that can threaten their survival [Taft, 2000]; they are also being employed to stop the spread of exotic organisms through natural and human-mediated pathways [Noatch & Suski, 2012]. The first major review of such guidance systems was conducted by Hocutt [1981], who focused on systems employed at power facilities in an attempt to attract or to repel fish away from intake structures. The literature reviewing effectiveness of behavioural deterrents is extensive, and the reader is directed towards them [EPRI, 1986, 1994, 1998, 2001, 2004; Carlson & Popper, 1997; Popper & Carlson, 1998; Michaud & Taft, 2000; Taft, 2000; Larinier & Travade, 2002;

Turnpenny & O’Keefe, 2005; Noatch & Suski, 2012; USACoE, 2012; Koth, 2014; Sheridan, 2014; Putland & Mensinger, 2019].

A multitude of stimuli have been used to attract, repel and guide fish [Turnpenny *et al.*, 1998], including: electrical screens [e.g. Bullen & Carlson, 2003; Dawson *et al.*, 2006], air bubble curtains [e.g. Kuznetsov *et al.*, 1971; Zielinski *et al.*, 2016], illumination [e.g. strobe lights - McIninch & Hocutt 1987, Hamel *et al.* 2008; continuous lights - Lowe, 1952], acoustics [e.g. Deleau *et al.*, 2020; Maes *et al.*, 2004; Sand *et al.*, 2000], changes in flow direction and velocity [e.g. Enders *et al.*, 2009; Goodwin *et al.*, 2014], pheromones [e.g. Johnson *et al.*, 2009; Wagner *et al.*, 2011], shade [e.g. Kemp *et al.*, 2005], and combinations of the above [e.g. air bubbles and sound, Welton *et al.*, 2002; Taylor *et al.*, 2005; air bubbles and strobe lights, Patrick *et al.*, 1985].

Data on the effectiveness of behavioural deterrents are often contradictory, particularly if inadequate testing has been performed [Hocutt, 1981], and successes often tend to be site-specific or reported for controlled environments which may not work under other conditions, species, or age classes [Webb *et al.*, 2008]. Many of the studies on use of sound to control fish behaviour are grey literature reports which makes it difficult to fully evaluate the effectiveness of techniques or to replicate the work with information available [Popper & Carlson, 1998]. As a result, while useful, the efficiency of behavioural screens generally tends to be lower than physical methods overall [Turnpenny *et al.*, 1998].

Recent and historical experience has shown that the response of fish to water flow can dominate their behaviour, potentially overriding their ability to respond adequately to behavioural stimuli. [Sager *et al.*, 1987; Carlson, 1994; Popper and Carlson, 1998]. When considering fish passage through aquatic structures such as hydroelectric facilities, flow fields should be considered as playing an essential part in redirecting fish to preferred routes [Popper and Carlson, 1998].

In addition to aiding the migration of species across man-made structures, non-physical barriers have been proposed to combat the movement of invasive fish [Noatch & Suski, 2012], to which new migration routes may have been opened as a result of engineered changes in waterways [Fuller *et al.* 1999; Chick & Pegg, 2001]. The use of screens and guidance systems to control invasive fish is a relatively new research area,

although there may be an increasing need for further investigation as more invasive species enter new environments.

Many successful invasive fish possess life history traits of r-selected species; which exhibit rapid growth rates, short generation times, exceptional dispersal capabilities, high reproductive output early in life, high density in the native range, and broad environmental tolerance [Ehrlich, 1984]. Colautti & MacIsaac [2004] proposed an invasional framework based on various models [Carlton, 1985; Williamson & Fitter, 1996; Richardson *et al.*, 2000; Kolar & Lodge, 2001] that breaks the invasion process into a series of consecutive, obligatory stages. The framework ranges from stage 0 - propagules residing in a donor region, to stage V - widespread and dominant.

Uncontrolled, invasive species will increasingly interfere with and jeopardise native species, communities, and ecosystems. The ability of such species to disperse and then establish themselves in novel locations is particularly problematic in rivers owing to the broad range and high connectivity among these systems [Junk *et al.* 1989]. Unlike fish protection where any reduction in stress, delay, or mortality is beneficial, a barrier that protects a waterway from an invader must be very nearly perfect because even one gravid female getting through can lead to establishment of a population beyond that barrier [Popper & Schilt, 2008].

Examples of invasive species include the topmouth gudgeon (*Pseudorasbora parva*) in Europe, and two species of Asian carp (silver carp - *Hypophthalmichthys molitrix*, and bighead carp - *H. nobilis*) in the Mississippi and Upper Illinois River in the US. The former has been described as Europe's most invasive fish [Gozlan *et al.*, 2005]. Following its introduction into Romania in 1960 as part of shipments of Chinese carp for aquaculture [Simon *et al.*, 2011], it is widespread and locally abundant within favourable European habitats, having first been recorded in the wild in the UK in 1996 [Gozlan *et al.*, 2002]. *P. parva* presents a risk to native fishes through the transmission of a novel fish pathogen (an obligate intra-cellular eukaryote parasite similar to *Sphaerothecum destruens*) and undesirable impacts arising from processes including increased inter-specific competition [Britton *et al.*, 2010].

Asian carp were originally imported to the Southern United States in the 1970s to control algal growth in sewage treatment and fish farming facilities. After heavy flooding, their subsequent escape into the wild resulted in detrimental environmental

effects [Pegg & Chick, 2001]. Their filter-feeding ability, fast growth, and high reproductive effort has allowed them to have a negative impact on native fish such as paddlefish, *Polyodon spathula* [Schrank *et al.*, 2003] and gizzard shad, *Dorosoma cepedianum* [Sampson *et al.* 2009]. The species have furthermore caused a decline of lower trophic level organisms and community shifts in zooplankton populations which in turn may have affected additional native aquatic species [Cooke *et al.*, 2009]. To limit their range expansion, especially into the Great Lakes, numerous US states are evaluating the efficacy of non-physical barriers to deter invasive carp [Kelly *et al.*, 2011].

### **1.3 Bubble Curtains and Combination Screens**

The recent push to develop cost-effective and easily deployable barriers to combat invasive carp species (such as *Cyprinus carpio*, *Hypophthalmichthys molitrix*, and *H. nobilis*) in North America, particularly in watersheds with multiple smaller tributaries, has generated a renewed interest in bubble curtains and combination screens [Taylor *et al.*, 2005; Ruebush *et al.*, 2012; Zielinski *et al.*, 2014b]. In contrast with the evaluations carried out at a number of sites on the Great Lakes in the 1970s and 1980s [Hocutt, 1981; Taft, 2000] recently greater efforts are being made to categorise the sound field generated by the bubble curtain [Zielinski *et al.*, 2014b; Zielinski & Sorensen, 2016].

Bubble curtains were developed in an attempt to overcome the need for expensive, automatically-cleaned, mechanical screens [Goodwin *et al.*, 2014]. A major advantage of bubble curtains over other behavioural screens is that they can be installed and maintained at relatively low cost, and can be readily repositioned or removed as needed [Zielinski & Sorensen, 2016]. They have been used with varying levels of success, depending on the species of fish involved, as a fishing aid for Atlantic herring (*Clupea harengus*) [Smith, 1961] and more widely to attract or repel fish from intakes [Bates & VanDerwalker 1964; Alvevras, 1974; Bibko *et al.*, 1974; Ray *et al.* 1976; Hocutt, 1981]. Information available can be contradictory [Kuznetsov, 1971], in fact impingement has been shown to increase when fish are attracted to the bubble screens [EPA 1973, 1976; Hanson *et al.*, 1977]. Herring, for instance, are attracted to bubble curtains under conditions of high illumination [Imamura & Ogura, 1959], as are juvenile salmon under certain combinations of approach velocity, angle and jet pressure

of the bubble curtain [Bates & VanDerwalker, 1964]. Deflection rates vary with illumination, air pressure, turbidity, and intake velocity [Bates & VanDerwalker, 1964].

It was originally thought that bubble curtains functioned as an entirely visual stimulus, a generalisation which work by Bibko *et al.* [1974] and Kuznetsov [1971] helped to dispel. Kuznetsov [1971] first proposed the idea that fish might be reacting to an acoustical stimulus. Sound is generated by bubbles as they detach from the diffuser [Leighton, 1994], but when present in large numbers their behaviour becomes influenced by the bubbles around them, causing them to emit low frequency (<1000 Hz) sound emissions [Nicholas *et al.*, 1994;]. Plumes of bubbles also generate turbulence with recirculation currents, which are dependent on the upward velocity and density of the bubble plume [Brevik & Kristiansen, 2002]. Bubble curtains may also serve as a visual barrier by obscuring a fish's line of sight past the barrier [Patrick *et al.*, 1985; Sager *et al.*, 1987]. Finally, since bubbles occur very regularly in the natural environment, fish tend to have previous experience of swimming through bubbly water. Bubbles lower the density of water and therefore a fish swimming through bubbly water would be required to inflate its swimbladder to remain at the same depth - which a fish may not always be sufficiently motivated to do [Leighton, pers comm.].

Best practice recommendations for bubble curtain installation have been provided by the UK's Environment Agency (EA) [Turnpenny and O'Keefe, 2005]. These include; (1) angling the curtain near-parallel to the water flow, (2) an air flow of 60 - 240 L min<sup>-1</sup> m<sup>-1</sup> of bubbler length to ensure that a uniform bubble sheet is maintained at all areas, and (3) a bore size of 0.5 – 2 mm to create bubbles that rise quickly enough [e.g. Gaudin, 1957; White & Beardmore, 1962; Baker & Chao, 1965; Scheid *et al.*, 1999] to maintain stability of the bubble curtain in running water. Spacings in the bubble wall should be assumed to be more or less analogous to separations in bar screens [Turnpenny & O'Keefe, 2005]. A key criticism is that none of these recommendations address bubble size. Bore size is not equivalent to bubble size, as was pointed out by Leighton *et al.*, [1991] because of coalescence at the bores which increasingly happens as small bores are used in an attempt, often in vain, to produce smaller bubbles.

In most lotic systems, periodic high water may decrease their visibility and integrity and it can be difficult to ensure equal air pressure across differing depths

[Noatch & Suski, 2012]. Bubblers are furthermore also vulnerable to clogging [e.g. Welton *et al.*, 2002]; the header should not be placed in areas of heavy siltation [EPRI, 1986]. Many fish species, including salmonids, clupeids and cyprinids can be deflected by a bubble barrier but habituation is rapid. Consequently they are best suited to deflection of migrating fish in rivers, or of fish moving with the tide in tidal systems [Turnpenny & O'Keefe, 2005].

Bubble curtains tend to be more effective when used with other stimuli. Examples include strobe lights and air bubbles (various freshwater and estuarine species [Patrick *et al.*, 1985]; Atlantic menhaden - *Brevoortia tyrannus*, spot - *Leiostomus xanthurus*, and white perch - *Morone americana* [McIninch & Hocutt, 1987]; Asian carp – *H. nobilis* [Ruebush *et al.*, 2012]); bubbles and electric fields (roundfish - *Pollachius spp.* and *Labrus mixtus* [Stewart *et al.*, 1981]); and low volume bubble curtains and sound (Atlantic salmon smolts [Welton, *et al.*, 2002]; Asian carp - *H. molitrix* and *H. nobilis* [Pegg & Chick, 2004]; Bighead carp - *H. nobilis* [Taylor *et al.*, 2005]).

Acoustic-bubble deterrents appear to have particular promise for Carp species. Common Carp (*Cyprinus carpio*) and related species like Asian carp (*H. molitrix*, *H. nobilis*) have a connection between the swim bladder and hearing organs which widens the range of sound frequencies they are sensitive to (**Fig 1.6.**). In a series of shallow-water laboratory experiments, bubble curtains with air flows that ranged between of 336 L min<sup>-1</sup> m<sup>-1</sup> to 6480 L min<sup>-1</sup> m<sup>-1</sup>, with or without sound, reduced passage of bighead and common carp by 75 - 85 % [Zielinski *et al.*, 2014a, 2014b]. This was likely due to the shallow-water environment which led to rapid attenuation of the sound field generated by the bubble curtains and insonified bubble curtains [Akamatsu *et al.*, 2002; Zielinski *et al.*, 2014a]. A field test in a small river showed that an air curtain could reduce passage of downstream swimming juvenile common carp by 60 %, but was ineffective against upstream migrating adults [Zielinski & Sorensen 2015].

A laboratory study using a split-passage experimental channel [Zielinski & Sorensen, 2016] found that a bubble curtain with an air flow of 180 L min<sup>-1</sup> m<sup>-1</sup> can reduce passage of both Asian and common carp by 75 – 80 %. Underwater cameras were used to observe swimming behaviour near the bubble curtain (< 20 cm) in three of the twenty trials. The study also mapped the acoustic near field of the bubble curtain (a

sound source distance less than the signal wavelength /  $2\pi$ ) where acoustic particle motion dominates the sound field [Kalmijn, 1988]. Within 25 cm of the bubble curtain, particle acceleration reached a maximum of 10 dB re 1 cm s<sup>2</sup> for frequencies < 300 Hz, exceeding the threshold that elicits avoidance behaviour [Knudsen *et al.*, 1992]. Since carp tended to be deflected approximately 25 cm away from the curtain, and also because hydrodynamic forces extended 50 - 100 cm away from similar curtains [Zielinski *et al.*, 2014a], this means that particle velocity may play a role in avoidance of bubble curtains by carp. A follow-up study with an underwater speaker in the absence of visual cues showed that although the initial avoidance response was mediated by acoustic pressure, fish swimming away from the speaker maintained a nearly perfect 0° orientation to the axes of particle velocity [Zielinski & Sorensen, 2017]. While not conclusive, this seems to indicate a likelihood that while avoidance response in carp may be pressure-mediated, oriented avoidance behaviour may at least be partially particle velocity-mediated [Zielinski & Sorensen, 2017].

Experiments carried out using bubble curtains in conjunction with other stimuli of relevance to the present study are: Welton *et al.*, [2002], Pegg & Chick, [2004] Taylor *et al.*, [2005], Ruebush [2012], and Dennis *et al.*, [2019]. The deflection efficiency of an insonified bubble curtain was tested in each of these studies, with Ruebush [2012] also testing a strobe light / sound / bubble curtain in a second experiment. In all cases, the system used was a Sound Projector Array Driven Bio Acoustic Fish Fence (SPA-BAFF, Fish Guidance Systems), which uses a combination of a sound source and bubble curtain to create a field largely contained within the bubble sheet through refraction [Nedwell & Turnpenny, 1997]. The system uses an electromagnetic or pneumatic sound transducer which generates a random series of cyclic sound bursts at a range of frequencies for the sound component of the stimulus [Turnpenny & O'Keefe, 2005].

Welton *et al.*, [2002] used an SPA-BAFF emitting a signal of 200 Hz to deflect Atlantic salmon smolts. Reported deflection efficiencies were greater at night (73 %) than in daylight (42 %) because smolt were able to detect gaps in the bubble barrier due to silting during the day. Pegg & Chick, [2004] tested two frequency ranges on bighead carp reporting efficiencies of 57 % (20 – 500 Hz) and 95 % (20 – 2000 Hz), the latter frequency range being the same used by Taylor *et al.*, [2005]. Finally, Ruebush [2012] tested upstream passage rates for both species of Asian carp. The rejection rate obtained



for a sound-bubble barrier in a hatchery raceway was 95 %. The second experiments involved the use of a sound-bubble-strobe light barrier in a tributary of the Illinois river (US). A total of 2 of 575 marked silver carp, and 85 of 2,937 marked fish of other species breached the barrier and were recaptured upstream. No marked bighead carp successfully passed upstream.

Dennis *et al.*, [2019] tested the deflection efficiency of outboard motor sound versus a proprietary sound in a darkened laboratory flume, and whether coupling either of these with a bubble curtain might enhance their effectiveness. The effects of these stimuli were tested on invasive bighead carp and common carp, as well as largemouth bass (*Micropterus salmoides*), which lacks a connection between the swim bladder and hearing organs. The proprietary sound was more effective than the outboard-motor sound at deflecting both carp species, but largemouth bass were less affected by both. When an air curtain was coupled to either sound, the combined stimulus became more effective at deflecting all three species; 90 - 97 % of bighead carp, 88 - 100 % of common carp, and 71 - 87 % of largemouth bass [Dennis *et al.*, 2019]. Results from these studies suggest that combined strobe light / bubble / sound barrier technologies could be used as a deterrent system to repel or redirect fish, however the current consensus is that these should not be used as an absolute barrier [Zielinski & Sorensen 2017].

Although literature investigating the effectiveness of bubble walls and combination barriers spans a number of decades (**Table 1.1**), the bulk of studies are either in the form of grey literature reports, or omit certain details for proprietary reasons. Barring some exceptions [e.g. Matousek *et al.*, 1988; Dawson, 2006; Zielinski & Sorensen, 2016], studies have generally failed to specify or measure the stimuli used, and feature set-ups and conditions which differ widely from one another, which precludes direct comparison between studies. Other studies have discussed but not tested the possibility that insonified bubble curtains produce strong sound pressure and particle acceleration gradients that are aversive to fish [Zielinski *et al.*, 2014; Dennis *et al.*, 2019]. While effective in the field, it is unclear so far whether effectiveness of bubble walls used in conjunction with sound is a result of the two stimuli acting separately, or in conjunction with one another using the resonant or refractive properties of bubbles.

## 1.4 Underwater Bubbles

A bubble is a quantity of gas suspended and surrounded by liquid water, entrained for instance by breaking waves, or injection by needles. Each bubble pulsates with a natural frequency which varies approximately inversely to its radius, undergoing a gradual amplitude decay. On entrainment the pulsations generate an acoustic “signature”, an exponentially decaying sinusoid, the frequency of which indicates the bubble size [Leighton *et al.*, 1997]. A few milliseconds after entrainment these passive emissions decay to below the level of the noise.

When driven by external sound fields a bubble will pulsate with a larger amplitude. When this sound field is at a frequency that is close to the natural frequency of the bubble, then the bubble is said to be close to resonance (from now on the looser phrase ‘at’ resonance will be used, but here in this sentence the term ‘close to’ is used because there are several different waves of defining resonance, which can lead to slightly different values for the resonance frequency; Leighton & Ainslie, 2009, 2011) . At resonance the bubble oscillates at its maximum and a maximum amount of energy is extracted from the incident sound wave. A portion of this energy is scattered in all directions by the pulsating bubble, and the remainder is converted into heat [Urick, 1983] either directly through irreversible thermal flux across the bubble wall, or through shear in the liquid around the bubble [Leighton, 1994]. Bubbles that are larger than the size resonant with the sound field will pulsate in antiphase to those smaller than resonance size (Leighton *et al.*, 1990), and the amplitude of pulsation tends to be largest closest to the resonance condition [Leighton 1994].

The loss in amplitude of a sound signal as it propagates from source to receiver through a bubble cloud is called attenuation, and is the result of scattering (where sound remains as sound but is diverted from its path between source and receiver) and absorption (where sound is converted to heat). Diffraction and refraction also play a part, and whilst these can produce interesting effects with bubble clouds (such as those employed by humpback whales (*Megaptera novaeangliae*) when hunting prey [Leighton, 2004; Leighton *et al.*, 2007, 2014; Qing *et al.*, 2019] they will not be further researched in this thesis). Bubbles that are much larger than resonance sound scatter strongly because they present large targets to the sound field, but do not pulsate to large amplitude, and so do not contribute as much to absorption as resonant bubbles. If the

bubble radius,  $R_0$ , is larger than the size which is resonant with the frequency,  $f$  of the sound field; the rule-of-thumb for air bubbles in water under 1 atmosphere (atm) of static pressure is that the bubble radius (mm) x resonance frequency (kHz)  $\sim 3$  [Minnaert, 1933; Leighton *et al.*, 1996].

How bubbly water affects the speed of sound depends on the driving frequency and the radius of the bubble population. If the bubble is much smaller than the resonant size, or if the frequency of the acoustic field is much less than the bubble resonance, the sound speed is reduced. If the bubble is much larger than resonant size, or if the frequency of the acoustic field is much greater than bubble resonance then the presence of bubbles will increase the speed of sound [Leighton 1998].

Bubbles produce “birthing wails” at their natural frequency as they are entrained into a medium (e.g. during wave breaking events) or as they separate from the hole used to introduce the bubble into that medium [e.g. Minnaert, 1933; Prosperetti, 1985]. Bubble clouds generated by breaking waves have, however, been observed to produce collective oscillations at frequencies far below those of the individual constituent bubbles. Carey & Bradley [1985], Carey & Browning [1988] and Prosperetti [1985] argued that since the bubbles in a cloud consist of a collection of coupled oscillators, one would expect to find modes of oscillation at frequencies far lower than those of individual bubbles. Yoon *et al.*, [1991]'s experiment, extended by Nicholas *et al.*, [1996] generated columns of bubbles using hypodermic needles to confirm that bubble clouds are indeed capable of these collective oscillations at frequencies far below those of individual constituent bubbles, and can be a major source of underwater sound at frequencies of a few hundred hertz.

The acoustic output  $F_0$  of a freely oscillating bubble of equilibrium radius  $R_0$  oscillating under a static pressure  $P_0$  in a liquid of density  $\rho$ , is given by **Eq. 1.1**. where  $K$  is referred to as the polytropic index, which takes values between unity and  $\gamma$  (the ratio of heat capacities at constant pressure and volume) depending on whether the gas behaves isothermally, adiabatically, or in some intermediate manner.

**Eq. 1.1:** 
$$F_0 \approx \frac{1}{2} \pi R_0 \left( 3K \frac{P_0}{\rho} \right)^{\frac{1}{2}}$$

**Table 1.1** Effectiveness of bubble barrier and combination bubble barriers used in previous studies. Flow refers to water flow, and air flow refers to the quantity of air used to generate the bubble curtain. *Note:* Rey *et al.*, [1976] contains several personal communications not included as references.

\* = species is acoustic pressure sensitive; \*\* = otophysian species; \*\*\*= study mapped or quantified the sound field; \*\*\*\* = study included information on bubble size; † = grey literature; ‡ = thesis. Negative effectiveness percentages indicate attraction to the stimulus.

Barrier / Deterrent	Species	Deployment conditions	Deflection Efficiency	Citation
Bubbles	Common carp **	Behavioural tank	73 %	Zielinski & Sorensen, 2016 ***
	Bighead carp **	Depth: 0.25 m; Flow: 5 cm s <sup>-1</sup>	83 %	
	Silver carp **	Air flow: 730 L min <sup>-1</sup> (180 L min <sup>-1</sup> m <sup>-1</sup> of barrier) PVC tubing with 3 mm holes at 5 cm intervals Sound produced by bubbles: 100 – 1000 Hz at 145 dB (re 1 µPa)	80 %	
	Roach **	Flume Depth: 0.20 m , Flow: 30 m s <sup>-1</sup> Air flow: 45 L min <sup>-1</sup> per air stone (225 L min <sup>-1</sup> m <sup>-1</sup> of barrier) 2 air stones (20 cm long) Tested effectiveness for :  a) Individuals b) Schooling groups	a) 47.5 % b) 65 %	Fullbrook, 2015 ‡
	Common carp **	Field test Air flow: 900 L min <sup>-1</sup> Bubble curtain sound: 100 – 2000 Hz at 150 dB (re 1 µPa)	59 ± 14 % (Downstream) 16 ± 11 % (Upstream)	Zielinski & Sorensen, 2015 ***
	Muskellunge	Field test – dam spillway Depth: 0.34 m; Flow: 6 cm/s, PVC tubing (20 mm diam.) with 0.39 mm holes at 16 mm intervals	Ineffective  Escape rate higher in daylight	Stewart <i>et al.</i> , 2014
	Common carp **	Behavioural tank Depth: 0.25 m; Flow: 5 cm s <sup>-1</sup> Three bubbler setups:	a) Ineffective b) 72 – 78 % c) 82 – 87 %	Zielinski <i>et al.</i> , 2014a ****

	<ul style="list-style-type: none"> <li>a) fine-graded – 23 <math>\mu\text{m}</math>, Air flow: 336 L <math>\text{min}^{-1}</math> ;</li> <li>b) graded – 23 <math>\mu\text{m}</math>, 1 mm, and 3 mm, Air flow: 1800 L <math>\text{min}^{-1}</math>;</li> <li>c) course – 3 mm, Air flow: 6480 L <math>\text{min}^{-1}</math>;</li> </ul>		
Eurasian ruffe	<p>Behavioural tank            Depth: 0.41 m            Air flow: 1.5 L <math>\text{min}^{-1}</math> (5 L <math>\text{min}^{-1}</math> <math>\text{m}^{-1}</math> of barrier);</p> <p>PVC Tubing, 30 cm long, two setups:</p> <ul style="list-style-type: none"> <li>a) 0.4 mm holes every 6.25 mm</li> <li>b) 1 mm holes every 12.5 mm</li> </ul>	<ul style="list-style-type: none"> <li>a) Ineffective</li> <li>b) Ineffective</li> </ul>	Dawson, 2006 ****
Chinook salmon American shad ** Panfish Other fish	<p>Submerged floating dry dock            Depth: 12 m            Air flow: 56,600 – 67,900 L <math>\text{min}^{-1}</math> (368 – 446 L <math>\text{min}^{-1}</math> <math>\text{m}^{-1}</math> of barrier)            PVC tubing (50 mm diam.), with 0.24 mm holes at 15 cm intervals.</p>	<p>77 %            92 %            Ineffective            - 127 %</p>	Sprott, 2001†
Various	<p>Field test – Pumping station intake (Blackdyke, Lincolnshire, UK)            Static / slow-moving conditions</p>	<p>Effective</p> <p>Decreased over time due to habituation</p>	EA, 1998 †
Catostomids ** Common carp ** Smallmouth bass Walleye Logperch Yellow perch White sucker ** Black crappie Largemouth bass Emerald shiner ** Other	<p>Field test – Power station intake (White Rapids Hydroelectric Project, Michigan, US)</p>	Ineffective	EPRI, 1998†

Bullhead *	Field test – Power station intake (Four Mile Hydroelectric project, Michigan, US) 3 parallel air lines, 15 cm apart	69 %	More effective at dawn, dusk, and night	McCauley <i>et al.</i> , 1996	
Shiner **		55 %			
Other species		43 %			
Bullhead *	Field test – Power station intake (Four Mile Hydroelectric project, Michigan, US) 3 parallel air lines, 15 cm apart	Ineffective		GLEC, 1994 †	
Shiner **					
Other species					
42 species	Field test – Power station intake (Heysham, UK) 70 m bubble curtain	37%	More effective at night	Turnpenny, 1993 †	
White perch	Field test – Power station intake (Roseton Generating Station, New York, US)  Air flow: 60 L min <sup>-1</sup> m <sup>-1</sup> of barrier Polyester fibre hose (5.7 cm diam.) around interior polyethylene tubing (0.95 cm diam.), with 15 mm holes, at 7.6 cm intervals  Bubble size: 0.16 cm diameter	Ineffective		Matousek <i>et al.</i> , 1988 ****	
Blueback herring **					
Bay anchovy **					
American shad **					
Alewife **					
Sockeye salmon	Field test – Power station intake (Seton hydro-electric station, British Columbia, Canada)	Ineffective		McKinley & Patrick, 1988 †	
White perch	Laboratory study Depth: 0.46 m; flow: 20 cm s <sup>-1</sup>  Three turbidity conditions:  a) Clear b) Low turbidity c) High turbidity	a) -11%	b) 12%	c) -40%	McIninch & Hocutt, 1987
Spot		a) 10%	b) 48%	c) 43%	
Atlantic menhaden **		a) 25%	b) 1%	c) N/A	
White perch	Behavioural tank	Ineffective		Sager <i>et al.</i> , 1987	
Spot	Flow: 30 – 50 cm s <sup>-1</sup>				

Atlantic menhaden \*\*

Alewife \*\*  
Gizzard shad \*\*  
Rainbow smelt

Behavioural tank

a) 70 %      b) 51 %  
a) 98 %      b) 80 %  
a) 92 %      b) N/A

Patrick, 1985

White perch  
Spot croaker \*\*  
Atlantic menhaden \*\*

Depth: 1 m; Flow: 11 - 12 cm s<sup>-1</sup>  
Porous plastic tubing (1 cm diam.), with intervals of 0, 5,  
10, 20 cm

*Marine species:*

15 cm s<sup>-1</sup> – a) 73 %; b) 71 %  
32 cm s<sup>-1</sup> – a) 59 %; b) 38 %

Treatments:

- a) Low light
- b) Dark

*Marine species -*

Depth: 1 m; Flow: i) 15 and ii) 32 cm s<sup>-1</sup>

Treatments:

- a) Turbid
- b) Clear

Saithe  
Pollack  
Cuckoo wrasse  
Plaice  
Lemon sole  
Common dab

Field test - Sea cages  
Confinement within sea cages

More effective for roundfish

Stewart, 1981

White perch  
Atlantic tomcod  
Striped bass

Field test – Power station intake

Ineffective

Leiberman & Muessig, 1978

Gizzard shad \*

Field study – Power station intake canal (Edison Company  
Quad Cities Generating Station, Illinois, US)

Ineffective

Latvaitis, 1976 †

Rainbow smelt Alewife *	Laboratory study Flow:  a) 15 cm s <sup>-1</sup> ; b) 37 cm s <sup>-1</sup> ; c) 69 cm s <sup>-1</sup> ;  Stainless steel tubing (1.3 cm diam.), with 0.87 mm holes at 5.1 cm intervals Air flow provided by compressor	57%  Velocity had no effect on deflection rate	Stone & Webster, 1976 †
Crappie Freshwater drum  Common carp ** Silver chub ** White bass	Field study – Power station intake (Prarie Island Nuclear Plant, Minnesota, US)	19 % 9.8 %  - 5.3 % - 40 % - 31.7 %  Overall: -7.1 %; but 30 – 65 % during Summer months.	Grotbeck, 1975 †
Yellow perch Walleye Gizzard shad ** Drum Alewife ** Smelt	Field study – Power station intake (Monroe Power Plant, Michigan, US)  System on or off over 7-day periods	Ineffective	Detroit Edison, 1975 †
Unknown	Field study – Power station intake (Indian Point Nuclear Powerplant, New York, US)	Ineffective during the daytime  May attract fish during periods of darkness	Alvebras, 1974 †
Striped bass Gizzard shad **	Field study – Power plant intake	Effective at 5 - 11 °C  Detected a 5 cm gap within the bubble screen - passed through it in single file.	Bibko <i>et al.</i> , 1974



Unknown	Unknown	Detected 15.2 cm gap and swam side by side in groups of 2 to 5. Ineffective	Mayo, 1974 †
Salmonids	Field study – Power plant intake Air bubbles in conjunction with a screen 30 ° to the flow	Ineffective due to breakup of screen in surface half.  100% in lower half of bubble screen.	Schuler & Larson, 1974 †
Salmonids	Unknown	Ineffective	Bell, 1973 †
Striped bass Perch	Field study – Power station intake Flow: 4.8 cm s <sup>-1</sup> – 18 cm s <sup>-1</sup> Air flow: 11,300 L min <sup>-1</sup> Two rows of seven horizontal PVC tubes, with 8 mm holes at 1.3 cm intervals	Ineffective  Fish attracted at night	EPA, 1973 †
Alewife **	Field study – Power station intake (Lake Michigan, US) Depth: 3.60 – 4.00 m; Flow: 18.3 m <sup>3</sup> s <sup>-1</sup> Air flow: 2830 L min <sup>-1</sup> at 60 psi PVC tubing (2.5 cm diam).	Effective	Maxwell, 1973 †
Unknown	Unknown	Ineffective	Anonymous, 1970 †
Juvenile migrant salmon	Field study – Power station intake  Treatments:  a) Day b) Night	a) 95 % b) 28 %	Bates & VanDerWalker, 1969
Alewife **	Field study – Milwaukee river 152 m PVC tubing 45 ° to flow, with 0.5 mm holes at 5 cm intervals	Effective  Results inconsistent	Kupfer & Gordon, 1966 †

Juvenile migrant salmon	Field study – Power station intake	90% at intake velocities of < 0.58 m/s	Bates & VanDerWalker, 1964
Marine fish	Behavioural tank	Effective Dependent on ability of fish to see bubbles	Enami, 1960
Jap. horse mackerel *	Field test Testing ability to drive / gather fish	Effective Rapid habituation	Inamura & Ogura, 1959a
Herring **	Field test  Treatments:  a) High illumination b) Low illumination	a) 79% b) 32%	Inamura & Ogura, 1959b
Various	Experimental tank Testing ability to drive / gather fish Perforated tubes (10 - 15 mm diam.)	Effective	Kobayashi <i>et al.</i> , 1959
Salmon smelt Cut-throat trout fry Kamloops trout fingerlings	Field test: Concrete / brick-lined canal (British Colombia, Canada) Flow: 91 cm s <sup>-1</sup> Bubble barrier placed 40 ° to flow	Ineffective	Brett & McKinnon, 1953
Atlantic herring **	Field test - Open water, fishing aid for sardines Air flow: 3738 L min <sup>-1</sup> (25 L min <sup>-1</sup> m <sup>-1</sup> of barrier) Polyethylene tubing (1 in. diam.), with 0.4 mm holes at 30 cm intervals	Effective	Smith, 1951
Common carp ** Northern pike Rainbow trout	No information	Effective Effective Ineffective	Bramsnaes <i>et al.</i> , 1942

Bubbles and Sound	Bighead carp ** Common carp ** Largemouth bass	Fibreglass Flume Depth: 0.30 m, Flow: 1.6 cms <sup>-1</sup> for bighead carp, no flow for other trials SPA-BAFF	<i>Experiment 1:</i> a) 76 %    b) 78 %    c) 60 % a) 42 %    b) 79 %    c) 64 % a) 46 %    b) 50 %    c) 68 %	Dennis <i>et al.</i> , 2019
		Treatments:  i) Experiment 1:  a) Outboard motor noise only b) Proprietary sound only c) Bubble curtain only  ii) Experiment 2:  a) Outboard motor noise + bubble barrier b) Proprietary sound + bubble barrier	<i>Experiment 2:</i> a) 90 %    b) 97 % a) 88 %    b) 100 % a) 71 %    b) 87 %	
	Common carp **	Behavioural tank Depth: 0.25 m, Flow: 5 cm/s Speaker array and fine bubble system Fine-graded – 23 µm, 336 L min <sup>-1</sup> air flow  The signal was a 10 s recording of the sound produced by the coarse-bubble system on a loop (130 dB re 1 µ Pa)	73 % - 76 %	Zielinski <i>et al.</i> , 2014a ***
	Silver carp ** Bighead carp ** Non-carp species	Field test – River (Quiver creek, Illinois, US) SPA-BAFF Air pressure at 25 psi Sound signal: 500 and 2000 Hz	<1% recapture rate upstream for asian carp  <3% recapture rate upstream for non-asian carp species	Ruebush <i>et al.</i> , 2012
	Bighead carp **	Behavioural tank / raceway SPA-BAFF Sound signal: 20 – 2000 Hz	95%	Taylor <i>et al.</i> , 2005

Bighead carp **	Behavioural tank / raceway SPA-BAFF	a) 57% b) 95%	Taylor <i>et al.</i> , 2003
	Sound signal treatments:  a) 20 - 500 Hz b) 20 - 2000 Hz		
Salmon smolts	Field test – Power station intake (small hydropower scheme, Backbarrow, Cumbria) Flow: 2 - 5 % of turbine flow  SPA-BAFF Sound signal: 50 - 600 Hz	56.9 % - 92.7 %  2.7 % - 7.3 % of fish estimated to be smolts	Spiby, 2004 †
Salmon smolts	Field test – Counting station intake (River Frome, UK) Air flow: 60 L min <sup>-1</sup> m <sup>-1</sup> of barrier  SPA-BAFF Sound signal: 200 Hz, 170 dB (re 1 μPa)  Treatments:  a) Night b) Day	a) 73 % b) 42%	Welton <i>et al.</i> , 2002
Unid. catostomids ** Common carp ** Smallmouth bass Walleye Logperch	Field test – Power station intake (White Rapids Hydroelectric plant, Michigan, US) Depth: 4.40 m, Flow: 15 – 27 cm s <sup>-1</sup> Air flow: 18,000 L min <sup>-1</sup> (738 L min <sup>-1</sup> m <sup>-1</sup> of barrier) at pressure of 0.71 kg/cm <sup>2</sup> Galvanised pipe (1.9 cm diam.) with 15 mm holes at 38 cm intervals Deterrent device mounted on trash racks  Sound signal: Five signal sound sequence played for 0.5s per signal, played through each transducer before moving on to the next	Ineffective	Michaud & Taft, 2000

	Salmon smolts	Field test – Power station intake (Halsou hydroelectric plant, Nive river, France) Depth: 3.00 m; Flow: 140 cm s <sup>-1</sup>  SPA-BAFF , 32 m long, 20° incline to canal axis Sound signal: 60 - 600 Hz - 3 pulses per second	<1 %	Gosset & Travade, 1999
	Salmon smolts	Field test – small shallow river, large bypass SPA-BAFF  Treatments:  a) Night b) Day	a) 70 % b) 30 %	Welton, 1997 †
	Salmon	Field test – River (Deer Creek, California, US) Air jet	Ineffective	Warner, 1956
Bubbles / Strobe Lights	Age-0 muskellunge	Field test – Power station spillway Depth: 0.34 m; Flow: 6 cm s <sup>-1</sup> Air pressure: 984.3 kg m <sup>-2</sup> 50 cm long PVC tubing (20 mm diam.) with 0.39 mm holes at 16 mm intervals  Strobe light signal - 60 flashes / minute, angled into bubble curtain	Ineffective	Stewart <i>et al.</i> , 2014
	Unid. catostomids ** Common carp ** Smallmouth bass Walleye Logperch	Field test – Power station intake (White Rapids Hydroelectric plant, Michigan, US) Depth: 4.40 m; Flow: 15 – 27 cm s <sup>-1</sup> Air flow 18,000 L min <sup>-1</sup> (738 L min <sup>-1</sup> m <sup>-1</sup> of barrier) at pressure of 0.71 kg/cm <sup>2</sup>  Deterrent device mounted on trash racks Galvanised tubing (1.9 cm diam.) with 15 mm holes, at 38 cm intervals  Strobe light signal -7.3 Hz, 24 strobe lights	Ineffective	Michaud & Taft, 2000

Bullhead *	Field test – Power station intake (Four Mile Hydroelectric project, Michigan, US) 3 parallel air lines, 15 cm apart Custom strobe light system	82 %	McCauley <i>et al.</i> , 1996
Shiner **		94 %	
Other species		81 % – ineffective during the day	
Salmon smolts	Field test – Water treatment intake (Walton water treatment works, River Thames, UK) Depth: 2.00 m 6 x 4 m PVC tubing (50 mm diam.) with 2 mm holes, at 25 mm intervals  Strobe light signal: 7.3 Hz	62.5 %	Solomon, 1992
Alewife **	Field test – Power station intake (Pickering Nuclear Power Station, Canada) Depth: 6.00 m Air flow: 60 L min <sup>-1</sup> m <sup>-1</sup> of barrier Polyester fibre hose (5.7 cm diam.) around interior polyethylene tubing (0.95 cm diam.), with 15 mm holes, at 7.6 cm intervals  Bubble size: 0.16 cm diameter Strobe light signal: 750 cd, 3.3 Hz, 100 µs duration	67.1 %	Ontario Hydro & LMS, 1989† / Patrick <i>et al.</i> , 1988
Blueback herring **	Field test – Power station intake (Roseton generating station, Hudson river, New York, US) Depth: 2.00 m – 6.00 m Air flow: 66 L min <sup>-1</sup> m <sup>-1</sup> Polyester fibre hose (5.7 cm diam.) around interior polyethylene tubing (0.95 cm diam.), with 15 mm holes, at 7.6 cm intervals  Bubble size: 0.16 cm diameter Strobe light signal: 4500 cd, 3.3 Hz, 100 µs duration  Treatments:  a) Day b) Dusk	46.9 %	Matousek <i>et al.</i> , 1988 ***
White perch		0.9 %	
Bay anchovy **		-77.8 %	
Alewife **		-2.4 %	
American shad **		31.4 %	
		Overall: 36 %	

	<ul style="list-style-type: none"> <li>c) Night</li> <li>d) Dawn</li> </ul>				
	Euryhaline conditions				
Sockeye salmon smolts	Field test – Power station intake (Seton hydro-electric station, British Colombia, Canada)	11%		McKinley & Patrick, 1988 †	
Atlantic menhaden **	Laboratory study	a) 36 %	b) 28 %	c) 40 %	McIninch & Hocutt, 1987
Spot **	Depth: 0.46 m; Flow: 20 cm s <sup>-1</sup>	a) 63 %	b) 69 %	c) 74 %	
White perch	Treatments:	a) 67 %	b) 59 %	c) N/A	
	<ul style="list-style-type: none"> <li>a) Clear;</li> <li>b) Low turbidity;</li> <li>c) High turbidity;</li> </ul>				
	Strobe light signal: 1 watt, 5 Hz, 80 μs duration				
White perch	Behavioural tank	a) 7 – 58 %	b) 3 – 6 %		Sager <i>et al.</i> , 1987
Spot **	Depth: 1.00 m; Flow: a) 20 cm s <sup>-1</sup> b) 50 cm s <sup>-1</sup>	a) 21 – 85 %	b) 24 – 46 %		
Atlantic menhaden **	Strobe light treatments:	a) 9 – 81 %	b) 9 – 51 %		
	<ul style="list-style-type: none"> <li>i) 0 Hz</li> <li>ii) 2 Hz</li> <li>iii) 5 Hz</li> <li>iv) 10 Hz</li> </ul>				
	Acclimated in darkness or light				
Alewife **	Behavioural tank	90 – 98 %			Patrick <i>et al.</i> , 1985
Gizzard shad **	<i>Freshwater species –</i>				
Rainbow smelt					
White perch	Depth: 1 m; Flow: 15 - 32 cm s <sup>-1</sup>				
Spot croaker **	Porous plastic tubing (1 cm diam.), with intervals of 0, 5,				
Atlantic menhaden **	10, 20 cm, placed 0.6 m in from of strobe light source				

Strobe light signal: 1 watt, 5 Hz, 80  $\mu$ s duration, 400 - 700 nm

*Marine species -*

Depth: 1 m; Flow: i) 20 and ii) 50  $\text{cm s}^{-1}$   
 Porous plastic tubing (1 cm diam.), with intervals of 0, 5, 10, 20 cm, placed 1.2 m in from of strobe light source

---

Bubbles / Sound / Strobe Lights	Sea Lamprey	Experimental raceway Two-choice experiment Depth: 0.50 m; Flow: 12 $\text{cm s}^{-1}$ Air pressure: 172 kPa Fine bubbles, perforations proprietary	No significant effect	Miehls <i>et al.</i> , 2017
		SPA-BAFF, 30° to parallel with the main channel Sound signal: 20-3000 Hz at 150 dB (re 1 $\mu$ Pa) Strobe light signal: 6 Hz		
	Juvenile Chinook Salmon	Field test: River (Sacramento – San Joaquin River Delta, California, US) Flow: 25 $\text{cm s}^{-1}$ Air flow: 120 $\text{L min}^{-1} \text{m}^{-1}$ of barrier	a) 92.3 % b) 77.7 %  Effectiveness declined with increasing river discharge	Perry <i>et al.</i> , 2014
		SPA-BAFF Sound signal: 5 – 600 Hz at 146 – 159 dB (re 1 $\mu$ Pa) Strobe light signal: 847.44 lx, 3 Hz		
		Treatments:  a) BAFF on b) BAFF off		
	Walleye	Hatchery pond Depth : 0.84 m; Flow: 4.2 $\text{m}^3 \text{s}^{-1}$ SPA-BAFF Air flow: 300 $\text{L min}^{-1}$ at 2.5 $\text{kg cm}^{-2}$ (164 $\text{L min}^{-1} \text{m}^{-1}$ of barrier)	Ineffective  Escapement rate up to 100% when light was on	Flammang <i>et al.</i> , 2014



Sound signal: 0 – 2000 Hz at four proprietary frequency ranges:

- a) Off;
- b) Low;
- c) Med;
- d) High;

Strobe light signal: 650 lumens at four treatments:

- i. Off
- ii. 8 Hz
- iii. 16 Hz

Silver / Bighead carp **	Field test – River (Quiver creek, Illinois, US) SPA-BAFF	< 1% recapture rate	Ruebush <i>et al.</i> , 2012
Non-carp species	Sound signal: 500 - 2000 Hz Strobe light signal: Two treatments:  a) Flashing intermittently; b) Constantly on;	< 3% recapture rate	
Riverine species	Field test – Power station intake (Kingsford Hydroelectric Project, Wisconsin; White Rapids Hydroelectric Project, Michigan, US)	Ineffective	Winchell <i>et al.</i> , 1997 †

---

This was confirmed by Leighton and Walton [1987], for bubbles in the size range of 0.1 – 1.0 mm. It was noted that **Eq 1.1**. ignores surface tension, and for smaller bubbles this becomes important in adding Laplace pressure terms to the pressure shown, such that a fuller description of the resonance frequency of a bubble driven to oscillation by a sound field,  $\omega_{res}$ , is:

$$\text{Eq 1.2} \quad \omega_{res} = \frac{1}{R_0 \sqrt{P_0}} \sqrt{3K \left( P_0 - P_v + \frac{2\sigma}{R_0} \right) - \frac{2\sigma}{R_0} + P_v - \frac{4\eta^2}{\rho R_0^2}}$$

Where  $P_0$  is the static pressure in the liquid outside the bubble,  $\eta$  and  $\rho$  are, respectively, the shear viscosity and density of the liquid (which is assumed to be incompressible),  $P_v$  is the vapour pressure,  $\sigma$  is the surface tension, and  $K$  is the polytropic index. [Leighton, 2004]. The Laplace pressure is the excess gas pressure in the bubble required to balance the tendency of surface tension to decrease the surface area of the bubble. The surface tension is defined as the energy required to create a unit area of new surface; and equivalently as the force per unit length in a surface perpendicular to that surface.

If one considers a bubble of radius  $R$ , there is an internal pressure,  $P_i$  within the bubble as a result of the pressure of the gas ( $P_g$ ), and the vapour pressure of the liquid ( $P_v$ ) so that:

$$\text{Eq 1.3} \quad P_i = P_g + P_v$$

The pressure within a bubble at rest is greater than the pressure in the liquid immediately outside the bubble as a result of surface tension forces. If the pressure in the liquid outside the bubble at the bubble wall is  $P_l$ , that within the bubble is:

$$\text{Eq 1.4} \quad P_i = P_l + P_\sigma$$

Where  $P_\sigma$  is the excess pressure. If an imaginary cut is made which divides the bubble in half, the excess pressure would tend to push the two halves of the bubble away from each other. The force which balances the excess pressure and so keeps the bubble intact

is the surface tension. The energy associated with a surface in a liquid is given by the product of the surface tension with the surface area, hence  $2\pi R\sigma$ . The force which balances this is  $2\pi R^2 P_\sigma$ , that is the excess pressure multiplied by the effective area as seen in the direction of the “push”,  $\pi R^2$ . One can show this more rigorously by imagining annuli along the surface of the bubble, and integrating the force on these. The radius of one such annulus would be  $2\pi R \sin\theta$ , and the force on such an annulus (the x-component) would be:

$$\text{Eq 1.5} \quad dF_x = (2\pi R \sin\theta)(P_\sigma \cos\theta)(R d\theta)$$

Integrating this from  $\theta = 0$  to  $\theta = \pi/2$  gives the required net force of  $\pi R^2 P_\sigma$ . Equating this to the surface tension force gives:

$$\text{Eq 1.6} \quad P_\sigma = \frac{2\sigma}{R}$$

This is the excess pressure inside a bubble which results from the surface tension, also known as the Laplace pressure. The Laplace pressure equals 1 Bar at a bubble radius of 1.5  $\mu\text{m}$ . Since the bubbles in this thesis ranged from just over  $10^1$  to  $10^4$   $\mu\text{m}$ , the effect of the Laplace pressure can be ignored.

The gas pressure in the bubble depends on its volume, not shape, and since changes in that pressure are what radiate acoustic waves, it is through bubble volume, not shape, that bubbles interact with sound field (unless the frequency is so much greater than resonance that the wavelength becomes comparable with the bubble radius [Phelps & Leighton, 1996], a regime that will not be used in this thesis). Therefore, in the seminal study of Leighton and Walton [1987], although photography of these bubbles showed distortions in the shape of the bubble due to buoyancy forces and shape oscillations, nevertheless equation 1.1 was experimentally validated, and used to count and size, for the first time, bubble entrainment in the natural world.

Following this, acoustic emissions from bubbles were categorised into a total of five groups by Medwin and Beaky [1989]: type A1, A2, B, C and D, each with their own specific emission type. A sixth emission type was identified which results from contact between bubbles [Leighton *et al.*, 1991], where sound is produced due to the rapid increase in bubble volume caused by the collapse of the neck of air joining the two

bubbles [Czerski, 2011]. While release of a single bubble at a nozzle (see **Fig. 1.1**) results in it oscillating between having the longer axis to the vertical (called here "needle shape" after the extreme form this shape would take) and the horizontal (called "pancake shape" after its extreme), increasing the air flow results in the formation of more complex bubbles [Leighton *et al.*, 1991].

Leighton et al [1991] identified that if a bubble, newly-released from a nozzle, does not move quickly enough away from the nozzle, it can coalesce with its successor bubble growing at the nozzle. This tends to happen if the nozzle creates small bubbles (which rise more slowly away from it than would larger bubbles), and also if the flow rate increases (causing the successor bubble to grow more quickly). They photographed how, under conditions of increased flow, a bubble detaching from the nozzle is contacted by its successor, still growing at the nozzle (see **Fig. 1.2**). This contact causes further shape oscillation in the initial bubble. The two merge, and the successor detaches from the nozzle. Both merging and detachment causes further shape oscillations which have the appearance of ripples on the surface of the bubble. The volume of the main bubble increases with each contact, which reduces the frequency of the sound. Increasing the flow further, increases the rate of growth of successor bubbles - more successors can be absorbed leading to a greater number of excitations by contact, and a larger final volume.

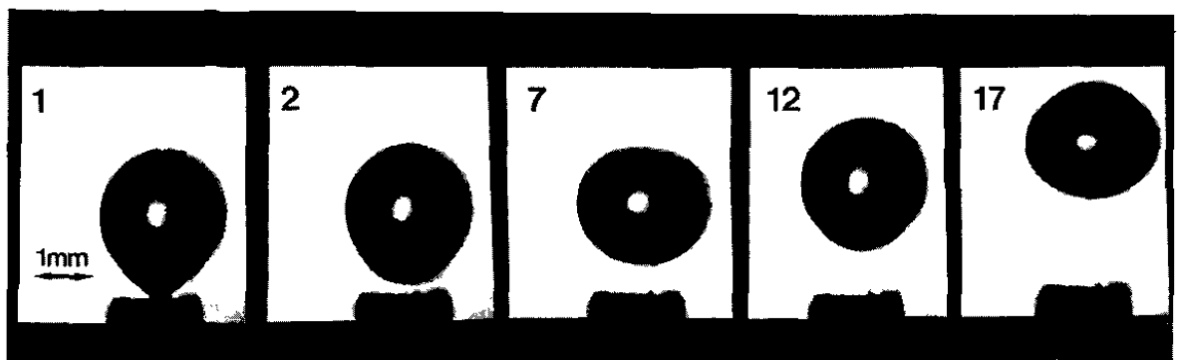


**Fig. 1.1:** Selected frames from a high-speed photographic sequence, showing a single bubble released from a metal nozzle (frame 1), depicting the "needle shape" (frames 2 and 12), and "pancake shape" (frames 7 and 17) [from Leighton *et al.*, 1991].

Further increases in air flow (**Fig. 1.3**) eventually lead to successors coalescing without detachment from the nozzle and the formation of intermediate bubbles. Eventually, fragmentation can be seen which contributes to high-frequency acoustic emissions. At the highest injectable flow rates obtained by Leighton *et al.*, [1991] the acoustic signal obtained was complex, indicating a system with little uniformity in the size of the bubbles produced.

Whilst the bubbles in natural brooks and waterfalls measured by Leighton and Walton [1987] produced clearly distinct acoustic ‘signatures’ from each bubble formation event (exponentially decaying sinusoids at the bubble natural frequency), as entrainment rates increase these signatures can overlap, making counting more difficult. Leighton *et al.*, [1997] explain a method by which a rising bubble population can be characterised using passive techniques despite the phenomenon of bubble coalescence. When bubble entrainment rates are high, bubble signatures overlap due to multiple excitations of the original bubble. However, if one performs a special type of Fourier transform (a Gabor transform), then plots a time-frequency representation of the coefficients, the frequency at which the final peak occurs is the one which relates to the size of the final bubble after it escapes contact with the nozzle.

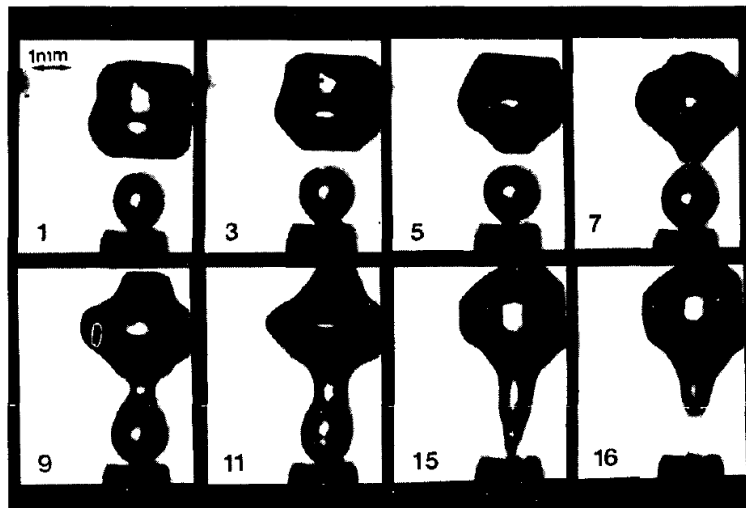


**Fig. 1.2:** Frames showing a bubble being released from a metal nozzle, excited by contact with and absorption of successor bubbles (Flow rate: 0.2 ml/s) [from Leighton *et al.*, 1991].

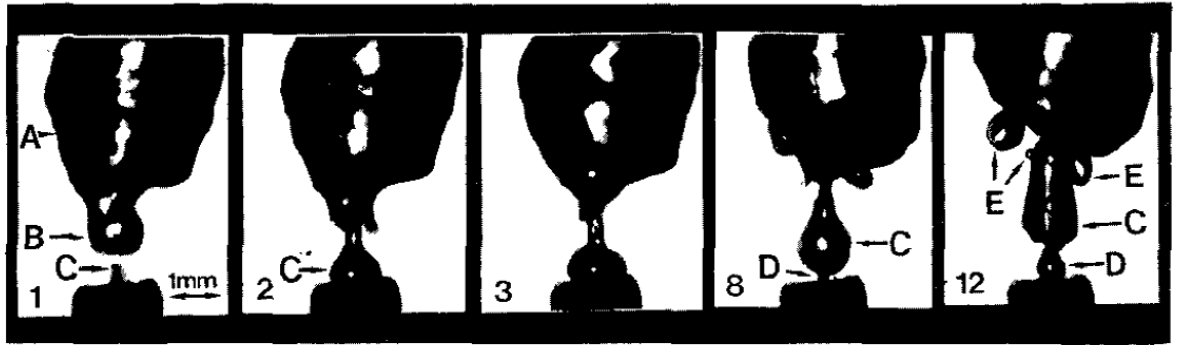


**Fig. 1.3** - Frames showing a characteristic multiple-bubble complex showing A: superior, B: intermediate, C: successor, D: replacement of successor, E: fragmentation. (Flow rate: 15 ml/s) [from Leighton *et al.*, 1991].

It is commonly thought that reducing the diameter of the hole used to introduce a bubble into a medium will generate smaller bubbles, but as explained above smaller bubbles will coalesce with successor bubbles so that the bubble which eventually travels into the liquid is large [Leighton *et al.*, 1991]. Leighton *et al.* [2012] describe of a set-up used to demonstrate to the general public the sound absorption in water due to bubbles, where bubbles are introduced into a water-filled pipe by a standard bone marrow biopsy needle. By attaching an inexpensive vibrating motor from a mobile phone using epoxy, coalescence can be prevented by vibrating the injection nozzle. A needle that would normally generate bubbles that are ineffective at absorbing sound would, when vibrated in this way, produce a cloud of much smaller bubbles because they did not coalesce at the nozzle. Being closer to resonance with the acoustic field, the generation of these smaller bubbles vastly increased acoustic absorption, even though the gas flow rate into the needle had not changed. A demonstration video in the electronic supplement to the paper demonstrated this effect.

Longuet-Higgins *et al.*, [1991] studied bubble formation at a nozzle in conditions where the gas flow through the nozzle was so slow as to produce bubbles in a very predictable way, without coalescence. This allowed for predictability, but the rate of generation of bubbles would be far too slow to produce a meaningful bubble curtain, or indeed for many practical applications. They showed that for a given nozzle size, assuming detachment occurs at the bubble "neck", there is a bubble of maximum volume and therefore a given acoustic frequency. The frequency, and hence the bubble size, depends on two factors. Firstly, the rate of air flow to the bubble: for slow rates of

flow the frequency is very close to the theoretical frequency. Secondly, whether the set-up used to generate the bubbles is in either a pressure-controlled or volume-controlled mode. This depends on the volume of air between the nozzle and the flow control valve. If the volume of air is large compared to the bubble volume, then the bubble released is said to be “*pressure-controlled*”. If small, then the release was “*volume-controlled*”.

However, such slow bubble generation would be impractical for the bubble screens generated here, which will use the vibrating needle method of Leighton *et al.* [2012] to generate a repeatable large number of bubbles at a predictable size that can be made close to the acoustic resonance. This is in order to absorb the sound, the theory for which is covered in the next section.

### **1.5 Absorption by Bubble Clouds**

Sound absorption by manmade bubble clouds dates back to the use of bubble curtains in the middle of the 20<sup>th</sup> century to hide the sound of submarines in Pearl Harbor [Loye & Arndt, 1948]. In 2004 Leighton proposed that cetaceans might have been using the acoustical properties of bubble nets for far longer, in order to catch fish. This proposal was refined over the years [Leighton, 2004; Leighton *et al.*, 2007, 2014; Qing *et al.*, 2019], showing how the net shape (circular or spiral) could be used to employ different phenomenon (absorption, refraction, reflection) to herd fish into a feeding zone with considerable sophistication.

It had been known for many decades that humpback whales form such bubble nets, but the use of acoustics in them had not previously been suggested. With the enhanced abilities in tagging whales in recent years, we now know that bubble-netting humpback whales employ a unique and complex foraging behaviour that involves swimming in either an upward spiral or a double loop [Wiley *et al.*, 2011] while expelling air underwater to form a vertical spiral of bubbles around prey [Leighton *et al.*, 2007]. When the whales form such nets, they emit very loud calls, containing energy up to at least 4 kHz [Leighton *et al.*, 2004] forming an insonified bubble net [Leighton *et al.*, 2004]. Prey attempting to leave enter a region where the sound is subjectively loud, are therefore startled and school [Leighton *et al.*, 2007].

Sound is trapped in these nets by refraction, since the presence of bubbles reduces the sound speed which happens when the bubbles controlling the sound speed are driven at frequencies lower than their resonance frequency [Leighton *et al.*, 2004, Leighton, 1998]. Huygen's principle can be used to explain how this occurs. The position of a wavefront (which is locally normal to the sound rays) can be determined from the envelope of small "Huygen's wavelets" which in turn can be thought of as propagating out from the position of the wavefront. In a cloud of bubbles the sound speed of the wavelets is smaller the closer one gets to the centre of the bubble cloud. This means the wavefront changes direction since one end is travelling faster than the other. The rays are therefore refracted back into the cloud (**Fig. 1. 4**). Whilst whales, in Leighton's hypoethisis, could use a combination of reflection, refraction and absorption, to make nets for fish, human use of bubble curtains has tended to focus on absorption and some reflection.

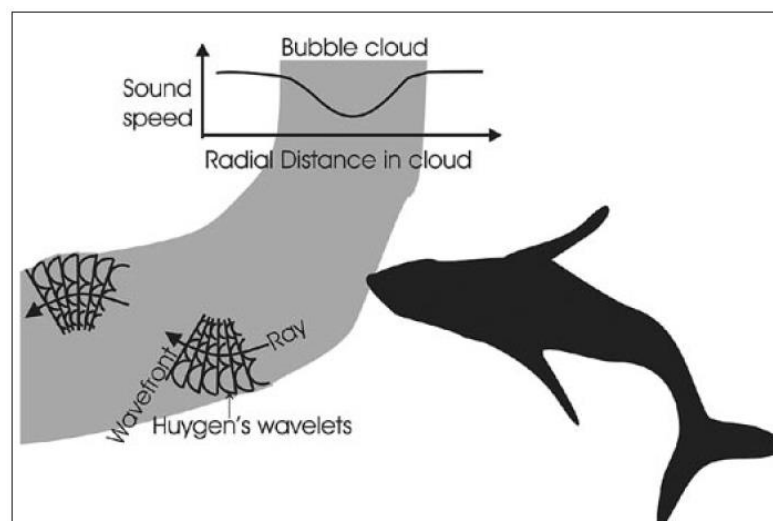


**Fig. 1.4** – Schematic of a whale insonifying a bubble-net. According to Hugen's principle, the position of a wavefront (locally normal to the rays) can be found from the envelope of small Huygens wavelets propagating out from the original position of the wavefront. [Leighton *et al.*, 2004]

Recent work by Bohne *et al.*, [2020] focused on modelling the acoustic transmission loss of bubble curtains used for mitigating noise pollution caused by underwater pile driving. A model of the bubble formation process was developed, allowing for prediction of the acoustic properties of a bubble curtain for different nozzle



hose configurations at different depths. This was validated by determining the transmission loss for a bubble curtain in a freshwater lake for two different nozzle configurations and comparing with measurements. [Bohne *et al.*, 2020]

The seminal work for the theory to predict the absorption of sound by bubbles in water was produced by Commander and Prosperetti [1989] (with a typographical error corrected by Baik, personal communication). In this thesis, equations (37) to (39) and (42) to (44) from Ainslie and Leighton [2011], were used to calculate attenuation of sound by a population of bubbles of different size distributions. The details of this method will be explained further in **Chapter 5**, with derivations for the equations used in **Appendices D** and **E**.

## **1.6 The Mechanics of Hearing in Fish**

The fact that fish can respond to sound has been recognised for a long time, indeed the earliest recorded discussion on the hearing abilities of fish was made by Pliny the Elder more than 2,000 years ago. Although Weber [1820] carried out the first anatomical description of fish ears, and Retzius [1881] published a comparative perspective on fish ears, it was Parker [1902, 1903] and others [von Frisch & Stetter, 1932; von Frisch, 1936; Dijkgraaf, 1960] who systematically demonstrated sound detection in fish. Hearing has been studied in a number of fish and has been reviewed extensively [e.g., Fay, 1988; Popper & Fay, 1993; Fay & Popper, 1999; Popper *et al.*, 2003; Ladich & Popper, 2004; Webb *et al.*, 2008].

It is likely that hearing in fish evolved to make use of environmental soundscapes, an important source of information [Fay, 2008]. Selective pressures which may have led to the evolution of hearing in fish include detection of distant predators and prey, detection of objects in the environment, the location of coral reefs [Fay, 2008]: an environment collectively known as the “auditory scene” [Bregman, 1990]. There is currently no clear link between the taxonomic position of a given species and hearing capabilities, and it is not yet possible to correlate such capabilities to ecological niches [Ladich & Popper, 2004].

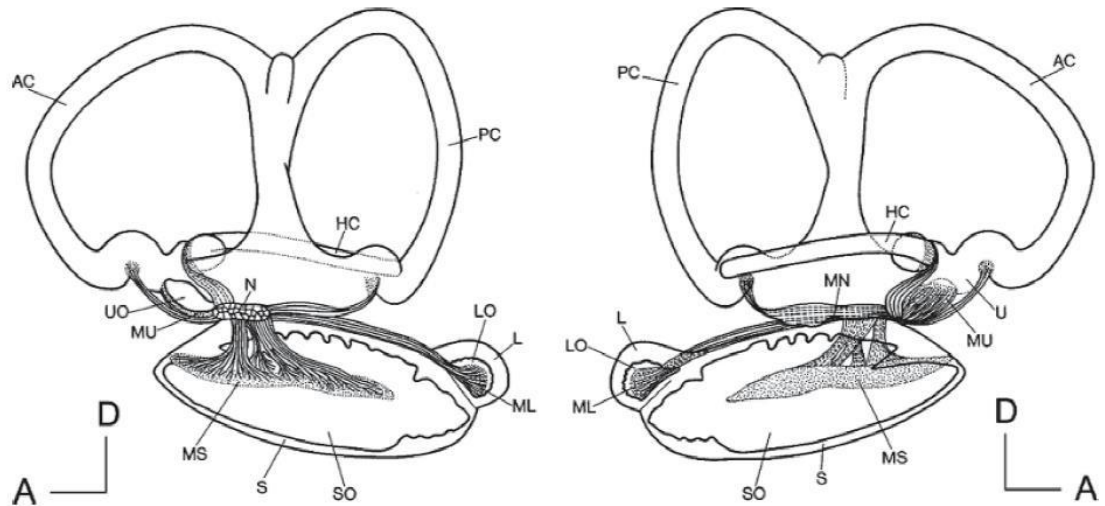


**Fig. 1.5:** Inner ear of a perch [from Ladich & Popper, 2004]. Medial view on the left and lateral view on the right. **AC, HC, PC** - anterior, horizontal, and posterior semicircular canals; **L** - lagena; **LO** - lagena otolith; **MN** - macula (papilla) neglecta; **MU** - utricular epithelium; **MS** - saccular epithelium; **N** - eighth cranial nerve; **S** - saccule; **SO** - saccular otolith; **UO** - utricular otolith.

Fish have been found to use soundscapes to orient themselves [Simpson *et al.*, 2005; Montgomery *et al.*, 2006], can distinguish between two sound sources at different distances [Schuijf & Hawkins, 1983], and certain species such as ballan wrasse (*Labris bergylta*) [Schuijf *et al.*, 1972], cod (*Gadus morhua*) [Chapman & Johnstone, 1974; Schuijf & Buwalda, 1975], goldfish (*Carassius auratus*) [Fay *et al.*, 2002], oyster toadfish (*Opsonus tau*) [Fay & Edds-Walton, 1997], and plainfin midshipman (*Porichthys notatus*) [Weeg *et al.*, 2002] are fully capable of distinguishing between two simultaneous but different sounds when processing the signals. It has been shown that Common carp (*Cyprinus carpio*) have the ability to discriminate blues recordings from classical music [Chase, 2002].

There is a large degree of interspecific variation in hearing capabilities among fish; ranging from the alosinae (a clupeid subfamily) that can detect sounds well into the ultrasonic range [Kynard & O'Leary, 1990; Mann *et al.*, 2001] to species able to detect infrasound [Sand & Karlsen 1986; Sand & Karlsen 2000; Sand *et al.*, 2000; Popper *et al.*, 2003]. Despite the huge variation (a detailed description of fish ears was written by Popper *et al.*, [2003]), fish share the same basic structures for detecting sound. The

inner ear (see **Fig. 1.5**) of sharks and bony fish consists of three semicircular canals, three pairs of otolith organs (the saccule, lagena, and utricle) which house calcareous structures known as otoliths, and in some species, a relatively diminutive macula neglecta. The sizes and shapes of otoliths vary considerably although there is currently a lack of understanding of the functional basis of the striking differences found in otoliths [Popper & Fay, 2011]. The sensory hair cells function as transducers. Each sensory hair cell has a typical cell body as well as an apically located ciliary bundle made up of one kinocilium and many stereocilia. Bending of the ciliary bundle results in a cascade of intracellular events that leads to the release of a neurotransmitter and the stimulation of the innervating eighth cranial nerve [Hudspeth 1985].

Each otolithic organ contains an epithelium composed of sensory and non-sensory hair cells. The sensory cells number in the thousands to hundreds of thousands depending on the species and the size of the fish, as the number of sensory cells increases as the fish ages [Corwin, 1981; Lombarte & Popper 1994]. The sensory epithelium lies close the otolith and they are separated by a thin otolithic membrane that mechanically couples them together [Popper *et al.*, 2003]. Hair cell stimulation results from the relative motion between the sensory epithelium and the otolith due to their different densities (see **Fig. 1.6**), and therefore otolith function in fish can be compared to that of an accelerometer.

The hair cells are organised into groups with different orientation patterns [Popper & Fay, 2011], based on the position of the kinocilium. All ciliary bundles in each region on the epithelium are in turn oriented with the kinocilium (see **Fig. 1.7**). Bending of the bundle results in responses proportional to the vector component in the axis of best physiological sensitivity [Popper, 1977; Hudspeth 1985; Lu & Popper 2001] and therefore sensory cells are potentially capable of computing the axis of particle motion of a sound source and provide information about its direction [Popper *et al.*, 2003; Rogers & Zeddies, 2008]. An increase in the number of hair cell orientation groups is closely correlated with greater hearing bandwidth and sensitivity when compared to fish that have the “standard” pattern [Popper & Fay, 2011]. However, whether the differences between species indicate different hearing capabilities or are different strategies to solve the same acoustic processing problems is unknown [Popper & Fay, 2011].

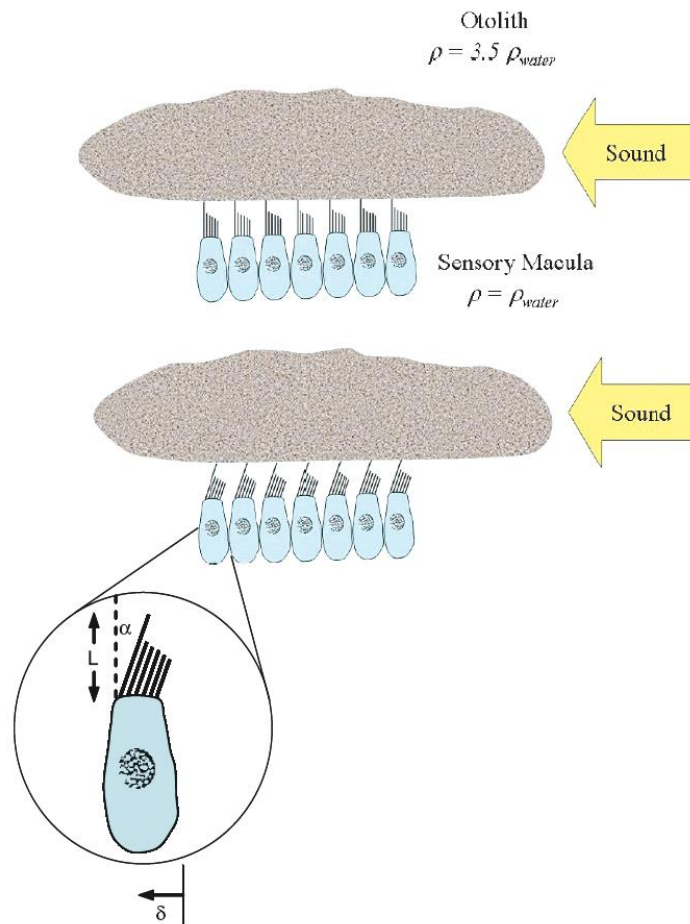


**Fig. 1.6:** The otolithic hearing mechanism. The dense otolith lags behind the sensory epithelium, which tends to move with the fluid. The cell output is proportional to the pivot angle:  $\alpha = \delta / L$ . The sensor is a dipole [from Rogers & Zeddies, 2008].

The disadvantage to using an accelerometer-like ear for hearing is that hearing sensitivity is limited to detection of particle motion [Popper & Fay, 2011]. Due to the high compressibility of gas compared with water, the existence of a swimbladder in teleosts provides an auditory advantage since the otoliths can be stimulated indirectly when sound pressure fluctuations are transformed into particle oscillations, increasing the hearing range of the fish. Approximately 7,800 species of fish, which include goldfish, catfish and carp, collectively referred to as otophysians, have a series of bones called Weberian ossicles which mechanically connect the swim bladder to the inner ear [Webb *et al.*, 2008]. The functions of the swim bladder in sound production and as an

accessory hearing organ are usually secondary to its function as a hydrostatic organ controlling buoyancy [Popper & Fay, 2011].

The now-common categorisation of fish under the strict dichotomy of "hearing specialists" or "hearing generalists" began with Dijkgraaf [1960], taking further hold following various other publications [Popper & Fay, 1973; Fay & Popper, 1974, 1975]. This designation has recently been called into question [Popper *et al.*, 2003] since it is overly simplistic. It is therefore more likely that there is a range of hearing capabilities across fish species that is more like a continuum, based on the contributions of acoustic pressure to the overall hearing capabilities of a given species [Popper *et al.*, 2003]. At one end of the continuum are species which have the most ancestral mode of hearing, which involves sensitivity to particle motion via direct inertial stimulation of the otoliths. This group includes elasmobranchs and jawless fish and other species such as gobies, flatfish and tuna [Popper *et al.*, 2003]. At the other end of the scale are a group of fish known as otophysians (e.g. squirrelfish, goldfish, cyprinids and herring), which have a connection composed of four pairs of bones known as Weberian ossicles between the inner ear and the swimbladder [Fay *et al.*, 2002; Popper *et al.*, 2003]. This connection allows the swimbladder to act as an acoustic pressure transducer, allowing a fish to detect the pressure component of a sound wave.

Between these two extremes are species that have swim bladders but lack known specialisations linking the swim bladder and the ears in which there is uncertainty regarding their pressure and particle motion sensitivity. In at least one case, an unspecialised species of fish has been shown to respond to sound pressure over the higher-frequency portion of their hearing range (in damselfish, *Pomacentridae* - Myrberg & Spires [1980]), while Tavalga & Wodinsky [1963] noted that some species may actually "switch" between detecting pressure and particle motion.

Whether a given species is most likely to respond to pressure, particle motion, or both is an important question with regard to assessing both the effects of anthropogenic noise, and developing suitable guidance systems for that species [Popper & Schilt, 2008]. The assumption that all fish with a swim bladder respond to acoustic pressure or that all hearing generalists respond only to particle motion, may not be useful. Despite the knowledge that fish hear particle motion [e.g. Cahn *et al.*, 1969], and bearing in mind that underwater sound waves have both a pressure and a particle-motion

component, few studies of underwater acoustic ecology have measured the particle-motion component of sound [Popper & Fay, 2011, Nedelec *et al.*, 2016]. Whereas the studies that examine sound pressure numbers in the thousands, field studies that measure particle motion are limited [Chapman & Hawkins 1973; Nedelec *et al.*, 2014, 2015], as are studies that provide insight on the relation between pressure and particle motion reception in different species [Chapman & Hawkins, 1973; Hawkins & Johnstone, 1978; Jerko *et al.*, 1989; Myrberg & Spires, 1980].

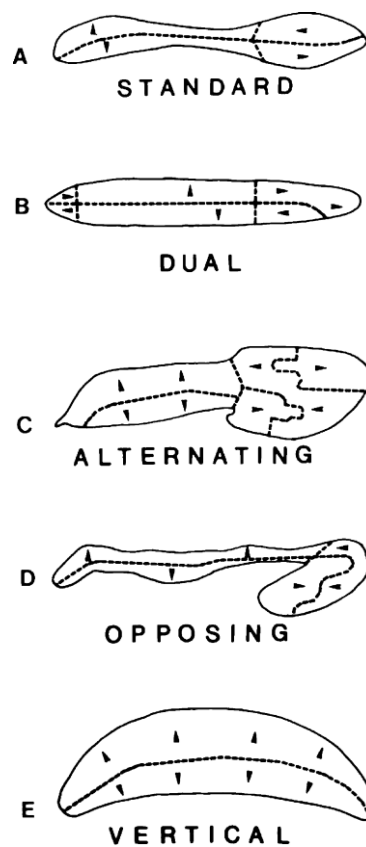


**Fig. 1.7:** Saccular hair cell orientation patterns from different fish. Anterior is to the right and dorsal to the left. The dotted lines are the areas of what is generally an abrupt transition in orientation between directions. Arrowheads indicate the direction of the kinocilia on the hair cells in each region of the epithelium. The “Standard” pattern is typically found in fish that are hearing generalists. Other patterns are most often found in hearing specialists. The same basic pattern can be found in taxonomically diverse fish [from Popper & Schilt, 2008].

In view of the highly specific responses of fish to the various components of underwater sound, it has been proposed that sound levels for detection thresholds, noise,

etc, be reported in terms that are meaningful for that species – i.e. either acoustic pressure, particle velocity, or both [Popper & Carlson, 2008; Hawkins 2015; Hawkins & Popper 2016; Popper & Hawkins 2018]. There is limited value in reporting the sensitivity data in acoustic pressure without translating these values to the component of the sound field that stimulates the fish’s sensory system [Kalmijn 1988; Rogers & Cox 1988]. For instance, it would be of more value to report the sensitivity of a salmonid in terms of particle velocity.

### **1.7 Directionality in Fish Hearing**

As explained in Section 1.5, all three otolith organs of fish (sacculle, lagena, and utricle) have different orientations in most fish species, and within each organ, hair cells are oriented along various axes [Popper, 1977]. It was assumed that the pattern of neural activity across hair cell arrays could encode the axis of acoustic particle motion, giving rise to directional hearing. This concept was called “vector detection” [Schuijf & Buwalda, 1975], and immediately gave rise to a new question; while the particle motion axis could be determined by arrays of hair cells, vector detection cannot determine which end of the axis points toward the source because this vector alternately points toward and away from the direction of the source. In addition, because the body of a fish is roughly the same density as that of the surrounding liquid, and because of the greater speed of sound in water, differences in arrival time between each ear are minimised and therefore unlike on land, inter-aural cues cannot be used for localisation [Rogers & Zeddis, 2008]. This became known as the “180 ° ambiguity problem” [Fay, 2011].

The question of whether fish are capable of directional hearing was first tackled in a series of experiments by Schuijf and colleagues in the 1970s and 1980s who demonstrated direction-dependent masking effects of noise [Chapman & Hawkins, 1973; Chapman & Johnstone, 1974] and that fish could distinguish sound sources with minimum audible angles of 15 ° – 20 ° in azimuth and elevation [Schuijf, 1975; Hawkins & Sand, 1977]. Schuijf & Buwalda [1975] opined that determining the phase angle between acoustic particle motion and sound pressure could resolve the 180 ° ambiguity. In simple terms, they proposed that if a sound propagates from a source to the right of a fish, then leftward particle accelerations would coincide with rising

pressure. This approach became known as the “phase model” and was evaluated experimentally by conditioning cod (a pressure sensitive fish) to discriminate between sound sources directly in front and behind [Schuijf & Buwalda, 1975] and is the best evidence supporting this model for sound source localisation [Braun & Grande, 2008; Fay, 2011].

Resolving the axis of acoustic particle motion does not automatically lead to knowledge of source location. The vector of particle motion only points toward the source for monopole sources, or specific regions of the field surrounding a dipole or higher order source [Kalmijn, 1989]. This means that a fish would need to have knowledge of the nature of the source, and sample it from multiple positions to determine its location [Kalmijn, 1989]. While behavioural data shows that fish can use their hearing for spatial analysis to a degree [e.g. Schuijf & Buwalda, 1975; Hawkins & Sand, 1977], it is still not entirely clear whether fish can directly locate a source.

In the acoustic far field of a sound source, the acoustic pressure and particle velocity decline at the same rate with distance. Closer to the source, however, in the hydrodynamic nearfield (see **Section 1.9** for further details), the magnitude of particle velocity is greater and declines more rapidly [Kalmijn 1988]. This means that the ratio of sound pressure to particle velocity increases at a constant rate with distance from the source, independent of source intensity. By comparing pressure and particle motion, fish could compute this ratio to determine source distance independently of intensity [Schuijf & Hawkins, 1983]

Current models of directional hearing in fish to resolve the 180 ° ambiguity include the “phase model”; an “orbital model” [de Munck & Schellart, 1987] where sound pressure and particle motion cause the otoliths to rotate either clockwise or anticlockwise depending on source location; a “computational model” [Rogers *et al.*, 1988]; and an “algorithmic model” [Kalmijn, 1997] where a fish can make their way to a sound source by swimming in a direction that maintains a constant angle between the fish and the axis of particle motion. Each of these models has their disadvantages; the “phase model” requires either pressure sensitivity from a gas-filled chamber (or swimbladder) or that the fish remain near surfaces and objects. Kalmijn [1997] also criticised this approach in that it assumed that sound source localisation in fish is similar to that of humans. Like the "phase" model, the “orbital” model also requires pressure



detection and only works for sinusoidal signals. Finally, the approach proposed by Kalmijn is limited to locating sources that broadcast throughout the duration of approach [Rogers & Zeddies, 2008].

A more recent mechanism, “the quadropole model”, by which fish could determine the direction to a sound source was proposed by Rogers & Zeddies [2008], although this still needs experimental testing [Fay, 2011]. Since fish ears are small compared to the wavelengths of sounds they are required to detect, they can be described in terms of "multipoles". Hair cells with an overlying otolith function as dipole sensors. Fish that possess a gas-filled chamber combine a dipole sensor with a monopole sensor to form what is known as a cardioid sensor. In fish without a swimbladder, hair cells that do not have an overlying otolith function as quadropole sensors. These are combined with a dipole sensor to form a dipole-quadropole cardioid. A dipole-quadropole cardioid is more directive than a monopole-dipole, and in the presence of omnidirectional ambient noise, or in situations where acceleration noise dominates, this can improve signal / noise ratios [Rogers & Zeddies, 2008].

The ability of fish to use particle motion vectors to swim towards a source of sound (known as the “algorithmic approach”) was demonstrated by Zeddies *et al.*, [2010, 2012]. Gravid plainfin midshipman (*Porichthys notatus*) females show phonotaxis toward an underwater loudspeaker broadcasting a male advertisement call (a signal with a fundamental frequency of about 90 Hz), or a low-frequency tone near the fundamental frequency of the male’s advertisement call [McKibben & Bass, 1998]. It was found that 73% of gravid females directed toward the sound source upon initial release and the subsequently followed straight to slightly curved pathways directed toward the source, in line with the local particle motion vectors (see **Fig. 1.8**) [Zeddies *et al.*, 2010].

A second, almost identical experiment using a dipole sound source showed that when released along the dipole axis, fish took straight paths to the source however, when released approximately 90 ° to the source’s axis, they took highly curved paths to the source that were in line with the local particle motion axes, which indicate that the acoustic cues used by fish during sound-source localisation include the axes of particle motion of the local sound field. [Zeddies *et al.*, 2010, 2012]. This finding seems to indicate that at least for certain species, there is evidence that fish are using the vectors

of particle motion to locate a source by moving towards it, although there is no conclusive evidence that fish can identify the source of an intermittent sound at a distance.

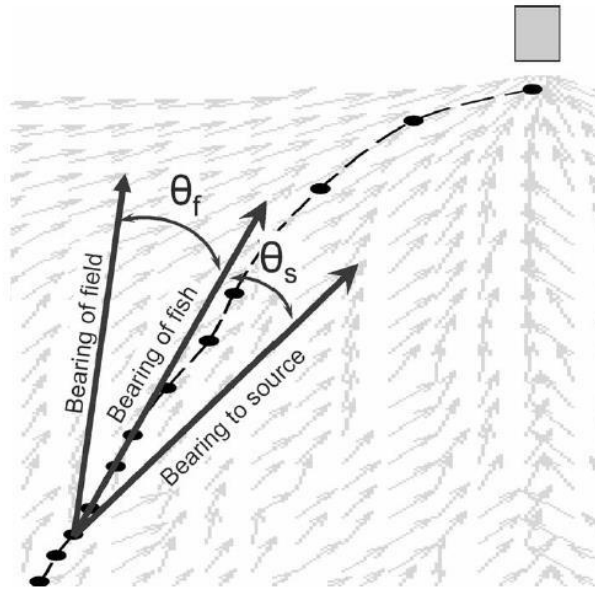


**Fig. 1.8:** An illustration of how the difference in the angles of the fish's bearing relative to the sound source and to the local particle motion vectors can be determined [from Zeddies *et al.*, 2010].

## 1.8 Measuring Auditory Sensitivity

By far the largest amount of data on comparative hearing in fish is in the form of behavioural audiograms [Popper & Fay, 2011]. Many studies have used behavioural or electrophysiological methods to detect fish hearing thresholds [Kojima *et al.*, 2005]. In the former, fish are conditioned to a pure tone using food as a reward, or by an electric shock which makes them avoid the sound source. The cardiac-conditioning method also conditions fish to a sound followed by an electric shock, but instead measures cardiac deceleration caused by the signal sound as an index to assess whether the fish can hear the sound or not. The key drawbacks to classical methods are the length of time to condition the fish to sound signals, a limited choice of organs on which electrodes can be placed, a potential need for surgically invasive procedures, and the degree of stress placed on the fish [Kojima *et al.*, 2005].

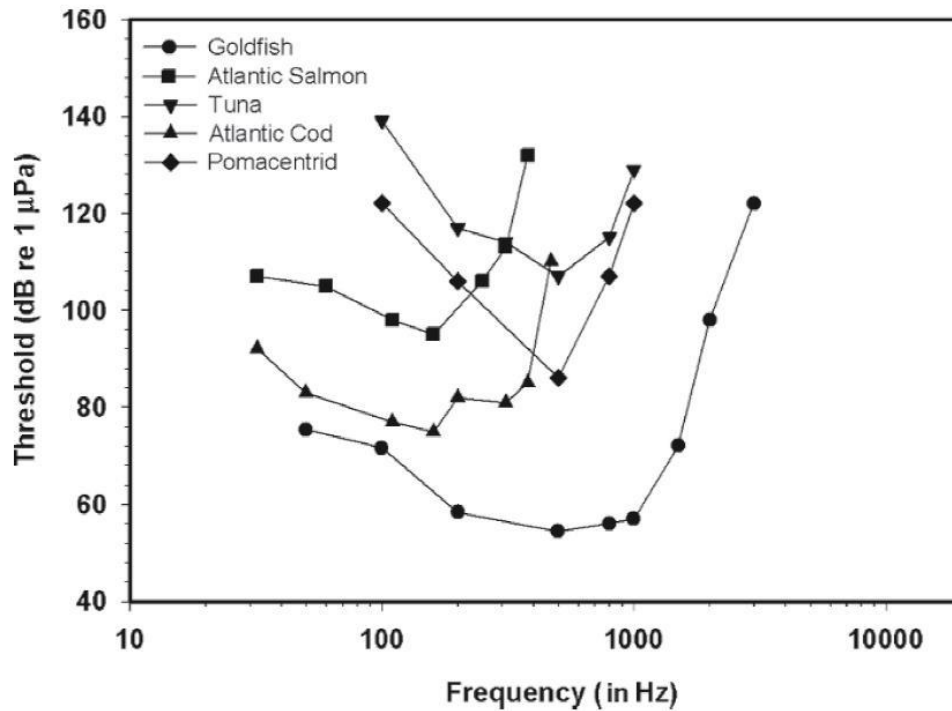


**Fig. 1.9:** Auditory thresholds from a select group of teleost fish [from Fay, 1988].

An alternative method is auditory brain response (ABR) first used by Kenyon *et al.* [1998] to determine the audiogram for the goldfish, (*Carassius auratus*) and oscar (*Astronotus ocellatus*). This method measures electrical potentials non-invasively from the skull surface over the region of the medulla, without the need for conditioning. The audiograms produced by Kenyon *et al.* [1998] did not differ significantly from two previously published behavioural curves and since the introduction of this method, more than 100 papers utilising this technique were published [Ladich & Fay, 2013]. Nedwell *et al.* [2004] drew together public domain information on the audiograms of 53 marine species, and Ladich & Fay [2013] described and compared the hearing abilities of 111 fish species out of 51 families.

A major challenge of researching the effects of sound on fish comes from the sparsity of data when compared with human audiology [Leighton *et al.*, 2020]. Results have tended to rely on a small number of fish subjects (averaged to represent a ‘typical’ member of the species), or a small number of well-studied model species. Leighton *et al.*, [2020] argue that despite the wealth of data on a significant number of humans over the past 50 years, including longitudinal studies of individuals, these are still considered

inadequate to predict the response of an individual on whom we have no data. Considering that over 33,000 living species of fish have been reported worldwide [Fishbase, 2015] and given the large gaps in knowledge for most of them, it is important that test signals and protocols for fish measurements are standardised (including, e.g. group response, and life history), so that direct comparisons can be made [Halvorsen *et al.*, 2020; Leighton *et al.*, 2020].

## 1.9 Underwater Sound and the Near and Far-Fields

The ratio between sound pressure and particle velocity is constant far from the source, and defines the acoustic impedance of the medium. In addition to generating sound, a vibrating sound source also produces hydrodynamic flows in its vicinity. These particle motions are independent of the elastic properties of the medium, and decay very steeply with distance from the source [Popper & Carlson, 1998]. Particle motions close to the source are therefore composed of both hydrodynamic flow and motions associated with the propagating sound.

Under free field conditions, attenuation of the sound pressure and the associated particle motions follow  $1/d$ , where  $d$  is the distance from the source. The hydrodynamic particle motions (which dominate close to the source) attenuate much more steeply, following  $1/d^2$  for a monopole source, which pulsates in volume, and  $1/d^3$  for a dipole source, which vibrates with constant volume. For an ideal monopole source, the distance at which hydrodynamic and pressure-associated particle motions have equal amplitude is  $1/2$  of the wavelength.

The near field of a source is the region close to a source where the sound pressure and acoustic particle velocity are not in phase. The far field of a source begins where the near field ends and extends to infinity. The measure often used for the transition between near and far field is a function of  $\lambda/2\pi$  ( $\lambda$  = wavelength), which is approximately one-sixth of a wavelength of the sound frequency. However, near- and far-field components of sound do not suddenly change at the point of  $\lambda/2\pi$ . The transition's precise distance is frequency dependent and depends on the way in which the sound source moves, for instance it is more extensive for a dipole source [van Bergeijk, 1967; Kalmijn, 1989]. Given the velocity of sound in water (1,500 m/s), the transition for a 100 Hz signal would be at 2.4 m from the sound source. Therefore,

higher frequency sound has a shorter transition distance, whereas lower-frequency sound has a longer one.

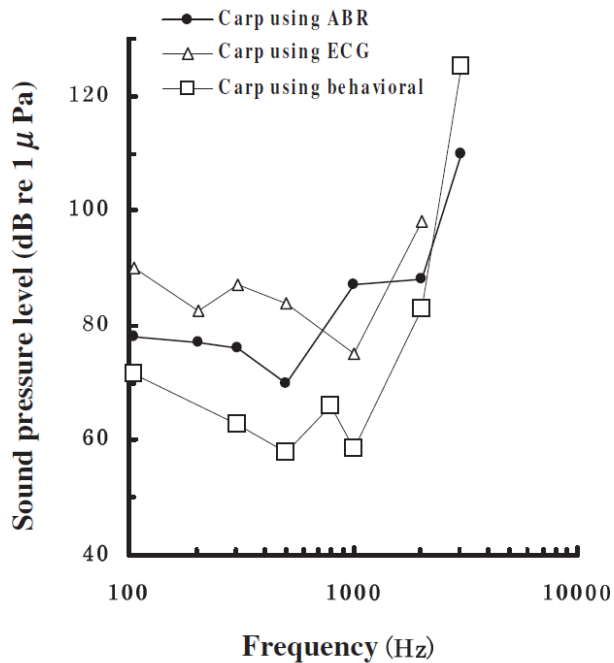


**Fig. 1.10:** Comparison of audiograms of carp obtained by a classical behavioural method, electrocardiogram (ECG), and auditory brainstem response (ABR) methods [from Kojima *et al.*, 2005; behavioural audiogram from Popper, 1972].

A significant number of species of fish spend at least part of their life history in the shallow waters of rivers and streams, where low-frequency sound propagates poorly. Both the pressure and particle velocity components of low frequency sound attenuate more rapidly with distance from the source in shallow rather than in deep water [Rogers & Cox, 1988], referred to as the shallow water ‘cutoff phenomenon’ [Akamatsu *et al.*, 2002]. For instance over a rocky bottom of 1 m depth, the lowest propagation frequency is around 300 Hz, whereas in waters of 10 m depth, the lower limit increases to 30 Hz. This means that fish in shallow habitats probably detect lower-frequency sounds only from sources that are extremely close to them.

### 1.10 Thresholds and criteria for injury and behavioural effects on fishes

Sound, at higher intensities, may have a diverse range of effects on an animal. These may include death, hearing impairment, damage to anatomical structures, and changes in physiology, neural function, behaviour, and development [Knight & Swaddle, 2011]. Currently there are no international standards for exposure of fish to impulsive or continuous sounds because few scientific data are available regarding the effects of sound for fishes, although interim criteria do exist [Popper *et al.*, 2014; Hawkins *et al.*, 2020].

The US National Marine Fisheries Service (NMFS) has developed interim criteria for pile driving using dual criteria [Woodbury & Stadler, 2008; Caltrans, 2009] which specify a maximum permitted SPL for a single pile driving event (206 dB re 1  $\mu$ Pa), and a maximum accumulated sound exposure level for lower level signals (187 dB re 1  $\mu$ Pa<sup>2</sup>s for fish  $\geq 2$  grams and 183 dB re 1  $\mu$ Pa<sup>2</sup>s for fish  $< 2$  grams). Guidelines for behavioural response are equally limited, and include an NMFS criterion of 150 dB re 1  $\mu$ Pa [Stadler & Woodbury, 2009], and the dBht (species) concept [Nedwell *et al.*, 2007]. It is unclear whether the former criterion is a peak or rms level [Popper *et al.*, 2014], or what evidence it is based on [Hastings, 2008]. Few independent experiments have been carried out to confirm the values proposed by Nedwell *et al.*, [2007], and since the relationship between the behavioural response and the hearing threshold may not necessarily be uniform [Sherlock & Formby, 2005] it may be incorrect to assume fish respond most strongly to frequencies that they are physiologically most sensitive to [Holgate, in prep].

Currently, the only set of widely accepted guidelines are those developed by Accredited Standards Committee S3/SC 1 Animal Bioacoustics [Popper *et al.*, 2014]. They include injury and behavioural guidelines for explosions, pile driving, air guns, low and mid frequency sonar, and continuous noise such as shipping. Where data is unavailable, a relative risk (high, medium, low) is given for animals at three distances from the source (near, intermediate, far). Fish are categorised into three major hearing groups based on the presence of a swimbladder and its adaptations for hearing, and criteria are given for each. Although the general opinion is that these guidelines are highly precautionary [Hawkins *et al.*, 2020], current consensus is that these should be

adopted until more data become available to update them (e.g. Andersson *et al.*, 2017; Faulkner *et al.*, 2018; Popper and Hawkins, 2019; Popper *et al.*, 2019).

For fish with swimbladders involved in hearing, which includes cyprinids such as common carp, SPL thresholds exist for recoverable injury (170 dB<sub>rms</sub> for 48 hours), and for temporary thresholds shifts in hearing sensitivity (158 dB<sub>rms</sub> for 12 hours). Given that sound levels of acoustic deterrents in the literature are at or well below 160 dB, the short exposure time of fish, and their ability to recover rapidly from acoustic disturbance [Bruintjes *et al.*, 2016], the effect of the behavioural deterrents tested for this thesis is expected to be temporary and negligible.

### **1.11 The relationship between the lateral line system and the ear**

The lateral line is a hydrodynamic receptor system that enables fishes to detect minute water motions generated by currents, conspecifics, predators or prey. It plays a role in a wide range of behavioral contexts including swimming, schooling, orientation to water flows (e.g., rheotaxis), predatory behaviour, and communication [Mogdans *et al.*, 2003; Webb *et al.*, 2008]. Other experimental work has demonstrated the ability of the lateral line system to detect moving objects in both still and running water. The sensory units of the lateral line are neuromasts which are distributed in canals and on the skin of the head and trunk. There are two types of neuromasts: 1) superficial, and 2) canal neuromasts. Superficial neuromasts are found on the surface of the skin and are sensitive to water velocity, whereas canal neuromasts are embedded in lateral line canals and sensitive to pressure gradients between canal pores [Coombs *et al.*, 1988].

Lateral line systems demonstrate a great deal of structural diversity among species and in the course of ontogeny, which suggests significant functional versatility in an evolutionary context and at different life history stages for individual species [Coombs *et al.*, 1988; Coombs & Montgomery 1999; Webb *et al.*, 2008]. Like the sensory epithelia (maculae) of the inner ear of fishes, neuromast receptor organs of the lateral line system are composed of a population of sensory hair cells and nonsensory support cells. Each sensory hair cell has one longer kinocilium and many stereocilia, which are graded in length and placed to one side of the kinocilium.

The similarities between hair cells in the lateral line and ear, and the presence of mechanical linkages between the ear, lateral line and swimbladder can blur distinctions

between acoustic and hydrodynamic receptors and between acoustic and hydrodynamic stimuli [Braun & Grande, 2008] and both the contributions of the mechanosensory lateral line system and the inner ear should be considered when interpreting acoustic stimuli in the near field [Webb *et al.*, 2008]. While bearing this in mind, there are distinct differences in the biomechanics of the lateral line system compared to the ears.

The lateral line system is activated by the relative motion between the water medium and the body of the fish. This can cause pressure gradients at adjacent lateral line canal pores, resulting in displacements of the fluid in the canals, which stimulates canal neuromasts that function as pressure gradient detectors [Kalmijn 1989]. Superficial neuromasts on the skin surface are activated by near-field hydrodynamic motions of the medium relative to the body surface, so these function as velocity detectors [Kalmijn, 1989; Engelmann *et al.*, 2000]. In general, these relative motions occur only in the acoustic near field where there are steep amplitude gradients of hydrodynamic motions. With the exception of fishes that have a link between the lateral line system and swim bladder (e.g. butterflyfishes) [Webb, 1998; Webb & Smith, 2000; Smith *et al.*, 2003], stimulation of the lateral line can therefore only occur in the near field of an acoustic source, within one or two body lengths [Webb *et al.*, 2008].

### **1.12 Response to stimuli in fish**

How information from the environment is received and processed by an individual fish depends on their sensory capabilities, and hence, as discussed earlier responses to extrinsic signals can differ between species [Schilt, 2007], lifehistory strategies and individuals [Budaev & Zworykin, 2002], developmental stage [Huntingford, 1993], physiological condition [Giorgi *et al.*, 1988], motivational status [Colgan, 1993], habituation [Knudsen *et al.*, 1992, 1997; Mueller *et al.*, 1998], and prior experience [Kieffer & Colgan, 1992]. In general, attractive stimuli are ones that an organism will voluntarily approach, and aversive stimuli are ones that an organism will try to escape or avoid. Labelling of a stimulus as attractive or aversive is based on an organism's behaviour, not on physical features of the stimuli themselves; therefore a stimulus that could be attractive to one species or life stage may well be aversive to another.

The reaction to exposure to a novel, high intensity, or aversive stimulus will always be within the normal behavioural repertoire of that species [Bui *et al.*, 2013]. A



common reaction to a potentially harmful signal is to escape and gain distance away from the source [Bui *et al.*, 2013; Millot *et al.*, 2009]. In fish, Flight behaviours are characterised by fast-start swimming: a high-energy burst and rapid acceleration in swimming speed [Domenici & Blake, 1997; Blaxter *et al.*, 1981], usually in the direction away from the disturbance [Domenici *et al.*, 2011]. The duration of stress responses are a trade-off between the potential risk represented by the signal and the cost of avoidance [Endler, 1991], and how long a stimuli elicits an effect is indicative of the magnitude of stress induced. For certain life-stages such as juvenile salmonids, behaviour in relation to passing barriers to downstream migration can be a key to determine successful seaward migration [Larinier & Travade, 2012].

Fish are adapted to detect changes in the visual environment [Gutherie & Muntz, 1993], which has a number of visual indicators. The intensity, spectral composition, and polarisation of light are factors that influence vision [Rader *et al.*, 2007]. Salmonids, for example, can detect polarised light and are sensitive to light of varying spectral composition including ultraviolet, blue, green, yellow, and red (346 nm - 690 nm; [Ali, 1961]). They have a strong behavioural response to acute changes in the light environment; four species of salmonids dived immediately to the bottom of tanks and swam with elevated activity after a transition from light-to-dark or dark-to-light environments [Monk & Gulbrandsen, 1994]. Abrupt exposure to artificial light can elicit strong avoidance responses across many taxa, including rainbow smelt (*Osmerus mordax*; [Hamel *et al.*, 2008]), zebrafish (*Danio rerio*; [Mesquita *et al.*, 2008]), yellow perch (*Perca fluvescens*), and largemouth bass (*Micropterus salmoides*) [Richards *et al.*, 2007].

Sound has also been explored as a potential behavioural modifier, Atlantic salmon are sensitive to acoustic particle motion, particularly at frequencies below 200 Hz [Hawkins & Johnstone, 1978] and well below 50 Hz [Popper & Fay, 1973]. Infrasound for example has been used to elicit avoidance responses in juvenile chinook salmon and rainbow trout [Knudsen *et al.*, 1997], cyprinids [Sonny *et al.*, 2006], and European eel [Sand *et al.*, 2000]. The mechanisms driving these responses are unclear, however the use of low frequency signals in the sound environment is common in communication [Hawkins & Myrberg, 1993], and may be analogous to the frequency produced by their predators [Enger *et al.*, 1989], or by particle displacement generated

by predator activity such as from birds or seals [Enger *et al.*, 1989; Huntingford *et al.*, 2012].

The importance of hydrodynamic relative to other sensory stimuli is still unclear in fish. For example, under experimental conditions overhead cover was found to induce avoidance in Pacific salmon smolts irrespective of discharge [Kemp *et al.*, 2005], however in the wild has been used to enhance guidance of downstream migrant brown trout, towards preferred passage routes at hydroelectric power dams [Greenberg *et al.*, 2012]. Vowles & Kemp [2012] and Vowles *et al.*, [2014] described elevated avoidance of velocity gradients when presented with a strong light stimulus, suggesting that visual cues may supplement information supplied by the mechanosensory system to increase responsiveness to hydrodynamic signals. This has links to overall fitness in the wild, since combined multisensory stimuli can increase detectability, discriminability and memorability of a stimulus in the receiving animal (Rowe, 1999). For example, multimodal signals enhance predator avoidance (e.g. Rowe & Guilford, 1999), mate selection (e.g. Uetz *et al.*, 2009) and communication (e.g. Partan *et al.*, 2009).

Finally, a lack of knowledge of the relationship between stimulus and response remains a key factor preventing progress in design of mitigation technology [Kemp *et al.*, 2011]. Current understanding tends to be based on defining thresholds of stimulus detection (e.g. Fay & Popper, 1974), measuring the auditory brainstem response of immobilized fish [Kenyon *et al.*, 1998] or by behavioural means based on the principles of classical or operant conditioning (e.g. Yan & Popper, 1992) which requires the training of the subject fish. These methods can be limited for defining the response of wild fish which may or may not be inclined to respond to a stimulus when they detect it [Kemp *et al.*, 2011].

### **1.13 Common carp (*Cyprinus carpio*) as a study species**

Common carp is originally native to the Black, Caspian and Aral seas [Balon, 1995]. The species was initially spread throughout Eurasia, and subsequently to every inhabited continent as a source of food and, more recently, for angling [Panek, 1987; Weber & Brown, 2009; FAO, 2017]. It is the most highly produced fish by tonnage, with upwards of 4 million tonnes produced in 2014 [FAO, 2017]. Along with other closely related species, it bears great economic and conservation value in many

countries [Newbold & Kemp, 2015]. In China, for instance, bighead carp, grass carp (*Ctenopharyngodon idella*), silver carp, black carp (*Mylopharyngodon piceus*), and common carp are commercially valuable fish species [Wu et al., 1992; Chen et al., 2004].

The duration and timing of common carp's spawning, growth, fecundity, and size at maturity differs between environments [Swee & McCrimmon, 1966; Shikhshabekov, 1972; Fida *et al.*, 1988; Smith & Walker, 2004] according to local temperature regimes [Alikunhi, 1966; Downing & Plante, 1993]. Size at maturity varies from 3-6 months or 90 - 140 mm SL in tropical regions [Alikunhi, 1966], to 3 - 5 years or 355 - 430 mm TL in temperate climates [English, 1951; Bishai *et al.*, 1974]. As long as conditions of >16 °C [Smith & Walker, 2004], a >12 h photoperiod [Crivelli, 1981; Smith & Walker, 2004], and appropriate habitat are met, common carp will spawn repeatedly [Alikunhi, 1966; Crivelli, 1981]. They are considered to be relatively strong swimmers in terms of speed and endurance [Tudorache *et al.*, 2007, 2008]. Optimal swimming speeds of  $30.59 \pm 4.36 \text{ cm s}^{-1}$  were obtained for carp of size 4.9 cm, with swimming speed increasing by  $7.5 \text{ cm s}^{-1}$  per additional cm of length [Tudorache *et al.*, 2007, 2008].

Construction of anthropogenic structures in riverine habitats inhabited by these species is contributing to their population decline [Fu *et al.*, 2003; Chen *et al.*, 2004] due to the fact that adults conduct large upstream migrations to spawning grounds and lateral movements as juveniles to lakes and other off-channel habitats [Jennings, 1988; Zhang *et al.*, 2012]. Carp has conversely been declared a pest in several countries [Koehn *et al.*, 2000; Smith & Walker, 2004], given that it negatively impacts aquatic ecosystems by consuming and uprooting submerged vegetation [Cahn, 1929; King & Hunt, 1967; Hanson & Butler, 1994] which leads to the suspension of sediment in the water column, limiting light and fuelling algal blooms [King & Hunt, 1967; Crivelli, 1983]. As mentioned previously, they have also caused a decline in lower trophic level organisms and community shifts in zooplankton populations which in turn may have affected additional native aquatic species [Cooke *et al.*, 2009]. The efficacy of non-physical barriers to deter invasive carp is currently being evaluated [Kelly *et al.*, 2011].

Common carp has been chosen as a study species for a number of reasons; it has a well-documented broad hearing range (100 – 4000 Hz) [Popper, 1972, Kojima *et al.*,

2005], and well-classified behaviour [e.g. Chase *et al.*, 2001; Amoser & Ladich, 2005; Tudorache *et al.*, 2007; Sisler & Sorensen, 2008; Bajer & Sorensen, 2010; Bajer *et al.*, 2010; Sloan *et al.*, 2013; Weber *et al.*, 2016]. Due to its high social learning and spatial memory skills, ease of acoustic conditioning and high retention rates applications of acoustical conditioning may prove useful as retention methods for the aquaculture industry [Bajer *et al.*, 2010; Sloan *et al.*, 2013]. Furthermore, Common Carp could serve as a potential surrogate for studies of how other carp species are influenced by bubble and acoustic deterrents in view of the high degree of overlap between hearing ranges and the similar deflection rates obtained by Pegg & Chick [2004], Taylor *et al.*, [2005], and Zielinski & Sorensen [2016] for Asian carp compared with common carp.



## Chapter 2

### Aims and Objectives

#### 2.1 Rationale

The following research gaps can be identified:

1. Previous work investigating the response of fish to bubble curtains and insonified bubble curtains have used widely varying testing protocols which makes direct comparison difficult. The number of studies in which the acoustic stimuli were categorised and mapped remains limited.
2. The idea of harnessing the resonant property of bubbles to improve existing technologies is, as yet, untried. Furthermore, literature has not taken the phenomenon of coalescence into consideration when attempting to compare streams of fine and coarse bubbles [e.g. Dawson 2006, Zielinski *et al.*, 2014b] When characterising the bubble population, previous studies have limited themselves to stating the gas flow rate and aperture size, under the assumption that the latter determines the size of the bubble;
3. There is a lack of understanding on what drives the effectiveness of bubble curtains and insonified bubble curtains especially with regard to how fish interact with the various stimuli elicited. The possibility that strong sound pressure and particle motion gradients generated by these bubble curtains elicits aversion in fish remains speculative;
4. Few studies account for the influence of visual cues when quantifying the guidance efficiencies of behavioural deterrents;
5. It is unclear what roles the two components of a sound field have on the behaviour of fish, and determining the extent of either remains a fundamental question;

## **2.2 Aim:**

To investigate the feasibility of insonified bubble curtains that exploit the resonant properties of bubbles as behavioural deterrents for fish, and help determine what drives fish behaviour when encountering such barriers.

## **2.3 Research Objectives:**

The research objectives, which built progressively on each other, were to:

- Ob 1: Test the reactions of common carp to a bubble curtain that uses a lower air flow than those used in industry, in the absence of visual cues;
- Ob 2: Divorce the effect of visual cues from stimuli generated by the bubble curtain by quantifying fish behaviour in the presence or absence of light when encountering insonified bubbles;
- Ob 3: Compare the effectiveness of resonant versus non-resonant insonified bubble curtains to deter passage, and determine the stimuli responsible for eliciting this response;
- Ob 4: Test to what extent the individual components of a sound field (i.e. acoustic pressure and particle motion) influence the behaviour and swimming trajectories of common carp (*Cyprinus carpio*) when reacting to a sound stimulus;

## **Reactions of juvenile common carp (*Cyprinus carpio*) to a bubble curtain with low air flow**

### **3.1 Abstract**

Bubble screens have previously been used as deterrents in an attempt to repel fish from intake structures, and to stop the spread of invasive species. Their key advantage is the ease at which they can be deployed, re-positioned and maintained. They have been used with varying levels of success, depending on the target species and deployment conditions, but show particular promise for carp. In line with industry recommendations, past studies have generally used bubble barriers with air flows greater than  $100 \text{ L min}^{-1} \text{ m}^{-1}$ , but generating this can be costly. In this pilot study fish reactions to a bubble curtain ( $30 \text{ L min}^{-1} \text{ m}^{-1}$  at atmospheric pressure) were tested. The bubble curtain was effective at reducing *Passes* ( $p < 0.001$ ) to 35% of the control. On encountering the barrier fish initially reacted by changing depth, and swimming along the front of the curtain. Passage most commonly occurred through the gap between the bubble and the flume wall when the air curtain was active, tending to bypass it. Results indicate that there is a potential for examining the effectiveness of lower flow bubble walls, in particular combining these with an acoustic field to which a high proportion of bubbles generated are resonant to.

### **3.2 Introduction**

Fish guidance technologies have long played a role in fisheries management efforts to reduce fish impingement at power generation facilities and to control the movement of invasive fish [Taft, 2000; Noatch & Suski, 2012]. Bubble screens were a type of behavioural deterrent developed in an attempt to overcome the need for expensive, automatically cleaned, mechanical screens [Welton *et al.*, 2002]. Although physical screens are preferred over behavioural screens due to their higher guidance efficiencies when installed correctly, the advantage of bubble curtains is that they are cheap, and easily deployable. While they do not provide a guaranteed barrier to fish passage, they are often used in less critical applications or where the alternative is to have no screening [Turnpenny & O'Keefe, 2005]. They are therefore ideal for areas such as the



upper Mississippi River in the US, which due its large network of tributaries makes the economic and environmental cost of physical screens prohibitive. In such areas bubble curtains are also preferable to other behavioural deterrents such as electrical screens, due the risk these can pose to human safety, and their potential to block valuable native fish [Noatch & Suski 2012, Zielinski & Sorensen, 2016].

Bubble curtains may influence fish visual, auditory, and lateral line systems by generating visual, sound, and tactile stimuli. Bubble curtains may serve as a visual barrier by obscuring a fish's line of sight past the barrier [Patrick *et al.*, 1985; Sager *et al.*, 1987, Welton *et al.*, 2002]. Bubbles detaching from a nozzle or diffuser generate sound due to the collapse of the neck of air formed immediately after bubble "pinch-off" [Leighton & Walton, 1987; Longuet-Higgins, 1990]. Clouds of bubble will also tend to oscillate collectively at frequencies far below those of the individual constituent bubbles [Yoon *et al.*, 1991; Manasseh *et al.*, 1994; Nicholas *et al.*, 1994], and are likely the source of natural oceanic ambient noise below 1 kHz [Yoon *et al.*, 1991]. Finally, a rising cloud of bubbles will create turbulence based on bubble density and rise velocity [Brevik & Kristiansen, 2002].

Although some laboratory and field studies have reported fish being deterred by bubble curtains [Enami, 1960; Bates & VanDerWalker, 1964; Bibko *et al.*, 1974; Stone & Webster, 1976; Stewart, 1981; Patrick, 1985; McIninch & Hocutt, 1987; Turnpenny, 1993; Turnpenny *et al.*, 1998; Sprott 2001] these studies did not quantify the sound field generated by the bubbles as they detach from the system used to generate them, or other physical characteristics needed to assess the factors driving the effectiveness of these systems. The varying conditions found in the field and differing setups used may indicate why results have been mixed or ineffective when such systems were deployed at power generation sites [EPRI, 1998; GLEC, 1994; Grotbeck, 1978; Latvaitis *et al.*, 1976; Hocutt, 1981; Taft, 2000].

Studies have sometimes reached opposite conclusions which may well be representative of interspecific variations in fish behaviour. For example Patrick *et al.*, [1985] found that light increased the deterrence of a bubble barrier by 20% for gizzard shad, alewife, and smelt. Conversely, Welton *et al.*, [1997] suggested that Atlantic salmon smolt were deterred more during the night due to their ability to identify and make use of gaps in walls during the day. McCauley *et al.*, [1996], Turnpenny [1993],

and Bibko *et al.*, [1974] reached similar findings. Other studies have reported attraction to bubble screens [Inamura & Ogura, 1959; Hanson *et al.* 1977; Alvevras, 1974; EPA 1973, 1976]. The implication is therefore that bubble curtains may be more effective at diverting fish with hearing specialisations since several unspecialised species such as Walleye, Muskellunge, Ruffe, White Perch and Atlantic salmon smolt are largely undeterred by them [Sager *et al.* 1987; Welton *et al.*, 1997; Dawson *et al.*, 2006; Flammang *et al.*, 2014; Stewart *et al.*, 2014].

A majority of the studies mentioned used bubble barriers with air flows greater than  $100 \text{ L min}^{-1} \text{ m}^{-1}$  [e.g. Sprott, 2001; Zielinski *et al.*, 2014a], although some reports did not always specify the air flow used to generate the bubble curtain. Despite the fact that generating large volumes of air can be costly, only two studies have used air flows lower than this: Welton *et al.* [2002] who used a bubble curtain in conjunction with sound, and Dawson *et al.*, [2006] who used a 30 cm long bubble barrier in a tank, with an air flow of  $1.5 \text{ L min}^{-1}$  (effectively  $5 \text{ L min}^{-1} \text{ m}^{-1}$  of barrier.) The latter found that while the presence of a bubble curtain increased the number of repels in Eurasian ruffe (a species which does not have a connection between the swim bladder and hearing organs) versus a control, the number of passes or attempts per fish remained unchanged [Dawson *et al.*, 2006]. In working towards the concept of a low flow insonified bubble curtain for use with species that possess hearing specialisations, a logical first step would therefore be to test the bubble barrier alone, using a lower flow than industrial recommendations.

Previous studies have also tended to assume that stating the bore size and gas flow is sufficient when categorising a bubble curtain. Although Dawson *et al.*, [2006] did observe that bubble size near the bottom of the barrier initially equaled the bore size, and then increased as the bubbles rose in the water column, this appears to have been a qualitative observation. As explained in **Chapter 1.4**, this is not sufficient to categorise a bubble curtain due to the phenomenon of coalescence. The next chapter will focus on this phenomenon and how to exploit it in more detail.

The present study investigates the impact of a bubble curtain on common carp (*Cyprinus carpio*), The species has been implicated in degrading considerable areas of shallow lake and wetland ecosystems across the globe [Weber & Brown 2009]. A bubbler was constructed using PVC piping, hypodermic needles as injection nozzles,

and vibrating motors used for haptic feedback purposes. The main objectives of the study were to: (1) develop and test the efficacy of a bubble curtain to inhibit carp movement in the absence of a visual stimulus; (2) contrast the efficacy of this set-up with a cloud of finer bubbles generated by vibrating the injection nozzles with attached haptic feedback motors.

### **3.3 Methodology**

#### **3.3.1 Experimental Set-up**

Experimental trials were carried out in an 8m x 4m stone annular raceway at the International Centre for Ecohydraulics Research (ICER) facilities at the University of Southampton (see **Fig. 3.1**). The raceway contained still conditioned tap water, due to the absence of a pumping system, with a depth of 60 cm. To aid recovery of fish after each trial an experimental section (8.0 m total length) was separated from the rest of the channel by wooden framed polyester mesh barriers (1 cm mesh size). While this set-up was asymmetrical due to presence of a walkway, attempts and passage efficiency did not differ with side of approach. A bubbler was constructed from two rows of 38 mm diameter grey PVC piping, with 3 mm holes drilled at 5 mm intervals. The two rows were 15 cm apart. A total of 36 gauge 21 (38.1 mm length, 0.8 mm internal diameter) hypodermic needles were used as injection nozzles and glued on top of each hole using polyacrylamide glue. Air (at  $60 \text{ L min}^{-1}$ , pressure: 1 bar, or  $30 \text{ L min}^{-1} \text{ m}^{-1}$  of bubbler) was supplied to the bubbler via 6.4 mm ID nylon tubing leading to a compressor (Clarke Bandit, 1HP), and flow monitored with an air flow meter (IDS, MR3000). A gap was present at the edges of the bubble curtain due to a combination of turbulence caused by rising bubbles, and a 7.5 cm spacing between the edge of the bubbler and the flume wall.

Bubble size distribution, determined post-experiment (see **Chapter 4.3.2**), ranged between 20 to 18,000  $\mu\text{m}$ ,  $\bar{x}$  diameter = 707  $\mu\text{m}$ . For distribution plots and examples of frames used for determining the size distribution, refer to **Appendix C**. Prior to running trials, acoustic measurements were taken to confirm that the sound made by the compressor could not be detected underwater due to impedance mis-match as a result of the different densities of air and water. To further eliminate any potential acoustic transmission, the compressor was positioned well away from the flume.

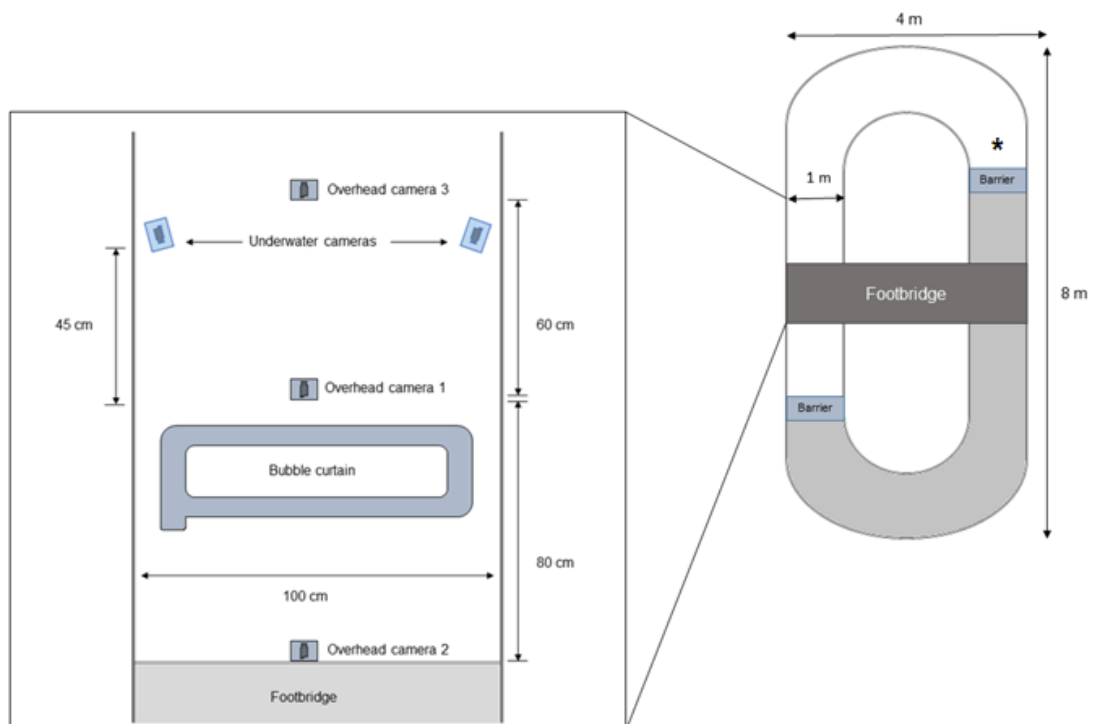


**Fig. 3.1** – Schematic of the experimental set-up. There was a 7.5 cm gap between the sides of the bubbler and the flume. The asterisk indicates the release point for fish at the start of each trial. The greyed-out section indicates the area of the flume not used during the experiment (drawing dimensions are not to scale).

### 3.3.2 Subject Fish

Common carp ( $n = 126$ ) used in the study were obtained from a commercial supplier ( $\bar{x}$  length ( $\pm$  SE):  $116.23 \pm 3.66$  mm;  $\bar{x}$  weight ( $\pm$  SE):  $23.59 \pm 2.30$  g), in July 2017. Fish were transported to the ICER facilities at the University of Southampton in well-oxygenated water, and held in 3,000 L holding tanks containing well aerated and filtered water under ambient temperature. Water quality was checked daily and maintained at optimum levels ( $[\text{NH}_4^+] < 0.125$  ppm;  $[\text{NO}_2^-] < 0.25$  ppm). At the end of each trial the subject fish were euthanised in accordance with Schedule 1 of the Animals (Scientific Procedures) Act 1986, and individual total body length ( $\pm 0.5$  mm) and mass ( $\pm 0.05$  g) recorded.

### 3.3.3 Experimental Trials

Trials were conducted at night (between the end of civil dusk: 21:45 to 21:20, and the start of civil dawn: 03:40 to 04:50) between 20 July and 10 August 2017 so as to reduce

visual stimuli to a minimum and because carp are more active at night [Bajer *et al.*, 2010]. Any lights in the experimental area were switched off and the experimental flume covered with tarpaulin. The temperature of the holding tank and experimental flume were measured prior to commencement of trials. Fish were then placed in perforated containers within the non-experimental section of the flume prior to the start of trials for the necessary time to acclimate (half an hour acclimatisation time for each 1°C difference).

For each trial, three carp of similar size were carefully removed from the containers and transferred into the experimental flume. This number was chosen to allow them to form shoals because carp are social and behave more naturally when tested as groups [Sisler and Sorensen, 2008; Huntingford *et al.*, 2010; Sloan *et al.*, 2013]. The fish were allowed to acclimatise by swimming freely in the experimental area for 15 minutes prior to each trial commencing. Low light overhead cameras, and underwater cameras were used to record behaviour under infra-red (IR) illumination (850 nm).

This experiment comprised of four treatments: a) the compressor switched on but unconnected to the bubbler (control), b) the compressor switched off and motors vibrating at 2 V (vibrating motors), c) a bubble curtain with a 30 L min<sup>-1</sup> m<sup>-1</sup> air flow (standard injection), d) a bubble curtain with a 30 L min<sup>-1</sup> m<sup>-1</sup> air flow and motors vibrating at 2 V (vibrated injection). Vibration of the injection nozzles was provided by a total of 36 haptic feedback motors attached to each nozzle (Precision microdrives 307-103). At 2V, the motors had an amplitude of 4 g and a frequency of 170 Hz. After the initial acclimation period, all trials consisted of a test (control or treatment) immediately followed by a post-test phase, each lasting 20 minutes.

### 3.3.3 Behavioural Analysis

Video recordings were analysed to quantify common carp response to the bubble curtains. Data were evaluated in two steps: (1) coarse-scale passage and rejection counts, and (2) Generalised additive modelling to test the influence of non-experimental factors.

The following coarse-scale metrics were recorded per individual fish: (1) *Number of approaches*, deemed to have occurred when a fish entered the visual field of

the cameras, (2) *Number of passes*, and (3) *Number of rejections*, based on whether or not an approach culminated in the fish passing through the bubble curtain. A rejection was defined as a change in direction of the swimming trajectory greater than 90 °, followed by sustained swimming away from the barrier and out of the field of view. For each trial, the *Number of approaches*, and *Passes* recorded were used to calculate the *Passage efficiency*, defined as the number of successful passes expressed as a proportion of the total number of approaches. As the majority of *approaches* (90%) were made by solitary fish, rather than by a shoal, approaches by fish were considered to be independent, regardless of whether these were made as part of a group or not.

When recording coarse-scale counts, the position of where a *Pass* took place along the length of the bubbler was also recorded. The bubbler was divided virtually into five areas of 20 cm each (seen from the same aspect as **Fig. 3.1**): *L* - left, *LC* - left centre, *C* - centre, *CR* – centre right, *R* – right. For each trial, the number of *Passes* from the sides (*L* and *R*) versus *Passes* from the centre (*LC*, *C*, *CR*) was recorded and these were used to calculate the *Inner passage fraction*. In view of the observation that fish tended to bypass the bubbler more often when this was in operation, by making use of the 7.5 cm spacing between the edge of the bubbler and wall of the flume, passage data were adjusted to control for passes from the sides prior to analysis.

#### 3.3.4 Statistical Analysis

Coarse-scale data were analysed by means of a two-way Anova with post-hoc Tukey pairwise comparisons. Bartlett's and Shapiro-Wilk tests revealed that the data showed mild signs of heterogeneity (K-squared = 13.87, df = 7, p-value = 0.05) but did not differ from normality (W = 0.98, p-value = 0.11). Data violated the assumptions of normality for *Number of passes* and homoscedasticity for *Number of rejections* for the treatment phase alone. Kruskal-Wallis rank sum tests, with a post-hoc Dunn test with Benjamini Hochberg corrections were used to verify whether treatment affected *Pass* and *Rejection* counts.

Generalised additive modelling (GAMS) using the *mgcv* package in RStudio (v 1.1.456: The R Foundation for Statistical Computing, Vienna, Austria, <http://www.r-project.org/>) was used to examine the impact of various experimental factors (subject, treatment, phase of experiment) and non-experimental factors (date, trial start time,

water level, water temperature) on the number of *Passes* and *Passage efficiency*. Starting from a saturated model, stepwise deletions were performed to identify non-significant terms, and model selection was based on residual deviance, generalised cross-validation score (GCV), R-Sq and the lowest Akaike Information Criterion (AIC). The minimum adequate model (MAM) was arrived at as the most parsimonious models with lowest AIC value [Burnham & Anderson, 2002]. For results of GAM checks see **Appendix B**.

### 3.4 Results

#### 3.4.1 Coarse Scale Results

*Number of passes* were lower in the presence of the bubble curtain than during the post-treatment control ( $F = 7.65$ ,  $p < 0.01$ ,  $p\text{-adj} < 0.01$  – see **Fig. 3.2**), and *Passage efficiency* was 47% lower ( $F = 4.44$ ,  $p < 0.01$ ,  $p\text{-adj} < 0.01$ ). There was no difference in the *Number of passes* between the vibrating control treatment and the post-treatment control ( $p\text{-adj} = 0.99$ ).

Treatment type had a significant effect on passage through the bubble curtain (Kruskal-Wallis rank sum test:  $\chi^2 = 10.494$ ; d.f. = 3;  $p = 0.012$ ). A post-hoc Dunn test with Benjamini Hochberg corrections indicated sizeable support for standard injection being more effective than the control ( $p = 0.031$ ), moderate support for vibrated injection vs control ( $p = 0.066$ ), and essentially no difference between both control treatments ( $p = 0.625$ ), or between both bubble treatments ( $p = 0.659$ ). Pairwise comparisons for *Rejection counts* showed that both bubble treatments, and vibrating motors increased the number of *Rejections* ( $p = 0.011$ ).

When the bubble curtain was operating, carp tended to pass it via a 7.5 cm gap at the flume wall, and the proportion of *Passes* at the wall was higher when the bubble curtain was in operation compared to the two controls. ( $\chi^2 = 23.18$ ,  $p < 0.01$  – see **Fig. 3.3**).

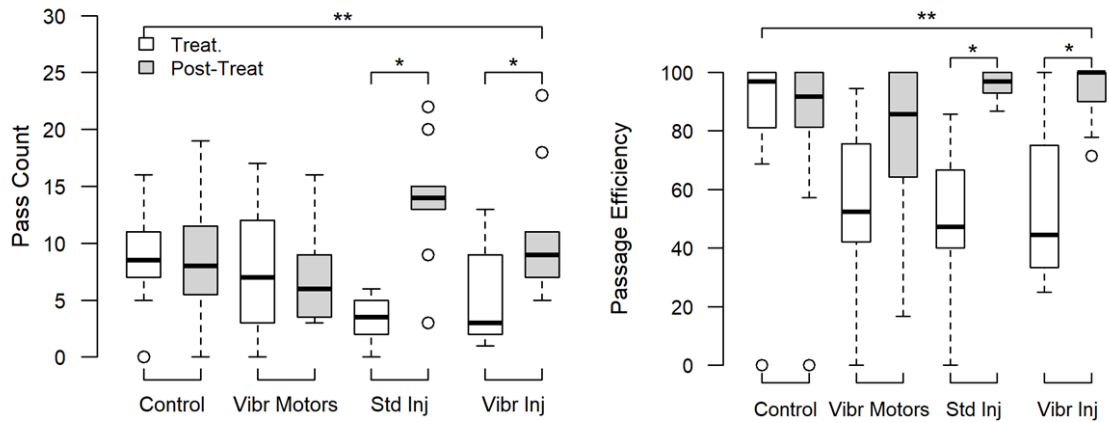


**Fig. 3.2** Box plots of *Number of passes* and *Passage efficiency* for all treatments for the 60 L min<sup>-1</sup> bubble curtain during test and post-treatment periods. Pairs with significant difference are denoted by an asterisk.

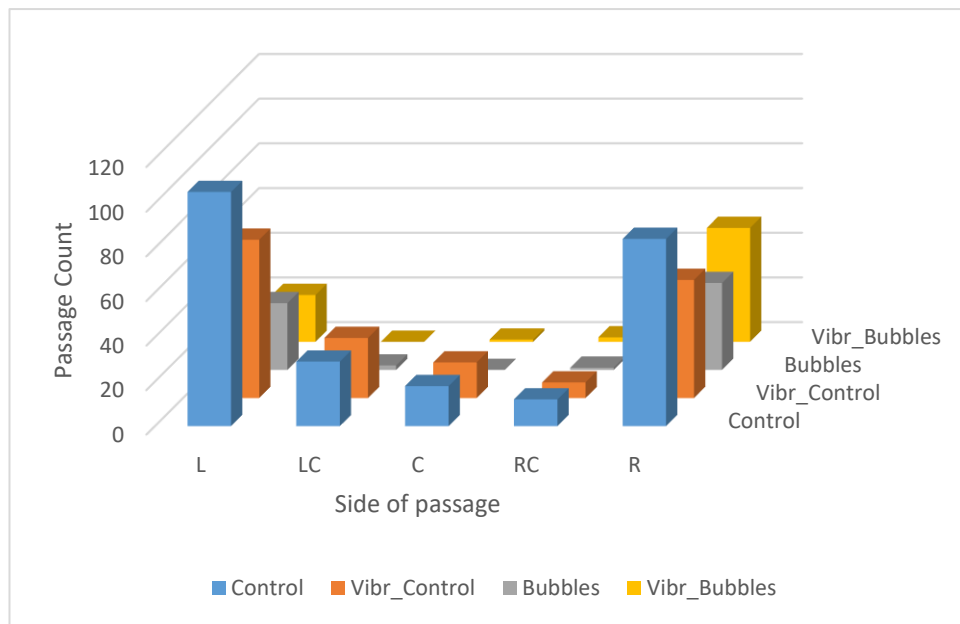


**Fig 3.3:** Count of *Passes* by location along the bubbler for fish during different treatments. *L* = left, *LC* = left centre, *C* = centre, *CR* = centre right, *R* = right.

### 3.4.2 Modelling in GAMS

Models obtained for the *Number of passes* (including or excluding passes that took place on the side of the bubbler) explained 64.2 and 32.4 % of the deviance versus the null (see **Table 3.1**). The interaction between phase and treatment phase alone, and date



of experiment explained the majority of the deviance, although trial date was less important for the second data set. Similar factors explained the results obtained for *Passage efficiency* (48.6 % deviance explained).

### 3.5 Discussion

Fish showed a high degree of exploratory behaviour, being generally side-oriented, and often swimming in loose to very loose groups of 2 – 3 fish. Contrary to expectations from literature fish largely tended to make attempts individually, which supports the decision to ignore whether approaches were made as a part of a group. In similar fashion to Zielinski *et al.*'s findings [2016] fish tended to react to the bubble curtain at short ranges, approximately at or less than 25 cm away from the curtain. Rejection was often preceded by the fish swimming upwards in the water column, potentially searching for possible routes where sound intensity was lower. This behaviour may in future be explained using high-resolution acoustic maps for multiple depths.

There is also scope for future analysis on the effect of shoaling on the decision making of individual fish due to the fact that there were a small number of occasions where fish clearly altered their trajectory due to the presence of other fish. It can be argued that to eliminate any such effects, trials should have been carried out with individual carp, however carp are social animals and tend to panic in the absence of other fish. Observing carp behaving more naturally was considered to be of greater benefit for the purpose of this test, which outweighed any group interaction effects. This assumption was confirmed by carrying out a limited number of trials with individual fish.

Results obtained show that the use of a simple bubble curtain generated using half the air flow used in similar walls in the literature can be effective at deflecting common carp, and that carp may be capable of detecting gaps through a bubble wall. Analysis of *Pass counts* controlling for side passage, showed a significant reduction in the number of *Passes*, and the vast majority of these were carried out by fish bypassing the bubble curtain through the gaps along the side. Analysis of all *Pass count* data (i.e. including side passage) suggests that the decision to reject passage may in part also take place at distances outside of the visual range of the underwater cameras due to the way

these were deployed (facing the bubbler). This is confirmed by the fact that when the bubble curtain was active the total number of approaches added up to 65 % of the value for the control. This can be analysed further in future experiments by using suspended underwater cameras which will also allow tracking of fish movements, overlaid onto acoustic and hydrodynamic maps.

**Table 3.1:** The deviance explained relative to null (%), estimated degrees of freedom (edf) and significance (p value) of variables within the minimum adequate models fitted to *Number of passes*, and *Passage efficiency*.

Data	Model terms	Deviance explained relative to null (%)	edf	p value
	s(Date, bs="ps", k=8) + Treatment:Phase	64.2 (Minimum adequate model)		
Passes (incl. from side)	Treatment:Phase	18.5		< 0.001
	Phase	23.2		< 0.001
	s(Date, bs="ps", k=8)	20.2	3.69	0.007
	Treatment	1.3		0.04
	s(Date, bs="ps", k=8) + Treatment:Phase	32.4 (Minimum adequate model)		
Passes (excl. from side)	Treatment:Phase	17.9		< 0.001
	Phase	10.1		0.003
	s(Date, bs="ps", k=8)	2.0	1.62	0.602
	Treatment	2.4		0.013
	s(Date, bs="ps", k=8) + Treatment:Phase	48.6 (Minimum adequate model)		
Passage Efficiency	Treatment:Phase	11.6		< 0.001
	Phase	17.8		< 0.001
	s(Date, bs="ps", k=8)	15.9	3.93	0.011
	Treatment	3.3		0.053

Despite the effectiveness of the bubble curtain, one of the aims of the study was not met as the vibration generated by the attached motors was insufficient to create the finer stream of bubbles sought after. This was a limitation imposed by the structural properties of the polyacrylamide glue used to fix the needles into place, which limited the motors to a voltage of 2V. Data for this treatment was retained because it could be used to verify whether the noise and vibrations of the haptic feedback motors used in the study affected fish behaviour. For this reason, this experiment is considered to be a viable pilot-study for follow-up experiments planned in view of the success of a simple low-flow bubble wall. Follow up experiments will remedy this issue by improving the

design of the bubbler by attaching the needle directly to the air tubing, allowing the needle to pivot freely, focusing in particular on the following aspects:

- The effect of visual cues on fish behaviour when encountering an insonified bubble curtain;
- Whether the resonant properties of bubbles can be used to create a more effective barrier;
- Whether the effectiveness of an insonified bubble curtain as a deterrent is the result of the two stimuli (sound and bubbles) acting separately, or in conjunction with one another using the resonant properties of bubbles. This can be tested by comparing the effectiveness of resonant versus non-resonant insonified bubble curtains to deter passage, and determining the stimuli responsible for eliciting this response.

### **3.6 Conclusions**

The present study shows agreement with prior experiments that examined the reactions of common carp (*Cyprinus carpio*) to bubble barriers, however also collected footage-based behavioural data. Passage rates were reduced to 34 % (standard injection) of the control rate. When the bubbler was in operation, the *Inner passage fraction* was reduced since the number of fish attempting passage through the space between the bubbler and the flume walls increased. Although this experiment did not specifically set out to test the ability of fish to detect and exploit spaces in the bubble wall for passage, this does hint at the ability of fish to sense gaps in the absence of visual stimuli. Follow-up experiments will focus on using the resonant properties of bubbles to improve acoustic bubble barriers, and examine how visual cues can affect their efficiency.

### **3.7 Ethics**

The study conformed to UK legal requirements and was approved by the University of Southampton's Ethics and Research Governance Office (Ethics ID: 27379).

## Chapter 4

### **Common carp (*Cyprinus carpio*) response to insonified bubbles with different size distributions, and influence of visual cues**

#### **4.1 Abstract**

Acoustic bubble curtains have been marketed as easily deployable behavioural deterrents for fisheries management. Their energy efficiency can be improved by reducing air flow and exploiting bubble resonance. In a series of two flume experiments, we: (1) compared the effectiveness of resonant versus non-resonant insonified bubble curtains (for the same volume flux of gas injected, through the nozzles) to deter passage, determining the stimuli responsible for eliciting deterrence, and (2) divorced the effect of visual cues from stimuli generated by the bubble curtain. This proof-of-concept study showed that bubble clouds with a higher proportion of resonant bubbles better deterred carp. Passage rejection was likely influenced by multimodal cues, specifically the changes in both particle displacement and sound pressure within a body length of the fish. All acoustic bubble curtains were less effective in the presence of visual cues, suggesting that visual stimuli dominate over those that act on the mechanosensory system. We discuss the importance of ascertaining the bubble size distribution, in addition to the gas flow rate and aperture size when characterising acoustically active bubble curtains.

#### **4.2 Introduction**

River off-takes, such as those that convey water to irrigation systems, hydropower turbines, power station cooling systems, or fish farms, can have multiple negative impacts on fish [Solomon, 1992]. Off-stream water use (e.g. irrigation) can remove fish from a population, whereas in-stream use (e.g. hydropower) can cause death, injury or delayed mortality at turbines and pump-mechanisms [Solomon, 1992]. Traditionally, physical or mechanical screens are used to protect fish at these structures, by blocking and/or guiding them to alternative, safer routes [Jansen *et al.*, 2007]. When designed and operated correctly, physical screen guidance efficiencies can range between 80-100% [Amaral *et al.*, 2003; Turnpenny & O'Keefe, 2005; Inglis *et al.*, 2015]. However, such methods can have several limitations; often being costly to deploy and maintain, particularly when there is debris accumulation [Solomon, 1992; Turnpenny & O'Keefe,

2005], and can themselves harm fish through impingement [Calles *et al.*, 2010]. Furthermore, their effectiveness at blocking and guiding larval and juvenile life-stages can be limited as these can pass through them [Turnpenny & O’Keefe, 2005; Kemp *et al.*, 2012] or lack the swimming capability to escape once impinged [Moser *et al.*, 2014]. Consequently, this had led to an interest in developing and testing non-physical guidance methods.

Behavioural guidance systems can use a diverse array of stimuli to repel and attract fish. Attractors, such as pheromones [Johnson *et al.*, 2009; Sorensen & Stacey, 2010]], are less frequently used than repellents. Repellents include electric fields (e.g. Eurasian ruffe, *Gymnocephalus cernuus* [Dawson *et al.*, 2006]), air bubbles (e.g. gizzard shad, *Dorosoma cepedianum* and striped bass, *Morone saxatilis* [Kuznetsov, 1976]; and common carp *Cyprinus carpio* and Asian carp, *Hypophthalmichthys spp.* [Zielinski & Sorensen, 2016]), strobe lights (e.g. Atlantic menhaden, *Brevoortia tyrannus*, spot, *Leiostomus xanthurus*, and white perch, *Morone Americana* [McIninch & Hocutt, 1987]) and continuous light (e.g. European eel, *Anguilla Anguilla* [Lowe, 1952]), acoustics, (e.g. silver carp, *Hypophthalmichthys molitrix* [Vetter *et al.*, 2015, 2018]; bighead carp, *H. nobilis* [Vetter *et al.*, 2017]; various estuarine species [Maes *et al.*, 2004]); European eel [Sand & Karlsen, 2000; Deleau *et al.*, 2019, 2020]; river lamprey, *Lampetra fluviatilis* [Deleau *et al.*, 2020]), hydrodynamics (e.g. chinook salmon, *Oncorhynchus tshawytscha* [Enders *et al.*, 2009, Goodwin *et al.*, 2014]), odours of decaying conspecifics (e.g. sea lamprey *Petromyzon marinus* [Wagner *et al.*, 2011]), and shade (e.g. Chinook salmon [Kemp *et al.*, 2005]). Efficiencies vary greatly between studies and are often much lower than those obtained for physical screens [Turnpenny *et al.*, 1998] that, as a consequence, are the preference of many regulatory agencies [Mefford, 2004; Turnpenny & O’Keefe, 2005]. However based on applying the Theory of Marginal Gains to fish screening [Deleau *et al.*, 2019], where many small incremental improvements in the system amount to a significant gains when added together, there remains considerable potential for developing behavioural deterrents to enhance the performance of physical devices when used in combination.

One of the potential explanations for the lower than expected performance of behavioural deterrents is that historically their development has often been based on a process of trial-and-error [Katopodis & Williams, 2012], rather than focusing on

fundamental principles and an understanding that responses to stimuli vary among species, life-stage and individuals [Noatch & Suski, 2012; Sonnichsen, 2012]. Results are often contradictory, particularly if insufficient rigour has been applied during testing [Hocutt, 1980; Noatch & Suski, 2012], and may reflect differences in site or approach adopted, e.g. field studies versus controlled experiments [Noatch & Suski, 2012; Zielinski et al., 2015; Leighton et al., 2020]. Concerns have also been raised with regard to a lack of habituation studies [Putland & Mensinger, 2019; Popper & Hawkins, 2019], insufficient quantitative data, and use of proprietary acoustic stimuli in previous studies, precluding testing by third parties [Putland & Mensinger, 2019]. As a result, river managers and environmental engineers can receive mixed messages, and so far the use of behavioural methods to complement physical screens remains limited [Turnpenny & O’Keefe, 2005].

The efficiency of behavioural guidance devices may be improved if more than one stimulus is used in combination [Popper & Carlson, 1998; Noatch & Suski, 2012]. Multiple stimuli have proven more effective in studies that compared them against their constituent stimuli alone. These include strobe lights with bubbles (e.g. Atlantic menhaden, Spot, and white perch [Lowe, 1952; Sager *et al.*, 1987], Alewife *Alosa pseudoharengus*, rainbow smelt *Osmerus mordax*, and Gizzard shad [Patrick *et al.*, 1985]), sound with electric fields (e.g. Atlantic salmon [IOE Group, 1994]), and bubbles with broadband sound (e.g. Atlantic salmon smolts [Welton et al., 2002]; bighead carp [Taylor *et al.*, 2005; Dennis *et al.*, 2019]). It is likely that these improvements in performance are the result of using multi-modal cues operating via different sensory systems in which stimuli can either act independently, or where one stimulus improves responsiveness to another [Vowles & Kemp, 2012; Vowles *et al.*, 2014].

Insonified bubble curtains present multi-modal acoustic, hydrodynamic, and visual stimuli. As mentioned earlier, bubbles introduced underwater generate sound and create turbulence that is influenced by bubble density and rise velocity [Brevik & Kristiansen, 2002]. Furthermore, they can create a visual barrier by obscuring a fish’s line of sight [Flammang *et al.*, 2014; Stewart *et al.*, 2014], although guidance efficiencies are generally higher at night for species such as walleye *Sander vitreus* [Flammang *et al.*, 2014], muskellunge *Esox masquinongy* [Stewart et al., 2014], largemouth bass *Micropterus salmoides* [Lewis *et al.*, 1968], and sockeye salmon *Oncorhynchus nerka*

[Brett & McKinnon, 1953]. This might be because fish can detect gaps during daylight hours through which they can pass, as suggested for Atlantic salmon smolts [Welton *et al.*, 2002]. Despite these examples, few studies account for the influence of visual cues when quantifying the guidance efficiencies of behavioural deterrents.

Although insonified bubble curtain deterrents are commercially available and can, under certain circumstances, attain high levels of efficiency [Welton *et al.*, 2002; Taylor *et al.*, 2005; Dennis *et al.*, 2019] there is potential to improve their cost-effectiveness. Reductions in air flows to below those recommended in industry best practice guidance (60 - 240 L min<sup>-1</sup> m<sup>-1</sup> of bubbler length [Turnpenny & O'Keefe, 2005]) could save power, which although not a trivial challenge, could be achieved by exploiting the little-explored fundamental principles of bubble resonance and coalescence. A bubble is at resonance with a sound field if its pulsation rate, which depends on the bubble size, matches the frequency of the sound. When driven by an external sound field a bubble will extract energy from it and pulsate, in the process radiating some sound energy and converting other sound energy ultimately to heat through viscothermal processes in the gas and liquid. However, if the size of the bubble is such that the sound field causes the bubble to pulsate close to resonance, then this effect is magnified resulting in greater absorption of the sound, and a local resonance peak in scattering [Leighton, 1994]. This property can be used to trap sound between bubble plumes of a size tuned to the sound field, creating a sharper sound gradient, and potentially improving the effectiveness of the insonified bubble curtain.

The control of the size of bubbles generated is challenging at high flow rates, such as those typically used in industry, because of bubble coalescence. When a series of air bubbles are introduced underwater these will tend to merge with growing successor bubbles at the nozzle, creating a bubble with a diameter much larger than that of the orifice [Leighton *et al.*, 1991]. This process occurs unpredictably leading to the production of a wide distribution of bubble sizes, and its effect increases with increased air flow [Leighton *et al.*, 1991]. Although this problem can be mitigated by significantly lowering the airflow to generate a more consistent bubble size, this reduces the throughput of gas, requiring more orifices, and has a limited effect for bubbles much smaller than a millimetre radius. Adding a simple mobile phone vibrator to the injection nozzle [Leighton *et al.*, 2012], allows the control of bubble size for the same volume of

gas flowing through it by preventing coalescence at the nozzle. Vibrating the nozzles at different rates while using identical apertures and gas fluxes allows for the generation of bubble clouds with distinct characteristics. This method is applied in this study to test the way changing the bubble size distribution, changes the acoustic effects and its effectiveness as a deterrent.

This study investigated the potential of resonant acoustic bubble curtains to provide an effective fish deterrent. The objectives were to: (1) divorce the effect of visual cues from stimuli generated by the bubble curtain by quantifying fish behaviour in the presence or absence of light when encountering insonified bubbles, and (2) compare the effectiveness of resonant versus non-resonant insonified bubble curtains to deter passage, and determine the stimuli responsible for eliciting this response.

### **4.3 Methodology**

#### **4.3.1 Experimental Set-up**

All experimental trials were conducted using an annular raceway at the ICER research facility, Chilworth (see **Fig. 4.1**). The channel (1.0 m wide) contained conditioned still tap water (0.60 m deep). To aid recovery of fish after each trial an experimental section (8.0 m total length) was separated from the rest of the channel by wooden framed polyester mesh barriers (1 cm mesh size). While this set-up was asymmetrical due to presence of a walkway, attempts and passage efficiency did not differ with side of approach. Four underwater cameras were suspended to just below the surface of the water. Each had an effective field of view of 60 x 60 cm of the channel floor that overlapped to ensure complete coverage of the approach to the bubble curtain. Trials were conducted during the day and night (Experiment 1), and at night only (Experiment 2). Infra-red light (850 nm) units were used to illuminate the experimental area during night trials for the purpose of recording fish behaviour in the absence of visual cues. The raceway was covered by a sheet of tarpaulin to prevent any natural or artificial sources of light affecting the experiment (luminous flux measured for night trials: 0.0 - 0.02 lx). While carp are known to be sensitive to near-IR [Matsumoto & Kawamura, 2005] and there may have been some visual cues, this does not invalidate any day or night differences.



An insonified bubble curtain was used for both Experiments 1 and 2 (see **Fig. 4.2**). The bubble curtain consisted of two bubble clouds, one on either side of an Electrovoice UW-30 underwater speaker. The cloud was generated using a device consisting of 18 linearly arranged, horizontal, gauge 21 needles secured using luer-to-barbed adaptors (Cole Parmer, WZ-45518-46), and housed within modified lengths of plastic trunking (FIG. 1). Air supply (at 2 bar) was provided individually to the needles, via manifold air tubes (4 mm ID silicone), and 6.4 mm ID nylon tubing leading to a compressor (Clarke Bandit, 1 HP). Fine-scale control of air flow was ensured by using a three way pressure reducing valve (Honeywell, PRV) and air flow meter (IDS, MR3030). Vibration of the nozzles was provided by a total of 36 haptic feedback motors each of which were attached to each injection nozzle (Precision microdrives,

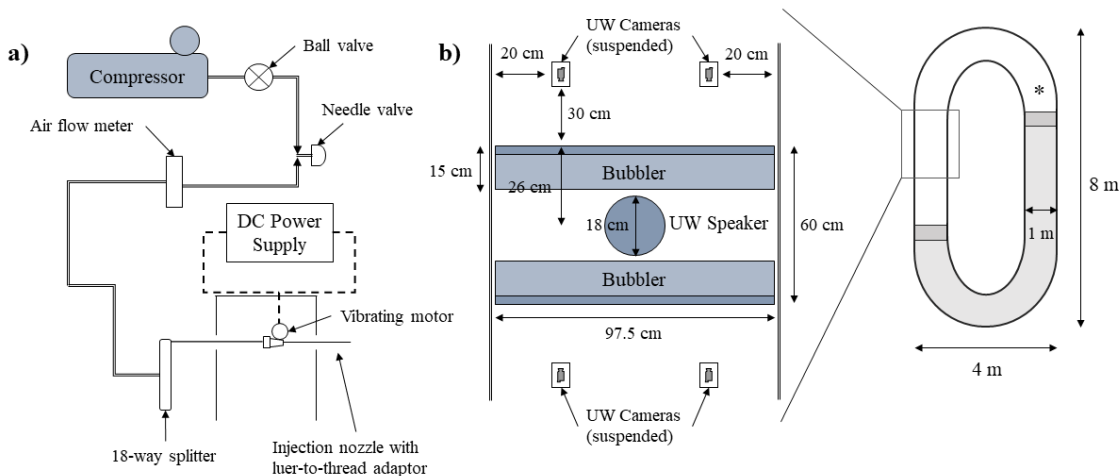


**Fig. 4.1 a)** Schematic of the bubble curtain and air supply system used for Experiments 1 and 2 of a study to investigate the response of common carp to insonified bubble curtains in the presence and absence of visual cues. A single needle is shown for simplification; **b)** plan of the experimental set-up used in Experiments 2 and 3. Grey areas indicate section of flume not used in experiment, dark grey blocks indicate mesh barriers. The asterisk indicates the release point for fish at the start of each trial. Set-up was asymmetrical due to presence of a walkway, although attempts and passage efficiency did not differ with side of approach.



**Fig. 4.2 – Left:** External view of one of the two bubblers used for this study. For health and safety reasons, injection needles were fitted into place once bubbler was positioned inside the flume. **Right:** Close-up of the 3D-printed cylindrical housing and vibrating motor.

307-103). Adjusting the voltage supplied to the motors, allowed control of the magnitude of the vibration. To protect the fragile flying leads, each motor was placed within a custom-made 3D printed cylindrical housing, and sealed in potting compound. Power was provided by two 30 V / 3 A DC Power blocks (Isotech, IPS 303DD). Each motor was connected in parallel using a series of terminal blocks.

For Experiment 1, two bubble populations were generated by injecting air (air flow: 10 L min<sup>-1</sup>, or 5 L min<sup>-1</sup> m<sup>-1</sup> of bubbler) through nozzles with or without vibration at 2.2 V. The bubbles were insonified by a continuous 1000 Hz pure tone signal emitted at a source level of 140 dB re 1 μPa at 1 m). For Experiment 2, two bubble populations were generated by injecting air (air flow: 6 L min<sup>-1</sup>, or 3 L min<sup>-1</sup> m<sup>-1</sup> of bubbler) through nozzles with or without vibration at 3V. The bubble clouds were either insonified by a 1750 Hz (144 dB re 1 μPa at 1 m) or a 4000 Hz (151 dB re 1 μPa at 1 m) continuous pure tone signal.

#### 4.3.2 Air Flow Rate selection and Bubble Sizing

To select and characterise the size distribution of the bubble populations, a short length of the bubbler used for Experiments 1 and 2 was tested in a glass tank (length: 80 cm; height: 40 cm; width: 40 cm). Air flow rates were chosen through informal testing with the short length bubbles based on two criteria: (1) as low, (2) as consistent a bubble size

as possible. For Experiment 1, a flow rate of 10 L min<sup>-1</sup> was selected as this was the lowest air flow measurable on the flow meter used with average bubble sizes resonant to 1000 Hz which carp are sensitive to. For Experiment 2, due to the availability of a flow meter sensitive over a range of 1 to 10 L min<sup>-1</sup>, a smaller flow rate of 6 L min<sup>-1</sup> was selected since the lower air flow made the changes in bubble size more distinct when the injection nozzles were vibrated.

The size of the bubbles generated for fluxes equivalent to 6.0, and 10 L min<sup>-1</sup> were determined at a pressure of 2 bar, and for vibration intensities of, 0 V, 2.2 V, and 3 V. For each set-up, five high-speed (1/800 s) photographs of the bubble streams were taken using a digital single-lens reflex (DSLR) camera with a macro lens, and processed in ImageJ (<http://fiji.sc/wiki/index.php/Downloads> Laboratory for Optical and Computational Instrumentation, University of Wisconsin-Madison, US). **Figure 4.3** shows the distribution of bubble sizes for the populations in the study, and **Figure 4.4** shows examples of the original high speed frames equivalent to 6 L min<sup>-1</sup> (3 L min<sup>-1</sup> m<sup>-1</sup>) with and without vibration at 3 V. Minnaert's equation [Minnaert, 1933] was used to identify a suitable incident sound frequency for each population. For further examples of high speed frames, refer to **Appendix C**.

#### 4.3.3 Determination of Extinction Cross-sections

The interaction of an acoustic field with an object, such as a bubble, can be characterised by three related quantities: the scattering ( $\sigma_s$ ), absorption ( $\sigma_a$ ), and extinction ( $\sigma_e$ ) cross-sections. The quantities define the power scattered, absorbed and lost from a plane wave incident on a bubble (see **Appendix D**) divided by the intensity of an incident plane wave, and so have dimensions of area. The ratio of the rate of energy loss by all mechanisms to the intensity of that incident plane wave is  $\sigma_e$  such that  $\sigma_e = \sigma_s + \sigma_a$  [Ainslie & Leighton, 2009]. To identify the bubbles with the greatest acoustic effect in each population, the extinction cross-sections ( $\sigma_e$ ) were determined for the bubble distributions in Experiments 2 and 3, for incident sound fields of 1000 Hz, 1750 Hz, and 4000 Hz. Here, equations (37) to (39) and (42) to (44) from Ainslie and Leighton [2011], based on work by Andreeva [1964] and Weston [1967] were used to calculate the damping factors ( $Q_{vis}$ ,  $Q_{rad}$ ,  $Q_{th}$ ), and cross-sections ( $\sigma_s$  and  $\sigma_e$ ), respectively (see **Appendix E** for details of equations used). Incoherent radiation is

assumed, allowing the cross-sections of individual bubbles to be summed to produce the cross-section of the cloud [Leighton, 1994].

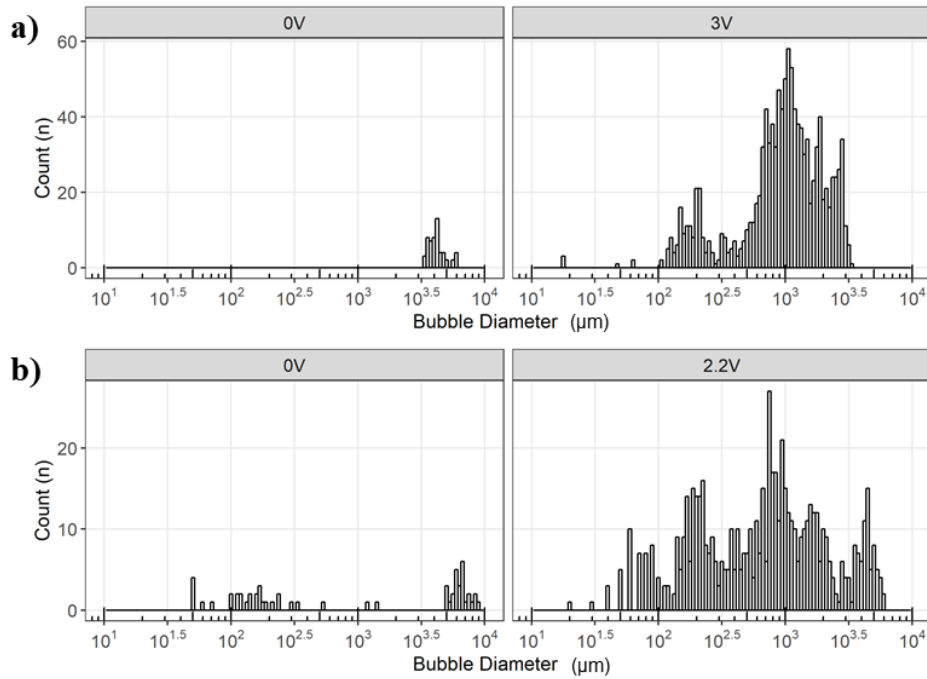


**Fig. 4.3** – Distribution of bubble diameters ( $\mu\text{m}$ ) at: **a)**  $6 \text{ L min}^{-1}$  ( $3 \text{ L min}^{-1} \text{ m}^{-1}$ ), with standard injection, and vibration at 3 V, **b)**  $10 \text{ L min}^{-1}$  ( $5 \text{ L min}^{-1} \text{ m}^{-1}$ ) with standard injection and vibration at 2.2 V. When the vibrating motors are activated, the general increase in bubble counts for the same volume gas flux is because the gas is distributed in more, smaller bubbles. Note that the volume of gas in the largest non-vibrating bubble peaks (diameters  $>10^{3.5}$  microns for (a) and  $>10^6$  microns for (b) disappear when vibration (3 V) is activated, and these peaks contain the bulk of the gas.

Each bubble population was characterised by a density function, where  $n(R)dR$  equals the number of bubbles (per  $\text{m}^2$  of bubble curtain, as the cloud is viewed from the horizontal direction) with an equivalent radius (i.e. the radius that a particular bubble would take had it been spherical and of the same volume) between  $R$  and  $R+dR$ . The population was divided into bins of such radii, and the power scattered, absorbed or lost from an incident plane wave by all the bubbles with equivalent radii was expressed as  $n(R)\sigma_s$ ,  $n(R)\sigma_a$ , and  $n(R)\sigma_e$ , respectively. The contribution of each bin to the acoustic scattering, absorption and extinction was determined to find which size of bubbles contributes the most. For each bin,  $\sigma_e$ ,  $\sigma_s$ , and  $\sigma_a$  were calculated for each combination

of bubble population and incident frequency and the results plotted. For each combination, the range at which the central 90 % of attenuation occurs,  $\sigma_e^{90}$ , was then determined (**Fig. 4.5**). This provided theory to explain the observed acoustical effects when identical volumes of gas are split between bubbles of different sizes (see **Appendix F** for modelled theoretical extinction coefficients of one bubble of each size for each frequency).

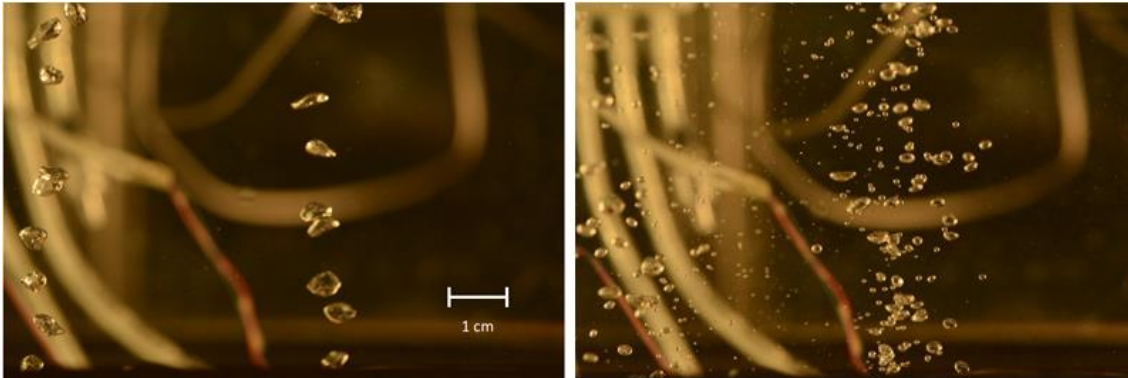


**Fig. 4.4** – Original frames of the two bubble populations equivalent to a flux of  $6 \text{ L min}^{-1}$  ( $3 \text{ L min}^{-1} \text{ m}^{-1}$ ) *left*: without vibration, *right*: with vibration at 3 V.

#### 4.3.4 Mapping of Stimuli

The acoustic spectra generated by the bubble clouds, speaker and vibrating motors alone, and all bubble/sound treatments used for Experiments 1 & 2 were recorded at a range of 1 m (see **Figs. 4.6** and **4.7**). For Experiment 3, the sound pressure level (SPL), and particle displacement (PD), were mapped at depths of 15, 30, and 45 cm, on a square grid of points with a 10 cm spacing up to a distance of 1 m from the speaker (see **Fig 4.8**). SPL measurements were made with a Brüel and Kjær 8103 hydrophone and pre-amplifier (Teledyne Reson VP2000). The signal was sampled at 44.1 kHz, using a USB 6341 data acquisition board (National Instruments, Austin, US). Data acquisition hardware was controlled using a custom virtual instrument in Labview (Labview 2017 64-bit, National Instruments, Austin, US).

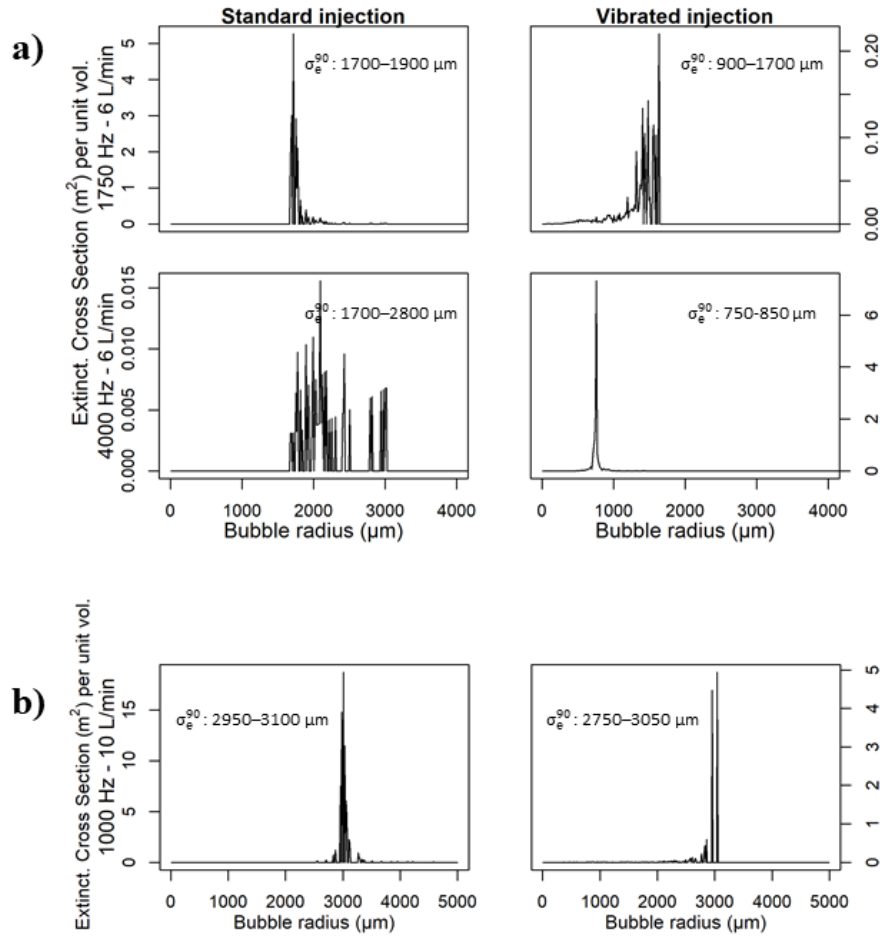


**Fig. 4.5.** – Modelled extinction cross sections for bubble distributions determined for Experiments 1 and 2: **a)** an air flow of  $6 \text{ L min}^{-1}$  ( $3 \text{ L min}^{-1} \text{ m}^{-1}$ ) insonified at either 1750 Hz or 4000 Hz, with either standard injection or vibration at 3 V, and **b)** an air flow of  $10 \text{ L min}^{-1}$  ( $5 \text{ L min}^{-1} \text{ m}^{-1}$ ) insonified at 1000 Hz with standard injection or vibration at 2.2 V.  $\sigma_e^{90}$  signifies the range of bubble diameters at which the central 90% of the attenuation occurs. The populations with a higher proportion of bubbles at resonance with the sound field are: 1750 Hz standard injection, 4000 Hz vibrated injection, 1000 Hz standard injection.

**Figure 4.6** shows spectra for Experiment 1. The highest peaks for both bubble populations were below 1000 Hz, and centred around 300 and 500 Hz. For the standard injection population, the intensity level for the 315 Hz and 500 Hz 1/3 octave bands were 107 and 104 dB re  $1 \mu\text{Pa}$  respectively. For vibrated injection (including motor noise), these were 110 and 108 dB re  $1 \mu\text{Pa}$ . Calculated band levels for the 200 Hz and 1250 Hz 1/3 octave bands produced by the vibrating motors (at 2.2 V) were 104 and 117 dB re  $1 \mu\text{Pa}$  at 1 m. The standard injection bubble population contained a greater

number of bubbles resonant to the 1000 Hz signal, which explains the differences between the spectra taken for both insonified set ups around 1000 Hz. **Figure 4.7** shows spectra for Experiment 2. Without vibration, the injected bubble cloud produced a broad spectrum of sound, with the highest peaks below 1000 Hz and centred around 500 Hz.

The intensity level for the 500 Hz 1/3 octave band was 97 dB re 1  $\mu$ Pa. The spectrum (which includes motor noise) obtained for the bubbles generated through vibrated injection at 3V shows peak frequencies at 100-150 Hz (128 dB re 1  $\mu$ Pa at 1 m) and at 250 – 500 Hz (115-120 dB re 1  $\mu$ Pa at 1 m), and 10-15 dB higher than that generated by the bubbles at frequencies above 1000 Hz. The calculated band levels for the 250 Hz and 500 Hz 1/3 octave bands produced by the vibrating motors were 127 and 132 dB re 1  $\mu$ Pa at 1 m. Key segments of the standard injection bubble population were resonant to the 1750 Hz signal, whereas the population generated through vibrated injection was resonant to the 4000 Hz treatment.

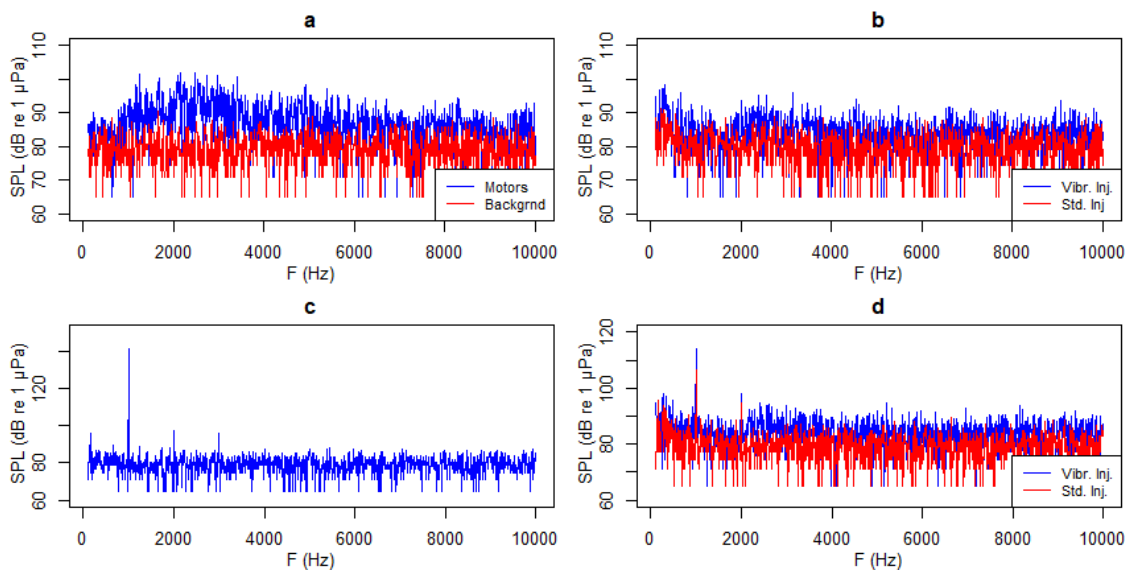


**Fig. 4.6** - Acoustic spectra for Experiment 1: a) background and vibrating motors (at 2.2V), b) both populations of bubbles, injected with standard injection, and vibrated injection, c) spectrum produced by the underwater speaker emitting a 1000 Hz tone, d) spectra for both bubble populations insonified by a 1000 Hz signal.

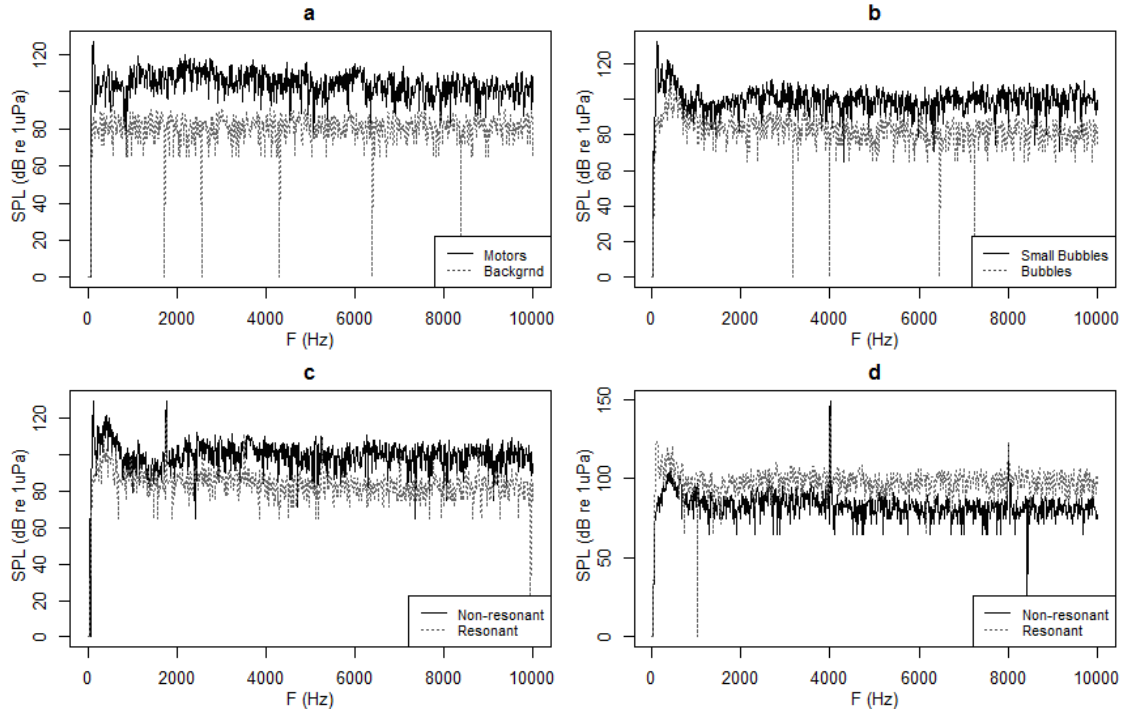


**Fig. 4.7** - Acoustic spectra for Experiment 2: a) background and vibrating motors (at 3V), b) both populations of bubbles, injected with standard injection (bubbles), and vibrated injection (small bubbles), c) spectra for both bubble populations insonified by a 1750 Hz signal, d) spectra for both bubble populations insonified by a 4000 Hz signal.

Particle velocity measurements were taken for Experiment 2 using four Brüel and Kjær 8105 hydrophones arranged tetrahedrally within a custom-built aluminium frame (See **Fig. 4.9** for assembly drawing of tetrahedral frame used to make particle velocity measurements), based on a set-up first proposed by Hickling & Wei [1995]. A custom Labview virtual instrument was used to record the magnitude and phase (relative to one hydrophone chosen as a reference) at each hydrophone. Measurements were taken at the driving frequency for the acoustic-bubble curtains, and at the peak frequency (400 Hz) for the vibrating motors. The discretised form of Euler's equation [Zeddies *et al.*, 2010], in a single dimension, was used to determine the particle velocity in the x, y, and z coordinates:

$$\text{Eq. 4.1} \quad \frac{P_1 - P_2}{\rho_0 d} = \frac{\partial u}{\partial t} \quad \text{where: } P_1 = Ae^{i\phi}$$



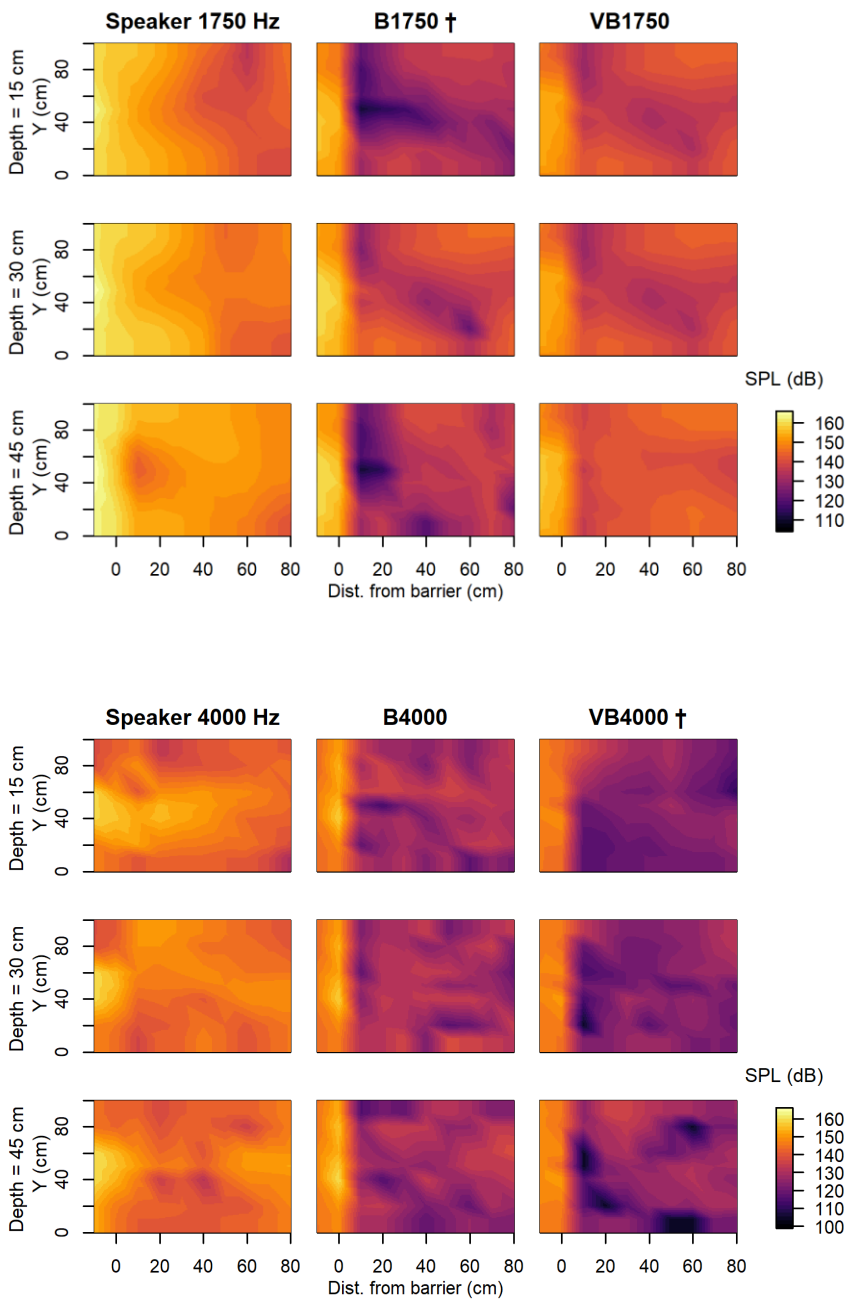


**Fig. 4.8** – Acoustic maps at 15, 30, and 45 cm depths for: *Top* - 1750 Hz bubble set-ups; *Bottom* - 4000 Hz bubble set-ups. Resonant treatments are marked by a dagger (Experiment 2). B = standard injection, VB = vibrated injection. On this scale the nearest edge of the loudspeaker is at horizontal position -17 cm, and the centre of the speaker at horizontal position -26 cm.

where  $P1$  and  $P2$  are the complex amplitudes measured at two points on the same plane, separated by distance  $d$ ,  $A$  is the zero-to-peak amplitude,  $\phi$  is the phase angle, and  $u$  is the velocity in line with the two points. The particle displacement was derived by dividing particle velocity with the square of the angular frequency,  $(2\pi f)^2$ .

The hydrodynamic field around the bubble cloud was quantified for Experiment 2 (see **Figs 4.11** and **4.12**). The presence of bubbles interferes with acoustic doppler-based instruments, so an electromagnetic flow meter (Valeport model 801, Valeport, Totnes, UK) was used to measure unidirectional velocity. Measurements were taken at 60 percent of the depth (36 cm from the surface) and at 10 cm intervals up to a distance of 1 m from the speaker. To quantify the turbulent flow induced by rising bubbles, the Turbulence intensity (TI) was used a metric. This was calculated by dividing the standard deviation by the mean water velocity.

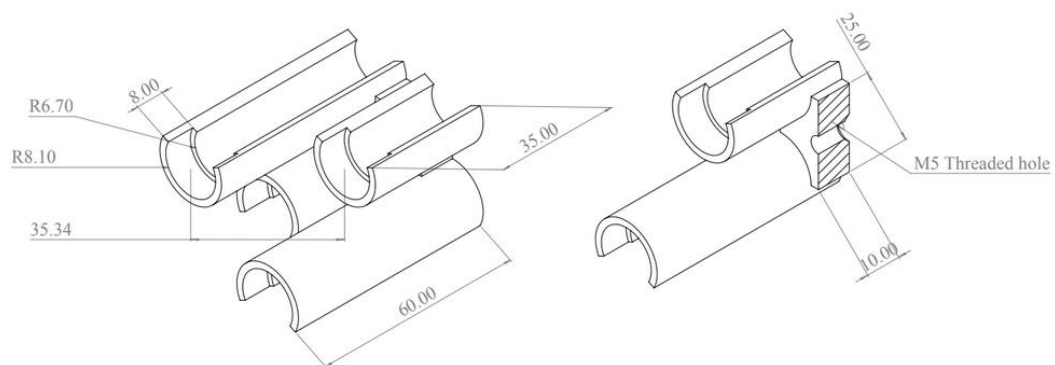


**Fig. 4.9** – Assembly drawing tetrahedral frame used to make particle velocity measurements. Material used was 6061-T6 aluminium, all measurements in mm.

#### 4.3.5. Subject fish

Common carp, a species with a connection between the swim bladder and hearing organs and known to be deterred by bubble barriers [Zielinski & Sorensen, 2016], was used as the model in this study. Fish were obtained from hatcheries in Hampshire, UK, and transported to the International Centre for Ecohydraulics Research (ICER) facilities at the University of Southampton in well-oxygenated water, and held in 3,000 L holding tanks containing well aerated and filtered water under ambient temperature. Water quality was checked daily and maintained at optimum levels ( $[\text{NH}_4^+] < 0.125$  ppm;  $[\text{NO}_2^-] < 0.25$  ppm).

At the end of each trial the subject fish were euthanized in accordance with Schedule 1 of the Animals (Scientific Procedures) Act 1986, and individual total body length ( $\pm 0.5$  mm) and mass ( $\pm 0.05$  g) recorded. Mean values were similar between experiments (see **Table 4.1**).

Experiment 1 was conducted with smaller fish, and water temperatures were lower than Experiment 2, and the previous chapter. Mean swimming velocity  $\pm$ SE was higher in Experiment 2 ( $0.099 \text{ ms}^{-1} \pm 0.0007$ ) than Experiment 1 (Mean:  $0.068 \text{ ms}^{-1} \pm 0.0006$ , Day:  $0.098 \text{ ms}^{-1} \pm 0.0011$ , Night:  $0.057 \text{ ms}^{-1} \pm 0.0005$ ). The number of approaches per hour did not vary considerably between Experiment 1 (Mean:  $36.40 \text{ hr}^{-1} \pm 1.89$ , day:  $37.56 \text{ hr}^{-1} \pm 3.55$ , night:  $35.28 \text{ hr}^{-1} \pm 1.65$ ) and Experiment 2 ( $34.43 \text{ hr}^{-1} \pm 2.49$ ). Despite the different durations of tests, all experiments were analysed separately, with results compared only within the same experiment.

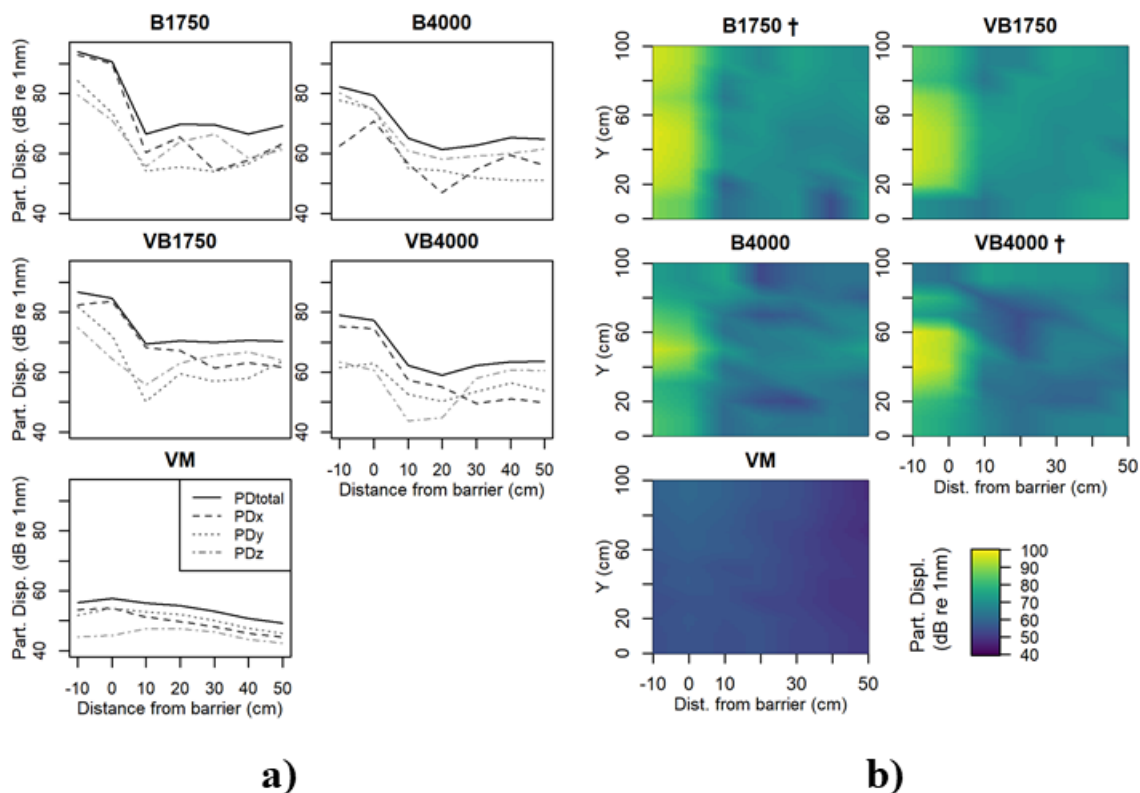


**Fig. 4.10** – Particle displacement in the: (a) xyz direction, and (b) maps at 20 cm depth. Resonant treatments are marked with a dagger (Experiment 2). B = standard injection, VB = vibrated injection.

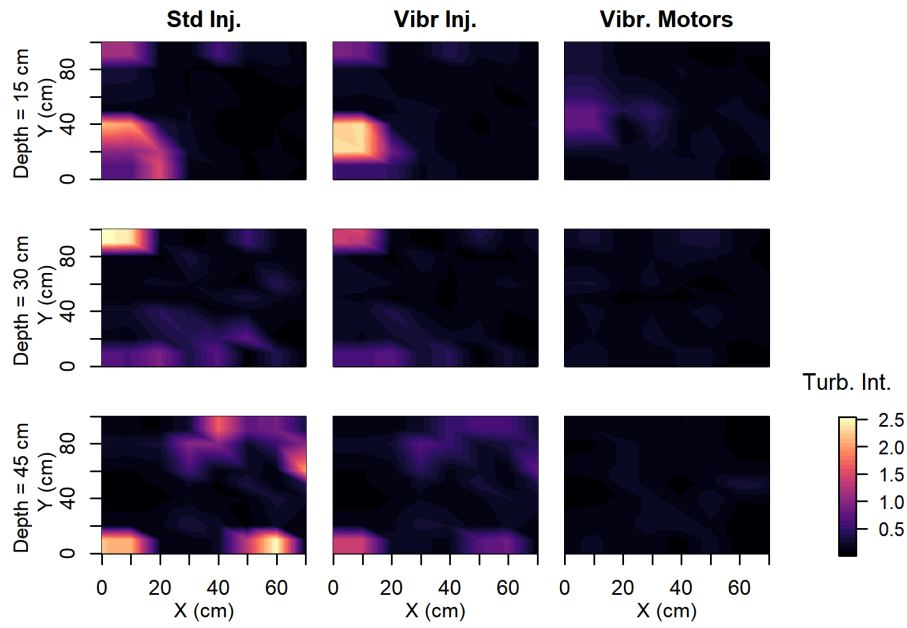


**Fig. 4.11** – Turbulence intensity for treatments in Experiment 2.

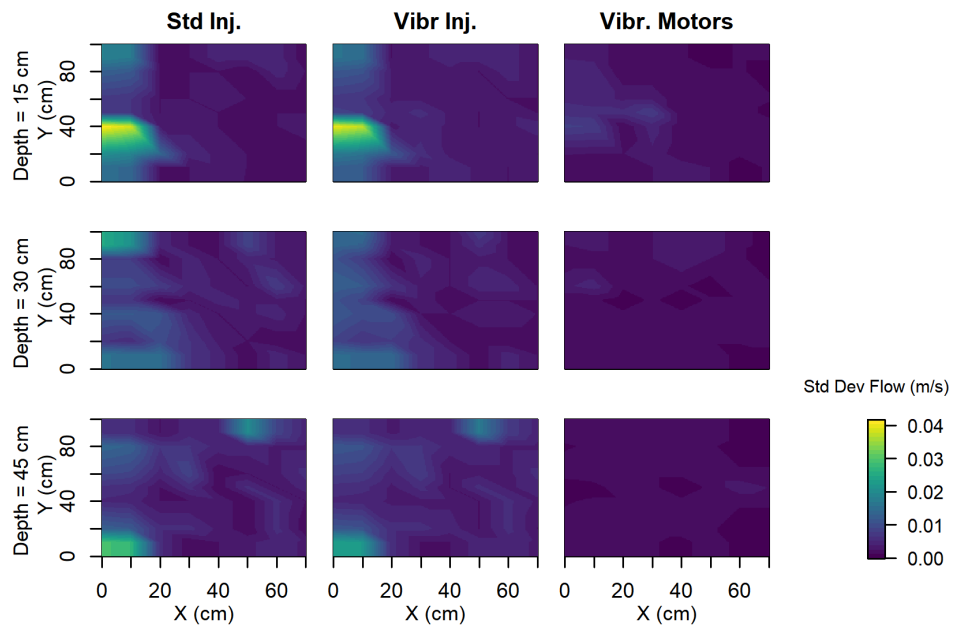


**Fig. 4.12** – Standard deviation of the flow ( $\text{ms}^{-1}$ ) for treatments in Experiment 2

**Table 4.1:** Mean length, weight, and holding tank temperature for common carp used in the two experiments to investigate their response to insonified bubble curtains.

<b>Experiment no.</b>	<b>Date</b>	<b>Mean (<math>\pm</math> SE) length (mm)</b>	<b>Mean (<math>\pm</math> SE) weight (g)</b>	<b>Mean (<math>\pm</math> SE) tank temperature (<math>^{\circ}</math>C)</b>
Experiment 1	Feb 2018	97.6 (0.6)	17.0 (0.4)	5.4 (0.4)
Experiment 2	Jul 2018	116.1 (0.7)	23.1 (0.5)	20.7 (0.3)

#### 4.3.6 Experiments

For each experiment, trials were conducted using groups of three similarly-sized individuals to enable shoaling behaviour typically exhibited by this species in the wild [Huntingford *et al.*, 2002; Sisler & Sorensen, 2008; Bajer *et al.*, 2010; Sloan *et al.*, 2013]. At the start of each set of trials, fish were placed in holding containers filled with water from the flume for the necessary time to acclimate to the flume water temperature (half an hour acclimatisation time for each  $1^{\circ}$ C difference). To ensure that the water temperature in the holding container remained within  $1^{\circ}$ C of the water temperature in the flume, a 50 % water change was carried out after every trial. Prior to each trial, naïve fish were carefully removed from the containers using a hand net and transferred to the experimental channel. The fish were allowed to acclimatise by swimming freely in the experimental area for 15 minutes prior to each trial commencing. Movement during trials was due to volitional behaviour.

##### *Experiment 1 – Influence of visual cues on fish response to an insonified bubble curtain:*

To investigate the influence of visual cues, a total of twenty-four 45 minute trials were conducted during hours of daylight (light) and a further twenty-four between the end of civil dusk (18:02 to 18:23 hrs) and midnight (dark) on the 16 to 28 February 2018. This experiment comprised 8 replicates of three treatments: a) injection with no vibration (i.e. standard injection), b) vibrated injection, c) no injection, but vibrating motors switched on (control). After the period of acclimation, the trials consisted successive phases defined as a pre-test (control), test (treatment or control), and post-test (control), each lasting 15 minutes.

##### *Experiment 2 - Comparing fish response to resonant and non-resonant bubble curtains:*

A total of sixty 80 minute trials were conducted at night (between the end of civil dusk: 21:15 to 20:45 and start of civil dawn: 03:40 to 04:50) between 1 and 22 August 2018. The experiment comprised 5 treatments: (a) 1750 Hz, standard injection (B1750, resonant), (b) 4000 Hz, vibrated injection (VB4000, resonant), (c) 1750 Hz, vibrated injection (VB1750, non-resonant), (d) 4000 Hz, standard injection (B4000, non-resonant), and e) vibrating motors only (control). After the initial acclimation period, twelve replicate trials were conducted for each treatment, each consisting of a 40 minute pre-test (control) phase immediately followed by a 40 minute test. The acoustic frequencies were selected by generating a sweep between 500 - 4500 Hz, with and without the bubble clouds to determine the effect of each population.

#### 4.3.7 Behavioural and Statistical Analysis

Video recordings were analysed to quantify common carp response to the insonified acoustic bubble curtains. Data were evaluated in three steps; (1) coarse-scale passage and rejection counts, (2) analysis of fish movement and orientation (sinuosity, swimming velocity, and angular dispersion), (3) fish response (binned rejection counts) relative to the gradients of the stimuli generated by an acoustic bubble barrier.

##### *1. Coarse-scale passage and rejection*

For all experiments, and for each trial, the coarse-scale metrics were recorded as per Chapter 3.3.3.

##### *2. Fish movement and orientation*

Swimming trajectories were determined for each approach by evaluating the position of the fish every fifth frame (450 ms) using Logger Pro (Vernier, USA). For every time step the following variables were recorded: Swimming velocity, step length, relative turning angle, and Euclidean distance from the bubble curtain. For approaches ending in a successful pass, the trajectories of fish before and after passage were analysed separately due to marked differences in trajectory directionality. Rejection tracks were also divided into two sections separated by the point of rejection, that is, the point after which fish showed directed and sustained swimming away from the barrier for more than one body length.

For approaches ending in a pass, the data collected were used to calculate indices of *Sinuosity* [Bovet & Benhamou, 1998; Benhamou, 2004]. For approaches

ending in a rejection, turning angles were binned at 5 cm intervals from the bubble curtain, and circular statistics used to calculate the mean angle, circular standard deviation, and mean vector,  $r$ , or *Angular dispersion* [Batschelet, 1981]. The Rayleigh test was used on each group of binned turning angles to test whether they differed from random [Batschelet, 1981] ( $p < 0.05$ ). See **Appendix G** for equations used to calculate mean angle, angular dispersion, and sinuosity, and **Appendix H** for checks of GAM models.

### 3. Response to stimuli generated by bubble curtains

Using data from Experiment 2, the relationships between fish trajectories and components of the stimulus: sound pressure level (SPL, dB re 1  $\mu$ Pa), particle displacement (PD, dB re 1 nm), and turbulence intensity (TI) generated by the insonified bubble curtain were analysed.

To determine whether SPL, PD or TI may act as thresholds for change in behaviour, the level of each at a fish's location was calculated for each time step using a custom Python script (Python v.3.7.3) in Ubuntu (Ubuntu v.18.04.2 LTS). For each time step, the gradients of each stimulus ( $\Delta$ SPL,  $\Delta$ PD, TI) to a virtual point one body length directly ahead of the fish were determined. The *Number of rejections* were binned at 5 cm intervals and the gradients within each interval were averaged. So as to reduce bias towards sound pressure values which showed a much wider range in pascals and also because response perception is often logarithmic [Fechner, 1860; Varshney & Sun 2013 Adler *et al.*, 2014], the sound pressure gradient was based on SPL, a logarithmic scale.

### 4. Statistical analysis

Coarse-scale and sinuosity data were tested for normality and homogeneity of variances using Shapiro-Wilk and Levene's tests. When these assumptions held, data were tested using two-way Anova with post-hoc Tukey HSD tests. Otherwise, a Kruskal-Wallis test with post-hoc Dunn Tests and Benjami Hochberg corrections was used.

For Experiment 1, generalised additive models (GAMs) were used to model the relationship between time of day (i.e. day or night), distance from the bubble curtain, direction (i.e. towards or away from the bubble curtain, prior to or after a *Pass* or *Rejection*), treatment, and phase (i.e. pre-treatment, treatment, post-treatment) on *Angular dispersion* and *Swimming velocity*, due to their non-linearity. For Experiment

2, GAMs with root-transformed gamma distributions were used to examine the relationship between the gradients of each stimulus, treatment, hydrodynamic treatment (i.e. standard injection, vibrated injection, or vibrating motors), and phase on *Angular dispersion* and *Swimming velocity*. Starting from a saturated model, stepwise deletions were performed to identify non-significant terms, and model selection was based on residual deviance and the lowest Akaike Information Criterion (AIC). The minimum adequate model (MAM) was arrived at as the most parsimonious models with lowest AIC value [Burnham & Anderson, 2002]. Finally, multiple regression with stepwise selection was used to test the relationship between the binned *Number of rejections* and stimuli gradients ( $\Delta$ SPL,  $\Delta$ PD,  $\Delta$ TI).

## 4.4 Results

### 4.4.1 Experiment 1: Influence of Visual Cues on Fish Response to an Insonified Bubble Curtain

Under conditions of daylight (see **Fig. 4.13**), the *Number of passes* were lower when a bubble curtain insonified by a 1000 Hz signal was active compared to a control ( $F = 4.97$ ,  $p = 0.01$ ,  $p\text{-adj} = 0.01$ ). Both treatments were more effective at night, resulting in lower *Passage efficiencies* ( $\chi^2 = 31.93$ ,  $p = < 0.01$ ) than during the day, with adjusted p-values of 0.048 and  $< 0.01$  for standard and vibrated injection, respectively. The vibrating motors treatment had no effect on either the *Number of passes* or *Passage efficiency*.

For carp that passed the bubble curtain, the approach trajectory was invariably more sinuous than when swimming away from the barrier after passage ( $\chi^2 = 64.05$ ,  $p < 0.01$ ) (see **Fig. 4.14**). *Sinuosity* was influenced by treatment and time of day (Table III). During daylight, fish exhibited more sinuous swimming trajectories during the test period than during the pre- and post-treatment phases for both the standard and vibrating injection treatments (*standard injection*:  $\chi^2 = 19.30$ ,  $p < 0.01$ ; *vibrated injection*:  $\chi^2 = 16.59$ ,  $p < 0.01$ ), while there was no influence on sinuosity when only the vibrating motors were operating ( $\chi^2 = 9.28$ ,  $p = 0.098$ ). At night, *sinuosity* was higher during the test period for all three treatments compared with the pre- and post-treatment control phases (*standard injection*:  $\chi^2 = 27.29$ ,  $p < 0.01$ ; *vibrated injection*:  $\chi^2 = 22.96$ ,  $p$



$< 0.01$ ; *vibrating motors*:  $\chi^2 = 12.74$ ,  $p = 0.03$ ). *Sinuosity* differed between treatments depending on whether it was day or night (*Day*:  $\chi^2 = 6.13$ ,  $p$ -value = 0.046; *Night*:  $\chi^2 = 8.22$ ,  $p = 0.02$ ); *sinuosity* was higher during the day only for the vibrated injection treatment ( $p = 0.04$ ), whereas at night it was higher for both bubble treatments versus the vibrating motors alone ( $p = 0.01$  for both).

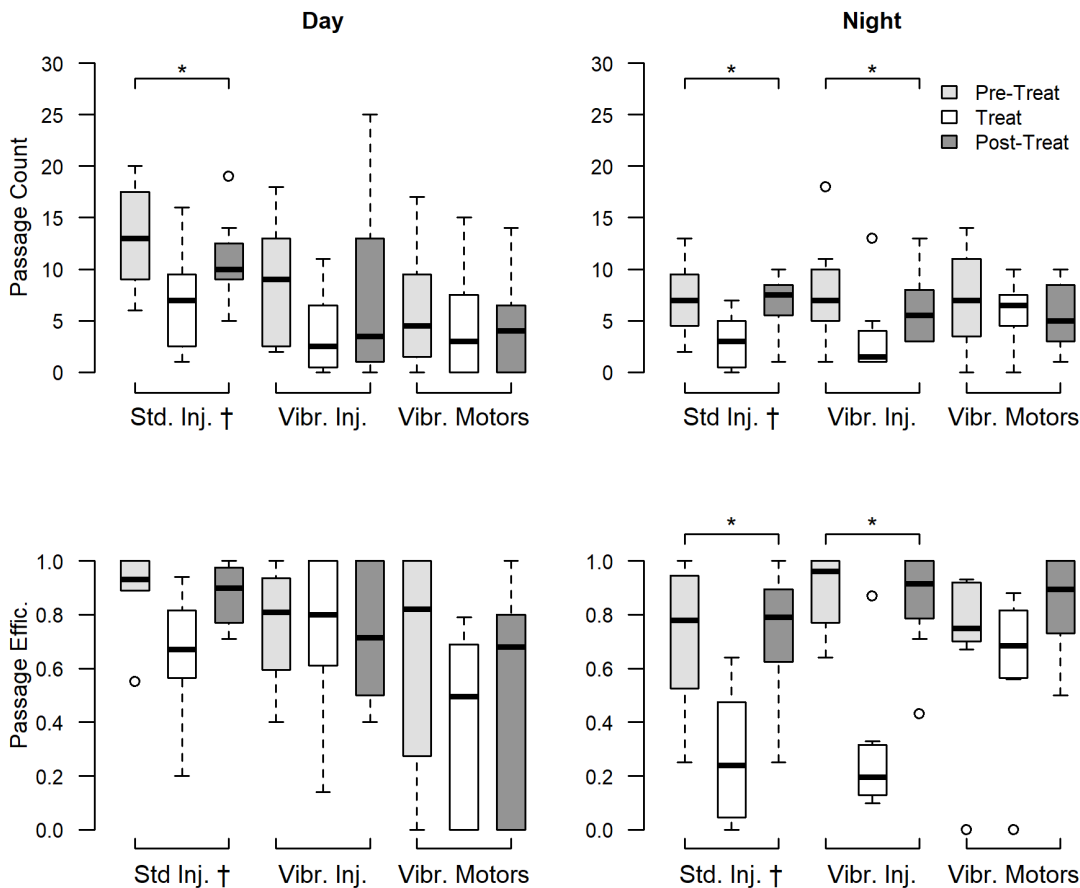


**Fig. 4.13** - The median, interquartile range and minimum/maximum whiskers of *Number of passes* and *Passage efficiency* for all treatments in Experiment 1 ( $10 \text{ L min}^{-1} / 5 \text{ L min}^{-1} \text{ m}^{-1}$  bubble curtain). Significant differences are denoted by an asterisk. Treatments with a greater number of bubbles at resonance with the sound field are marked by a dagger.

The presence of visual cues did not influence the trajectories of fish as they rejected the bubble curtain (see **Fig. 4.15**). The *Angular dispersion*,  $r$ , depended on distance from the bubble curtain, time of day, direction and phase. Using these parameters, the model explained 34% of the deviance. Trajectories were more sinuous during the treatment phase compared to the pre/post-treatment controls ( $p < 0.01$ ), and during the

vibrated injection treatment ( $p = 0.012$ ). *Swimming velocity* was dependent on distance from the bubble curtain, experimental phase, treatment, and time of day, with the model explaining 27.4% of the deviance when approaching the bubble curtain, and 28.4% when swimming away. In both cases, *Swimming velocity* was lower at night ( $p < 0.01$ ), and during the treatment phase compared to the rest of the trial ( $p < 0.01$ ). When approaching the bubble curtain *Swimming velocity* was lower nearer to it ( $p < 0.01$ ) for both bubble treatments compared to the vibrating motors only treatment ( $p < 0.01$ ). When swimming away, velocities were higher further away from the bubbler ( $p < 0.01$ ), and highest for vibrated injection ( $p < 0.01$ ).

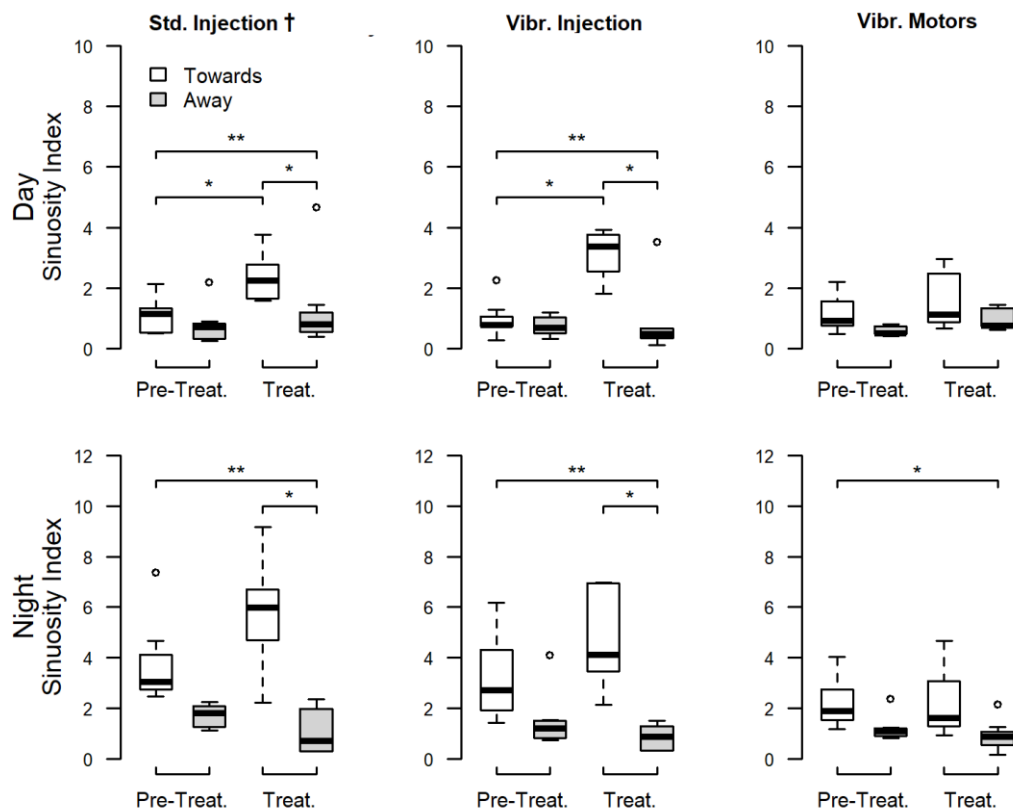


**Fig. 4.14** - The median, interquartile range and minimum/maximum whiskers of mean sinuosity indices per trial for passes ( $10 \text{ L min}^{-1} / 5 \text{ L min}^{-1} \text{ m}^{-1}$  bubble curtain). Pairs with significant differences are denoted by an asterisk. Treatments with a greater number of bubbles at resonance with the sound field are marked by a dagger.

#### 4.4.2 Experiment 2: Comparing fish response to resonant and non-resonant bubble curtains

The *Number of passes* were lower when the acoustic bubble curtain with a  $6 \text{ L min}^{-1} \text{ m}^{-1}$  airflow was operational than a pre-test control (*phase*:  $F = 61.46$ ,  $p < 0.01$ ; *treatment*:  $F = 3.27$ ,  $p = 0.014$  – see **Fig. 4.16**); both resonant treatments (B1750 and VB4000) and one of the non-resonant treatments (VB1750) had lower *Number of passes* ( $p\text{-adj} = 0.014$ ,  $< 0.01$ ,  $< 0.01$  respectively) than the pre-test control. The two resonant treatments reduced *Passes* by 65% compared to 45-50% for non-resonant treatments (B4000, VB1750), and 30% for vibrating motors alone ( $F = 4.20$ ,  $p < 0.01$ ). However, the difference between resonant and non-resonant treatments were not significant, with the difference existing between the two resonant treatments and vibrating motors alone ( $p\text{-adj} = 0.013$  and  $0.011$ , respectively). Passage efficiency was lower for all treatments compared to the pre-test control, with the exception of B4000 (B1750:  $\chi^2 = 15.27$ ,  $p < 0.01$ ; VB1750:  $\chi^2 = 11.25$ ,  $p < 0.01$ ; B4000:  $\chi^2 = 3.59$ ,  $p = 0.06$ ; VB4000:  $\chi^2 = 5.63$ ,  $p = 0.018$ ; VM:  $\chi^2 = 5.92$ ,  $p = 0.014$ ).

*Number of rejections* correlated with the gradient of all three stimuli ( $F_{3,46} = 9.11$ ;  $p < 0.01$  - **Fig. 4.17**), and stepwise selection determined that the most parsimonious model was the one that excluded the turbulence intensity term. Post-hoc modelling of the stimuli gave information on the individual contributions of each stimulus to the model ( $\Delta\text{SPL}$ :  $F_{1,48} = 11.59$ ,  $p < 0.01$ ;  $\Delta\text{PD}$ :  $F_{1,48} = 24.35$ ,  $p < 0.01$ ;  $\Delta\text{TI}$ :  $F_{1,48} = 2.68$ ,  $p = 0.11$ ). Visual inspection of the maps of SPL, and density maps of location of rejection showed that fish tended to switch direction and swim away from the bubble curtain in zones with the lowest SPL and PD, i.e. regions with the highest gradients.

For fish that successfully passed during the treatment phase, *Sinuosity index* values were higher on approach to the bubbler compared with when swimming away (**Fig. 4.18**). These differences were not observed during the pre-test control period (B1750  $\chi^2 = 13.93$ ,  $p < 0.01$ ; B4000  $\chi^2 = 11.54$ ,  $p < 0.01$ ; VB1750  $\chi^2 = 17.35$ ,  $p < 0.01$ ; VB4000  $\chi^2 = 14.42$ ,  $p < 0.01$ ; VM:  $\chi^2 = 12.03$ ,  $p < 0.01$ ).

Distance from the barrier was the most important explanatory variable in the MAM of *Swimming velocity* for successful passage approaches (**Table 4.2**), explaining 15.5% of residual deviance. *Swimming velocity* was also correlated with swimming direction, the hydrodynamic gradient, and treatment. For fish rejecting passage, the significant predictors were distance from the barrier, sound pressure gradient,

hydrodynamic gradient, and treatment. Models obtained for the difference angle data explained comparatively lower percentages of deviance in comparison with the swimming velocity models. Distance from the curtain ( $p < 0.01$ ), and swimming direction ( $p < 0.01$ ) explained 9.5 % of the variation for passage data, whereas rejection was influenced by distance from the curtain ( $p < 0.01$ ), and PD gradient ( $p < 0.01$ ), explained 8.5 % of deviance. Results of distribution and GAM checks for both models can be seen in **Appendix H**.

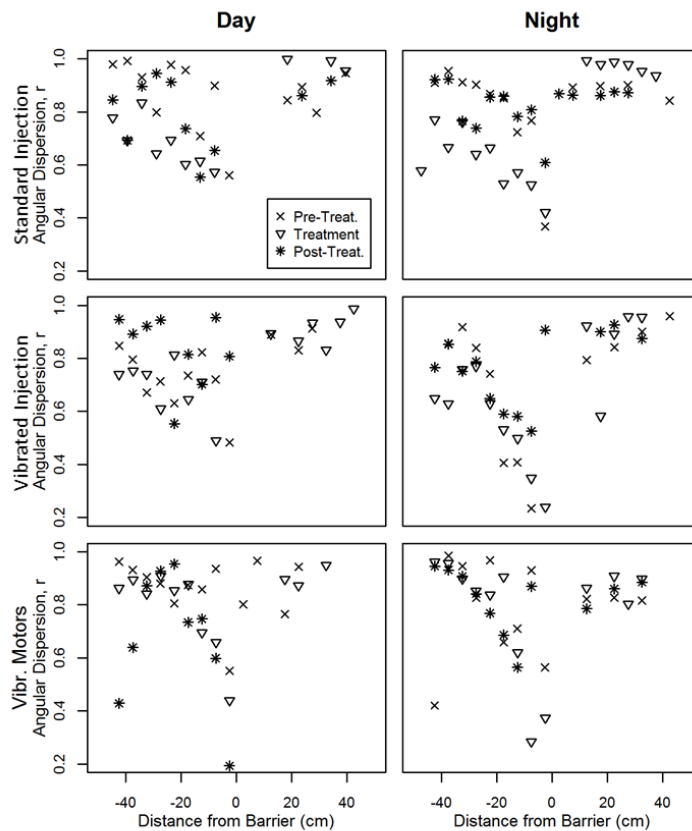


**Fig. 4.15** – Scatterplots of *Angular dispersion* for rejected attempts from Experiment 1 ( $10 \text{ L min}^{-1} / 5 \text{ L min}^{-1} \text{ m}^{-1}$  bubble curtain). Values nearer to 1.0 indicate greater directionality. Negative x-axis values indicate motion towards the barrier, positive x-axis values indicate motion away from the barrier.

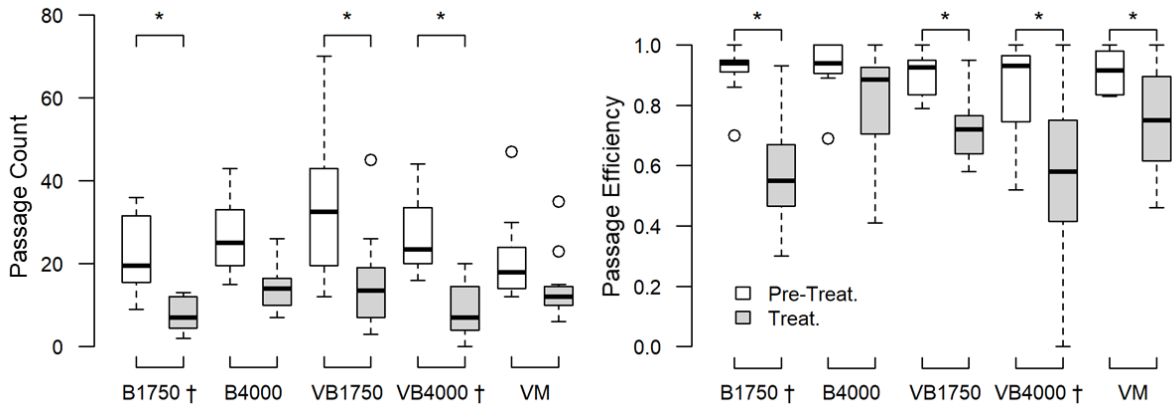


**Fig. 4.16** – The median, interquartile range and minimum/maximum whiskers of *Number of passes* and *Passage efficiency* for all treatments for Experiment 2 ( $6 \text{ L min}^{-1} / 3 \text{ L min}^{-1} \text{ m}^{-1}$  bubble curtain) during pre-treatment and test periods. Pairs with significant difference are denoted by an asterisk. Resonant treatments are marked by a dagger. B = standard injection, VB = vibrated injection.

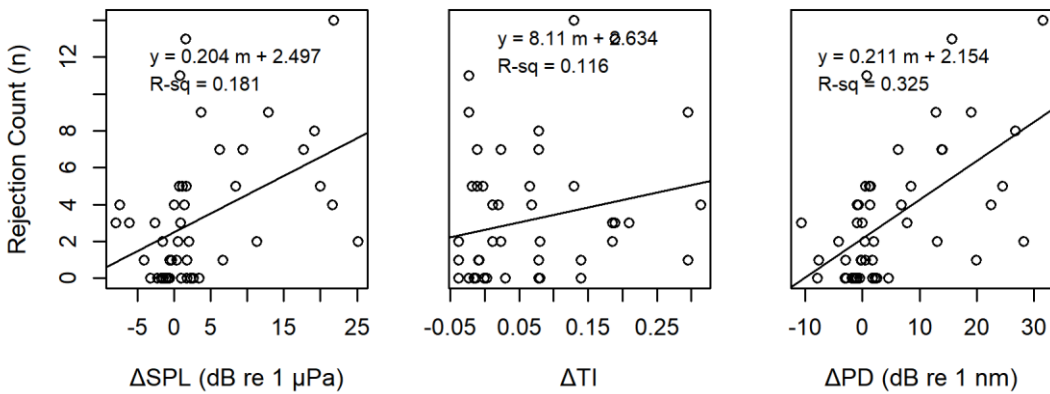


**Fig. 4.17** – Scatter plots of rejection counts against gradients (averaged for 5 cm bins) of all three stimuli generated by the bubble curtains.

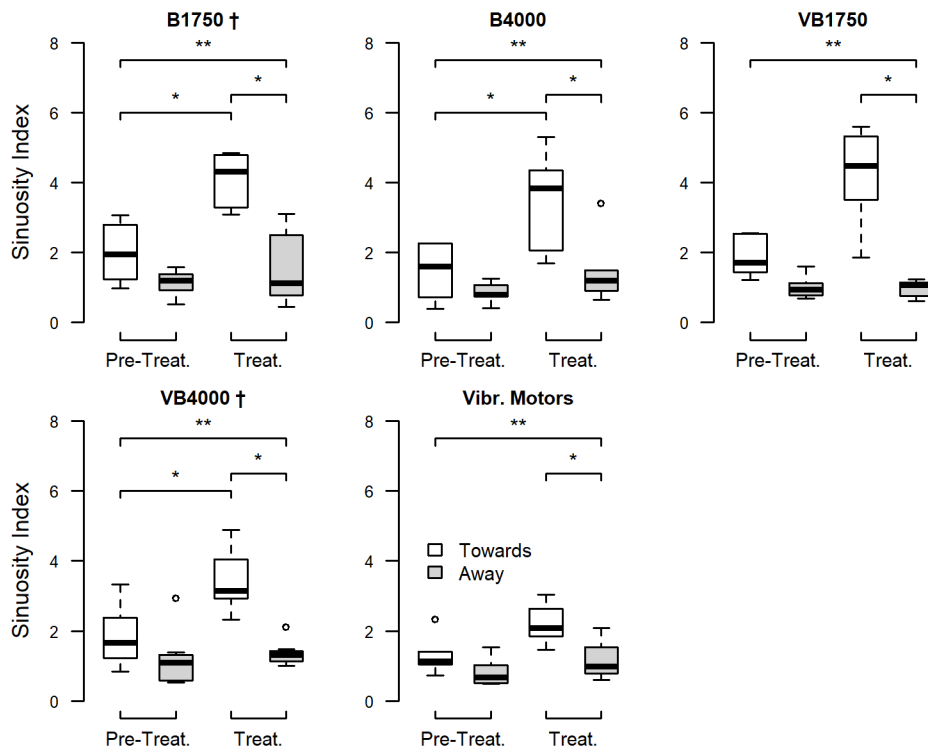


**Fig. 4.18** - The median, interquartile range and minimum/maximum whiskers of the mean sinuosity indices per trial for *Passes* during Experiment 2 ( $6 \text{ L min}^{-1} / 3 \text{ L min}^{-1} \text{ m}^{-1}$  bubble curtain). Pairs with significant difference are denoted by an asterisk. Resonant treatments are marked by a dagger.

#### 4.5 Discussion

The novelty of this study relates to three main elements; it is the first to: (1) compare the effectiveness of resonant versus non-resonant insonified bubble curtains to deter passage, determining the stimuli responsible for eliciting deterrence, and (2) consider the effect of visual cues in relation to acoustic and hydrodynamic stimuli generated by the bubble curtain by conducting trials under conditions of illumination and darkness. This was achieved by implementing the first flume deployment of a method to control bubble size using the same orifices and gas flow, by considering bubble coalescence [Leighton *et al.*, 2012]. To accomplish this in a small test tank, the air flow was much lower than what would be used in the field, so the fish responses were expected to be small. However in principle the system could readily be scaled up for field-scale facilities.

Resonant insonified bubble curtains were more effective at reducing passage in carp than non-resonant bubble curtains. A bubble population that contains more bubbles in resonance with the driving sound field will extract more energy from that field compared with a population that contains a less resonant bubbles. We can therefore postulate that the more abrupt changes in the acoustic stimuli due to the presence of a resonant bubble population were more likely to initiate avoidance in carp. Movement of carp away from an insonified bubble curtain appears to have been strongly influenced by the gradients of both particle displacement ( $\Delta PD$ ) and the sound pressure level ( $\Delta SPL$ ), and these findings seem to match previous literature.

**Table 4.2:** Results obtained for the modelled effects of the stimuli generated by an insonified bubble curtain on fish swimming velocity (Experiment 2). The deviance explained relative to null (%), estimated degrees of freedom (edf) and significance (p-value) of the terms in the minimum adequate model fitted to swimming velocity are listed. Brackets indicate smoothed terms.

Dataset	Model terms	Deviance explained relative to null (%)	edf	p value
Swimming velocity (Passage)	Treatment + Direction + s(Distance from barrier)	21.5 (minimum adequate model)		
	s(Distance from barrier)	16.9	8.27	<0.01
	Direction	4.2	-	<0.01
	Treatment	0.4	-	<0.01
Swimming velocity (Rejection)	Treatment + HydroTreatment + s(Distance from barrier) + s(SD Flow) + s(SPL) + s(PD)	17.6 (minimum adequate model)		
	s(Distance from barrier)	9.47	8.95	<0.01
	s(PD)	5.72	6.91	<0.01
	Hydrotreatment	1.41	-	<0.01
	Treatment	0.4	-	<0.01
	s(SD Flow)	0.5	3.8	<0.01
	s(SPL)	0.1	1.01	0.023

A previous study carried out with an acoustic bubble curtain ( $720 \text{ L min}^{-1}$ , or  $180 \text{ L min}^{-1} \text{ m}^{-1}$  of bubble curtain) [Zielinski & Sorensen, 2016] argued that deterrence is likely caused by acoustic particle motion in the near field of the bubble curtain. This

conclusion was reached by observing that carp rejected passage within 25 cm of the bubble curtain, which coincided with the region of maximum particle acceleration, whereas hydrodynamic forces generated by the bubbles extended 50 – 100 cm away from it. In this study hydrodynamic forces decreased rapidly beyond a distance of 25 cm away from the bubble curtain, whereas the higher air flows used to create the bubble curtain in the previous study [Zielinski & Sorensen, 2016] likely explain their larger hydrodynamic signatures. Despite the overlap with particle displacement and acoustic pressure, results showed that the gradient of turbulence intensity had no significant effect on the rejection count.

In the presence of daylight, insonified bubble curtains reduced passage in carp relatively less. Although course-scale efficiencies of bubble curtains have been known to vary between daylight and night [Welton *et al.*, 2002; Leander *et al.*, 2021], our findings quantified this behaviourally. In all three experiments, when encountering a bubble curtain in darkness, carp tended to engage in exploratory behaviour, and repeatedly swam along the front of or held position facing it, prior to a pass or rejection. Carp also reduced their swimming speed, and the degree to which this happened, as well as the distance at which reductions were observed was dependent on treatment type. It is likely that non-resonant treatments were better at reducing swimming speeds because the acoustic stimuli could be detected farther away. In daylight, however, these behaviours became less pronounced, noticeable from the higher passage efficiencies, higher swimming speeds, and a decrease in the sinuosity index. While this supports Welton *et al's* [2002] conclusions, Leander *et al.*, [2021] found that bubble curtains alone were more effective at guiding salmon smolts into a fishway during the day. This indicates that in the absence of other sensory cues such as a sound field, visual detection of the bubble curtain is important for eliciting deterrence [Leander *et al.*, 2021].

Earlier work suggests that fishes are highly dependent on the mechanosensory system in darkness, but when available, visual cues may be given more importance than hydrodynamic and acoustic signals [Rowe, 1999; Vowles *et al.*, 2014]. This could explain our video footage observations in Experiment 3, where fish swam through gaps in the bubble wall during the day, caused by needles moving out of alignment. Although this observation was qualitative, similar conclusions were drawn for Atlantic salmon smolts, which during the day appear to detect gaps in a bubble curtain that occur due to deposition



of silt on the perforated pipe, thus reducing the efficiency of the bubble curtain [Welton *et al.*, 2002].

While results from the two experiments are not directly comparable due to the different trial lengths, and the colder winter conditions and smaller sized fish in Experiment 1, nevertheless a pattern is apparent when looking at passage efficiency data. The 1000 Hz sound signal (from Experiment 1) appears to have been more effective at eliciting rejection, followed by the 1750 Hz, and the 4000 Hz signal in that order. This is largely in line with our knowledge of hearing sensitivities of carp. Although 4000 Hz is not the most sensitive range for carp, they may have reacted to the particle motion or hydrodynamic field generated by the bubble curtain for which behavioural audiograms do not currently exist. Given the reduced sensitivity to acoustic pressure at 4 kHz, the resonant 4000 Hz set-up was less effective than the resonant 1750 Hz one.

Testing was carried out in still water and fish behaviour was entirely volitional; they were not motivated or rewarded. This was largely due to limitations with the raceway; namely the absence of a pump, although using a flume with a hard bottom was acoustically preferable to the alternative of a glass flume. This, in conjunction with the fact that water temperatures were low during Experiment 1 means that care should be taken when extrapolating these results more generally given that carp behaviour changes with season [Bajer *et al.* 2010], time-of-day [Benito *et al.*, 2015], and temperature [Rome *et al.*, 1985]. While the ideal place for the barrier would have been in the middle of two symmetrical areas of the flume, this was not possible due to the presence of a walkway over the centre axis of the flume. Initial tests were conducted with the bubble curtain in that location however tracking fish and illuminating the flume in that region using IR lighting proved challenging due to the shadows created by the walkway, and the custom built structures that suspended the cameras underwater. This decreased the contrast, making it very difficult to track the fish in the near vicinity of the bubble curtain.

For both experiments, the range of  $\sigma_e^{90}$  was narrow for every insonified bubble curtain tested, and narrowest for the resonant set-ups. This implies that if past or future bubble curtain deployments injected a suboptimal bubble size; either by injecting a very wide range such that much of the gas pumped in does not contribute to the acoustical effect, or by generating a bubble cloud that does not contain resonant bubbles, they could

be highly inefficient. By altering the size of bubble generated, a large-scale deployment could change from not being cost-effective, to being practicable, efficient and affordable.

While the main scope of this work was a proof of concept study, it is important to draw attention to certain historical pitfalls when conducting experiments with underwater bubbles. The use of bubble curtains to contain sound fields through backscattering or attenuation dates back to 1948 [Love & Arndt, 1948]. Evaluations of bubble curtains used as behavioural deterrents for fish were also carried out at a number of sites on the Great Lakes in the 1970's [Hocutt, 1980], although many of these studies were grey literature reports, and lacked methodological details or in-depth categorisation of the stimuli used [Popper & Carlson, 1998]. Results were mixed and research into their use dropped. Recently, however, the interest in bubble curtains has been renewed due to the need to develop cost-effective and easily deployable barriers to prevent the spread of invasive carp in North America [Kelly *et al.*, 2011] and Australia [Koehn *et al.*, 2000], and also to protect them in their native range [Wu *et al.*, 1992; Chen *et al.*, 2004]. Despite the historical body of work on bubble curtains, the push towards specifying and measuring the stimuli they generate is a fairly recent one [Dawson *et al.*, 2006; Zielinski & Sorensen, 2016]. It is essential that this continues, and for the behavioural scientist to be able to carry out valid research and properly compare and interpret the results of others.

When using bubbles to create a multimodal stimulus (e.g. with sound) great care should be taken to consider what determines the size of a bubble, and how this may affect its properties and the replicability of the study. For a given nozzle size, there is a bubble of maximum volume, and its size depends on: (1) the rate of air flow to the bubble, and (2) whether the system is operated in a pressure-controlled or volume-controlled mode [Clift *et al.*, 1978; Longuet-Higgins *et al.*, 1991]. When introducing air underwater, as gas flow is increased, rising bubbles come into contact with one another and coalesce to form larger bubbles. Higher flow rates (e.g. 30 mL s<sup>-1</sup> per nozzle) result in a wide range of bubble sizes growing at the orifice or generated by the fragmentation of existing bubbles [Leighton *et al.*, 1991]. Since detachment and fragmentation occur unpredictably, using the size of the orifice to measure the bubble size used in an experiment is unreliable.

Our study used the tactic of generating bubble curtains using the same apertures and gas fluxes, but activated with different levels of needle vibration, to determine how fish react to bubble curtains. Leighton *et al.*, [2012] first demonstrated (with video at

[www.isvr.soton.ac.uk/fdag/PIPE\\_DEMO/index.htm](http://www.isvr.soton.ac.uk/fdag/PIPE_DEMO/index.htm) ) how the mass flux of gas through a needle could be made to deliver varying but controllable changes to the acoustic absorption, by vibrating the needle with a mobile phone vibrator. A needle that would normally generate bubbles that are ineffective at absorbing sound would, when vibrated, produce a cloud of much smaller bubbles because they did not coalesce at the nozzle [Leighton *et al.*, 1991]. Being closer to resonance with the acoustic field, these smaller bubbles attenuated sound better, even though the gas flow rate into the needle was unchanged. This demonstrates that simply stating the gas flow rate and aperture size is not sufficient to characterise an acoustically-active bubble curtain, because the bubble size distribution also has to be known. Knowing the size composition of the bubble population (obtained through photography, or acoustic measurement methods [Longuet-Higgins *et al.*, 1991; Leighton *et al.*, 1998]), gas flow rate, and the gas pressure in addition to mapping the fields for the various stimuli generated should be considered a starting point for future experiments involving bubbles and sound. Determining,  $\sigma_e^{90}$ , the size fractions responsible for 90% of the extinction of the energy from an incident wave could prove a useful tool to determine the most effective range of frequencies to use for a given bubble population.

Given that this study focused on the comparing the deflection efficiencies of resonant vs non-resonant bubble curtain set-ups, the deflection efficiencies of the same in daylight vs night, in an effort to limit the number of treatment and to limit the number of animals used, controls with just the speaker and with just a bubble curtain were not included. For completeness, it would be advisable to carry out such controls in future work. While 4000 Hz is not within the most sensitive range of carp hearing [e.g. Vetter *et al.*, 2018], the approach taken here was to match the sound frequencies to the bubbles generated. In line with carp audiograms, in Experiment 2 the 4000 Hz set-ups were relatively less effective than their respective 1750 Hz treatments. However, carp also reacted to the particle motion or hydrodynamic field for which behavioural audiograms do not currently exist [Popper & Hawkins, 2019]. Furthermore, the ability of a fish to detect a sound may not necessarily evoke a response [Putland & Mensinger, 2019; Leighton *et al.*, 2020].

Much scope remains for research and a logical next step would be to maximise deterrence. Using slightly higher air flows (e.g. 10 – 20 L min<sup>-1</sup> m<sup>-1</sup>) the deterrent effect of resonant bubble curtains insonified by: (1) a single tone versus, (2) multiple tones, and

(3) broadband signals, each selected specifically to drive one or more bubble size ranges to resonance, could be compared. The influence of group effects [e.g. Currie *et al.*, 2020] and long-term habituation could also be considered [Putland & Mensinger, 2019]. We echo earlier calls [e.g. Deleau *et al.*, 2019] that such technologies should not be used as an absolute barrier, but incrementally improved to deflect, or redirect fishes; e.g towards fish passes where even moderate improvements in passage rates could help conserve sensitive species. To avoid habituation such deterrents are best used in situations where fish will be in contact with the stimulus for a brief period of time such as during a migration, or in tidal areas [Turnpenny & O’Keefe, 2005, Zielinski & Sorensen, 2016].

#### **4.6 Conclusion**

This study used injection nozzles and vibrating motors to generate populations of underwater bubbles of different size and composition while using the same air flow. These were insonified by sound fields of different frequencies to test the effectiveness of resonant versus non-resonant insonified bubble curtains as deterrents for fish passage, and in the absence or presence of light. Results show that bubble clouds in resonance with a sound field are more effective deterrents, and that passage rejection in common carp is likely mediated by multimodal cues. The presence of visual cues significantly increased passage efficiency and swimming velocity, and fish followed less sinuous trajectories compared to the same conditions in the dark. This indicates that visual cues are likely prioritised by carp.

When working with bubble curtains, due consideration should be given to what influences the size of a bubble, and how this affects the way a bubble cloud interacts with an incident sound field. Care should be taken to ensure replicability and better control over the stimuli generated through detailed categorisation.

#### **4.7 Ethics**

The study conformed to UK legal requirements and was approved by the University of Southampton's Ethics and Research Governance Office (Ethics IDs: 40073, 42546).



## Chapter 5

### **Reactions of common carp to sound fields with varying acoustic pressure to particle displacement ratios.**

#### **5.1 Abstract**

Sensitivity to particle motion is an ancestral mode of hearing among fish, and their spectrum of hearing runs between fish that can only detect particle motion, to fish with anatomical specialisations which link the swimbladder to the hearing organs allowing them to sense acoustic pressure. Recent discussions in the field of underwater sound have identified a need to improve the understanding of fish response to particle motion. In this study, the phase of a signal emitted by two speakers positioned opposite each other was manipulated to create areas with stronger or weaker ratios of sound pressure to particle motion. When swimming across a 1 m<sup>2</sup> rejection zone, fish were significantly more likely to reject passage when encountering a region of high acoustic pressure. Despite a higher than expected level of behavioural noise, binomial models revealed changes in the significance of variables as fish moved closer to the centreline of the reaction zone, and with successive crossing attempts. Models had greater predictive power within  $\pm 10$  cm of the centreline, where experimental phase and  $\Delta PD$  and SPL played a consistent role at eliciting rejection. Swimming speed was dependent on the distance from both speakers, time, mean light flux, location of the fish in the X plane, PD, and the  $\Delta SPL$ .

#### **5.2 Introduction**

Understanding the physical properties of sound is critical when considering the impact of acoustic deterrents on fish. Sound is a waveform that travels through a medium accompanied by a transfer of energy from place to place [Urick, 1983]. The waves consist of alternating pressure deviations, which cause localised regions of compression and rarefaction, called sound pressure. The particles within the medium do not travel with the propagating sound wave, but transmit the oscillatory motion to their neighbours. This is referred to as particle motion and contains information about the direction of the propagating wave. Particle motion can be expressed as displacement

(m), velocity ( $\text{ms}^{-1}$ ) or acceleration ( $\text{ms}^{-2}$ ). These three quantities are directly related through the following equations:

$$\text{Eq. 5.1} \quad a = u \times 2\pi f$$

$$\text{Eq. 5.2} \quad \xi = \frac{u}{2\pi f}$$

Where:  $a$  = acceleration ( $\text{ms}^{-2}$ ),  $u$  = particle velocity ( $\text{ms}^{-1}$ ),  $2\pi f$  = angular frequency ( $f$  = frequency in Hz), and  $\xi$  = displacement (m)

Recent advancements in understanding fish hearing have shown that there is a continuum of hearing capabilities across species based on the contributions of acoustic pressure to the overall hearing capabilities of a given species [Popper *et al.*, 2003; Hawkins & Popper, 2016]. Popper *et al.* [2014], for example, suggested four key groups. Firstly, species which have the most ancestral mode of hearing which involves sensitivity to particle motion via direct inertial stimulation of the otoliths (e.g. elasmobranchs) [De Vries, 1950] Secondly, fish with a swim bladder where the organ does not appear to play a role in hearing. Such species (e.g. salmonids) show sensitivity only to particle motion and a narrow band of frequencies. Thirdly, species with swimbladders that are close, but not connected to the ear (e.g. codfishes, drums and croakers), which show a more extended hearing range of up to 500 Hz. Finally, species with specialised skeletal adaptations e.g. the Weberian ossicles that connect the swimbladder to the inner ear. The swimbladder acts as a pressure transducer, extending the hearing sensitivity of such species (e.g. cyprinids, clupeids) to several kHz.

Although some fish are sensitive to acoustic pressure, most detect particle motion [Popper & Fay 2011]. Many elasmobranch species detect and respond to underwater sounds [Myrberg, 2001; Casper *et al.*, 2012], and particle velocity plays an important role in locating sound sources through directional hearing [Schuijf & Hawkins, 1983; Hawkins & Popper, 2016]. In the natural environment, there are a number of circumstances where the magnitudes of particle motion are much greater than for a given sound pressure; for example close to the water surface and in shallow water [Popper & Hawkins, 2018], or in channels constructed or heavily modified for human

use [Leighton *et al.*, 2020]. As a consequence, it is important to take into account the acoustical habitats that fish are occupying, and the possible conversion of sound pressure into particle motion, when assessing whether they can detect sounds from a particular source.

In spite of recent regulatory work on the impacts of anthropogenic noise on fish and invertebrates, and efforts to standardise metrics and methodologies [Ainslie *et al.*, 2019], reviews of research gaps have pointed out that sounds and thresholds are currently mostly described in terms of acoustic pressure [Hawkins *et al.*, 2015; Nedelec *et al.*, 2016; Popper & Hawkins, 2018; Popper *et al.*, 2019]. The need for the following has been highlighted [Hawkins *et al.*, 2015; Nedelec *et al.*, 2016; Popper & Hawkins, 2018]:

- Consensus on the adoption of relevant and universally acceptable metrics for sound pressure and particle motion so that sounds may be described appropriately;
- Further fundamental work on whether particular species are sensitive to sound pressure or particle motion, and respective hearing thresholds;
- Obtain information on the background levels of particle motion in the sea and other aquatic environments.

Given that focus on this area is relatively recent, it is perhaps not surprising that few studies of underwater acoustic ecology have measured the particle-motion component of sound [Popper & Fay, 2011; Nedelec *et al.*, 2016; Popper *et al.*, 2019]. Field studies that measured particle motion are limited [e.g. Chapman & Hawkins 1973; Nedelec *et al.*, 2014, 2015; Sprague *et al.*, 2016; Campbell *et al.*, 2019], as are studies that provide insight on the relation between pressure and particle motion reception in different species [Chapman & Hawkins, 1973; Hawkins & Johnstone, 1978; Jerko *et al.*, 1989; Myrberg & Spires, 1980; Zielinski & Sorensen, 2016, 2017; Campbell *et al.*, 2019]. Two of these studies examined the roles that sound pressure and particle motion might play at mediating common carp response first to a bubble curtain [Zielinski & Sorensen, 2016], then to broadband noise [Zielinski & Sorensen, 2017] in the absence of visual cues. In their work they showed that fish responded to acoustic pressure levels



greater than 140 dB by negative phonotaxis, but maintained a nearly perfect 0 orientation to the axes of particle acceleration swimming away from a speaker. This indicates that carp avoid complex sounds in darkness and while initial responses may be informed by sound pressure, sustained oriented avoidance behaviour is likely mediated by particle motion [Zielinski & Sorensen, 2017].

Particle motion also appears to have played a key role in the previous chapter, where, in the vicinity of an insonified bubble curtain the change in the gradient of particle displacement played a key role in eliciting avoidance in carp. Explicitly examining the separate roles of either particle motion or sound pressure generated by a bubble barrier is challenging, however this can be achieved by manipulating sound fields using speakers to create sound fields with stronger or weaker ratios of sound pressure to particle motion [Zielinski, pers. comm.].

One can generate areas of low acoustic pressure through destructive interference or incoherent addition, termed; “acoustic holes”. This can be done by creating two sound waves: 1) a first sound wave,  $A_{\max}\sin(\omega t)$ , of amplitude  $A_{\max}$  and angular frequency  $\omega t$ ; and 2) a second sound wave  $A_{\max}\sin(\omega t + \phi)$ , with a phase shift,  $\phi$ , of e.g. 180°. The location of the “acoustic hole” can be changed by further manipulating the phase of the signal. Given that in a plane wave, particle displacement lags the acoustic pressure and particle velocity by 90°, areas of low acoustic pressure would correspond to areas of higher particle displacement.

This experiment investigated the reaction of common carp, a species with a connection between the swim bladder and hearing organs, to manipulated sound fields using speakers to create areas with stronger or weaker ratios of acoustic pressure to particle motion. The objectives were to: 1) determine whether regions with different levels of acoustic pressure to particle-motion influenced fish behaviour; 2) determine the stimuli responsible for eliciting the response.

### 5.3 Methodology

#### 5.3.1 Experimental Set-up

All experimental trials were conducted using an annular raceway at the ICER research facility, Chilworth (see **Fig. 5.1**). The channel (1.0 m wide) contained conditioned tap

water (0.40 m deep). An experimental section (3.0 m total length) was separated from the rest of the channel by wooden framed polyester mesh barriers (1 cm mesh size). Two cameras (Swann PRO-A850 720P) were suspended 2 m above the bottom of the flume, and each had an effective field of view of half of the channel floor (1.5 m x 1.0 m of the flume bottom), which overlapped to ensure complete coverage. Trials were conducted during the day. The raceway was covered by a sheet of tarpaulin to prevent any fluctuations in natural light affecting the experiment, illumination was provided by two fluorescent aquarium lights (10 W) which faced the ceiling of the tarpaulin, so as to avoid directly illuminating the flume but also to avoid triggering the infrared (IR) sensor in the cameras (i.e. > 1.0 lx; luminous flux measured for trials: 1.5 – 5.2 lx).

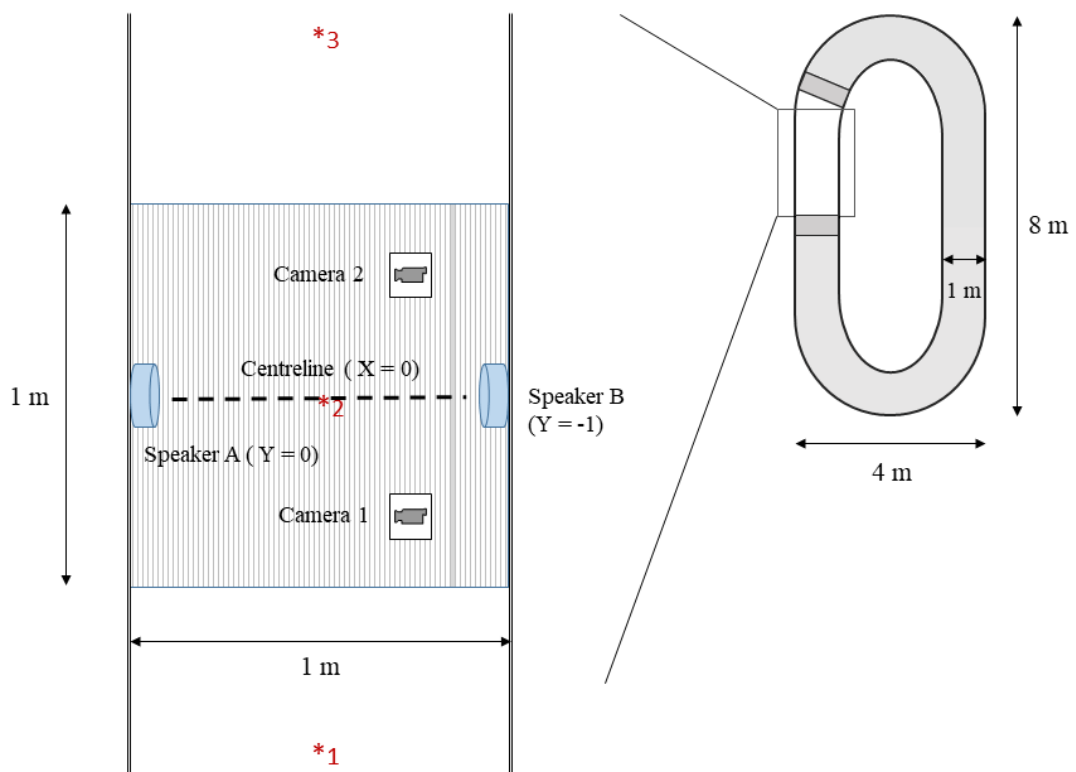


**Fig. 5.1** - Schematic of the experimental setup. Area marked with grey vertical lines indicates the “reaction zone”, and asterisks mark the three randomly selected fish release points. Due to the location of the cameras, for tracking purposes, the left-most speaker (Speaker A) in the diagram was considered to be  $Y = 0$ , the right-most speaker (Speaker B) was  $Y = -1$ . The virtual “centreline” running between both speakers was considered to be  $X = 0$ , with the limits of the reaction zone at  $X = 0.5$  and  $X = -0.5$ . The dark grey boxes indicate location of the mesh barriers, and light grey sections indicate areas of the flume not used in the experiment.

Two Electrovoice UW-30 underwater speakers were positioned opposite to one another on either side of the flume, separated by a distance of 1 m. The centre of each speaker was placed at a depth of 15 cm. Two lines were marked out on the flume bottom using waterproof tape, 50 cm away from a virtual “centreline” between the two speakers. This 1 m x 1 m area was considered to be the “reaction zone”.

### 5.3.2 Experimental trials

Trials were conducted using groups of five similarly-sized individuals to enable shoaling behaviour typically exhibited by this species in the wild [Huntingford *et al.*, 2002; Sisler & Sorensen, 2008; Bajer *et al.*, 2010; Sloan *et al.*, 2013]. At the start of each set of trials, fish were placed in holding containers filled with water from the flume for the necessary time to acclimate to the flume water temperature (half an hour acclimatisation time for each 1°C difference). To ensure that the water temperature in the holding container remained within 1°C of the water temperature in the flume, a 50 % water change was carried out after every trial ( $\bar{x}$  temp flume ( $\pm$  SE):  $15.42 \pm 0.11$  °C ;  $\bar{x}$  temp. holding tank ( $\pm$  SE):  $15.66 \pm 0.10$  °C).

Prior to each trial, fish were carefully removed from the containers using a hand net and transferred to the experimental channel. The fish were allowed to acclimatise by swimming freely in the experimental area for 20 minutes prior to each trial commencing. The initial location (i.e. far left, centre, or far right of the experimental arena) of fish was randomly chosen at the beginning of each trial.

*Experiment - Reactions of common carp to regions of sound with high acoustic pressure, and high particle displacement:*

To investigate the influence of the two components of a sound field a total of 32 trials, each 60 minutes long, were conducted during hours of daylight, (between 08:00 and 20:00) on the 18<sup>th</sup> through to 30<sup>th</sup> June 2019. After the period of acclimation, the trials consisted of two successive experimental phases defined as a pre-test (control), and test (treatment or control), each lasting 30 minutes.

This experiment comprised of 8 replicates of two treatments, both speakers emitting a 1750 Hz pure tone (146 dB re 1  $\mu$ Pa at 1 m) with: a) no shift in phase (0-0), and b) one speaker phase-shifted by 270° (0-270). Signals were generated on a laptop

using a custom virtual instrument in Labview (Labview 2017 64-bit, National Instruments, Austin, US), signals were generated on a separate channel for each speaker. The laptop was connected to a USB 6341 data acquisition board (National Instruments), and connected to an amplifier via two BNC cables. Speakers were plugged into a two-channel power amplifier (HH Electronic VX-200).

Common carp demonstrate schooling behaviour, and therefore the speakers were only activated when a group of three fish or more swam into the reaction zone. This was termed a *Crossing attempt* which composed of an “on” and “off” (or rest) period each 1 minute long. For the acoustic treatments, the speaker was active during the “on” period, but switched off during the “off” period. To compare behaviours between treatments and controls, *Crossing attempts* were also recorded for the pre-test, and the control with the speaker inactive.

### 5.3.3 Experimental Fish

Common carp ( $n = 280$ ) used in the study were obtained from a commercial supplier ( $\bar{x}$  length ( $\pm$  SE):  $88.94 \pm 0.47$  mm;  $\bar{x}$  weight ( $\pm$  SE):  $10.79 \pm 0.29$  g), in May 2019. Fish were obtained from a hatchery in Hampshire, UK, and transported to the ICER facilities at the University of Southampton in well-oxygenated water, and held in 3,000 L holding tanks containing well aerated and filtered water under ambient temperature. Water quality was checked daily and maintained at optimum levels ( $[\text{NH}_4^+] < 0.125$  ppm;  $[\text{NO}_2^-] < 0.25$  ppm).

At the end of each trial the subject fish were euthanised in accordance with Schedule 1 of the Animals (Scientific Procedures) Act 1986, and individual total body length ( $\pm 0.5$  mm) and mass ( $\pm 0.05$  g) recorded.

### 5.3.4 Mapping

To identify a frequency of interest preliminary measurements were made using pure tone signals of 1750 – 1850 Hz given that the exact space between speakers was 85 cm. A frequency of 1750 Hz was selected since this gave the best acoustic nulls during tests. The acoustic spectrum for the background, one speaker emitting a 1750 Hz tone (146 dB re 1  $\mu$ Pa at 1 m), and the acoustic treatments (see **Fig. 5.2**) were recorded. For the

acoustic treatments, recordings were made at 20 cm depth, in the centre of the flume, 90 cm away from the virtual centreline between the speakers.

The sound pressure level (SPL), and particle displacement (PD), were mapped at depths of 20 and 30 cm, on a square grid of points with a 10 cm spacing up to a distance of 70 cm from the speaker (see **Fig. 5.3**). Sound pressure level measurements were made with a Brüel and Kjær 8105 hydrophone and pre-amplifier (Teledyne Reson VP2000). The signal was sampled at 44.1 kHz, using a USB 6341 data acquisition board (National Instruments, Austin, US). Data acquisition hardware was controlled using a custom virtual instrument in Labview (Labview 2017 64-bit, National Instruments, Austin, US). Particle velocity measurements were taken as per Chapter 4.3.4 (see **Fig. 5.4**). Due to one speaker being underpowered, the location of the acoustic pressure minima for the 0-0 treatment was anomalously immediately in front of  $y = 0$ , and contrary to expectations when conducting preliminary measurements the 0-270 treatment had a stronger null than a set-up tested with one speaker phase shifted by  $180^\circ$ .

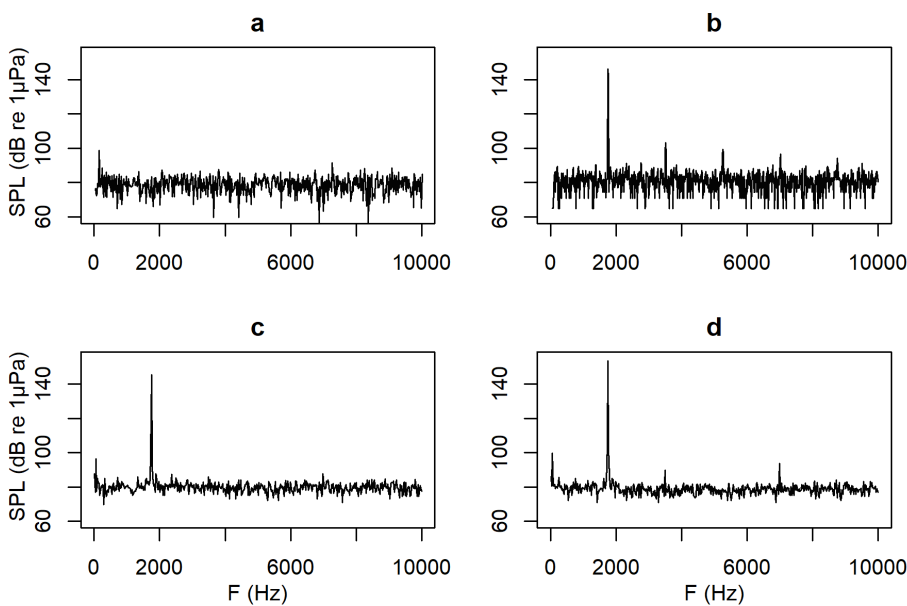


**Fig. 5.2** - Acoustic spectra : a) background; b) 1750 Hz signal (146 dB re 1  $\mu$ Pa at 1 m); c) 0-0 speaker treatment (145 dB re 1  $\mu$ Pa at 1 m); d) 0-270 speaker treatment (154 dB re 1  $\mu$ Pa at 1 m). All measurements taken at 20 cm depth, in the centre of the flume, 90 cm away from the virtual centreline between the speakers.

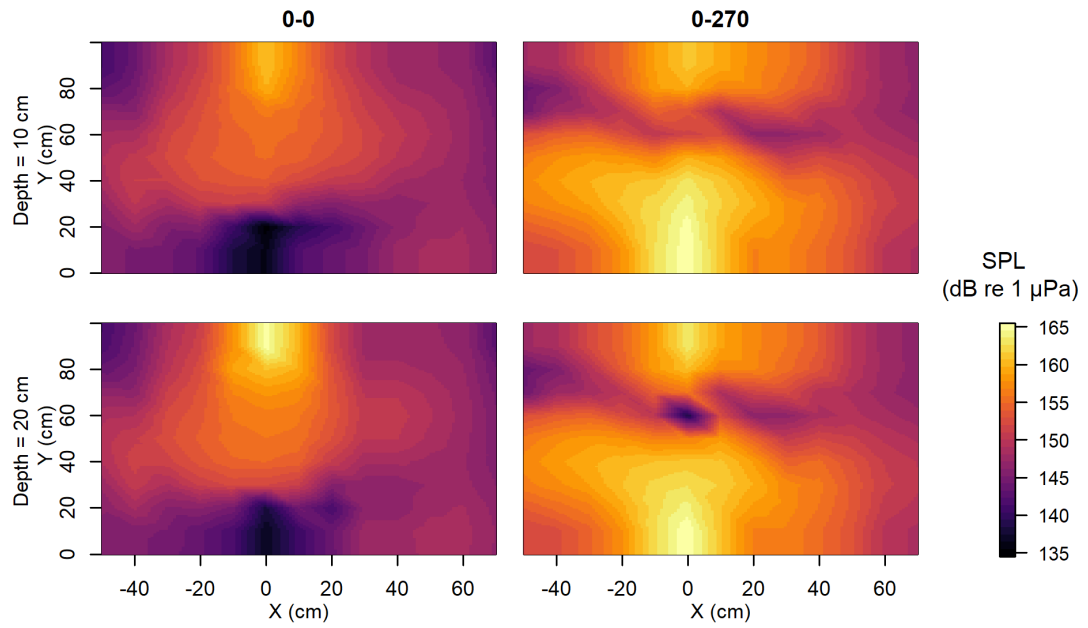


**Fig. 5.3** - Acoustic pressure maps for 0-0 and 0-270 treatments at 10 and 20 cm depth. Location of speaker A is at  $x = 0, y = 100$ , Speaker B is at  $x = 0, y = 0$ . Location of acoustic pressure minima was due to one speaker being underpowered.

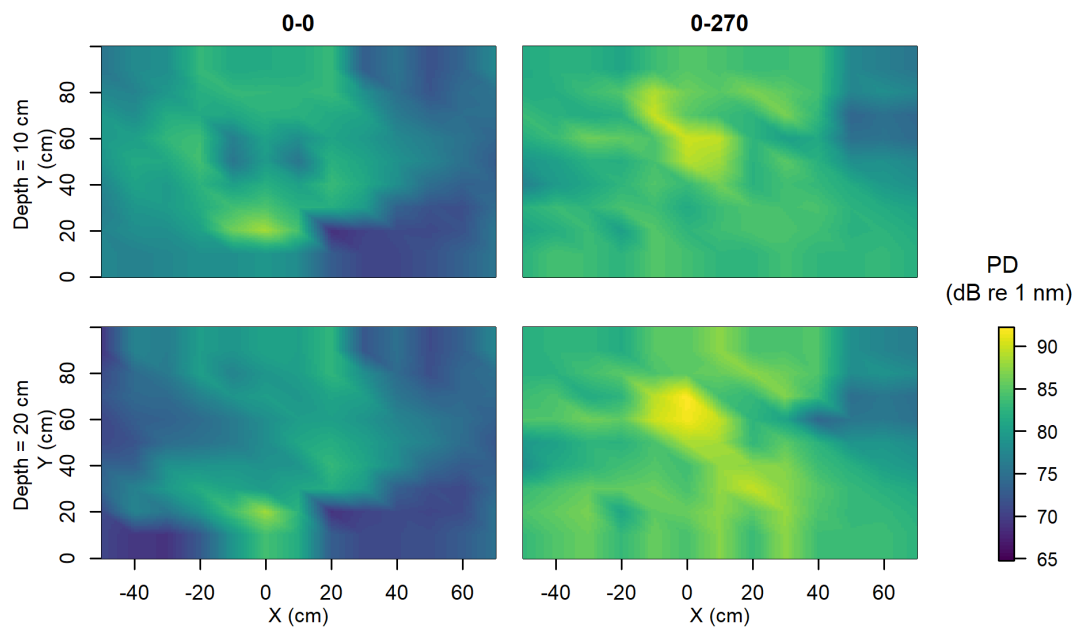


**Fig. 5.4** – Particle displacement maps for 0-0 and 0-270 treatments at 10 and 20 cm depth. Location of speaker A is at  $x = 0, y = 100$ , Speaker B is at  $x = 0, y = 0$ .

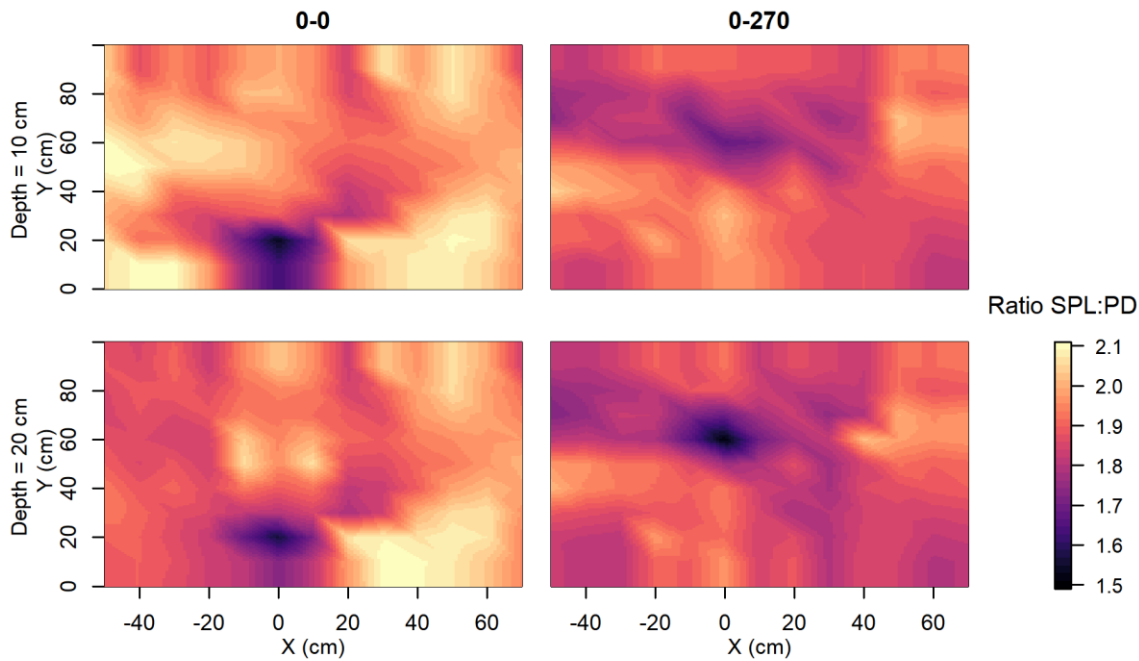


**Fig. 5.5** – Maps showing the ratio of acoustic pressure : particle motion for 0-0 and 0-270 treatments at 10 and 20 cm depth. Location of speaker A is at  $x = 0$ ,  $y = 100$ , Speaker B is at  $x = 0$ ,  $y = 0$ .

### 5.3.5 Statistical analysis

To simplify the fish tracking process and data analysis, only footage of each *Crossing attempt*, excluding the 1 minute rest period, was analysed. Video clips of each *Crossing attempt* were extracted from the full length footage using the open source video editing program Avidemux (<https://www.ffmpeg.org/Avidemux.html>). Lens distortion was removed using a semi-automated script (3DE4 Radial – Fisheye, Degree 8) in Fusion 9 (Blackmagic design, Australia). The video clips from both video camera channels were then merged in Handbrake (v. 1.3.3, <https://handbrake.fr/>). Swimming trajectories were determined for each *Crossing attempt* by evaluating the position of the fish every fifth frame ( $\approx 0.2$  s) using Logger Pro (Vernier, USA). For every time step the following variables were recorded: location of fish, location of fish within the upper, or *high* ( $Y \geq -0.5$ ) or *low* ( $Y < -0.5$ ) half of the reaction zone, swimming velocity, step length, relative turning angle, Euclidean distance from the central axis (i.e. the centreline) of the experimental arena, and Euclidean distance from either speaker. To eliminate pseudo-replicates from repeat attempts, once a fish left the reaction zone after the start of a *Crossing attempt*, any further re-entries into the reaction zone were not considered.

Video recordings were analysed to quantify common carp response to the sound fields, or control. Data were evaluated in four steps: (1) coarse-scale *Rejection count*, (2) analysis of fish movement and orientation (*Straightness*, *Sinuosity*, *Swimming velocity*, *Turning angles*), (3) fish response (*Rejection count*) relative to the stimuli generated by the speakers (SPL, PD,  $\Delta$ SPL,  $\Delta$ PD), and (4) group behaviours (*Position of centroid*, *Group swimming velocity*). For equations used to calculate straightness and sinuosity, see **Appendix G**. These metrics were used to test whether location of the acoustic pressure minima and particle motion maxima affected rejections, swimming trajectories, and swimming speed.

### 1. Coarse-scale rejection counts

The *Rejection count* was determined by analysing footage from each *Crossing attempt*. A rejection was defined as a change in direction of the swimming trajectory greater than  $90^\circ$ , followed by sustained swimming of more than one body length (i.e.  $> 10$  cm) within four frames, and the fish leaving the reaction zone. The location of rejections relative to the upper or *high* ( $Y \geq -0.5$ ) or *low* ( $Y < -0.5$ ) half of the reaction zone was also recorded.

Differences in *Rejection counts* between and within treatments were analysed by means of two-way Anova with post-hoc Tukey pairwise comparisons. Levene's and Shapiro-Wilk tests revealed that the variances were homogenous ( $F = 1.50$ ,  $df = 5$ ,  $p = 0.21$ ) with mild departures from normality ( $W = 0.95$ ,  $p = 0.05$ ).

### 2. Fish movement and orientation

Trajectory data collected were used to calculate indices of *Straightness* and *Sinuosity* [Bovet & Benhamou, 1998; Benhamou, 2004]. Differences in indices of *Straightness* and *Sinuosity* between and within treatments were analysed by means of a Kruskal-Wallis with post-hoc pairwise Dunn tests and BH corrections. Levene's and Shapiro-Wilk tests revealed heterogeneity of variances (*Straightness*:  $F = 3.92$ ,  $df = 5$ ,  $p = 0.002$ ; *Sinuosity*:  $F = 3.15$ ,  $df = 5$ ,  $p = 0.008$ ) and departures from normality (*Straightness*:  $W = 0.90$ ,  $p = <0.001$ ; *Sinuosity*:  $W = 0.94$ ,  $p = <0.001$ ). *Straightness* data were modelled as a GAM to test the importance of treatment type (0-0, 0-270, control), experimental phase (pre-test, test), and three indices of location along the Y-axis. These were: *Mean Y* – the mean location of the fish on the Y axis throughout the



*Crossing attempt*; *Initial Y* - location of the fish on the Y axis at the start of the Crossing attempt; and  $Y_{0.1}$  the mean location of the fish on the Y axis when the fish was within  $\pm 0.1$  m of the centreline. Due the heavy tails in the data (Skewness = -0.88, Kurtosis = 2.08), a scaled t model was used.

GAMs were used to model the influence of various experimental variables on *Swimming speed* and *Turning angles* within the reaction zone. Time steps with swimming speed greater than  $0.5 \text{ m s}^{-1}$  were filtered out of the data set so as to remove outliers and allow a better fit. Variables tested were as follows: distance from speakers A and B (i.e. DistA, DistB), time, stimuli generated by the speakers (SPL, PD,  $\Delta$ SPL,  $\Delta$ PD), mean light flux, location in the X and Y plane, treatment, and experimental phase.

Using the *fitdistrplus* package in RStudio (v 1.1.456: The R Foundation for Statistical Computing, Vienna, Austria, <http://www.r-project.org/>), data distribution was checked and fitted. If data were heavily skewed, they were transformed appropriately. Results of distribution checks and R code used for all models can be found in Appendix H. For all models, starting from a saturated model, stepwise deletions were performed to identify non-significant terms, and model selection was based on residual deviance and the lowest Akaike Information Criterion (AIC). The minimum adequate model (MAM) was arrived at as the most parsimonious model with lowest AIC value [Burnham & Anderson, 2002].

### *3. Fish response to stimuli generated by the speakers*

To determine whether SPL, PD,  $\Delta$ SPL, and  $\Delta$ PD may act as thresholds for change in behaviour, the level of each at a fish's location was calculated for each time step using a custom Python script (Python v.3.7.3) in Ubuntu (Ubuntu v.18.04.2 LTS). For each time step, the gradients of each stimulus to a virtual point 10 cm directly ahead of the fish were determined.

Binary logistic regression models were used to determine whether the probability of a rejection within the reaction zone was influenced by the stimuli generated by the speakers (SPL, PD,  $\Delta$ SPL,  $\Delta$ PD), distance from either speaker, light levels in the flume, and *Crossing attempt* number (i.e. whether behaviour was influenced by subsequent entries into the reaction zone). Data were filtered into four

sets to examine: (a) the first crossing attempt for each trial; (b) all crossing attempts for each trial; (c) and (d) the same respectively, but for sections of the track within 10 cm of the reaction zone centreline. Fit distribution and determining the significance of the terms was carried out as above. Results of distribution and GAM checks can be found in **Appendix I**.

#### 4. Group behaviours

The influence of various experimental variables on *Group swimming speed* and *Group distance* within the reaction zone was modelled as a GAM. Variables tested were as follows: time, position of the centroid (X and Y coordinates), treatment, and experimental phase. For both models, fit distribution and determining the significance of the terms was carried out as above. Results of distribution and GAM checks can be found in **Appendix I**.

## 5.4 Results

### 5.4.1 Coarse rejection counts

The *Number of rejections* were higher when either sound treatment was active compared to a control (*treatment*:  $F = 6.72$ ,  $p = 0.003$ ; *high / low*:  $F = 1.84$ ,  $p = 0.182$ ; *treatment: high/low*:  $F = 2.61$ ,  $p = 0.085$  - see **Fig. 5.6**). Tukey HSD post-hoc tests indicate that both acoustic treatments significantly increased *Number of rejections* (0-0:  $p\text{-adj} = 0.003$ ; 0-270:  $p\text{-adj} = 0.034$ ). *Number of rejections* were higher for both sound treatments versus a pre-test control (0-0:  $F = 16.69$ ,  $p < 0.001$ ; 0-270:  $F = 11.39$ ,  $p = 0.002$ ). For the 0-0 treatment, the region of the reaction zone with higher acoustic pressure elicited a higher *Number of rejections* ( $F = 4.84$ ,  $p = 0.04$ ).

### 5.4.2 Analysis of fish movement and orientation

*Straightness indices* were lower for either acoustic treatment versus a pre-test control ( $\chi^2 = 30.10$ ,  $p < 0.001$ ; *treatment*:  $p < 0.001$ ; *phase*:  $p = 0.004$ ; *treatment: phase*:  $p = 0.30$ ). This was likely due to differences between the pre-test and test experimental phase for both acoustic treatments (0-0:  $p\text{-adj} = 0.052$ ; 0-270:  $p\text{-adj} = 0.020$ ). *Sinuosity* was not affected by the acoustic treatments ( $p = 0.115$ ) (see **Fig. 5.7**).

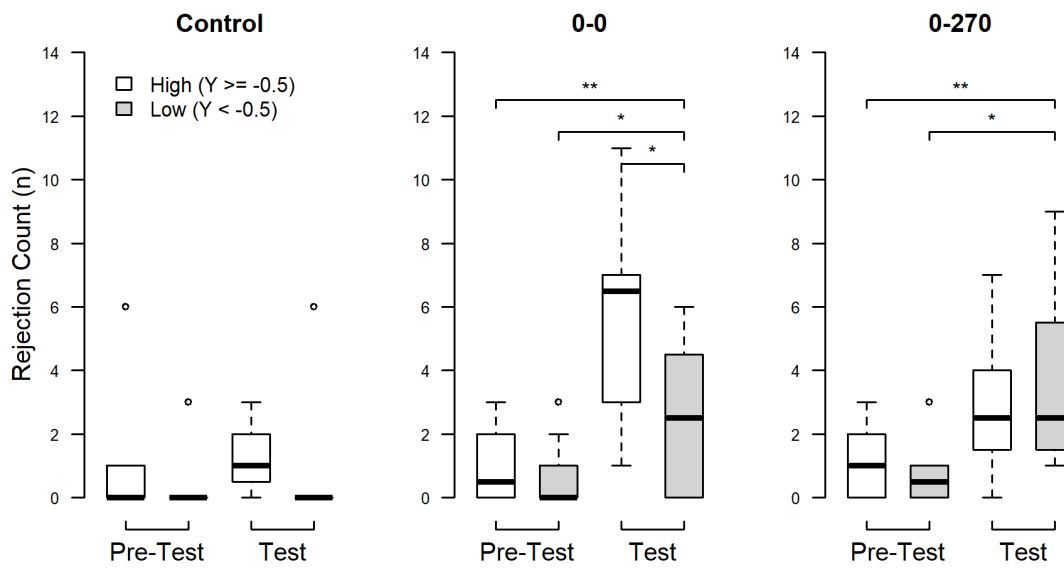


**Fig. 5.6** – The median, interquartile range and minimum/maximum whiskers of *Number of rejections* for both experimental treatments and the control. Asterisks mark significance at a  $p < 0.05$  level.

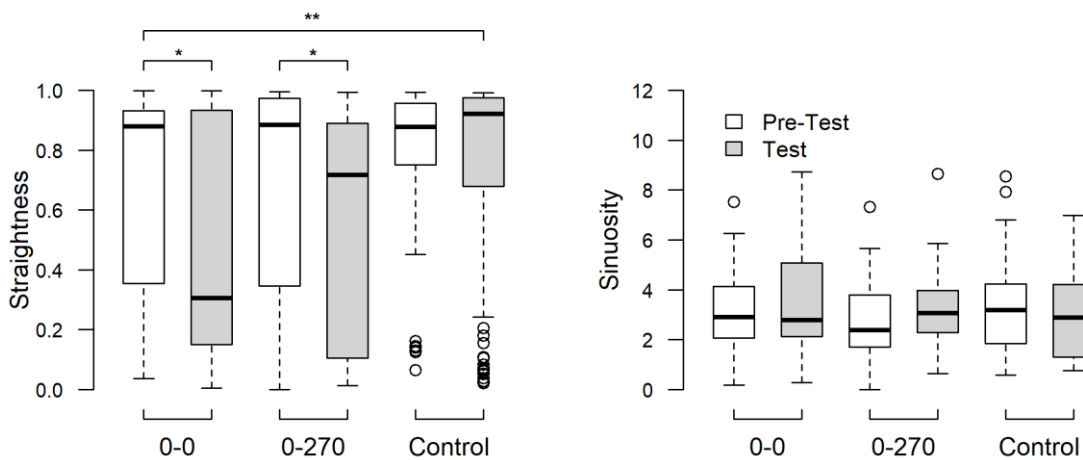


**Fig. 5.7** – The median, interquartile range and minimum/maximum whiskers for the indices of *Straightness* and *Sinuosity*. Asterisks mark significance at a  $p < 0.05$  level.

Models obtained for the *Straightness* data show that the most important terms influencing the straightness of fish tracks were treatment, experimental phase, and position on the y-axis within  $\pm 0.1$  m of the centre line (see **Table 5.1**). Position on the y-axis,  $Y_{0.1}$  was the most important term, explaining 5.4 % of the deviance compared to the null. Treatment ( $p < 0.01$ ) and experimental phase ( $p < 0.01$ ) explained 4.76 and 2.34 % of the deviance, and their interaction ( $p < 0.01$ ) a further 0.9 %. Due to the

heavy tails in the data, *Swimming speed* data were filtered and inverse transformed. *Swimming speed* was mainly influenced by the distance from the two speakers, time, (Dist A and Dist B), time, mean light flux, location of the fish in the X plane, PD level,  $\Delta$ SPL, and the interaction between treatment and experimental phase (see **Table 5.2**).

*Turning angles* were modelled as an inverse gamma distribution against the following terms: location (X and Y position), distance from the two speakers (Dist A and Dist B), the components of the stimulus (SPL, PD,  $\Delta$ SPL,  $\Delta$ PD), and the interaction between treatment and experimental phase. Since the saturated model had limited explanatory power (5.47 %), the relative importance of each term was not determined (see **Appendix I** for GAM plots of each candidate variable).

**Table 5.1** – Results obtained for the modelled effects of the terms affecting the *Straightness index* of fish trajectories. The deviance explained relative to null (%), estimated degrees of freedom (edf) and significance (p value) of variables within the minimum adequate model (MAM) are listed. Exp. Phase refers to the experimental phase of the trial (i.e. pre-test / test). Brackets indicate smoothed terms.

Data	Model terms	Deviance explained relative to null (%)	edf	p value
	$s(Y_{0,t}) + s(\text{MeanY}) + s(\text{InitialY}) + \text{Treatment: Exp. Phase}$	14.2 (saturated model)		
	$s(\text{MeanY})$	0.1	1	0.647
	$s(\text{InitialY})$	0.7	1.974	0.325
Straightness	$s(Y_{0,t}) + \text{Treatment: Exp. Phase}$	13.4 (minimum adequate model)	3.113	<0.01
	Treatment: Exp. Phase	0.9		<0.1
	Treatment	4.76		<0.01
	Phase	2.34		<0.01
	$s(Y_{0,t})$	5.4	3.173	<0.01

#### 5.4.3 Fish Response to Speaker Stimuli

A binary logistic regression model showed that the terms which influenced the *Number of rejections* changed as fish moved closer to the centreline of the reaction zone, and also with successive crossing attempts (see **Fig. 5.9** and **Table 5.3**). In general, models had greater predictive power within  $\pm 10$  cm of the centreline. When including all *Crossing attempts*, SPL and  $\Delta$ PD played a consistent role at eliciting rejection (deviance explained: 15.0 %). When modelling only the first crossing attempt for each trial, PD

played a greater role than SPL; with phase, PD, and  $\Delta$ PD being the most important terms influencing *Number of rejections*, the model explaining 20.0% of the deviance.

**Table 5.2** – Results obtained for the modelled effects of the terms affecting the inverse *Swimming speed* of fish. The deviance explained relative to null (%), estimated degrees of freedom (edf) and significance (p value) of variables within the MAM are listed. Exp. Phase refers to the experimental phase of the trial. Brackets indicate smoothed terms.

Data	Model terms	Deviance explained relative to null (%)	edf	p value
	s(DistA) + s(DistB) + s(SPL) + s(PD) + s( $\Delta$ SPL) + s( $\Delta$ PD) + s(X) + s(Y) + s(Approach) + s(MeanLight) + Treatment: Exp. Phase	19.4 (Minimum adequate model and Saturated model)		
	s(DistB)	8.03	30.16	<0.001
	s(Time)	1.15	17.05	<0.001
	s(DistA)	4.12	16.22	<0.001
	s(MeanLight)	3.00	16.25	<0.001
1 /	s(X)	1.10	11.95	<0.001
Swimming	s(PD)	0.40	11.2	<0.001
speed	s(Approach)	0.50	6.797	<0.001
	s( $\Delta$ SPL)	0.50	9.784	<0.001
	s(SPL)	0.10	5.226	<0.001
	s(Y)	0.10	14.592	<0.001
	s( $\Delta$ PD)	0.10	4.759	0.008
	Treatment	0.10	-	0.04
	Exp. Phase	0.00	-	0.17
	Treatment:Exp. Phase	0.30	-	<0.001

#### 5.4.4 Analysis of group behaviours

*Group distance* was mostly influenced by time, and location of the centroid (see **Fig. 5.10** and **Table 5.4**) These terms combined described 60.3 % of the deviance (Centroid Y – 27.9 % ; Time – 18.7 % ; Centroid X – 13.0 %). *Group swimming speed* was modelled as a log gamma distribution, against time, centroid position (x and y axis), and an interaction between treatment and experiment phase (see **Fig. 5.11** and **Table 5.4**). The model obtained showed that time, location of the centroid, and treatment had the greatest effects on *Group swimming speed* with the model explaining 12.1% of the deviance (Centroid X – 4.32% ; Time – 3.72% ; Centroid Y – 1.41% ; Treatment – 2.39%).

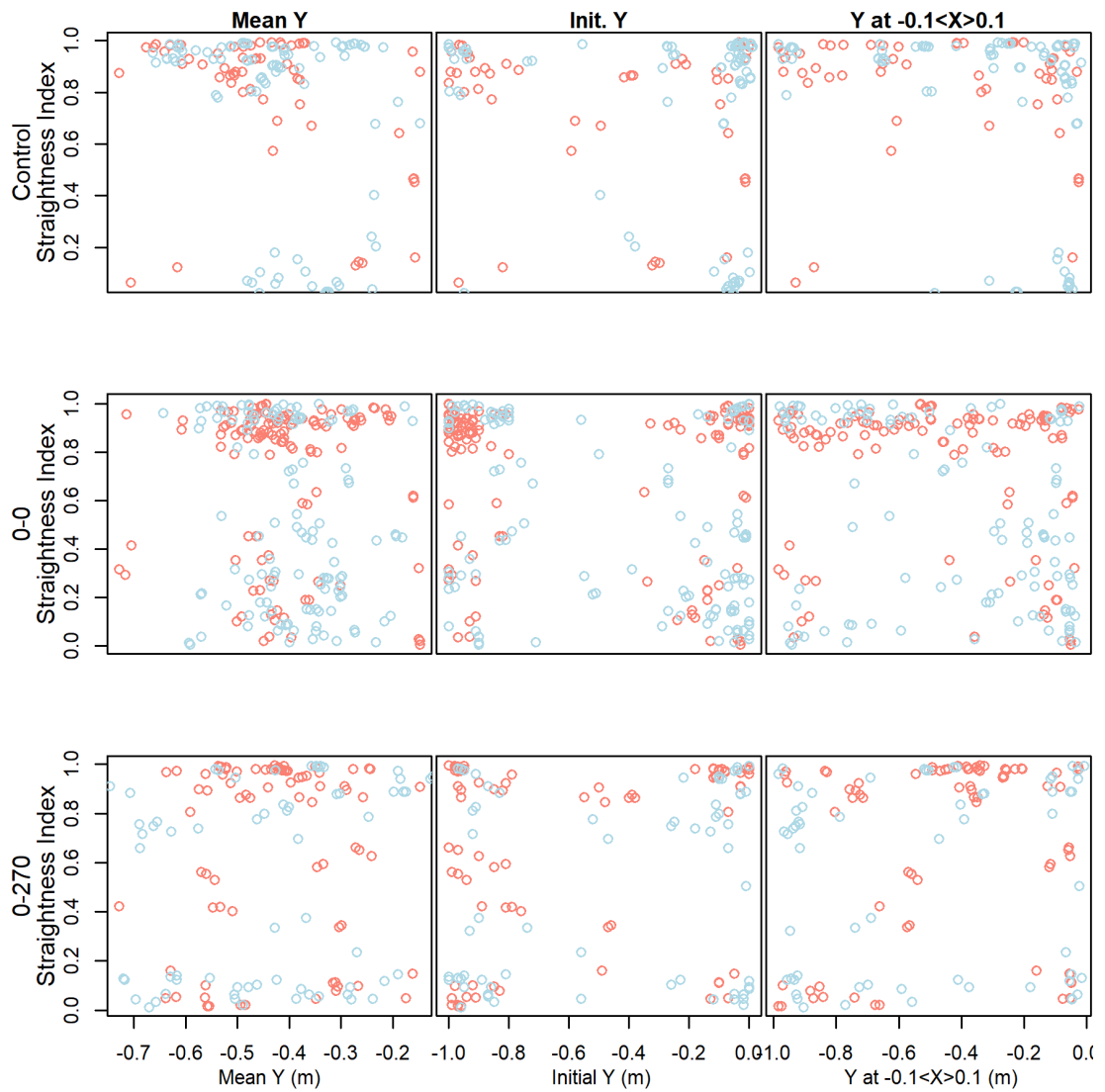


**Fig. 5.8** – Values obtained for *Straightness index* plotted against location of the fish on the Y axis / centreline. *Mean Y* - mean location of the fish on the Y axis throughout the *Crossing attempt*; *Initial Y* - location of the fish on the Y axis at the start of the *Crossing attempt*; and  $Y_{0.1}$  - mean location of the fish on the Y axis when the fish was within  $\pm 0.1$  m of the centreline. Red circles indicate pre-test experimental phase, blue circles indicate test experimental phase.

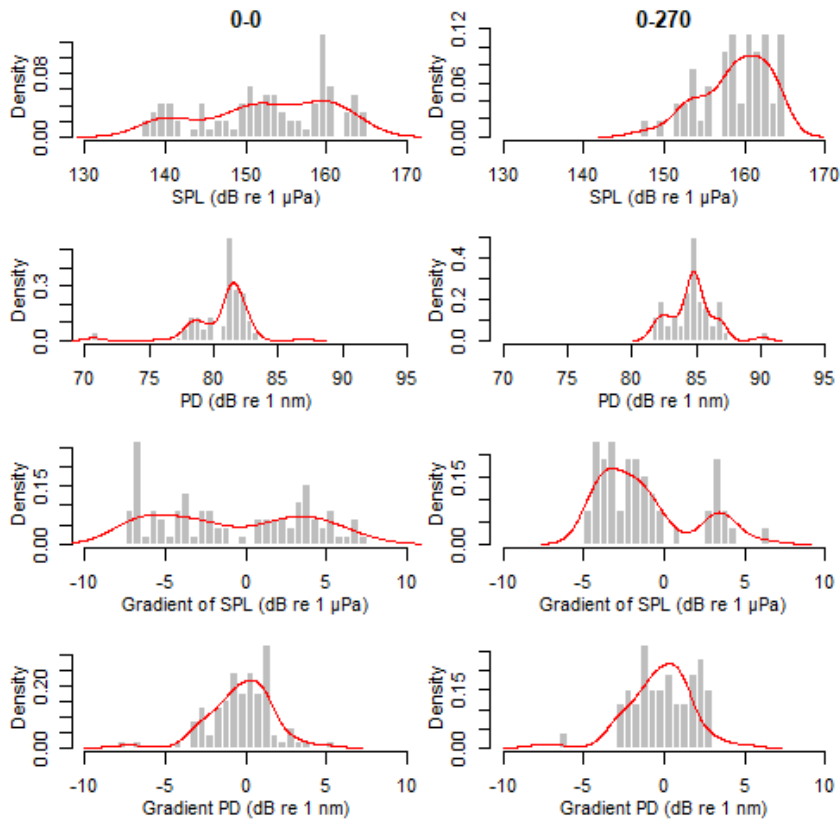


**Fig. 5.9** – Binned *Number of rejections* for the 0-0 and 0-270 acoustic treatments against stimuli generated by the speakers. The solid red line indicates density. SPL = Sound pressure level; PD = Particle displacement.

## 5.5 Discussion

This study found that in low light conditions, common carp tended to exhibit negative phonotaxis when exposed to regions with a high ratio of acoustic pressure to particle displacement, versus regions with a low ratio. All treatment trials showed at least one rejection per crossing attempt. Avoidance behaviours tended to be elicited when acoustic pressure reached about 150 - 160 dB (re 1  $\mu$ Pa), where fish often held position before initiating a reaction to the stimulus. The location of the high acoustic pressure and high particle displacement regions affected the number of rejections observed in the upper and lower regions of the reaction zone. Regions of high acoustic pressure significantly increased the number of *Rejections*.

**Table 5.3** - Results obtained for the modelled effects of the terms affecting the *Number of rejections*. The deviance explained relative to null (%), estimated degrees of freedom (edf) and significance (p value) of variables within the MAM fitted for each of the four datasets ((a) to (d)) are listed. Exp. Phase refers to the experimental phase of the trial. Brackets indicate smoothed terms.

Data subset	Model terms	Deviance explained relative to null (%)	edf	p value
	s(MeanLight) + s(SPL) + s(PD) + s( $\Delta$ PD) + s(DistA) + s(DistB) + s(Approach) + Exp. Phase:Treatment	9.88 (Minimum adequate model)		
(a) reaction zone data, all crossing attempts	Exp. Phase	2.87	-	<0.001
	s(SPL)	2.77	2.32	<0.001
	s(DistA)	1.41	5.88	<0.001
	s(DistB)	0.84	2.77	<0.001
	Treatment	0.04	-	0.48
	s(PD)	0.65	3.03	0.05
	s(Approach)	0.30	2.77	0.24
	s( $\Delta$ SPL)	0.00	1.45	0.27
	s( $\Delta$ PD)	0.34	2.48	0.32
	s(MeanLight)	0.02	1.00	0.41
Exp. Phase : Treatment	0.78	-	0.55	
	s(SPL) + s( $\Delta$ SPL) + s(DistA) + s(DistB) + Exp. Phase	8.22 (Minimum adequate model)		
(b) reaction zone data, first crossing attempt	Exp. Phase	3.59	-	<0.001
	s(DistB)	0.39	1.00	0.05
	s(DistA)	2.02	1.00	<0.001
	s(SPL)	2.22	1.00	<0.001
	s( $\Delta$ SPL)	0.10	1.00	0.46
	s(MeanLight) + s(SPL) + s( $\Delta$ PD) + s(DistA) + s(Approach) + Exp. Phase	15.0 % (Minimum adequate model)		
(c) $\pm$ 10 cm from centre line, all crossing attempts	Exp. Phase	5.35	-	<0.001
	s(SPL)	5.45	1.00	<0.001
	s(DistA)	0.50	1.00	0.03
	s( $\Delta$ PD)	2.30	6.12	0.02
	s(Approach)	1.10	3.27	0.04
	s(MeanLight)	0.30	1.00	0.18
	s(MeanLight) + s(SPL) + s(PD) + s( $\Delta$ PD) + s(DistA) + s(Approach) + Exp. Phase + Treatment	20.0 % (Minimum adequate model)		
(d) $\pm$ 10 cm from centre line, first crossing attempt	Exp. Phase	8.72	-	<0.001
	s(PD)	5.58	2.06	<0.001
	s( $\Delta$ PD)	4.80	2.99	0.03
	s(DistA)	0.00	1.33	0.29
	Treatment	0.50	-	0.36
	s(SPL)	0.30	1.00	0.53
s(MeanLight)	0.20	1.00	0.52	



**Table 5.4** - Results obtained for the modelled effects of the terms affecting the *Group distance*, and log of *Swimming speed*. The deviance explained relative to null (%), estimated degrees of freedom (edf) and significance (p value) of variables within the MAM are listed. Exp. Phase refers to the experimental phase of the trial. Brackets indicate smoothed terms.

Data	Model terms	Deviance explained relative to null (%)	edf	p value
Distance	s(Time) + s(CentroidY) + s(CentroidX) + Treatment:Exp. Phase	60.3 (minimum adequate model)		
	s(Time)	18.70	10.4	< 0.001
	s(Centroid Y)	27.90	25.34	< 0.001
	s(Centroid X)	13.00	28.26	< 0.001
	Exp. Phase	0.60		< 0.001
	Treatment	0.00		< 0.001
	Treatment: Exp. Phase	0.10		< 0.001
Log Speed	s(Time) + s(CentroidY) + s(CentroidX) + Treatment + Exp. Phase	12.1 (minimum adequate model)		
	s(Centroid X)	4.32	11.43	<0.001
	s(Centroid Y)	1.41	12.76	<0.001
	s(Time)	3.72	9.237	<0.001
	Exp. Phase	0.26		<0.001
	Treatment	2.39		<0.001

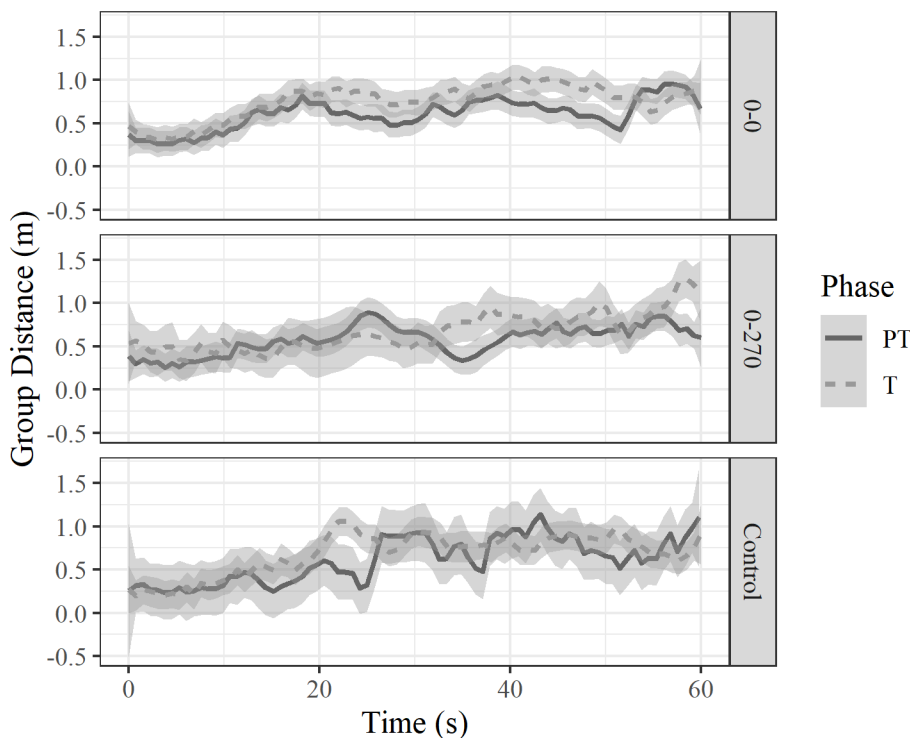


**Fig 5.10** - Locally estimated scatterplot smooth (smooth parameter = 0.05) of group *Distance* plotted against time. Phase refers to Experimental phase, PT = Pre-test, T = Test.

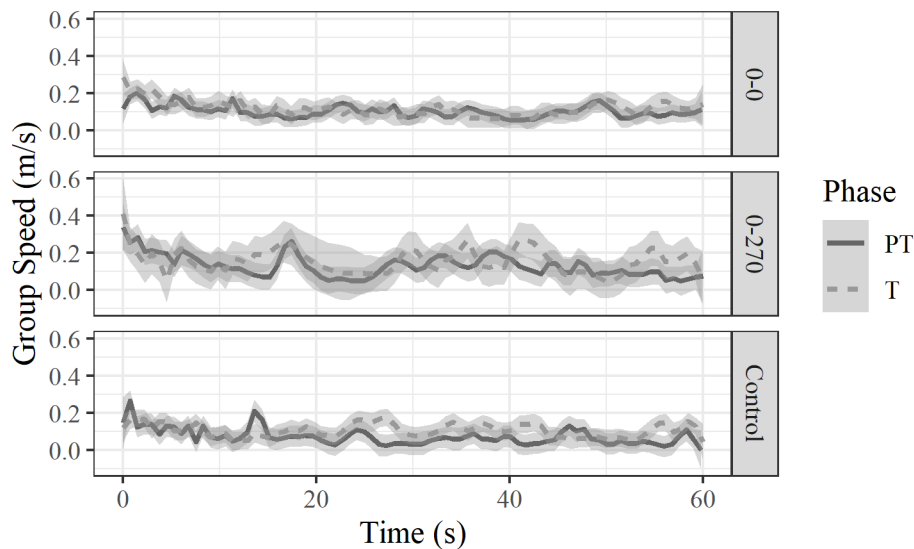


**Fig 5.11** - Locally estimated scatterplot smooth (smooth parameter = 0.05) of group *Swimming speed* plotted against time. Phase refers to Experimental phase, PT = Pre-test, T= Test.

The binomial models gave an indication of greater complexity, although in every case experimental phase had a significant influence. Responses changed in two ways depending on: (1) distance of a fish to the centreline, and (2) number of attempts. The greater explanatory power of the models within 10 cm of the centreline matches earlier findings in Chapter 4, and previous work that found that carp reacted to acoustic stimuli within one to two body lengths. Magnitude of SPL appears to have been the likely cause for eliciting rejection, although at closer ranges to the centreline, PD and  $\Delta$ PD gained more importance.

There is some evidence that *Straightness* indices are affected by the position of the fish along the y-axis of the flume, especially within 10 cm of the centreline. Given the effect of regions of high acoustic pressure on rejection counts, this seems to indicate that fish follow a straighter trajectory when encountering regions of high particle displacement. The curved nature of the swimming paths observed in this study were consistent with avoidance behaviours of bighead and common carp reported for low frequency (< 5000 Hz) sound sources produced by air curtains in darkness [Zielinski *et al.*, 2014; 2015; 2016; Zielinski & Sorensen, 2017]. It is also consistent with behaviours observed in the previous two chapters, where fish held position at the front of the bubble curtain and either turned away from, or continued swimming through the bubble barrier.

Although experimental treatments, and the stimuli generated by the speakers did have an effect on swimming speed, this appears to have been limited compared to non-experimental variables. The effect of time was likely due to fish having relatively high swimming speeds at the start of a crossing attempt, and as an initial reaction to the speaker, which meant they were more likely to slow down as time progressed. Distance from the two speakers, time, (Dist A and Dist B), time, mean light flux, and location of the fish in the X plane had the greatest effect.

The initial experimental plan consisted of an additional treatment ( $n = 8$ ), with both speakers phase-shifted by  $90^\circ$ . The purpose of this was to compare rejection counts with the 0-0 treatment, to control for any behavioural effects of the sound wave being generated at the peak. No differences were found between the 90-90 and 0-0 treatments, hence for the coarse scale metrics 8 out of a total of 16 trials were selected at random, and for the modelling steps all data were pooled.

Higher than expected levels of behavioural noise probably accounts for the low deviance explained by the models for swimming speed, group swimming speed, turning angle, and group distance. Fish were obtained from the same hatchery as previous experiments, however in contrast to previous stock, their behaviour remained restive despite extending the amount of time to acclimate to their holding tank environment, and a decrease in the lighting intensity used for the experiment. Given the behavioural noise, model explanatory power was considered to be adequate in terms of providing an indication of the relative importance of the model terms.

Popper *et al.*, [2019] and Nedelec *et al.*, [2016] discussed a number of priorities with regard to particle motion measurements. This included comparing the effects of sound on fish where the pressure is maintained constant, but particle-motion levels are varied for species that (1) can detect acoustic pressure, and (2) can only detect particle motion. Popper *et al.*, [2019] suggest a focus on behavioural studies of fish species that reflect hearing over broad groups defined by hearing rather than taxonomy, to gain a better understanding of what fish can actually hear and respond to. This could include testing the behavioural reaction of naïve fish of a given species to different frequencies and different levels of particle motion, or the use of behavioural conditioning in a similar fashion to Hawkins & Chapman., [1975]. Fish could be trained to react to a

sound signal, and their ability to recognise and react appropriately to the same signal with different ratios of acoustic pressure to particle motion could then be tested.

## **5.6 Conclusion**

This study used two speakers emitting a 1750 Hz signal, with or without a phase difference of 270 degrees, to create regions of high particle motion or high acoustic pressure. Regions of high acoustic pressure caused fish to reject crossing the reaction zone, more often than regions of high particle displacement. Fish swimming through regions of high particle displacement tended to have a straighter trajectory. While results of modelled behaviour indicate that the location of fish along the y axis had a consistently important effect on trajectory straightness, it is unclear whether regions with different ratios of acoustic pressure and particle displacement affect metrics such as swimming speed, group swimming speed, turning angle, and group distance.

## **5.7 Ethics**

The study conformed to UK legal requirements and was approved by the University of Southampton's Ethics and Research Governance Office (Ethics ID: 47181).



## Thesis Discussion

Addressing the global challenges faced by climate change led to the UN Paris Agreement in 2016, with several countries having since drafted ambitious strategies to meet the targets set by the agreement. In the EU, for instance, clean energy is expected to play a crucial role at reaching climate objectives as part of the European Green Deal [COM, 2019; 2020]. The Green Deal aims to make the EU climate neutral by 2050, the key target being a reduction in greenhouse gas emissions of at least 55 % (from 1990 levels) by 2030 [COM, 2020], and at least a 32 % share for renewable energy [Renewable Energy Directive (2018/2001/EU)].

The UK's approach to tackling and responding to climate change was legislated in the Climate Change Act 2008, which introduced a long-term legally binding 2050 target to reduce greenhouse gas emissions by at least 80% relative to 1990 levels. The devolved Welsh and Scottish governments introduced similar measures through The Environment (Wales) Act 2016, and the Climate Change (Scotland) Act 2009. In 2017, the UK Government also published its Clean Growth Strategy (CGS) setting out policies and proposals, through to 2032 and beyond, to reduce emissions across the economy and promote clean growth.

Worldwide, hydropower is expected to play a key role in implementing these strategies. Global hydropower generation increased by 2.5 per cent in 2019, with projects totalling 15.6 GW in capacity were put into operation in 2019 [IHA, 2020]. Given that it is the number one renewable energy source in Europe [Eurostat, 2017], its contribution to the implementation of the Renewable Energy Directive and EU energy targets for 2020-2030 is expected to be considerable.

As with all other water-based activities, hydropower must conform to the requirements of EU environmental law, which has been introduced to protect and restore Europe's rivers and lakes. These legal requirements are laid down in the Water Framework Directive, the Floods Directive, the Birds and Habitats Directives, the Eels Regulation, and the Environmental Assessments Directives (Environmental Impact Assessment - EIA and Strategic Environmental Assessment - SEA Directives) [EC, 2018]. In the United States, the Clean Water Act (CWA) requires that water intakes

incorporate the best technology for minimising adverse environmental impact [US Clean Water Act, 1972].

Much of Europe depends on water from rivers for drinking, food production and the generation of hydropower, which is essential for meeting the European Union (EU) renewable energy target. Yet only half the EU surface waters have met the Water Framework Directive's (WFD) 2015 target of good ecological status, due in part to the fragmentation of habitats caused by tens of thousands of dams and weirs [Kerr *et al.*, 2016]. Barriers such as these can cause a number of effects to riverine ecosystems, including delayed migration [Caudill *et al.*, 2007], and injury through blade strikes or barotrauma [Cada *et al.*, 2006; Brown *et al.*, 2009; Brown *et al.*, 2014]. Poor river connectivity is considered one of the main reasons for declines in many European [Larinier, 2001] and other freshwater fish populations worldwide [Jungwirth *et al.*, 1998; Thorncraft & Harris, 2000].

A wide range of measures can be introduced for both existing and new hydropower plants to reduce their ecological effects. These measures can include restoration of river continuity by removing old or obsolete structures or building fish passes; reducing fish mortality by installing screens at inlets or special "fish-friendly" turbines; and the restoration of adequate flow [Kerr *et al.*, 2016; EC, 2018] As discussed in Chapter 4, non-physical behavioural barriers, such as acoustic deterrents, have increasingly been introduced globally to help guide fish away from water intakes, pumping stations, hydroelectric power plants, and weirs towards fish passes, reducing the number of impinged fishes [Patrick *et al.* 1988; Piper *et al.* 2019]. In such cases, given that the primary goal is to reduce fish mortality or improve connectivity, any reduction in mortality or increase in migration numbers may be desirable, and a consensus efficacy could be reached between the company, fisheries managers and the public [Putland & Mensinger, 2019].

Ecological challenges are not only limited to aquatic infrastructure, but also the introduction of invasive alien species (IAS). Globalised commerce and recreation has increased connectivity between many large bodies of water, resulting in more invasive species being introduced and expanding outside their native range [Keller *et al.* 2011]. At present, the European network of inland waterways is made up of 28000 km of navigable rivers and canals, connecting 37 countries in Europe and beyond [Panov *et*

*al.*, 2009]. This aquatic network now connects the previously isolated catchments of the southern European seas (Caspian, Azov, Black, and Mediterranean seas) and the northern European seas (Baltic, North, Wadden, White), providing invasion corridors for alien species. Europe has 30 main canals with a further 100 branch canals and 350 ports [Bij de Vaate *et al.*, 2002; Ketelaars 2004; Galil *et al.*, 2007]. There are plans to deepen many of these canals to accommodate larger vessels and to prepare for the lower anticipated water levels as a result of climate change. Nunes *et al.*, [2015] identified priority pathways and gateways of introductions, a priority for the development of adequate control strategies. In Europe, where the number of invasive alien species (IAS) showed an increase of 76 % between 1970 and 2007 [Butchart *et al.* 2010], aquaculture, pet/aquarium trade and stocking activities were of major importance in their introduction [Nunes *et al.*, 2015].

Stocking, and accidental escape of aquaculture or ornamental fish, were also the introduction methods for Asian and Common carp in the upper Mississippi, and the Murray-Darling river basins in the US and Australia [Bajer & Sorensen, 2010] where they have been reported to reach especially high, damaging densities [Panek 1987; Koehn 2004]. Their reproductive success can be linked to the environmental instability of these regions [Bajer & Sorensen, 2010]. The upper Mississippi is a network of interconnected rivers and lakes whose shallow basins frequently experience severe winter hypoxia and fish mortality ('winterkill') as a consequence of prolonged snow cover [Magnuson *et al.*, 1985], whereas the Murray-Darling system features floodplain lakes and prolonged droughts which cause summer hypoxia [Gehrke *et al.*, 1995;].

In line with the internationally agreed three-stage approach to tackle invasive species based on: (1) prevention, (2) early detection and eradication, and (3) control and containment measures [Genovesi & Shine, 2004], Bajer & Sorensen [2010] suggested that efforts to control the abundance of these species must focus on hindering the ability of migratory adults to access unstable habitats and/or reduce the severity of instability processes. As discussed in Chapter 1, many fish (including common and Asian carp species) have adaptations which make them sensitive to a wide range of acoustic frequencies, and avoid intense acoustic stimuli generated by acoustic speakers, bubble barriers, or combinations of the two [Taylor *et al.*, 2005; Ruebush *et al.*, 2012; Vetter *et al.*, 2015; Zielinski & Sorensen, 2016].



Electrical barriers are not a viable option in the upper Mississippi River and its large network of tributaries because of high costs, the risk they can pose to human safety, and their potential to block valuable native fish [Noatch & Suski 2012]. As discussed, this has sparked a renewed interest in the use of acoustic and bubble barriers to retard or alternatively to use sound to herd and concentrate these species for removal. Due to their low cost and ease of deployment, bubble curtains could ultimately be used to guide carp away from critical habitat or passageways either towards traps [Johnson *et al.* 2014)] or toward low-velocity waters, such as tributaries and oxbow lakes, where large numbers of Asian carp have been observed [Varble *et al.*, 2007; Kolar *et al.*, 2007; Wilson 2014] where they can be captured with seine nets [Bajer & Sorensen, 2010]. The Mississippi River lock chambers offer unique opportunities to deploy bubble curtains because they have a well-defined channel, shallow and slow moving water, and already have much of the infrastructure necessary to operate bubble curtains. Despite not being 100 % effective, such barriers would not be expected to act as permanent barriers, but rather reduce propagule pressure while allowing trapping methods, or commercial fishing to keep the population in control [Zielinski & Sorensen, 2016; Putland & Mensinger 2019], and preventing expansion by making use of available barriers impassable to fish, such as the lock at Upper St. Anthony Falls which was permanently closed in 2014 [Invasive Carp Work Group, 2014].

Although the use of bubble curtains or screens to, by attenuation and backscattering, contain sound fields to particular regions, dates back to 1948 [Love and Arndt, 1948], as touched upon in earlier chapters, fisheries managers face two substantial challenges when evaluating acoustic barrier technology: (1) the variable guidance efficiencies reported, and (2) the frequent absence of details such as frequency range, sound pressure level, particle motion data, type of equipment, or bubble size distribution [Hocutt, 1981; Popper & Carlson, 1998; Putland & Mensinger, 2019]. The variety of set-ups described in the literature also appear to suggest that to a certain extent, many studies have "*re-invented the wheel*", making little cumulative progress.

Putland & Mensinger, [2019] raised a number of concerns on previous studies on bubble curtains. First, the lack of quantitative data makes it impossible for third parties to recreate the results. This is compounded by acoustic stimuli being considered proprietary which precludes rigorous testing by other laboratories. Secondly, the small

number of deterrent technologies available for use and their capabilities were mainly described in the grey literature, with many of the reports including authors who developed or sold the systems - a potential conflict of interest. Finally, few if any studies determined the driving force behind the negative phonotaxis given that efficiencies reported vary substantially.

Building on the work done by Zielinski & Sorensen [2016], this thesis has worked towards both determining the likely driving force behind negative phonotaxis in carp when encountering an insonified bubble wall (Experiments 2 and 3), and the relative importance of acoustic pressure and particle motion (Experiment 4) in eliciting such reactions. It also highlights the importance of properly categorising the stimuli and acoustic environment when testing the effectiveness of a bubble curtain, while bearing in mind that pressure, air flow, and the volume of air between the nozzle and the flow control valve can all effect the final size of the bubbles produced. While the received wisdom regarding bubble barriers is to use an air flow of 60-240 L min<sup>-1</sup> m<sup>-1</sup>, this study (Experiment 1, 2, 3) has shown that it is possible to elicit rejection in carp with flows of 30 L min<sup>-1</sup> m<sup>-1</sup>. If the properties of bubbles as scatters of sound energy are harnessed, the air flow can be dropped further, thus reducing the power required. A quick comparison with set-ups used previously in the field (e.g. Welton *et al.*, 2002; Zielinski *et al.*, 2015) suggests that a ten-fold decrease in air flow could mean an equivalent decrease in hourly energy consumption due to the ability to switch to less powerful compressors of 750-1500 W. While this is significant, it should be pointed out that the construction costs involved in setting up and maintaining a large scale bubble curtain are generally larger than the cost of running air compressors [Zielinski, *pers comm.*]. The same concept has been used in the marine renewable energy industry, where stationary arrays of large tethered encapsulated bubbles are used abate low frequency underwater noise from anthropogenic sources such as pile driving. Both the systems designed by AdBm [Lee *et al.*, 2016], and Offnoise Solutions [Elmer *et al.*, 2012] are considered to be cheaper to run than the more traditional big bubble curtains [Verfuss *et al.*, 2019].

A major message of this thesis is a cautionary tale for researchers, fisheries managers, and developers of acoustic-bubble deterrents, illustrated particularly by the differences that could be made to the soundscape simply by vibrating the injection

nozzles and changing the size distribution of a bubble cloud. This ties into the larger discussions within the bioacoustics field to improve standardisation [Erbe *et al.*, 2016; Halvorsen & Ainslie, 2018; Hawkins *et al.*, 2020], and to avoid common pitfalls that occur when fish biologists carry out cross-disciplinary studies in acoustics [Parvulescu, 1964; Rogers *et al.*, 2016; Grey *et al.*, 2016], ensuring replicability. International quality standards for measuring procedures do not yet exist [Ainslie *et al.*, 2019] for fish audiograms, although Halvorsen *et al.*, [2019] reported on the start of a programme to establish these. There is a clear need for standardisation of test signals and protocols for fish measurements, so that direct comparisons can be made. The methodologies used to date are diverse, and behavioural studies exhibit a variety of methods and conditioning types, some of which are species specific.

In the discussion paper of a plenary talk at the 2019 “Effects of Noise on Aquatic Life” conference (Den Haag, The Netherlands, July 7-12, 2019) Leighton *et al.*, [2020] identified underlying challenges that can serve as lessons learnt from human audiology. This echoes similar calls by Parvulescu [1964], Akamatsu *et al.*, [2002], and Grey *et al.*, [2016] who drew attention to certain challenges faced when conducting experiments inside small tanks, and advised that hearing measurements and behavioural experiments on fish should be conducted in an acoustic environment as close as possible to that of the animal’s natural environment.

When arguing the relevance of utilising environments as close as possible to the subject’s natural environment, Leighton *et al.*, [2020] opined that the acoustic environment of freshwater systems and heavily modified channels bear more similarity to laboratory flumes and tanks, than free field conditions found in open water. Freshwater systems are extremely variable, shallow watered (often < 1 m depth) and highly modified environments with banks and riverbeds that introduce a wide range of sediment properties, flow rates, turbulence and bubble populations. They are often subject to significant manmade infrastructure, such as fish passes, dams and weirs [Johnson *et al.*, 2014], or the concrete-lined Levada's in Madeira, open channels which date from the 15<sup>th</sup> century [Leighton *et al.*, 2020]. Rivers flowing through urban areas are often channelised and lined with concrete, to improve flow and expedite drainage. Environments like these produce strong wall reflections, and the shallow water means that fish would be close to the nearly pressure-release air/water interface at the top of the water column [Leighton *et al.*, 2020]. Propagation of sound would also be hampered

in depths of less than roughly a quarter of a wavelength [Akamatsu *et al.*, 2002; Leighton *et al.*, 2020]. Although received wisdom is vital to avoid common pitfalls, given proper understanding of the concepts involved, valid acoustic experiments can be made. Since a behavioural deterrent is more likely to be deployed in such environments (e.g. the tailrace of a hydropower dam, or a small shallow tributary), with adequate categorisation of the stimulus, it is more useful to gauge fish reactions in such conditions.

Much scope remains for future research. For flume-based work, as discussed in **Chapter 4**, one avenue could be to test the effect of an increased number of bubbles, for example by adding additional nozzles, or alternatively by generating bubble swarms through electrolysis in a controlled manner [Birkin *et al.*, 2015]. The effect of varying the mode of bubble generation (e.g. continuous or pulsed) could be tested. All three bubble curtains used in **Chapter 3** and **4** showed a wide range of bubble sizes. Given that carp tend to show stronger negative phonotaxis in response to broadband sound versus pure tones [Vetter *et al.*, 2015, 2017], the deterrent effect of resonant bubble clouds insonified by a (1) single tone versus, (2) multiple tones and (3) a broadband signal, each covering a range of several matching bubble sizes could be compared. Furthermore, while it is known that fish can detect particle motion, it is currently still unclear whether they react to particle velocity, particle displacement, or particle acceleration [White, P.R. pers. comm.]. It has been suggested that thresholds for particle motion-sensitive fish be reported in terms of particle acceleration [Popper *et al.*, 2019] since in the infrasound range, audiograms related to particle velocity and particle displacement incorrectly tend to register a loss in sensitivity [Sand & Karlsen, 2000]. Determining this for a number of frequencies and/or for a small number of species would be a useful fundamental question.

All experiments in this thesis used small groups of 3 – 5 fish, although collective group behaviour was not considered at this stage. There is a lack of understanding of how behavioural deterrents impact collective behaviour, such as shoaling or schooling [Herbert Read *et al.*, 2017, Neo *et al.*, 2014; Currie *et al.*, 2020]. Groups of fish are made up of several individuals working within that collective, dependent on a complex feedback matrix through interactions with other individuals and the surrounding environment which facilitates foraging [Pitcher & House, 1987; Bajer *et al.*, 2010],

social information exchange, and anti-predator defence [Riley, 2014]. Individual fish within a group will also show variations in auditory sensitivities and motivation to respond. Carp [Bajer *et al.*, 2010], and their close relatives, goldfish [Pitcher & House, 1987], have been known to learn quickly from each other's foraging behaviour, while more strongly schooling cyprinids such as minnows show strong group responses to acoustic stimuli [Currie *et al.*, 2020]. Potential work in this area could involve how group decisions affect the deflection efficiency of a behavioural barrier.

Field-testing the concept of a bubble curtain that functions using resonance in a scenario more applicable to management and implementation would be a logical final step. Bearing in mind that the bubblers used in this thesis should not be considered to be a finished design, the concept could be modified to work in flow conditions encountered in the field. Currently, best practice for bubble barriers is to deploy them in water no deeper than 3 m, and to use bubbles of 2 mm or larger to ensure that their rise time is fast enough not to cause break-up of the bubble curtain [Turnpenny & O'Keefe, 2005]. Bearing in mind the approximate water depths that can be expected in the field, and the cut-off phenomenon, bubbles with a diameter of approximately 2 mm - 6 mm insonified by a frequency that falls between 1000 - 3000 Hz could prove viable.

This proposed set-up is based on the assumption that bubble curtains are roughly analogous to bar screens [Turnpenny & O'Keefe, 2005], however resonant bubbles can function as very effective absorbers even at low concentrations and significant reductions in sound speed can be achieved using void fractions of 1 % [Rino & Ngo, 1991; Yoon *et al.*, 1991]. Given that, for example, the wavelengths of sound used to insonify the bubble curtains in this thesis ranged between 0.35 – 1.5 m, it is possible that the "bar rack" analogy may be too conservative when applied to resonant bubble curtains. Further testing could include comparisons between a more traditional insonified bubble curtain (as above), and a "diffuse" setup, more similar to a cloud of bubbles than a defined curtain. It is expected that such a set-up would work best as behavioural guidance system to deflect migratory fish towards fish passes in lower-flow and lower-energy environments such as chalk streams. Given that the system is based on deterring fish by using a sudden sound gradient, an insonified bubble curtain would be expected to have a lower deflection efficiency in areas with higher background noise levels such as higher energy rivers, areas with sediments that have a large grain size,

and estuaries with large tidal ranges. Similarly, based on findings in the noise mitigation industry, it is generally not recommended to deploy bubble curtains in water flows greater than 0.75 m/s [Nehls *et al.*, 2007].

Finally, with regard to the fish used in the experiments, these were sourced from hatcheries. Two major reasons for this were (1) the ease of obtaining fish of a similar size, thus reducing the factors to control for, and (2) the difficulty in sourcing wild common carp from UK rivers. That said, it is important to discuss the drawbacks of using hatchery-based fish. They are often morphologically different [Fleming *et al.*, 1994] to their wild counterparts, and will often display different behaviour from wild individuals [Vowles & Kemp, 2014]. Although fish sourced from the wild tend to provide an increased applicability of results, applications of behavioural deterrents also include preventing fish from escaping aquaculture sites – such as in China, where aquaculture of carp species is of major economic importance. For such applications, therefore, results obtained from hatchery-raised fish would be representative of their behaviour.

Furthermore, hatchery-raised fish may differ from wild fish in terms of lifetime prior noise exposure, and while they are more likely to have a known or traceable-life history, in the absence of standards there might be no records of this [Leighton *et al.*, 2020]. Controlling sound exposure, and assessing to what extent this resembles the experience of the wild fish to which one wishes to apply the laboratory results would therefore not be possible [Leighton *et al.*, 2020].

## **6.1 Conclusions**

The research reported in this thesis was conducted in pursuit of two aims. The first was to assess the feasibility of an insonified bubble curtain that exploits the resonant properties of bubbles as a behavioural deterrent for fish, while the second was to help determine what drives fish behaviour when encountering such barriers. To realise these aims, four research objectives were identified (see Chapter 2). Conclusions drawn from this body of research in relation to each objective are presented below.

*Ob 1: Test the reactions of common carp to a bubble curtain that uses a lower air flow than those used in industry, in the absence of visual cues*

Coarse-scale carp response to a bubble curtain (air flow:  $30 \text{ L min}^{-1} \text{ m}^{-1}$ ) was tested. Passage rates were reduced to 34 % (standard injection) of the control rate. When the bubbler was in operation, the *Inner Passage Fraction* was reduced since the number of fish attempting passage through the space between the bubbler and the flume walls increased. This hinted at the ability of fish to sense gaps in a bubble curtain in the absence of visual stimuli.

*Ob 2: Divorce the effect of visual cues from stimuli generated by the bubble curtain by quantifying fish behaviour in the presence or absence of light when encountering insonified bubbles.*

Chapter 3 (Experiment 1) was the first study to quantify the effect of visual cues on fine-scale metrics of fish behaviour in the presence of an insonified bubble curtain. The presence of visual cues significantly increased passage efficiency and swimming velocity, and fish followed less sinuous trajectories compared to the same conditions in the dark. This indicates that visual cues are likely prioritised by carp when encountering a bubble curtain during the day.

*Ob 3: Compare the effectiveness of resonant versus non-resonant insonified bubble curtains to deter passage, and determine the stimuli responsible for eliciting this response.*

Behavioural metrics indicated that bubble clouds in resonance with an insonifying sound field are more effective deterrents, and that for the set-up used, passage rejection appears to be mediated by particle displacement and hydrodynamics (specifically the SD of the flow). For all treatments the acoustic pressure and particle displacement fields were mapped. A model based on work by Andreeva [1964], Weston [1967], and Baik [2013] was developed to identify the bubbles with the greatest acoustic effect in each population. The extinction cross-sections were determined for each radius bin. This provided theory to explain the observed acoustical effects when

identical volumes of gas are split between bubbles of different sizes, confirming that the treatments with the highest acoustic gradients contained bubbles at resonance with the sound field.

*Ob 4: Test to what extent do the individual components of a sound field (i.e. acoustic pressure and particle velocity) influence the behaviour and swimming trajectories of Common carp (Cyprinus carpio) when reacting to a sound stimulus*

Common carp tended to exhibit negative phonotaxis when exposed to regions with a high ratio of acoustic pressure to particle displacement, versus regions with a low ratio. They also tended to follow straighter trajectories when swimming through regions of high particle displacement. Due to high amounts of behavioural noise, it is still unclear whether regions with different ratios of acoustic pressure and particle displacement affect metrics such as swimming speed, group swimming speed, turning angle, and group distance.

## **6.2 Contributions to existing knowledge and thinking**

As a result of this thesis a number of original contributions to existing thinking have been made to the field of fish passage and underwater noise.

- In Chapter 1, a narrative review of fish passage and behavioural deterrent literature outlined a number of research gaps and flaws in some traditional research approaches when testing behavioural deterrents. These were namely; frequent absence of experimental details, reporting results in grey literature, use of proprietary signals or equipment preventing independent testing, a low number of studies determining the driving force behind the negative phonotaxis, and a lack of appreciation of the effects of bubble coalescence and how this could reduce control of the stimulus and thus reproducibility. The review also identified that no previous studies had examined the potential of using the resonant properties of bubbles to create a behavioural barrier using a much reduced air flow.



- Taking an approach where the experiments built progressively on each other, this work developed and tested an insonified bubble curtain that uses the resonant properties of bubbles by: (1) testing a bubble barrier curtain that uses a lower air flow than those found in the literature (Chapter 3), (2) divorcing the effect of visual cues from stimuli generated by the bubble curtain by quantifying fish behaviour in the presence or absence of light when encountering insonified bubbles (Chapter 4 – Experiment 1), (3) comparing the effectiveness of resonant versus non-resonant insonified bubble curtains to deter passage, and determining the stimuli responsible for eliciting this response (Chapter 4 – Experiment 2). This work has been submitted to the International Journal of the Acoustical Society of America as: Flores Martin, N., Leighton, T.G., White, P.R., Kemp, P.S. (in prep) The response of common carp (*Cyprinus carpio*) to insonified bubble curtains. The findings from Chapter 4 - Experiment 2 were also presented at the 178th Meeting Acoustical Society of America, San Diego, USA, 2 – 6 December 2019 as: Flores Martin, N., Leighton, T.G., White, P.R., Kemp, P.S. (2019) Influence of resonance-driven bubble clouds on fine-scale behaviour of common carp (*Cyprinus carpio*).
- The effect of visual cues on fish encountering an insonified bubble curtain was quantified. This work appears to explain the findings of Welton *et al.*, (2002), and matches the observations of Bibko *et al.*, [1974], who described similar behaviour in striped bass, and gizzard shad.
- Building on the work of Zielinski & Sorensen [2016], this study was the first to quantify which of the stimuli generated by an insonified bubble curtain are most likely to influence a fishes decision to swim away from it.
- A model was created to calculate the extinction, scattering, and absorption coefficients of the bubble sizes within a bubble population. This was based on the pioneering work of Andreeva [1963], Weston [1967], and Baik [2013]. The differences in the acoustic fields generated by each bubble / sound treatment could be confirmed. The model also confirmed that a small amount of bubbles at resonance have an effect which is disproportionate to their size and numbers. This

model could be used as a tool for future work when testing insonified bubble curtains. The model can be accessed on [GitHub](#).

- In line with calls by the international bioacoustics community to examine the importance of particle motion in addition to that of acoustic pressure, and also building on work by Zielinski & Sorensen [2017], the final experiment (Chapter 5) of this thesis looked at how regions of high acoustic pressure but low particle displacement (and vice versa) generated by shifting the phase of a speaker signal affect common carp behaviour. It is likely that regions of high acoustic pressure play more of a role in eliciting negative phonotaxis in fish, however results were not conclusive.
- During my candidature, I was given the opportunity to participate in collaborative and cross-disciplinary research in two other projects:
  1. Understanding the impact of an invasive nematode on the function of the European eel swimbladder. The aim of this interdisciplinary study was to use tensile tests to characterise rupture strength and elasticity of the swimbladder wall at various stages of infection. The swimbladder functions as a buoyancy aid and allows the eel to control its depth in the water column. Since the European eel is critically endangered, any reduction in swimbladder function can be fatal for eels undergoing their spawning migration to the Sargasso sea. The findings were published in the *Journal of Experimental Biology* as: Currie, H.A.L., Flores Martin, N., Espindola Garcia, G., Davis, F.M., Kemp, P.S. (2020), A mechanical approach to understanding the impact of the nematode *Anguillicoloides crassus* on the European eel swimbladder;
  2. Testing the effects of simulated passage through a hydropower turbine on a commercially important species of fish, *Prochilodus lineatus*. The research was carried out at the Ouro Branco campus of USJ, Minas Gerais, Brazil, using a custom built manually controlled barotrauma chamber to simulate the rapid changes in pressure that occur as a migrating fish passes through a hydropower turbine. The findings were

presented at two conferences as: Currie, H.A.L., Flores Martin, N., Espindola Garcia, G., Silva, L.G.M., Kemp, P.S., Castro A.L.F. (2017) Barriers to Migration: The impacts of barotrauma on the physiology of a commercially important species (*Prochilodus lineatus*), American Fisheries Society 147th Annual Meeting, Tampa, 20 - 24 August 2017, and: Castro, A.L.F., Currie, H.A.L., Flores Martin, N., Espindola Garcia, Kemp, P.S., G., Silva, L.G.M. (2017) Barriers to Migration: The impacts of barotrauma on the physiology of a commercially important species (*Prochilodus lineatus*), XXII Encontro Brasileiro de Ictiologia, Universidade Federal do Sul da Bahia, Porto Seguro, Brazil, 29 January - 3 February 2017;

Research presented in this thesis highlights the importance of properly characterising the properties of an insonified bubble barrier: i.e. recording the bubble size distribution, airflow, pressure, nozzle size, sound frequency and level, in addition to fine-scale mapping of the acoustic and particle motion fields generated by the set-up. This should ensure that studies can be compared and replicated, avoiding a repeat of the same oversights highlighted earlier in the chapter.

## References:

- Aarestrup K., Nielsen C., & Koed A. (2002) Net ground speed of downstream migrating radio-tagged Atlantic salmon (*Salmo salar L.*) and brown trout (*Salmo trutta L.*) smolts in relation to environmental factors. *Hydrobiologia*. 483, pp. 95–102.
- Adler, M., Mayo, A., & Alon, U. (2014). Logarithmic and Power Law Input-Output Relations in Sensory Systems with Fold-Change Detection. *PLoS Comput Biol* 10(8): e1003781.
- Ainslie, M.A., Robinson, S.P., Halvorsen, M.B., & de Jong, C.A.F. (2019) International standardisation in underwater bioacoustics, paper presented to The Effects of Underwater Noise on Marine Life, The Hague, NL, 7-13 July 2019.
- Ainslie, M.A. & Leighton, T.G. (2011) Review of scattering and extinction cross-sections, damping factors, and resonance frequencies of a spherical gas bubble, *J. Ac. Soc. Am.* 130(5), pp. 3184–3208.
- Ainslie, M.A. & Leighton, T.G. (2009) Near resonant bubble acoustic cross-section corrections, including examples from oceanography, volcanology, and biomedical ultrasound, *J. Acoust. Soc. Am.*, 126(5), pp. 2163-2175.
- Andreeva, I.B. (1964) Scattering of sound by air bladders of fish in deep sound-scattering ocean layers, *Sov. Phys. Acoust.* 10, pp. 17–20.
- Akamatsu, T., Okumura, T., Novarini, N., & Yan, H.Y. (2002) Empirical refinements applicable to the recording of fish sounds in small tanks. *J. Acoust. Soc. Am.* 112, pp. 3073–3082
- Ali, M.A. (1961) Histophysiological studies on the juvenile Atlantic salmon (*Salmo salar*) retina. *Can J Zool* 39, pp. 511–525.
- Alikunhi, K. H. (1966) Synopsis of Biological Data on Common Carp *Cyprinus carpio* Linnaeus, 1758 (Asia and the Far East). Rome: FAO.
- Alvevras, R. A. (1974) Status of air bubble fish protection system at Indian Point Station on the Hudson River, pp. 289-291. In: Jensen, L. D. (Ed.), *Entrainment and intake screening*. Proc. 2nd Entrain. & Intake Screen. Work., Johns Hopkins Univ., Baltimore, Maryland.

American Rivers, Friends of the Earth & Trout Unlimited. (1999) Dam Removal success stories: Restoring rivers through selective removal of dams that don't make sense. Washington, D.C.

Amaral, S.V., Winchell, F.C., McMahon, B.J., & Dixon, D.A. (2003) Evaluation of angled bar racks and louvers for guiding silver phase American eels, pp. 367–376. In: Dixon, D.A. (Ed.) Biology, management and protection of catadromous eels. Bethesda, MD: American Fisheries Society, Symposium 33.

Amoser, S. & Ladich, F. (2005) Are hearing sensitivities of freshwater fish adapted to the ambient noise in their habitats? *J. Exper. Biol.* 208, pp. 3533-3542.

Andersson, M.H., Andersson, S., Ahlsen, J., Andersson, B.L., Hammar, J., Persson, L.K., Pihl, J., Sigray, P., & Wissstrom, A. (2017). "A framework for regulating underwater noise during pile driving. A technical Vindal report," Environmental Protection Agency, Stockholm, Sweden.

Andreae, M.O., (1986) In: The role of air-sea exchange in geochemical cycling, Buat-Menard, P. (Edit.), Reidel, Dordrecht, The Netherlands, pp. 331-363.

Andreeva, I.B. (1964) Scattering of sound by air bladders of fish in deep sound-scattering ocean layers, *Sov. Phys. Acoust.* 10, pp. 17–20.

Anonymous. 1970. Fish protection at Indian Point, Unit No. 1. Consolidated Edison Co., New York, N. Y.: 34pp. (mimeo).

Baik, K. (2013) Comment on 'Resonant acoustic scattering by swimbladder-bearing fish' [*J. Acoust. Soc. Am.* 64, 571–580 (1978)] (L)," *J. Acoust. Soc. Am.* 133 (1), pp. 5-8.

Bajer, P.G. & Sorensen, P.W. (2010) Recruitment and abundance of an invasive fish, the common carp, is driven by its propensity to invade and reproduce in basins that experience winter-time hypoxia in interconnected lakes. *Biol. Invasions.* 12, pp. 1101–1112.

Bajer, P.G., Lim, H., Travaline, M.J., Miller, B.D., & Sorensen, P.W. (2010) Cognitive aspects of food searching behavior in free-ranging wild Common Carp. *Environ. Biol. Fish.* 88, pp. 295–300.

Baker, J. L. L. & Chao, B. T. (1965), An experimental investigation of air bubble motion in a turbulent water stream. *AIChE J.* 11, pp. 268–273.

- Balon, E.K. (1995) Origin and domestication of the wild carp, *Cyprinus carpio*—from Roman gourmets to the swimming flowers. *Aquaculture*. 129, pp. 3–48.
- Batschelet, E. (1981) *Circular Statistics in Biology*. London, Academic Press.
- Bates, D. W. & VanDerwalker, J.G. (1964) Exploratory experiments on the deflection of juvenile salmon by means of water and air jets. *Fish Passage Res. Prog., Rev. Prog., U. S. Bur. Comm. Fish.*, 3(14), 6 pp.
- Baumgartner, L.J., Reynoldson, N., & Gilligan, D.M. (2006) Mortality of larval Murray Cod (*Maccullochella peelii peelii*) and Golden Perch (*Macquaria ambigua*) associated with passage through two types of low-head weirs. *Mar. Fresh. Res.* 57, pp. 187-191.
- Baxter, R.M. (1977) Environmental Effects of Dams and Impoundments. *Ann. Rev. Ecol. Sys.* 8, pp. 255-283.
- Beasley, C.A. & Hightower, J.E. (2000) Effects of a low-head dam on the distribution and characteristics of spawning habitat used by striped bass and American shad. *Trans. Am. Fish. Soc.* 129, pp. 1316–1330.
- Bejder, L., Samuels, A., Whitehead, H., Finn, H., & Allen, S. (2009) Impact assessment research: use and misuse of habituation, sensitisation and tolerance in describing wildlife responses to anthropogenic stimuli. *M. E. P. S.* 395, pp. 177–185.
- Bell, M.C. (1973) *Fisheries handbook of Engineering requirement and biological criteria*. U.S. Army Corps of Engineers. Portland, Oregon.
- Benhamou, S. (2004) How to reliably estimate the tortuosity of an animal's path: straightness, sinuosity, or fractal dimension? *J. Theor. Biol.* 229, pp. 209-220.
- Benito, J., Benejam L., Zamora, L., Garcia-Berthou, E. (2015). Diel Cycle and Effects of Water Flow on Activity and Use of Depth by Common Carp, *Trans. Am. Fish. Soc.* 144, 491-501.
- Bibko, P. N., Wirtenan, L., & Kueser, P.E. (1974) Preliminary studies on the effects of air bubbles and intense illumination on the swimming behavior of the striped bass (*Morone saxatilis*) and the gizzard shad (*Dorosoma cepedianum*), pp. 293-304. In: Jensen, L. D.(ed.), *Entrainment and intake screening*. Proc. 2nd Entrain. In-take Screen. Work., Johns Hopkins Univ., Baltimore, Md.

- Bij de Vaate, A., Jazdzewski, K., Ketelaars, H.A., Gollasch, S., & Van der Velde, G. (2002) Geographical patterns in range extension of Ponto-Caspian macroinvertebrate species in Europe. *Can. J. Fish. Aq. Sci.*, 59, pp 1159 – 1117.
- Blaxter, J.H.S., Gray, J.A.B., & Denton, E.J. (1981) Sound and startle responses in herring shoals. *J Mar Biol Assoc UK* 61, pp. 851–869.
- Bishai, H. M., Ishak, M. M., & Labib, W. (1974) Fecundity of the mirror carp *Cyprinus carpio* L. at the Serow Fish Farm (Egypt). *Aquacult.* 4, pp. 257–265.
- Bovet, P. & Benhamou, S. (1998) Spatial analysis of animals' movements using a correlated random walk model. *J. Theor. Biol.* 131, pp. 419-433.
- Burnham, K.P. & Anderson, D.R. (2002) *Model Selection and Multimodel Inference. A Practical Information-Theoretical Approach.* Springer-Verlag, New York, USA.
- Bohne, T., Griebmann, T., Rolfes, R., (2020) Integral modelling of the bubble formation process to predict the transmission loss of a bubble curtain. *Int. J. Multiph. Flow*, 132, 103436.
- Bramsnaes, F., Morgens, J., & Otterstrom, C.V. (1942) Barriers against fishes by means of electricity of veils of air. *Rept. Danish. Biol. Stn.*, 47, pp. 39-46.
- Bregman, A.S. (1990) *Auditory Scene Analysis: The Perceptual Organization of Sound.* Cambridge, MA: MIT Press.
- Brett, J. R. & MacKinnon, K.D. (1953) Preliminary experiments using lights and bubbles to deflect migrating young spring salmon. *J. Fish. Res. Bd. Can.*, 10(8), pp. 548-559.
- Brevik, I. & Kristiansen, Ø., (2002) The flow in and around air-bubble plumes. *Int. J. Multiph. Flow.* 28, pp. 617–634
- Britton, J.R., Davies, G.D. & Brazier, M. (2010) Towards the successful control of the invasive *Pseudorasbora parva* in the UK. *Biol. Invasions.* 12, pp. 125–131.
- Braun, C.B. & Grande, T. (2008) Evolution of Peripheral Mechanisms for the Enhancement of Sound Reception, In: Webb, J.F., Fay, R.R., Popper, A.N. (Eds.), *Fish bioacoustics:* Springer, pp. 99-144.

- Brown, L., Haro, A. & Castro-Santos, T. (2009) Three-Dimensional Movement of Silver-Phase American Eels in the Forebay of a Small Hydroelectric Facility. *Am. Fish. Soc. Sympos.* 58, pp. 277–291.
- Brown, R.S., Ahmann, M.L., Trumbo, B.A. & Foust, J. (2012) Fish protection: cooperative research advances fish friendly turbine design. *Hydro Review.* 31 (8), pp. 48-53.
- Brown, R.S., Carlson, T.J., Welch, A.E., Stephenson, J.R., Abernethy, C.S., Ebberts, B.D., Langeslay, M.J., Ahmann, M.L., Feil, D.H., Skalski, J.R. & Townsend, R.L. (2009) Assessment of barotrauma from rapid decompression of depth-acclimated juvenile Chinook salmon bearing radiotelemetry transmitters. *Trans. Am. Fish. Soc.* 138(6), pp.1285-1301.
- Brown, R.S., Colotelo, A.H., Pflugrath, B.D., Boys, C.A., Baumgartner, L.J., Deng, Z.D., Silva, L.G.M., Brauner, C.J., Mallen-Cooper, M., Phonekhangpeng, O., Thorncraft, G., & Singhanouvong, D. (2014) Understanding barotrauma in fish passing hydro structures: A global strategy for sustainable development of water resources. *Fisheries.* 39(3), pp. 96-122.
- Bruintjes, R., Purser, J., Everley, K.A., Mangan, S., Simpson, S.D., & Radford, A.N. (2016) Rapid recovery following short-term acoustic disturbance in two fish species. *R. Soc. open sci.* 3(1), 150686.
- Bruintjes, R. & Radford, A.N. (2014) Chronic playback of boat noise does not impact hatching success or posthatching larval growth and survival in a cichlid fish. *Peer. J.* 2, e594.
- Budaev S.V. & Zworykin, D.D. (2002) Individuality in fish behavior: ecology and comparative psychology. *J. Ichthy.* 42 (2), pp. 189–195.
- Budy, P., Thiede, G.P., Bouwes, N., Petrosky, C.E., & Schaller, H. (2002) Evidence linking delayed mortality of Snake River salmon to their earlier hydrosystem experience. *N. Am. J. Fish. Manage.* 22, pp. 35–51.
- Bui, S., Oppedal, F., Korsøen, Ø.J., Sonny, D., & Dempster, T. (2013) Group Behavioural Responses of Atlantic Salmon (*Salmo salar* L.) to Light, Infrasound and Sound Stimuli. *PLoS ONE* 8(5): e63696.
- Bullen, C.R. & Carlson, T.J. (2003) Non-physical fish barrier systems: their development and potential applications to marine ranching. *Rev. Fish Biol. Fish.* 13 (2), pp. 201–212.
- Burnaby, F. (1874) *A ride to Khiva*, Cambridge University Press, UK.



Butchart, S.H.M., Walpole, M., Collen, B., van Strien, A., Scharlemann, J.P.W., Almond, R.E.A., Baillie, J.E.M., Bomhard, B., Brown, C., Bruno, J., Carpenter, K.E., Carr, G.M., Chanson, J., Chenery, A.M., Csirke, J., Davidson, N.C., Dentener, F., Foster, M., Galli, A., Galloway, J.N., Genovesi, P., Gregory, R.D., Hockings, M., Kapos, V., Lamarque J-F., Leverington, F., Loh, J., McGeoh, M.A., McRae, L., Minasyan, A., Hernández Morcillo, M., Oldfield, T.E.E., Pauly, D., Quader, S., Revenga, C., Sauer, J.R., Skolnik, B., Spear, D., Stanwell-Smith, D., Stuart, S.N., Symes, A., Tierny, M., Tyrrell, T.D., Vié, J-C., & Watson, R. (2010) Global biodiversity: indicators of recent declines. *Science*, 328, pp. 1164–1168.

Cada, G. F., Coutant, C.C. & Whitney, R.R. (1997) Development of biological criteria for the design of advanced hydropower turbines. U.S. Department of Energy, Idaho Operations Office, Report DOE/ID-10578, Idaho Falls.

Cahn, A.R. (1929) The effect of carp on a small lake: the carp as a dominant. *Ecology*. 10, pp. 271–274.

Cahn, P.H., Siler, W., & Wodinsky, J. (1969) Acoustico-lateralis system of fishes. Tests of pressure and particle-velocity sensitivity in grunts, *Haemulon sciurus* and *Haemulon parrai*. *J. Acoust. Soc. Am.*. 46, pp. 1572–1578.

Calles, O., Olsson, I.C., Comoglio, C. Kemp, P.S., Blunden, L., Schmitz, M., & Greenberg, L.A. (2010) Size-dependent mortality of migratory silver eels at a hydropower plant, and implications for escapement to the sea, *Freshw. Biol*, 55, pp. 2167–2180.

Caltrans (California Department of Transportation) (2009) Technical guidance for assessment and mitigation of the hydroacoustic effects of pile driving on fish (<http://ter.ps/3xk> ). Appendix I, revised 2012, Compendium of pile driving sounds (<http://ter.ps/3x1> ).

Campbell, J., Shafiei Sabet, S., & Slabbekoorn, H. (2019) Particle motion and sound pressure in fish tanks: A behavioural exploration of acoustic sensitivity in the zebrafish. *Behav. Process*. 164, pp. 38–47.

Capranica R. R. & Moffat A. J. M. (1983) Neurobehavioral correlates of sound communication in anurans. In *Advances in Vertebrate Neuroethology* (ed. Ewert J. P., Capranica R. R. and Ingle D. J.), pp. 701-730 New York: Plenum Press.

Carey, W. M. & Bradley, M.P. (1985) Low-frequency ocean surface noise sources. *J. Acoust. Soc. Am. Suppl.* 1 78, S1-S2.

- Carey, W. M. & Browning, D. G. (1988) Low-frequency ocean ambient noise: Measurements and theory. In: Sea Surface Sound, Kerman, B.R. [Ed.] (Kluwer, Dordrecht), pp. 361-376.
- Carlson, T.J. (1994) Use of sound for fish protection at power production facilities: A historical perspective of the state of the art. Phase I Final Rep., Proj. 92-071, Bonneville Power Admin., Portland OR, 58 pp.
- Carlson, T.J.B. & Popper, A.N. (1997) Using Sound To Modify Fish Behavior At Power-Production And Water-Control Facilities: A Workshop December 12-13, 1995 Portland State University Portland, Oregon, Phase II: Final Report, Report to Bonneville Power Administration, Contract No. 1986BP62611, Project No. 199207101, 360 pp.
- Carlton, J.T. (1985) Transoceanic and interoceanic dispersal of coastal marine organisms: the biology of ballast water. *Oceanog. Mar. Biol. Ann. Rev.* 23, pp. 313–371.
- Carr, J. (2000) Atlantic salmon (*Salmo salar* L.) smolt migration patterns in the dam-impacted St John river systems. In: *Advances in fish telemetry* (Ed. A. More & I. Russell). CEFAS, Lowestoft, pp. 47-72.
- Carr, J.W. & Whoriskey, F.G. (2008) Migration of silver American eels past a hydroelectric dam and through a coastal zone. *Fish. Mgmt. Ecol.* 15, 393–400.
- Casper, B.M., Halvorsen, M.B., Matthews, F., Carlson, T.J., & Popper, A.N. (2013) Recovery of barotrauma injuries resulting from exposure to pile driving sound in two sizes of hybrid striped bass. *PLoS ONE* 8 (9), e73844.
- Casper, B.M., Popper, A.N., Matthews, F., Carlson, T.J., & Halvorsen, M.B. (2012) Recovery of barotrauma injuries in Chinook salmon, *Oncorhynchus tshawytscha* from exposure to pile driving sound. *PLoS ONE* 7 (6), e39593.
- Castro Santos, T., Cotel, A., & Webb, P. (2009) Fishway evaluations for better bioengineering: an integrative approach, AFS, Symposium 69, pp. 557-575.
- Chapman, C.J. & Johnstone, A.D.F. (1974) Some auditory discrimination experiments on marine fish. *J Exp Biol.* 61, pp. 521-528.
- Chapman, C.J. & Hawkins, A.D. (1973) A field study of hearing in the cod, *Gadus morhua* L. *J. Comp. Physiol.* 85, pp. 147-167.

- Charlson, R.J., Lovelock, J.E., Andreae, M.O., & Warren, S.G. (1987) Oceanic phytoplankton, sulphur, cloud albedo and climate. *Nature*, 326, pp. 655-661.
- Chase, A. (2002) Music discriminations by carp (*Cyprinus carpio*), *Anim. Learn. Behav.* 29 (4), pp. 336-353.
- Chen, D., Duan, X., Liu, S. & Shi, W. (2004) Status and management of fishery resources of the Yangtze river. In: Welcomme, R., & Petr, T. (Eds.), *Proceedings of the Second International Symposium on the Management of Large Rivers for Fisheries*, vol. I. FAO Regional Office for Asia and the Pacific, Bangkok, Thailand, pp. 173–182.
- Chick, J.H. & Pegg, M.A. (2001) Invasive carp in the Mississippi River basin. *Science*, 292(5525), pp. 2250–2251.
- Clift, R., Grace, J.R., & Weber, M.E. (1978) *Bubbles, Drops and Particles*, Academic Press, London, UK.
- Codarin, A., Wysocki, L.E., Ladich, F., & Picciulin, M. (2009) Effects of ambient and boat noise on hearing and communication in three fish species living in a marine protected area (Miramare, Italy). *Mar. Poll. Bull.* 58, pp. 1880-1887.
- Colautti, R.I. & MacIsaac, H.J. (2004) Diversity. *Distrib.* 10, pp. 135–141.
- Commander, K.W., & Prosperetti, A. (1989) Linear pressure waves in bubbly liquids: Comparison between theory and experiments, *J. Acoust. Soc. Am.*, 85(2), pp. 732-746.
- Cooke S.L., Hill W.R., & Meyer K.P. (2009) Feeding at different plankton densities alters invasive bighead carp (*Hypophthalmichthys nobilis*) growth and zooplankton species composition. *Hydrobiologia.* 625, pp. 185-193.
- Coombs, S., Janssen, J., Webb, J.F. (1988) Diversity of lateral line systems: evolutionary and functional considerations. In: Atema, J., Fay, R.R., Popper, A.N., Tavolga, W.N. (eds) *Sensory Biology of Aquatic Animals*. New York: Springer, pp. 553–593.
- Coombs, S., & Montgomery, J.C. (1999) The enigmatic lateral line system. In: Fay, R.R., Popper, A.N. (eds) *Comparative Hearing: Fish and Amphibians*. Springer Handbook of Auditory Research. New York: Springer, pp. 319–362

Copp, G., Bianco, P., Bogutskaya, N.G., Eros, T., Falka, I., Ferreira, M., Fox, M.G., Freyhof, J., Gozlan, R., Grabowska, J., Kovác, V., Moreno-Amich, R., Naseka, A., Pawson, M.G., Penáz, M., Povž, M., Przybylski, M., Robillard, M., Russell, I., & Wiesner, C. (2005). To be, or not to be, a non-native freshwater fish?. *J. App. Ichtyol.* 21, pp. 242-262.

Corwin, J.T. (1981) Audition in elasmobranchs. In: Tavolga, W.N., Popper, A.N., Fay, R.R. (Eds.), *Hearing and Sound Communication in Fishes*. Springer-Verlag, New York, pp. 81-105.

Crivelli, A.J. (1983) The destruction of aquatic vegetation by carp—a comparison between Southern France and the United-States. *Hydrobiologia.* 106, pp. 37–41.

Cultured Aquatic Species Information Programme. *Cyprinus carpio*. Cultured Aquatic Species Information Programme. Text by Peteri, A. In: FAO Fisheries and Aquaculture Department [online]. Rome. Updated 1 January 2004.

Currie, H.A.L., White, P.R., Leighton, T.G., & Kemp, P.S. (2020) Group behavior and tolerance of Eurasian minnow (*Phoxinus phoxinus*) in response to tones of differing pulse repetition rate, *J. Acoust. Soc. Am.* 147(3), pp. 1709-1718.

Czerski, H. (2011) A candidate mechanism for exciting sound during bubble coalescence. *J. Acoust. Soc. Am.* 129(3), EL83-EL88.

Dadswell, M.J., Kaluda, R.J., Moffitt, C.M., Saunders, R.L., Rulifson, R.A., & Cooper, J.E. (Eds.) (1987) *Common Strategies of Anadromous and Catadromous Fishes*. American Fisheries Society Symposium 1. Bethesda, MD: American Fisheries Society.

Dawson, H.A., Reinhardt, U.G., & Savino, J.F. (2006) Use of electric or bubble barrier to limit the movement of Eurasian Ruffe (*Gymnocephalus cernuus*). *J. Great Lakes Res.* 32, pp. 40–49.

Deleau, M.J.C., White, P.R., Peirson, G., Leighton, T.G., & Kemp, P.S. (2019) Use of acoustics to enhance the efficiency of physical screens designed to protect downstream moving European eel (*Anguilla anguilla*), *Fish. Manag. Ecol.*, 27(1), pp. 1-9.

Deleau, M.J.C., White, P.R., Peirson, G., Leighton, T.G., & Kemp, P.S. (2020) The response of anguilliform fish to underwater sound under an experimental setting, *River Res. Applic.* 36 (3), pp. 441-451.

Dennis, C.D., Zielinski, D.P., & Sorensen, P.W. (2019) A complex sound coupled with an air curtain blocks invasive carp passage without habituation in a laboratory flume, *Biol. Inv.* 21, pp. 2837–2855.

Department for Business, Energy, and Industrial Strategy (2019) The UK's Draft Integrated National Energy and Climate Plan (NECP), 139 pp.

de Munck, J.C. & Schellart, N., (1987) A model for the nearfield acoustics of the fish swimbladder and its relevance for directional hearing, *J. Ac. Soc. Am.*, 81(2), pp. 556-60.

De Vries, H. L. (1950) The mechanics of labyrinth otoliths. *Acta oto-laryngol.* 38, pp. 262-273.

Dijkgraaf, S. (1960) Hearing in bony fishes. *Proc. R. Soc. Lond. Ser. B.* 152, pp. 51-54.

Domenici, P., Blagburn, J.M., Bacon, J.P. (2011) Animal escapology II: escape trajectory case studies. *J Exp Biol* 214, pp. 2474–2494.

Downing, J. A. & Plante, C. (1993) Production of fish populations in lakes. *Can. J. Fish. Aq. Sci.* 50, pp. 110–120.

Dudgeon, D. (1992) Endangered ecosystems: a review of the conservation status of tropical Asian rivers. *Hydrobiologia.* 248, pp. 167-191.

Ehrlich, P. R. (1984). Which animal will invade? Pp 79–95 in Mooney, H.A., & Drake, J.A. (Eds.) (1984) *Ecology of biological invasions of North America and Hawaii.* Springer-Verlag, New York.

Electric Power Research Institute (EPRI), (1998) Evaluation of Fish Behavioral Barriers. Technical Report 109483. Palo Alto, CA.

Electric Power Research Institute (EPRI), (2004) Chapter 22: Behavioral Methods, Fish Passage Manual Chapter Updates. Technical Report 1011448. Palo Alto, CA.

Electric Power Research Institute, (1986) Assessment of downstream migrant fish protection technologies for hydroelectric application. EPRI Report No. 2694-1. Palo Alto, CA.

Electric Power Research Institute, (1994) Research Update on Fish Protection Technologies for Water Intakes. Prepared by Stone & Webster Engineering Corporation, EPRI TR-104122.

Elmer, K.H., Gattermann, J., Kuhn, C., & Bruns, B., (2012) Hydroschalldämpfer (HSD) zur Schallminderung bei Offshore Rammarbeiten, DUH Conference „Herausforderung Schallschutz beim Bau von Offshore Windparks, 25/26 September 2012, Deutsche Umwelthilfe, Berlin.

Enami, S. (1960) Studies on the bubble net. II. Experiments on some sea water fishes performed on the driving and intercepting effects. Bull. Japan. Soc. Sci. Fish. 26(3), pp. 269-272.

Enders, E.C., Gessel, M.H., & Williams, J.G. (2009) Development of successful fish passage structures for downstream migrants requires knowledge of their behavioural response to accelerating flow. Can. J. Fish. Aquat. Sci. 66, pp. 2109–2117.

Endler, J.A. (1991) Interactions between predators and prey. In: Krebs JR, Davies NB (eds). Behavioural Ecology: An Evolutionary Approach. Oxford: Blackwell Scientific Publications. 169–196.

Engås A., Løkkeborg S., Ona E., & Soldal, A.V. (1996). Effects of seismic shooting on local abundance and catch rates of cod (*Gadus morhua*) and haddock (*Melanogrammus aeglefinus*). Canadian Journal of Fisheries and Aquatic Sciences 53, pp. 2238–49.

Engelmann, J., Hanke, W., Mogdans, J., & Bleckmann, H. (2000) Hydrodynamic stimuli and the fish lateral line. Nature 408, pp. 51–52.

Enger, P.S., Kalmijn, A.J., & Sand, O. (1989) Behavioural investigations on the functions of the lateral line and inner ear in predation. In: Coombs S, Gorner P, Münz H (eds). The Mechanosensory Lateral Line. New York: Springer Verlag. 575–587.

English, T. S. (1951). Growth studies of the carp, *Cyprinus carpio* Linnaeus, in Clear Lake, Iowa. Iowa Stat. J. of Sci. 24, pp. 537–540.

Environmental Protection Agency (1973) Development document for proposed best technology available for minimizing adverse environmental impact of cooling water intake structures. U. S. Environ. Protect. Agency, EPA 440/ 1-74/015, 175 pp.

Environmental Protection Agency (1976) Development document for best technology available for the location, design, construction and capacity of cooling water intake structures for minimizing adverse environmental impact. U. S. Environ. Protect. Agency, EPA 440/1-76/015-a, 263 pp.

Erbe, C., Ainslie, M.A., de Jong, C.A., Racca, R. & Stocker, M. (2016) Summary Report Panel 1: The need to protocols and standards in research on underwater noise impacts on marine life. In *The Effects of Noise on Aquatic Life II*. New York: Springer.

EU (2020) COM/2020/562 Communication from from the Commission to the European Parliament, the European Council, the Council. Stepping up Europe's 2030 climate ambition Investing in a climate-neutral future for the benefit of our people, 26 pp.

EU (2019) COM/2019/640 Communication from the Commission to the European Parliament, the European Council, the Council. The European Economic and Social Committee and the Committee of the Regions, *The European Green Deal*, 24 pp.

EU (2018) Directive (EU) 2018/2001 of the European Parliament and of the Council of 11 December 2018 on the promotion of the use of energy from renewable sources, *Off. J. Eur. Commun. Legis. L 328*, pp. 82–209.

EU (2018) Guidance on The requirements for hydropower in relation to EU Nature legislation, Publications Office of the European Union, Luxembourg, 87 pp.

EU (2014) Regulation (EU) No 1143/2014 of the European Parliament and of the Council on the prevention and management of the introduction and spread of invasive alien species, *Off. J. Eur. Commun. Legis. L 315*, pp. 35 – 55.

EU (2000) Directive 2000/60/EC of the European Parliament and of the Council of 23 October 2000 establishing a framework for Community action in the field of water policy, *Off. J. Eur. Commun. Legis. L 327(1)*, pp. 1–71.

Faulkner, R.C., Farcas, A., & Merchant, N.D. (2018) Guiding principles for assessing the impact of underwater noise. *J. Appl. Ecol.* 55, pp. 2531–2536.

Fay, R.R. (1988) *Hearing in Vertebrates: A Psychophysics Handbook*. Winnetka, IL: Hill-Fay Associates.

Fay, R.R. (2008) Sound source perception and stream segregation in non-human vertebrate animals. In: Yost, W.A., Popper, A.N., & Fay, R.R. (Eds.) *Auditory Perception of Sound Sources*.

Fay, R.R. (2009) Soundscapes and the sense of hearing of fishes. *Integrative Zoology*. 4: pp. 26-32.

- Fay, R.R. (2011) Directional Hearing in Fishes, Advances in Sound Localization, In: Dr. Pawel Strumillo (Ed.), Advances in Sound Localization, Intech, pp. 493-512.
- Fay, R.R. & Edds-Walton, P.L. (1997) Directional response properties of saccular afferents of the toadfish, *Opsanus tau*. Hear Res. 111, pp. 1-21.
- Fay, R.R. & Popper, A.N. (Eds.) (1999) Comparative Hearing: Fish and Amphibians. New York: Springer-Verlag.
- Fay, R.R. & Popper, A.N., (1974) Acoustic stimulation of the ear of the goldfish (*Carassius auratus*). J. Exp. Biol. 61, pp. 243-260.
- Fay, R.R. & Popper, A.N., (1975) Modes of stimulation of the teleost ear. J. Exp. Biol. 62, pp. 379-387.
- Fay, R.R., Coombs, S., & Elepfandt, A. (2002) Response of goldfish otolithic afferents to a moving dipole sound source. Bioacoustics. 12(2-3), pp. 172-174.
- Fechner, G.T. (1860). Elemente der Psychophysik, Leipzig: Breitkopf & Härtel, 1860.
- Fida, S., Qadri, M. Y., & Siddiqi, M. (1988) Influence of environmental conditions on the ovarian cycle and serum chemistry of *Cyprinus carpio* in the Dal Lake, Kashmir (India). Freshwater Biol. 20, pp. 61–67.
- Flammang, M. K., Weber, M.J., & Thul, M.D. (2014) Laboratory evaluation of a bioacoustic bubble strobe light barrier for reducing Walleye escapement. N. Am. J. Fish. Manage. 34, pp. 1047–1054.
- Fu, C., Wu, J., Chen, J., Wu, Q., & Lei, G. (2003). Freshwater Fish Biodiversity in the Yangtze River Basin of China: Patterns, Threats and Conservation. Biodiversity and Conservation - Biodivers. Conserv. 12. pp. 1649-1685.
- Fullbrook, L. (2015) The Influence of Schooling Behaviours on the Effectiveness of Non-Physical Screens. MSc Thesis, University of Southampton. 38 pp.
- Fuller, P. L., Nico, L.G., & Williams, J.D. (Eds.) (1999) Non-indigenous fishes introduced into inland waters of the United States. American Fisheries Society Special Publication 27.



Galil, B.S., Nehring, S., & Panov, V.E. (2007) Waterways as invasion highways – Impact of climate change and globalization. In: Nentwig, W. (ed), Biological Invasions. Ecological Studies Nr. 193, Springer, Berlin, pp 59–74.

Gaudin, A.M. (1957) Flotation, McGraw-Hill, New York

Gehrke, P.C., Brown, P., Schiller, C.B., Moffatt, D.B., Bruce, A.M. (1995) River regulation and fish communities in the Murray-Darling River System, Australia. Regul. Rivers. Res. Manag., 11, pp. 363–375.

Genovesi, P. & Shine, C. (2004). European strategy on invasive alien species. Nature and Environment 137. Strasbourg (FR): Council of Europe. 67 pp.

GLEC, 1994. Report on fish diversion at Four Mile Dam using strobe lighting and air bubble curtain techniques.

Goodwin, R.A., Politano, M., Garvin, J.W., Nestler, J.M., Haye, D., Anderson, J.J., Weber, L., Dimperio, E., Smith, D.L., & Timko, M. (2014) Fish navigation of large dams emerges from their modulation of flow field experience. PNAS. 111 (14), pp. 5277–5282.

Gosset C. & Travade F., (1999) Etude de dispositifs d'aide à la migration de dévalaison des salmonidae: barrières comportementales (A study of facilities to aid the downstream migration of salmonids: behavioural screens). Cybium. 23(1), pp. 45-66.

Gowans, A.R.D., Armstrong, J.D., & Priede., I.G. (1999) Movements of adult Atlantic salmon through a reservoir above a hydroelectric dam: Loch Faskally. J. of Fish Biol. 54, pp. 727–740.

Gozlan, R.E., Pinder, A.C., & Shelley, J. (2002) Occurrence of the Asiatic cyprinid *Pseudorasbora parva* in England. J. Fish. Biol. 61, pp. 298–300.

Gozlan, R.E., St-Hilaire, S., Feist, S.W., Martin, P., & Kent, M.L. (2005) An emergent infectious disease threatens European fish biodiversity. Nature. 435, pp. 1046.

Graham, A.L. & Cooke, S.J. (2008) The effects of noise disturbance from various recreational boating activities common to inland waters on the cardiac physiology of a freshwater fish, the largemouth bass (*Micropterus salmoides*). Aquatic Conserv: Mar. Freshw. Ecosyst. 18, pp. 1315–1324.

- Gray, M., Rogers, P.H. & Zeddies, D.G. (2016) Acoustic particle motion measurement for bioacousticians: principles and pitfalls, *Proceedings of Meetings on Acoustics*, 27, 010022
- Green, D.M. & Swets, J.A. (1966) *Signal Detection Theory and Psychophysics*, Wiley, New York, US.
- Greenberg, L., Calles, O., Andersson, J., Engqvist, T. Effects of trash diverters and overhead cover on downstream migrating brown trout. *Ecol. Eng.* 48, pp. 25-29.
- Grotbeck, L. M. (1975) Evaluation of an air curtain as a fish deterrent device at the Prairie Island Nuclear Generating Plant cooling water intake. Section Z.8, pp.1-25. In: Northern States Power 1975 Annual Report, *Environ. Ecol. Stud. Prog.*, Prairie Island Nuclear Gener. Plant.
- Gutherie, D.M., & Muntz, W.R.A. (1993) Role of vision in fish behaviour. In *Behaviour of Teleost Fishes*, 2nd edition (ed TJ Pitcher). Chapman & Hall, London. 90–128.
- Halfwerk, W. & Slabbekoorn, H. (2009) A behavioural mechanism explaining noise dependent frequency use in urban birdsong. *Animal Behaviour*. 78, 1301–1307.
- Halvorsen, M.B., Ainslie, M.A., Hawkins, A.D., Popper, A.N., Rogers, P.H., Sisneros, J.A., Slabbekoorn, H., & Zeddies, D.G. (2019) Auditory thresholds in fishes: towards international standard measurement procedures. *The Effects of Noise on Aquatic Life* (Den Haag, NL, 7-12 July 2019) Book of Abstracts, page 65.
- Halvorsen, M.B., & Ainslie, M.A. (2018). Auditory threshold in fishes: Towards international standard measurement procedures. *J. Ac. Soc. Am.*, 144(3), pp. 1662-1662.
- Halvorsen, M.B., Casper, B.M., Woodley, C.M., Carlson, T.J., & Popper, A.N. (2012a) Threshold for onset of injury in Chinook salmon from exposure to impulsive pile driving sounds. *PLoS ONE* 7 (6), e38968.
- Halvorsen, M.B., Zeddies, D.G., Ellison, W.T., Chicoine, D.R., & Popper, A.N. (2012b) Effects of mid-frequency active sonar on hearing in fish. *J. Acoust. Soc. Am.* 131 (1), pp. 599–607.
- Hamel, M.J., Brown, M.L., & Chipps, S.R. (2008) Behavioral response of rainbow smelt to in situ strobe lights. *N. Am. J. Fish. Manage.* 28 (2), pp. 394–401.

Hanson, C. H., White, J.R., & Li, H.W. (1977) Entrapment and impingement of fishes by power plant cooling-water intakes: an overview. *Mar. Fish. Rev.* 39 (10), pp. 7-17.

Hanson, M.A. & Butler, M.G. (1994) Responses to food-web manipulation in a shallow waterfowl lake. *Hydrobiologia* 279, pp. 457–466

Hawkins, A.D., & Johnstone, A.D.F. (1978) The hearing of the Atlantic salmon, *Salmo salar*. *J. Fish. Biol.* 13, pp. 655-673.

Hawkins, A.D., Johnson, C., & Popper, A.N. (2020) How to set sound exposure criteria for fishes, *The Journal of the Acoustical Society of America*, 147 (3), pp. 1762-1777.

Hawkins, A.D., & Myrberg, A.A. Jr (1983) Hearing and sound communication under water. In: Lewis B (ed). *Bioacoustics, A Comparative Approach*. London: Academic Press. 347–405.

Hawkins, A. D. & Popper, A. N. (2018). “Effects of Man-Made Sound on Fishes”. In: *Effects of Anthropogenic Noise on Aquatic Life*, H. Slabbekoorn, R. J. Dooling, A. N. Popper, and R. R. Fay (eds.), Springer Science + Business Media, LLC, New York.

Hawkins, A.D. & Popper, A.N. (2017) A sound approach to assessing the impact of underwater noise on marine fishes and invertebrates *ICES J. Mar. Sci.* 74 (3), pp. 635–651.

Hawkins, A.D. & Popper, A.N. (2015) Developing Sound Exposure Criteria for Fishes, *Adv. Exp. Med. Biol.* 875, pp. 431-439.

Hawkins, A.D. & Sand, O. (1977) Directional hearing in the median vertical plane by the cod. *J. Comp. Physiol. A.* 122: pp. 1–8.

Hawkins, A.D., Pembroke, A.E., & Popper, A.N. (2015) Information gaps in understanding the effects of noise on fishes and invertebrates. *Rev. Fish. Biol. Fisheries.* 25, pp. 39–64.

Herbert-Read, H.E., Kremer, L., Bruintjes, R., Radford, A.N., & Ioannou, C.C. (2017) Anthropogenic noise pollution from piledriving disrupts the structure and dynamics of fish shoals, *Proc. R. Soc. Lond. B.* 284(1863), 20171627.

Hickling, R. & Wei, W. (1995) Use of pitch-azimuth plots in determining the direction of a noise source in water with a vector sound-intensity probe, *J. Acoust. Soc. Am.* 97 (2), pp. 856-886.

- Hocutt, C.H. (1981) Behavioral barriers and guidance systems. In: Hocutt, C.H., Stauffer, J.R. Jr, Edinger, J.E., Hall, L.W. Jr, & Morgan, R.P. II (Eds.), *Power Plants: Effects on Fish and Shellfish Behavior*. New York: Academic Press, pp. 183–205.
- Hoffbeck, S.R. (2001) “Without careful consideration”: why carp swim in Minnesota's waters. *Minn. Hist.* 57, pp. 305–320
- Hudspeth, A.J. (1985) The cellular basis of hearing: the biophysics of hair cells. *Science*. 230, pp. 745–752.
- Huntingford, F.A., (1993) Development of behaviour in fish. In: Pitcher, T.J. (Ed.), *Behaviour of Teleost Fishes.* , second edition. Chapman and Hall, London, pp. 57–84.
- Huntingford, F. A., Andrew, G., Mackenzie, S., Morera, D., Coyle, S.M., & Pilarczk Kadri, S. (2010) Coping strategies in a strongly schooling fish, the Common Carp *Cyprinus carpio*. *Journal of Fish Biology*. 76, pp. 1576–1591.
- Huntingford, F.A, Coyle, S., Hunter, W. (2012) Avoiding Predators. In: Huntingford F, Jobling M, Kadri S (eds). *Aquaculture and Behavior*. London: Wiley-Blackwell. 220–247.
- Imamura, Y. & Ogura, M. (1959a) Study on the response of *Trachurus japonicus* to air-bubbles. *J. Tokyo Univ. Fish.* 45 (2): pp. 195-203.
- Imamura, Y. & Ogura, M. (1959b) Study on the fish gathering effects of air curtain. *J. Tokyo Univ. Fish.*, 45(2): 173-177.
- Inglis, M.L., McCoy, G.L., & Robson, M. (2016) Testing the effectiveness of fish screens for hydropower intakes, Environment Agency, Bristol, UK.
- International Hydropower Association (2020) 2020 Hydropower Status Report, 54 pp. Caudill, C.C., Daigle, W.R., Keefer, M.L., Boggs, C.T., Jepson, M.A., Burke, B.J., Zabel, R.W., Bjornn, T.C., & Peery, C.A. (2007) Slow dam passage in adult Columbia River salmonids associated with unsuccessful migration: delayed negative effects of passage obstacles or condition dependent mortality? *Can. J. Fish. Aq. Sci.*, 64, pp. 979 - 995.
- Invasive Carp Work Group (2014) Minnesota invasive carp action plan, 31 pp.

Jansen, H.M., Winter, H.V., Bruijs, M.C.M., & Polman, J.G. (2007) Just go with the flow? Route selection and mortality during downstream migration of silver eels in relation to river discharge, ICES J. Mar. Sci., 64, pp. 1437–1443.

Jennings, D.P., (1988). Bighead carp (*Hypophthalmichthys nobilis*): a biological synopsis. U.S. Fish and Wildlife Service Biological Report, vol. 88. U.S. Fish and Wildlife Service, Washington, DC, pp. 1–47.

Jerko, H., Turunen-Rise, I., Enger, P.S., & Sand, O. (1989) Hearing in the eel (*Anguilla anguilla*). J. Comp. Physiol. A 165, pp. 455-459.

Johnson, G.E. & Dauble, D.D. (2006) Surface flow outlets to protect juvenile salmonids passing through hydropower dams. Rev. Fish. Sci. 14, pp. 213-244.

Johnson, N.S., Yun, S.S., Thompson, H.T., Brant, C.O., & Li, W. (2009) A synthesized pheromone induces upstream movement in female sea lamprey and summons them into traps. Proc. Natl. Acad. Sci. U.S.A. 106 (4), pp. 1021–1026.

Jones, D. & Marten, K. (2016) Dredging sound levels numerical modelling and EIA. Terra et Aqua. 144, pp. 21-29.

Jonsson, N. (1991) Influence of water flow, water temperature and light on fish migration in rivers. Nord. J. Fresh. Res. 66, pp. 20–35.

Jungwirth, J., Schmutz, S., & Weiss, S. (eds) (1998). Fish Migration and Fish Bypasses. Oxford: Fishing News Books. Blackwell Science Publications, 448 pp.

Junk, W., Bayley, P.B., & Sparks, R.E. (1989) The flood pulse concept in river-floodplain systems. Pp. 110-127 in D.P. Dodge, (Ed.). Proceedings of the International Large River Symposium (LARS). Canadian Special Publication of Fish. Aq. Sci. 106.

Kalmijn, A. J. (1988) Hydrodynamic and acoustic field detection. pp. 83–130, In: Atema, J., Fay, R.R., Popper, A.N., & Tavolga, W.N., (Eds.), Sensory biology of aquatic animals. Springer-Verlag, New York.

Kalmijn, A.J. (1989) Functional evolution of lateral line and inner ear sensory systems. In: Coombs S, Görner P, Münz H (Eds.) The Mechanosensory Lateral Line: Neurobiology and Evolution. New York: Springer-Verlag, pp. 187–216.

- Kalmijn, A.J. (1997) Electric and near-field acoustic detection, a comparative study. *Acta Physiol. Scand.* 161, pp. 25–38.
- Kastelein, R.A., van der Heul, S., van der Veen, J., Verboom, W.C., Jenings, N., & de Haan, D. (2007) Effects of acoustic alarms, designed to reduce small cetacean bycatch in gillnet fisheries, on the behaviour of North Sea fish species in a large tank. *Mar. Env. Res.* 64, pp. 160-180.
- Kastelein, R.A., van der Heul, S., van der Veen, J., Verboom, W.C., Jenings, N., & de Haan, D. (2008) Startle response of captive North Sea fish species to underwater tones between 0.1 and 64 kHz. *Mar. Env. Res.* 65, pp. 369-377.
- Katopodis, C. & Williams, J.G. (2012) “The development of fish passage research in a historical context,” *Ecol. Eng.* 48, 8-18.
- Keller, R.P., Geist, J., Jeschke, J.M., & Kühn, I. (2011) Invasive species in Europe: ecology, status, and policy. *Env. Sci. Eur.* 23: 23 pp.
- Kelly A.M., Engle C.R., Armstrong M.L., Freeze M., & Mitchell A.J. (2011) History of 19 introductions and governmental involvement in promoting the use of grass, silver, and bighead carps. *Invasive Asian Carps in North America, American Fisheries Society Special Symposium.* 74, pp. 163-174.
- Kemp, P.S, Anderson, J.J., & Vowles, A.S. (2012) Quantifying behaviour of migratory fish: Application of signal detection theory to fisheries engineering. *Ecol. Eng.* 41, pp. 22– 31.
- Kemp, P.S., Gessel, M.H., & Williams, J.G. (2005) Seaward migrating subyearling Chinook salmon avoid overhead cover, *J. Fish Biol.* 67, pp. 1381–1391.
- Kenyon, T.N., Ladich, F., & Yan, H.Y. (1998) A comparative study of hearing ability in fishes: the auditory brainstem response approach. *J. Comp. Physiol. A.* 182, pp. 307-318.
- Kerr, J., Vowles, A.S., O’Hanley, J., & Kemp, P.S. (2016) D.1.1 Guidance on Stream Barrier Surveying and Reporting. Part A: Locating, Surveying and Prioritising Mitigation Actions for Stream Barriers, 58 pp.
- Ketelaars, H.A.M.. (2004). Range extensions of Ponto-Caspian aquatic invertebrates in continental Europe. In: Dumont, H.J., Shiganova, T.A., Niermann, U., (eds.) *Aquatic invasions in the Black, Caspian, and Mediterranean seas.* Dordrecht (NL): Kluwer Academic. pp 209–236.

- Kieffer, J.D., & Colgan, P.W. (1992) The role of learning in fish behaviour. *Rev. Fish Biol. Fish.* 2, pp. 125–143.
- King, D.R. & Hunt, G.S. (1967) Effect of carp on vegetation in a Lake Erie marsh. *J. Wildl. Manag.* 31, pp. 181–188.
- Knight, C.R., & Swaddle, J.P. (2011) How and why environmental noise impacts animals: an integrative, mechanistic review. *Ecol Lett* 14, pp. 1052-1061.
- Knudsen, F.R., Enger, P.S., & Sand, O. (1992) Awareness reactions and avoidance response to sound in juvenile Atlantic salmon, *Salmo salar* L. *J. Fish Biol.* 40, pp. 523–534.
- Knudsen, F.R., Schreck, C.B., Knapp, S.M., Enger, P.S., & Sand, O., (1997) Infrasound produces flight and avoidance responses in Pacific juvenile salmonids. *J. Fish Biol.* 51, pp. 824–829.
- Kobayashi, K., Igarashi, S., Abiko, Y., & Hayashi, K. (1959) Studies on air screen in water. I. Preliminary observation of behavior of fish school in relation to air screen. *Bull. Faculty Fish., Hokkaido Univ.*, 10 (3), pp. 222-228.
- Koehn, J., Brumley, A., & Gehrke, P. (2000) *Managing the Impacts of Carp*. Bureau of Rural Sciences (Department of Agriculture, Fisheries and Forestry – Australia), Canberra. 261 pp.
- Kojima, T., Ito, H., Komada, T., Taniuchi, T., & Akamatsu, T., (2005) Measurements of auditory sensitivity in common carp *Cyprinus carpio* by the auditory brainstem response technique and cardiac conditioning method. *Fish. Sci.* 71, pp. 95–100.
- Kolar, C. S., Chapman, D.C., Courtenay, W.R. Jr., Housel, C.M, Williams, J.D., & Jennings, D.P. (2007) *Bigheaded Carps: a biological synopsis and environmental risk assessment*. American Fisheries Society, Special Publication 33, Bethesda, Maryland
- Kolar, C.S. & Lodge, D.M. (2001) Progress in invasion biology: predicting invaders. *Trends Ecol. Evol.*, 16, pp. 199–204.
- Koth, R. (2014) "Lock and Dam #1, Asian carp barrier alternatives analysis; the known unknowns". International Conference on Engineering and Ecohydrology for Fish Passage. Paper 15.
- Kupfer G.A. & Gordon, W.G. (1966) An evaluation of the air bubble curtain as a barrier to alewives. *Comm. Fish. Rev.* 28(9), 1-9.

- Kuznetsov, Y. A. (1971) The behavior of fish in the zone affected by a curtain of air bubbles, pp. 103-110. In: Alekseev, A. P. (ed.), Fish behavior and fishing techniques. Nat. Mar. Fish. Serv., NOAA, Nat. Tech. Info. Serv., Translation No. TT 71-50010.
- Kynard, B. & O'Leary, J. (1990) Behavioral guidance of adult American shad using underwater AC electrical and acoustic fields. Proceedings of the International Symposium on Fishways '90 in Gifu, Japan, October 8–10, 1990, pp. 131–135.
- Ladich F. & Popper A.N. (2004) Parallel evolution in fish hearing organs. In: Manley, G.A., Popper, A.N., & Fay, R.R. (Eds.), Evolution of the Vertebrate Auditory System. New York: Springer-Verlag, pp. 95–127.
- Ladich, F. & Fay, R.R. (2013) Auditory evoked potential audiometry in fish. Rev. Fish. Biol. Fisheries. 23, pp. 317–364.
- Larinier, M. & Travade, F. (2002) Downstream migration: problems and facilities. Bull. Fr. Peche Piscic. 364 suppl. pp. 181-207
- Latvaitis, B., Bernhard, H.F., & MacDonald, D.B. (1976) Impingement studies at Quad-Cities Station, Mississippi River, pp. 269-290. In: Jensen, L. D. (Ed.), Proc. 3rd Natl. Work. Entrain. Impinge., New York, N. Y.
- Lee, K. M., Wochner, M. S., & Wilson, P. S. (2016). "Passive Underwater Noise Attenuation Using Large Encapsulated Air Bubbles". In: Popper, A., Hawkins, A. (Eds.), The Effects of Noise on Aquatic Life II. Advances in Experimental Medicine and Biology, vol 875. Springer, New York, pp. 607-614.
- Leighton, T.G., (1994) The Acoustic Bubble. Academic Press, San Diego, CA, pp. 913.
- Leighton, T.G. (2004) From seas to surgeries, from babbling brooks to baby scans: The acoustics of gas bubbles in liquids, Int. J. Mod. Phys. B, 18(25), pp. 3267-3314 (Invited Review Article).
- Leighton, T.G., Currie, H.A.L., Holgate, A., Dolder, C.N., Lloyd Jones, S., White, P.R., & Kemp, P.S. (2019) Analogies in contextualizing human response to airborne ultrasound and fish response to acoustic noise and deterrents," Proceedings of Meetings on Acoustics, 37, 010014.
- Leighton, T.G., Fagan, K.J., & Field, J.E. (1991) Acoustic and photographic studies of injected bubbles. Eur. J. Phys. pp. 77 - 85.



Leighton, T.G., Finfer, D.C., & White, P.R., (2007) An acoustical hypothesis for the spiral bubble nets of humpback whales, and the implications for whale feeding. *Ac. Bull.* 32, pp. 17-21.

Leighton, T.G., Jiang, J., & Baik, K. (2012) Demonstration comparing sound wave attenuation inside pipes containing bubbly water and water droplet fog. *J. Acoust. Soc. Am.* 131 [3] pt. 2, pp 2413–2421.

Leighton, T.G., Phelps, A.D., & Ramble, D.G., (1997) The detection of tethered and rising bubbles using multiple acoustic techniques. *J. Acoust. Soc. Am.* 101(5), Pt. 1.

Leighton, T.G., Phelps, A.D., Ramble, D.G., & Sharpe, D.A, (1996) Comparison of the abilities of eight acoustic techniques to detect and size a single bubble. *Ultrasonics* 34: pp. 661-667.

Leighton, T.G., Ramble, D.G., Phelps, A.D., Morfey, C.L., & Harris, P.P. (1998) Acoustic detection of gas bubbles in a pipe. *Acta Acustica united with Acustica.* 84, pp. 801–814.

Leighton, T.G., Richards, S.D., & White, P.R., (2004) Trapped within a ‘wall of sound’: A possible mechanism for the bubble nets of humpback whales. *Ac. Bull.* 29, pp. 24-29.

Leighton, T.G. & Walton, A.J., (1987) An experimental study of the sound emitted from gas bubbles in a liquid. *Eur. J. Phys.* 8, pp. 98-104.

Leighton, T.G., Walton, A.J., & Pickworth, M.J.W (1990) Primary Bjerknes forces, *Eur. J. Phys.*, 11, pp. 47-50.

Leighton, T. G. & White, P. R. (2014) Dolphin-inspired target detection for sonar and radar, *Archives of Acoustics*, 39(3), pp. 319-332.

Leighton, T.G., White, P.R., Morfey, C.L., Clarke, J.W.L., Heald, G.J., Dumbrell, H.A., & Holland, K.R. (2002) The effect of reverberation on the damping of bubbles, *J. Acoust. Soc. Am.* 112(4), pp. 1366–1376.

Lewis, W.L., Heidinger, R., & Konikoff, M. (1968) Loss of fishes over the drop box spillway of a lake, *Trans. Am. Fish. Soc.* 97, pp. 492–494.

Li, J., Roche, B., Bull, J., White, P.R., Leighton, T., Provenzano, G., Dewar, M., & Henstock, T. (2020) Broadband acoustic inversion for gas flux quantification - application to a methane plume at Scanner Pockmark, central North Sea. *J. Geophys. Res. Oc.* 125(9), e2020JC016360.

- Lieberman, J. T. & P. H. Muessig. MS. Evaluation of an air bubbler to mitigate fish impingement at an electric generating plant. Texas Instruments, Inc., Buchanan, N. Y. 21pp.
- Lombarte, A. & Popper, A.N., (1994) Quantitative analyses of postembryonic hair cell addition in the otolithic endorgans of the inner ear of the European hake, *Merluccius merluccius* (Gadiformes, Teleostei). J. Comp. Neurol. 345, pp. 419-428.
- Longuet-Higgins, M.S. (1990) An analytic model of sound produced by raindrops, J. Fluid Mech. 214, pp. 395–410.
- Longuet-Higgins, M.S., Kerman, B.R., & Lunde, K. (1991) The release of air bubbles from an underwater nozzle. J. Fluid. Mech. 230, pp. 365-390.
- Louzada, M.O. (2017) Migratory fish habitat fragmentation by hydropower dams: History and trends for the São Francisco and Paraíba do Sul river basins. MSc Dissertation. pp. 41.
- Loye, D.P. & Arndt, W.F. (1948) An acoustic screen for making underwater noise reduction tests in Pearl Harbor, J. Acoust. Soc. Am. 20, 224.
- Lowe, R.H. (1952) The influence of light and other factors on the seaward migration of the silver eel (*Anguilla anguilla* L.). J. Anim. Ecol. 21, pp. 275–309.
- Lu, Z. & Popper, A.N. (2001) Neural response directionality correlates of hair cell orientation in a teleost fish. J. Comp. Physiol. A. 187, pp. 453–465.
- Lucas M.C. & Baras E. (2001) Migration of Freshwater Fishes. Blackwell Science, Oxford.
- Lucas, M.C., Bubb, D.H., Jang, M., Ha, K. & Masters, J.E.G. (2009) Availability of and access to critical habitats in regulated rivers: effects of low-head barriers on threatened lampreys. Freshwater Biology. 54, pp. 621-632.
- Maes, J., Turnpenny, A.W.H., Lambert, D.R., Nedwell, J.R., Parmentier, A., & Ollevier, F., (2004) Field evaluation of a sound system to reduce estuarine fish intake rates at a power plant cooling water inlet. J. Fish Biol. 64, 938–946
- Magnuson, J.J., Beckel, A.L., Millis, K., & Brandt, S.B. (1985) Surviving winter hypoxia: behavioural adaptations of fishes in a northern Wisconsin winterkill lake. Environ. Biol. Fishes. 14, pp. 241–250.

- Mann, D.A., Higgs, D.M., Tavalga, W.N., Souza, M.J., & Popper, A.N. (2001) Ultrasound detection by clupeiform fishes. *J. Acoust. Soc. Am.* 109, pp. 3048–3054.
- Matousek, J. A., Wells, A.W., & McGroddy, P.M. (1988) Field Testing of Behavioral Barriers for Fish Exclusion at Cooling-Water Intake Systems Central Hudson Gas & Electric Roseton Generating Station. Electric Power Research Institute (EPRI). RP 2214-6.
- Matsumoto, T., & Kawamura, G. (2005). The eyes of the common carp and Nile tilapia are sensitive to near-infrared. *Fish. Sci.* 71(2), pp. 350-355.
- Maxwell, W. A. (1973) Fish diversion for electrical generating station cooling systems a state-of-the-art report. Southern Nuclear Engineering Inc. Report SNE-I23, NUS Corporation, Dunedin, Fla., 78 pp.
- Mayo, R. D. (1974) Conventional fish screening systems and some promising alternatives, pp.277-280. In: Jensen, L. D. (Ed.), Proc. 2nd Entrainment and Intake Screening Workshop, Feb. 5-9, 1973, Baltimore, MD.
- McCauley, D.J., Montuori, L., Navarro, J.E., & Blystra, A.R. (1996) Using strobe lights, air bubble curtains for cost-effective fish diversion. *Hydro Review*, 25(2), pp. 42-51.
- McCauley, R.D., Fewtrell, J., & Popper, A.N. (2003) High-intensity anthropogenic sound damages fish ears. *J. Acoust. Soc. Am.* 113, pp. 638–42.
- McIninch, S.P. & Hocutt, C.H., (1987) Effects of turbidity on estuarine fish response to strobe lights. *J. Appl. Ichthyol.* 3, pp. 97–105.
- McKibben, J. R. & Bass, A. H. (1998) Behavioral assessment of acoustic parameters relevant to signal recognition and preference in a vocal fish. *J. Acoust. Soc. Am.* 104, pp. 3520-3533.
- McLaughlin, K.E. & Kunc, H.P. (2013) Experimentally increased noise levels change spatial and singing behaviour. *Biology Letters.* 9, 20120771.
- Medwin, H. & Beaky, M.M. (1989) Bubble sources of the Knudsen sea noise spectrum. *J. Acoust. Soc. Am.* 83, pp. 1124-1130.
- Mefford, B. (2014) Pocket Guide to Screening Small Water Diversions - A guide for understanding fish screening and selection of screens for small diversions, US Bureau of Reclamation, 43 pp.

- Mesquita, F.O., Godinho, H.P., Azevedo, P.G., Young, R.J. (2008) A preliminary study into the effectiveness of stroboscopic light as an aversive stimulus for fish. *Appl Anim Behav Sci* 111, pp. 402–407.
- Michaud, D.T. & Taft, E.P. (2000) Recent evaluations of physical and behavioral barriers for reducing fish entrainment at hydroelectric plants in the upper Midwest. *Environmental Science & Policy* 3 (2000) pp. S499-S512
- Miehls, S.M., Johnson, N.S., & Hrodey, P.J. (2017) Test of a Nonphysical Barrier Consisting of Light, Sound, and Bubble Screen to Block Upstream Movement of Sea Lampreys in an Experimental Raceway. *N. Am. J. Fish. Manag.* 37, pp. 660–666.
- Millot, S., Bégout, M.L., & Chatain, B. (2009) Exploration behaviour and flight response toward a stimulus in three sea bass strains (*Dicentrarchus labrax* L.). *Appl Anim Behav Sci* 119, pp. 108–114.
- Minnaert, M. (1933) On musical air-bubbles and the sound of running water. *Philos. Mag.* 16, pp. 235–248.
- Mogdans, J., Engelmann, H.W., & Kröther, S. (2003) The fish lateral line: how to detect hydrodynamic stimuli. In: Barth, F.G., Humphrey, J.A.C., Secomb, T.W. (eds) *Sensors and Sensing in Biology and Engineering*. New York: Springer-Verlag, pp. 173–185.
- Montgomery, J.C., Jeffs, A., Simpson, S.D., Meekan, M., & Tindle, C. (2006) Sound as an orientation cue for the pelagic larvae of reef fishes and decapod crustaceans. *Advances in Marine Biology* 51, pp. 143–96.
- Mork, O.I., & Gulbrandsen, J. (1994) Vertical activity of four salmonid species in response to changes between darkness and two intensities of light. *Aquaculture* 127, pp. 317–328.
- Moser, M.L., Jackson, A.D., Lucas, M.C., & Mueller, R.P. (2014) Behavior and potential threats to survival of migrating lamprey ammocetes and macrophthalmia, *Rev. Fish Biol. Fish.*, 25, pp. 103-116.
- Mueller, R.P., Neitzel, D.A., Mavros, W.V., & Carlson, T.J. (1998) Evaluation of low and high frequency sound for enhancing the capacity of fish screening facilities to protect outmigrating salmonids. Contract Number DE-A179-86BP62611. Bonneville Power Administration, Portland, OR.

- Myrberg Jr., A.A. & Spires, J.Y., (1980) Hearing in damselfishes: an analysis of signal detection among closely related species. *J. Comp. Physiol.* 140, pp. 135-144.
- Nedelec, S.L., Campbell, J., Radford, A.N., Simpson, S.D., & Merchant, N.D. (2016) Particle motion: the missing link in underwater acoustic ecology. *Meth. Ecol. Evol.* 7, pp. 836–842.
- Nedelec, S.L., Radford, A.N., Simpson, S.D., Nedelec, B., Lecchini, D., & Mills, S.C. (2014) Anthropogenic noise playback impairs embryonic development and increases mortality in a marine invertebrate. *Scientific Reports.* 4, 5891.
- Nedelec, S.L., Simpson, S.D., Morley, E.L., Nedelec, B., & Radford, A.N. (2015) Impacts of regular and random noise on the behaviour, growth and development of larval Atlantic cod (*Gadus morhua*). *Proc. R. Soc. B: Biol. Sci.* 282, 20151943.
- Nedwell, J.R. & Turnpenny, A.W.H. (1997). Fish guidance using evanescent sound. American Fisheries Society 127th Annual Meeting, “Fisheries at Interfaces: Habitats, Disciplines, Cultures”, Monterey, CA, 24-28th August 1997.
- Nedwell, J., Turnpenny, A.W.H. & Lambert, L. (2003). Objective Design Of Acoustic Fish Deterrent Systems. Symposium on Cooling Water Intake Technologies to Protect Aquatic Organisms, Arlington, Virginia, USA, 6-7 May 2003, pp.200-206.
- Nedwell, J.R., Turnpenny, A.W.H., & Lovell, J. (2007) A validation of the dBht as a measure of the behavioural and auditory effects of underwater noise. Subacoustech Report No 534R1231
- Nedwell, J.R., Edwards, B., Turnpenny, A.W.H., & Gordon, J. (2004) Fish and Marine Mammal Audiograms: A summary of available information. Subacoustech.
- Nehls, G., Betke, K., Eckelmann, S. & Ros. M. (2007) Assessment and costs of potential engineering solutions for the mitigation of the impacts of underwater noise arising from the construction of offshore windfarms. BioConsult SH report, Husum, Germany. On behalf of COWRIE Ltd.
- Neo, Y.Y., Seitz, J., Kastelein, R.R., Winter, H.W., ten Cate, C., & Slabbekoorn, H. (2014) Temporal structure of sound affects behavioural recovery from noise impact in European seabass, *Biol. Cons.* 178, pp. 65-73.

- Nestler, J.M., Goodwin, R.A., Smith, D.L., Anderson, J.J., & Li, S. (2008) Optimum fish passage and guidance designs are based in the hydrogeomorphology of natural rivers, *River Res. Appl.* 24, pp. 148–168.
- Newbold, L.R., & Kemp, P.S., (2015) Influence of corrugated boundary hydrodynamics on the swimming performance and behaviour of juvenile common carp (*Cyprinus carpio*). *Ecol. Eng.* 82, pp. 112-120.
- Nicholas, M., Roy, R.A., Crum, L.A., Oguz, H., & Prosperetti, A., (1994) Sound emissions by a laboratory bubble cloud. *J. Acoust. Soc. Am.* 95 (6), pp. 3171–3182.
- Noatch, M.R. & Suski, C.D. (2012) Non-physical barriers to deter fish movements, *Environ. Rev.* 20, pp. 1-12.
- Nunes, A.L., Tricarico, E., Panov, V.E., Cardoso, A.C., & Katsanevakis, S (2015) Pathways and gateways of freshwater invasions in Europe, *Aq. Inv.* 10(4), pp. 359-370.
- Odeh, M. (2000) *Advances in Fish Passage Technology: Engineering Design and Biological Evaluation*. Am. Fish. Soc., Bioengineering Section, Bethesda, Maryland.
- Ontario Hydro & LMS (1989) Field testing of behavioural barriers for fish exclusion at cooling-water intake systems (Ontario Hydro Pickering Nuclear Generating Station). EPRI GS-6246
- Panek, F. (1987) Biology and ecology of carp. In: Cooper, E. (Ed.), *Carp in North America*. Am. Fish. Soc., Bethesda, MD, pp. 1–15.
- Panov, V.E., Alexandrov, B., Arbačiauskas, K., Binimelis, R., Copp, G.H., Grabowski, M., Lucy, F., Leuven, R.S.E.W., Nehring, S., Paunović, M., Semenchenko, V., & Son, M.O. (2009) Assessing the risks of aquatic species invasions via European inland waterways: from concepts to environmental indicators. *Int. Env. Ass. Manag.* 5, pp. 110–126.
- Parker, G.H. (1902) Hearing and allied senses in fishes. *Bull. U.S. Fish. Comm.* 22, pp. 45–64.
- Parker, G.H. (1903) The sense of hearing in fishes. *Am. Nat.* 37, pp. 185–203.
- Partan, S.R., Larco, C.P., & Owens, M.J. (2009) Wild tree squirrels respond with multisensory enhancement to conspecific robot alarm behaviour. *Animal Behaviour* 77, 1127e1135.
- Parvulescu, A. (1964) Problems of propagation and processing. In: Tavalga, W.N. (ed.) *Marine bio-acoustics*. Pergamon, Oxford, pp. 87–100.

Patrick, P.H., Christie, A.E., Sager, D., Hocutt, C., & Stauffer Jr., J. (1985) Responses of fish to a strobe light/air-bubble barrier. *Fish. Res.* 3, pp. 157–172.

Patrick, P.H., McKinley, R.S., & Micheletti, W.C. (1988) Field testing of behavioural barriers for cooling water intake structures - Test site I - Pickering Nuclear Generating Station - 1985/86. In: Proceedings of the Electric Power Research Institute Conference on Fish Protection at Steam and Hydro Plants, San Francisco, Ca., Oct. 28-30, 1987. EPRI CS/EA/AP-5663-SR

Pegg, M.A. & Chick, J.H. (2004) Aquatic nuisance species: an evaluation of barriers for preventing the spread of Bighead and Silver carp to the Great Lakes. Illinois–Indiana Sea Grant, Final Report A/SE (ANS)-01-01, Urbana, Illinois.

Perry, R. W., Romine, J. G., Adams, N. S., Blake, A. R., Burau, J. R., Johnston, S. V. & Liedtke, T. L. (2014), Using a non-physical behavioural barrier to alter migration routing of juvenile chinook salmon in the Sacramento-San Joaquin river delta. *River Res. Applic.*, 30: 192–203.

Phelps, A.D. & Leighton, T.G. (1996) High-resolution bubble sizing through detection of the subharmonic response with a two frequency excitation technique, *J. Acous. Soc. Am*, 99, pp. 1985-1992.

Piper, A.T., White, P.R., Wright, R.M., Leighton, T.G., & Kemp, P.S. (2019) Response of seaward-migrating European eel (*Anguilla anguilla*) to an infrasound deterrent, *Ecol. Eng.* 127, pp. 480–486.

Pitcher, T.J. (1983) Heuristic definitions of fish shoaling behavior, *Anim. Behav.* 31, pp. 611-613.

Pitcher, T.J. & House, A.C. (1987) Foraging rules for group feeders: area copying depends upon food density in shoaling goldfish. *Ethology*, 76, pp. 161–167.

Popper, A.N. (1977) A scanning electron microscopic study of the sacculus and lagena in the ears of fifteen species of teleost fishes. *J. Morphol.* 153, pp. 397-418.

Popper, A.N. & Carlson, T.J. (1998) Application of sound and other stimuli to control fish behavior. *Trans. Am. Fish. Soc.* 127, pp. 673–707.

Popper, A.N., & Fay, R.R. (1973) Sound detection and processing by teleost fishes: a critical review. *J Acoust Soc Am* 53, pp. 1515–1529.

- Popper, A.N. & Fay, R.R. (1993) Sound detection and processing by fish: a critical review. *J. Acoust. Soc. Am.* 53, pp. 1515-1529.
- Popper, A.N. & Fay, R.R. (2011) Rethinking sound detection by fishes. *Hear. Res.* 273, pp. 25-36.
- Popper, A.N., Fay, R.R., Platt, C., & Sand, O., (2003) Sound detection mechanisms and capabilities of teleost fishes. In: Collin, S.P., Marshall, N.J. (Eds.), *Sensory Processing in Aquatic Environments*. Springer-Verlag, New York, pp. 3-38.
- Popper, A.N., Halvorsen, M.B., & Kane, A. (2007) The effects of high-intensity, low-frequency active sonar on rainbow trout. *J. Acoust. Soc. Am.* 122, pp. 623–635.
- Popper, A.N. & Hawkins, A.D. (2018) The importance of particle motion to fishes and invertebrates. *J. Ac. Soc. Am.* 143, 470 pp.
- Popper, A.N., & Hawkins, A.D. (2019). An overview of fish bioacoustics and the impacts of anthropogenic sounds on fishes. *J. Fish. Biol.* 94(5), pp. 692-713.
- Popper, A.N., Hawkins, A.D., Fay, R.R., Mann, D.A., Bartol, S., Carlson, T.J., Coombs, S., Ellison, W.T., Gentry, R.L., Halvorsen, M.B., Lokkeborg, S., Rogers, P.H., Southall, B., Zeddies, D., & Tavalga, W.A. (2014). *ASA S3/SC1. 4 TR-2014 Sound Exposure Guidelines for Fishes and Sea Turtles: A Technical Report prepared by ANSI-Accredited Standards Committee S3/SC1 and registered with ANSI* (Springer, New York).
- Popper, A.N., Hawkins, A.D., & Halvorsen, M.B. (2019). “Anthropogenic sound and fishes,” Washington State Department of Transportation, Olympia, WA.
- Popper, A. N., Hawkins, A.D., Sand, O. and Sisneros, J. (2019) Examining the hearing abilities of fishes. *J. Ac. Soc. Am.* 146(2), pp. 948 - 955.
- Popper, A.N. & Schilt, C.R. (2008) Hearing and Acoustic Behavior: Basic and Applied Considerations. In: Webb, J.F., Fay, R.R., Popper, A.N. ed. *Fish bioacoustics*: Springer, pp. 17-48.
- Popper, A.N., Smith, M.E., Cott, P.A., Hanna, B.W., MacGillivray, A.O., Austin, M.E., & Mann, D.A. (2005) Effects of exposure to seismic airgun use on hearing of three fish species. *J. Acoust. Soc. Am.*, 117, pp. 3958–3971.



- Prosperetti, A. (1985) Bubble-related ambient noise in the ocean. *J. Acoust. Soc. Am. Suppl.* 1, 78, S2.
- Putland, R.L. & Mensinger, A.F. (2019) Acoustic deterrents to manage fish populations, *Rev. Fish. Biol. Fisheries*, 29, pp. 789–807.
- Qing, X., White, P.R., Leighton, T.G., Liu, S., Qiao, G. and Zhang, Y. (2019) Three-dimensional finite element simulation of acoustic propagation in spiral bubble net of humpback whale. *J. Acoust. Soc. Am.*, 146(3), pp. 1982-1995.
- Rader, R.B., Belish, T., Young, M.K., & Rothlisberger, J. (2007) The scotopic visual sensitivities of four species of trout: a comparative study. *West North Am Nat* 67, pp. 524–537.
- Radford, A.N., Lebre, L., Lecaillon, G., Nedelec, S.L., & Simpson, S.D. (2016) Repeated exposure reduces the response to impulsive noise in European seabass. *Glob. Ch. Biol.* 22, pp. 3349–3360.
- Radford, A.N., Purser, J., & Brintjes, R. (2015) Beyond a simple effect: variable and changing responses to anthropogenic noise. In: *The Effects of Noise on Aquatic Life, II* (eds Popper AN, Hawkins AD), pp. 901–907. Springer Science+Business Media, New York, NY.
- Ray, S. S., Snipes, R.L. & Tomljanovich, D.A. (1976) A state-of-the art report on intake technologies. TVA, Chattanooga Pow. Res. Staff, Publ. No. PR-Z64874:82pp.
- Retzius, G. (1881) *Das Gehörorgan der Wirbelthiere*, Vol. I. Stockholm: Samson and Wallin.
- Richardson, D.M., Pysek, P., Rejmánek, M., Barbour, M.G., Panetta, F.D. & West, C.J. (2000) Naturalization and invasion of alien plants: concepts and definitions. *Diversity Distrib.* 6, pp. 93–107.
- Richards, N.S., Chips, S.R., & Brown, M.L. (2007) Stress response and avoidance behavior of fishes as influenced by high-frequency strobe lights. *N Am J Fish Manage* 27, pp. 1310–1315.
- Riley, J., (2014) *Auguries of Discord*, Performance Research, 19, pp. 41-44.
- Rino, C.L. & Ngo, H.D (1991) Low frequency acoustic scatter from subsurface bubble clouds. *J. Acoust. Soc. Am.* 90, 406-415.

- Rogers, P.H. & Cox, M. (1988) Underwater sound as a biological stimulus. In: Atema, J., Fay, R.R., Popper, A.N., & Tavolga, W.N. (Eds.) *Sensory Biology of Aquatic Animals*. New York: Springer-Verlag, pp. 131–149.
- Rogers, P.H., Hawkins, A.D., Popper, A.N., Fay, R.R., & Gray, M.D. (2016) Chapter 115 Parvulescu Revisited: Small Tank Acoustics for Bioacousticians, In: Popper, A.N., Hawkins, A.D. (eds.), *The Effects of Noise on Aquatic Life II, Advances in Experimental Medicine and Biology*, Springer Science+Business Media New York, 875, pp. 933-941.
- Rogers, P.H., Popper, A.N., Cox M., & Saidel, W.M. (1988) Processing of acoustic signals in the auditory system of bony fish., *J. Acoust. Soc. Am.*, 83, pp. 338–349.
- Rogers, P.H. & Zeddies, D.G. (2008) Multipole mechanisms for directional hearing in fish. In: Webb, J.F., Fay, R.R., Popper, A.N. (Eds.), *Fish bioacoustics*: Springer, pp. 233-252
- Rome, L.C., Loughna, P.T., Goldspink, G. (1985). Temperature Acclimation: Improved Sustained Swimming Performance in Carp at Low Temperatures, *Science* 228 (4696), 194-196.
- Rosell, R., Evans, D., & Allen, M. (2005) The eel fishery in Lough Neagh, Northern Ireland – an example of sustainable management? *Fish. Manage. Ecol.* 12, pp. 377-385.
- Rowe, C. (1999) Receiver psychology and the evolution of multicomponent signals, *Anim. Behav.* 58, pp. 921-931.
- Rowe, C., & Guilford, T. (1999) The evolution of multimodal warning displays. *Evolutionary Ecology* 13, 655e671.
- Ruebush, B.C., Sass, G.G., Chick, J.H., & Stafford, J.D., (2012) In-situ tests of sound-bubble-strobe light barrier technologies to prevent range expansions of Asian carp. *Aquat. Inv.* 7, pp. 37–48.
- Sager, D.R., Hocutt, C.H., & Stauffer, J.R., (1987) Estuarine fish responses to strobe light, bubble curtains and strobe light/bubble-curtain combinations as influenced by water flow rate and flash frequencies. *Fish. Res.* 5, pp. 383–399.
- Sampson S.J., Chick J.H., & Pegg M.A. (2009) Diet overlap among two asian carp and three native fishes in backwater lakes on the Illinois and Mississippi rivers. *Biol. Invasions.* 11, pp. 483-496.

- Sand, O. & Karlsen, H.E. (1986) Detection of infrasound by the Atlantic cod. *J. Exp. Biol.* 125: pp. 197–204.
- Sand, O. & Karlsen, H.E. (2000) Detection of infrasound and linear acceleration in fish. *Philos. Trans. R. Soc. Lond. B.* 355, pp. 1295–1298.
- Sand, O., Enger, P.S., Karlsen, H.E., Knudsen, F., & Kvernstuen, T. (2000) Avoidance responses to infrasound in downstream migrating European silver eels, *Anguilla anguilla*. *Environ. Biol. Fishes.* 57 (3), pp. 327–336.
- Scheid, C.M.; Puget, F.P.; Halasz, M.R.T., & Massarani, G. (1999) Fluid dynamics of bubbles in liquid. *Braz. J. Chem. Eng.* 16(4), pp. 351-358.
- Schellart, N. & De Munck, J. (1987) A model for directional and distance hearing in swimbladder-bearing fish based on the displacement orbits of the hair cells. *J. Acoust. Soc. Am.* 82. pp. 822-829.
- Schilt, C.R., (2007) Developing fish passage and protection at hydropower dams. *Appl. Anim. Behav. Sci.* 104, 295–325.
- Scholik, A.R. & Yan, H.Y. (2001) Effects of underwater noise on auditory sensitivity of a cyprinid fish. *Hear. Res.* 152, pp. 17–24.
- Scholik, A.R. & Yan, H.Y. (2002) The effects of noise on the auditory sensitivity of the bluegill sunfish, *Lepomis macrochirus*. *Comp. Biochem. Physiol. A.* 133, pp. 43–52.
- Schrank S.J., Guy C.S., & Fairchild J.F. (2003) Competitive interactions between age-0 bighead carp and paddlefish. *Trans. Am. Fish. Soc.* 132, pp. 1222-1228.
- Schuijf, A. & Buwalda, R.J.A. (1975) On the mechanism of directional hearing in cod (*Gadus morhua*). *J. Comp. Physiol., A.* 98, pp. 333-344 .
- Schuijf, A. & Hawkins, A.D. (1983) Acoustic distance discrimination by the cod. *Nature*, 302, pp. 143-144.
- Schuijf, A., (1975). Directional hearing of cod (*Gadus morhua*) under approximate free field conditions. *J. Comp. Physiol. A.* 98, pp. 307-332.
- Schuijf, A., Baretta, J.W., Wildschut, J.T., (1972) A field investigation on the discrimination of sound direction in *Labrus berggylta* (Pisces: Perciformes). *Neth. J. Zool.* 22, pp. 19-43.

- Schuler, V.J. & Larson, L.E. (1974) Experimental studies evaluating aspects of fish behavior as parameters in the design of generating station systems. Presented at the meeting of the American Society of Civil Engineers, Water Resources Engineering Program held at Los Angeles, California
- Sheridan, S. (2014) Screening at intakes and outfalls: measures to protect eel. Environment Agency.
- Sherlock, L.P. & Formby, C. (2005). Estimates of Loudness, Loudness Discomfort, and the Auditory Dynamic Range: Normative Estimates, Comparison of Procedures, and Test-Retest Reliability. *J. Am. Ac. Audiol.* 16(2), pp. 85-100.
- Shikhshabekov, M. M. (1972) The annual cycle of the gonads in wild carp (*Cyprinus carpio* L.) from the Terek Delta. *J. Ichthyol.* 5, pp. 855–859.
- Simon, A., Britton, R., Gozlan, R., Oosterhout, C., Volckaert, F.A.M., & Halnfling, B. (2011) Invasive cyprinid fish in Europe originate from the single introduction of an admixed source population followed by a complex pattern of spread. *PLoS ONE* 6(6), e18560.
- Simpson, S.D., Meekan, M., Montgomery, J., McCauley, R., & Jeffs, A. (2005) Homeward sound. *Science.* 308, 221.
- Simpson, S.D., Purser, J., & Radford, A.N. (2015) Anthropogenic noise compromises antipredator behaviour in European eels. *Glob. Change Biol.* 21, pp. 586–593.
- Simpson, S.D., Radford, A.N., Nedelec, S.L., Ferrari, M.C.O., Chivers, D.P., McCormick, M.I., & Meekan, M.G. (2016) Anthropogenic noise increases fish mortality by predation. *Nature Communications.* 7, 10544.
- Sisler, S.P. & Sorensen, P.W. (2008) Common carp and goldfish discern conspecific identity using chemical cues. *Behaviour.* 145, pp. 1409-1425.
- Skalski, J.R., Pearson, W.H., & Malme, C.I. (1992) Effects of sounds from a geophysical survey device on catch-per-unit-effort in a hook and line fishery for rockfish. *Can. J. Fish. Aquat. Sci.* 49, pp. 1357-1365.
- Sloan, J.L., Cordo, E.B., Mensinger, A.F. (2013) Acoustical conditioning and retention in the common carp (*Cyprinus carpio*). *J. Great Lakes Res.* 39, pp. 507–512.

- Smith, B.B. & Walker, K.F. (2004) Spawning dynamics of common carp in the River Murray, South Australia, shown by macroscopic and histological staging of gonads. *J. Fish. Biol.* 64, pp. 336–354.
- Smith, K. A. (1961) Air-curtain fishing for Maine sardines. *Comm. Fish. Rev.* 23(3), pp. 1-14.
- Smith, M.E., Coffin, A.B., Miller, D.L., & Popper, A.N. (2006) Anatomical and functional recovery of the goldfish (*Carassius auratus*) ear following noise exposure. *J. Ex. Biol.* 209, pp. 4193–202.
- Smith, M.E., Kane, A.S., & Popper, A.N. (2004) Noise-induced stress response and hearing loss in goldfish (*Carassius auratus*). *J. Ex. Biol.* 207, pp. 427–35.
- Smith, W.L., Webb, J.F., & Blum, S.D. (2003) The evolution of the laterophysic connection with a revised phylogeny and taxonomy of butterflyfishes (Teleostei: Chaetodontidae). *Cladistics* 19, pp. 287–306.
- Solomon D.J. (1992). Diversion and entrapment of fish at water intakes and outfalls. R & D Report No. 1, National Rivers Authority, Bristol: 51 pp.
- Song, J., Mann, D.A., Cot, P.A., Hanna, B.W., & Popper, A.N. (2008) The inner ears of northern Canadian freshwater fishes following exposure to seismic air gun sounds. *J. Acoust. Soc. Am.* 124, pp. 1360-6.
- Sonnichsen, J. C. (1975) Fish protective devices: a compilation of recent designs, concepts, and operating experience of water intakes used in the United States. Hanford Eng. Devel. Lab. Rept. HEDL-TME 75-38VC-79, 82 pp.
- Sonny, D., Knudsen, F.R., Enger, P.S., Kvernstuen, T., & Sand, O. (2006) Reactions of cyprinids to infrasound in a lake and at the cooling water inlet of a nuclear power plant. *J Fish Biol* 69, pp. 735–748.
- Sorensen, P.W. & Stacey, N.E. (2010) Brief review of fish pheromones and discussion of their possible uses in the control of non-indigenous teleost fishes, *New Zeal. J. Mar. Fresh.*, 38, pp. 399–417.
- Spiby, D. (2004). A pilot study into the effectiveness of a bubble/acoustic screen designed to divert migrating fish away from hydroelectric turbines. Unpublished report, Environment Agency, North-West Region, February 2004.

- Sprague, M. W., Krahforst, C. S., & Luczkovich, J. J. (2016). Noise propagation from vessel channels into nearby fish nesting sites in very shallow water, POMA 27, 010012.
- Sprott, T.A. (2001) The National Shipbuilding Research Program, Preliminary Report on the Field Testing of an Air-Curtain Screen to Minimize Fish Passage onto Submerged Floating Drydocks. In: The National Shipbuilding Research Programme, NSRP 0589. 20 pp.
- Stadler, J.H., & Woodbury, D.P. (2009) Assessing the effects to fishes from pile driving: application of new hydroacoustic guidelines. Inter-Noise 2009.
- Stewart, H. A., Wolter, M.H., & Wahl, D.H. (2014) Laboratory investigations on the use of strobe lights and bubble curtains to deter dam escapes of age- 0 Muskellunge. N. Am. J. Fish. Manage. 34, pp. 571–575.
- Stewart, P.A.M. (1981). An investigation into the reactions of fish to electrified barriers and bubble curtains. Fish. Res. 1, pp. 3–22.
- Stone & Webster Engineering Corporation. (1976) Studies to Alleviate Fish Entrapment at Power Plant Cooling Water Intakes, Final Report. Prepared for Niagara Mohawk Power Corporation and Rochester Gas & Electric Corporation.
- Swee, U. B. & McCrimmon, H. R. (1966) Reproductive biology of the carp, *Cyprinus carpio* L., in Lake St Lawrence, Ontario. Trans. Am. Fish. Soc. 95, pp. 372–380.
- Taft, E.P. (2000) Fish protection technologies: a status report. Environ. Sci. Policy. 3 (1), pp. 349–359.
- Tavolga, W.N. & Wodinsky, J. (1963) Auditory capacities in fishes. Pure tone thresholds in nine species of marine teleosts. Bull. Am. Mus. Nat. Hist. 126, 177–240.
- Taylor, R. M., Pegg, M.A., & Chick, J.H. (2005) Response of Bighead Carp to a bioacoustic behavioural fish guidance system. Fish. Manage. Ecol. 12:283–286.
- Taylor, R.M., Pegg, M.A., & Chick, J.H. (2003) Some observations on the effectiveness of two behavioral fish guidance systems for preventing the spread of bighead carp to the Great Lakes. Aq. Invas. 14, pp. 1–5
- Tesch, F.W. (1999) Tracking of silver eels in the Rivers Weser and Elbe. Fischökologie. 7, pp. 47–59.

Thorncraft, G. & Harris, J.H. (2000) Fish Passage and fishways in New South Wales: A status report. Office of Conservation NSW Fisheries, Sydney. Cooperative Research Centre for Freshwater Ecology Technical Report 1/2000. 32 pp.

Thorstad, E.B., Økland, F., Kroglund, F., & Jepsen, N. (2003) Upstream migration of Atlantic salmon at a power station in the River Nidelva, Southern Norway. *Fish. Manage. Ecol.* 10, pp. 1-8.

Tudorache, C., Viaene, P., Blust, R., Vereecken, H., & De Boeck, G. (2008) A comparison of swimming capacity and energy use in seven European freshwater fish species. *Ecology of Freshwater Fish*, 17, pp. 284–291.

Tudorache, C., Viaene, P., Blust, R., & De Boeck (2007) Longer flumes increase critical swimming speeds by increasing burst–glide swimming duration in carp *Cyprinus carpio*, L. *J. Fish Biol.* 71, pp. 1630–1638.

Turner, J., Wiltshire, P., & Wood, M. (2011) Part IV Undergraduate Group Design Project: An Underwater Particle Velocity Sensor. BSc Thesis, University of Southampton, 155 pp.

Turnpenny, A.W.H. (1993). Bubble curtain fish exclusion trials at Heysham 2 Power Station. Fawley ARL Ltd, Client Report to Nuclear Electric plc, Report No. FCR 037/93.

Turnpenny, A.W.H. & O'Keefe, N. (2005) Screening for intake and outfalls: a best practice guide. Vol. W6-103/TR. Environment Agency, Bristol.

Turnpenny, A.W.H., Struthers, G., & Hanson, K.P., (1998). A UK guide to intake fish screening regulations, policy and best practice. ETSU H/06/00052/00/00. Department of Trade and Industry, Energy Technology Support Unit, Harwell, UK, 127 pp.

Uetz, G.W., Roberts, J.A., & Taylor, P.W. (2009) Multimodal communication and mate choice in wolf spiders: female response to multimodal versus unimodal signals. *Animal Behaviour* 78, 299e305.

U.S. Army Corps of Engineers (2012) Sensory Deterrent Systems. 8 pp.

US Clean Water Act (1972) Federal Water Pollution Control Act, Government, E. P. A. a. U., (ed).

Urick, R.J. (1983) Principles of Underwater Sound. 3rd Edition, McGraw-Hill, New York.

- van Bergeijk, W.A. (1967) The evolution of vertebrate hearing. In: Neff WD (Ed.) Contributions to Sensory Physiology, Vol. 2. New York: Academic Press, pp. 1–49.
- Varble, K. A., Hoover, J.J., George, S.G., Murphy, C.E., & Kilgore, K.J. (2007) Floodplain wetlands as nurseries for Silver Carp, *Hypophthalmichthys molitrix*: a conceptual model for use in managing local populations. Aquatic Nuisance Species Program, ERDC/TNANSRP- 07-4, Vicksburg, Mississippi.
- Varshney, L.R., & Sun J.Z. (2013). Why do we perceive logarithmically? Significance 10(1), pp. 28-31.
- Verfuss, U.K., Sinclair, R.R. & Sparling, C.E. (2019). A review of noise abatement systems for offshore wind farm construction noise, and the potential for their application in Scottish waters. Scottish Natural Heritage Research Report No. 1070.
- Vetter, B.J., Cupp, A.R., Fredricks, K.T., Gaikowski, M.P., Mensinger, A.F. (2015) Acoustical deterrence of silver carp (*Hypophthalmichthys molitrix*). Biol Invasions 17, pp. 3383–3392.
- Vetter, B., Murchy, K., Cupp, A., Amberg, J.J., Gaikowski, M.P., & Mensinger, A.F. (2017) Acoustic deterrence of bighead carp (*Hypophthalmichthys nobilis*) to a broadband sound stimulus, J. Great Lakes Res. 43(1), pp. 163-171.
- Vetter, B. J., Brey, M. K., & Mensinger, A. F. (2018). Re-examining the frequency range of hearing in silver (*Hypophthalmichthys molitrix*) and bighead (*H. nobilis*) carp. PLoS ONE 13(3): e0192561.17
- von Frisch, K. (1936) Über den Gehörsinn der Fische. Biol. Rev. 11. pp. 210–246.
- von Frisch, K. & Stetter, H. (1932) Untersuchungen über den Sitz des Gohörsinnes bei der Elritze. Z. vergl. Physiol. 17, pp. 686-801.
- Vowles, A.S. & Kemp, P.S. (2012) Effects of light on the behaviour of brown trout (*Salmo trutta*) encountering accelerating flow: application to downstream fish passage, Ecol. Eng., 47, pp. 247-253.
- Vowles, A.S., Anderson, J.J., Gessel, M.H., Williams, J.G. & Kemp, P.S. (2014) Effects of avoidance behaviour on downstream fish passage through areas of accelerating flow when light and dark, Anim. Behav. 92, pp. 101-109.



- Wagner, C.M., Stroud, E.M., Meckley, T.D., & Kraft, C. (2011) A deathly odor suggests a new sustainable tool for controlling a costly invasive species. *Can. J. Fish. Aquat. Sci.* 68 (7), pp. 1157–1160.
- Warner G.H. (1956) Report on the air-jet fish-deflection tests. *Progressive Fish. Cult.* 18 (1), pp. 39–41.
- Webb, J.F., Popper, A.N., & Fay, R.R. (2008) Fish bioacoustics. Popper, A.N., Fay, R.R. (eds.), Springer.
- Webb, J.F. (1998) Laterophysic connection: a unique link between the swim bladder and the lateral-line system in *Chaetodon* (Perciformes: Chaetodontidae). *Copeia* 1998, pp. 1032–1036.
- Webb, J.F., Montgomery, J.C., & Mogdans, J. (2008) Bioacoustics and the Lateral Line System of Fishes. In: Webb, J.F., Popper, A.N., & Fay, R.R. (eds) *Fish Bioacoustics*. New York: Springer, pp. 145-182.
- Webb, J.F., Smith, W.L. (2000) The laterophysic connection in chaetodontid butterflyfish: morphological variation and speculations on sensory function. *Philos Trans Roy Soc Lond B* 355, pp. 1125–1129.
- Weber, E.H. (1820) *De aure et auditu hominis et animalium. Pars I. De aure animalium aquatiliium*. Leipzig.
- Weber, M.J. & Brown, M.L. (2009) Effects of common carp on aquatic ecosystems 80 years after “Carp as a Dominant”: ecological insights for fisheries management. *Rev. Fish. Sci.* 17, pp. 524–537.
- Weber, M.J., Hennena, M.J., Brown, M.L., Matthew J. Hennena, Lucchesi, D.O., & Sauver, T.R.St (2016) Compensatory response of invasive common carp *Cyprinus carpio* to harvest *Fisheries Research*. 179, pp. 168–178.
- Weeg M, Fay RR, Bass A (2002) Directional response and frequency tuning in saccular nerve fibers of a vocal fish, *Porichthys notatus*. *J. Comp. Physiol. A* 188, 631–41.
- Welton, J.S., Beaumont W.R.C., Ladle M., Masters J.E.G., (1997) Smolt Trapping Using Acoustic Techniques. Environment Agency, R&D Technical Report W66, 79 pp.

- Weston, D.E. (1967) Sound propagation in the presence of bladder fish, In: V. M. Albers, (Ed.) Underwater Acoustics, Proc. NATO Advanced Study Institute, Copenhagen (Plenum, New York, 1967), Vol. II, pp. 55–88.
- White, E.T., Beardmore, R.H. (1962) The Velocity of Rise of Single Cylindrical Air Bubbles through Liquid Contained in Vertical Tubes. Chem. Eng. Sci. 17(5), pp. 351-361.
- Wiley, D., Ware, C., Bocconcelli, A., Cholewiak, D., Friedlaender, A., Thompson, M., & Weinrich, M. (2011) Underwater components of humpback whale bubble net feeding behaviour. Behav. 148(56), pp. 575–602.
- Williamson, M., & Fitter, A. (1996) The characters of successful invaders. Biol. Conserv. 78, pp. 163–170.
- Winchell, F. C., Amaral, S.V., Taft, E.F., Cook, T.C., Plizga, A.W., Paolini, E.M., & Sullivan, C.W. (1996) Results of Field Evaluations of the New Modular Inclined Fish Diversion Screen. In: Fish Passage Workshop, Milwaukee, Wisconsin, May 6-8, 1997. Sponsored by Alden Research Laboratory, Conte Anadromous Fish Research Laboratory, Electric Power Research Institute, and Wisconsin Electric Power Company.
- Woodbury, D., & Stadler, J. (2008) A proposed method to assess physical injury to fishes from underwater sound produced during pile driving. Bioacoustics 17, pp. 289—291.
- Wu, X., Rao, J., & He, B. (1992). The history of the Chinese freshwater fisheries. In: Liu, J., He, B (Eds.), Cultivation of the Chinese Freshwater Fishes. Science Press, Beijing, China, pp. 5–29.
- Wysocki, L.E., Dittami, J.P., & Ladich, F. (2006) Ship noise and cortisol secretion in European freshwater fishes. Biol. Conserv. 128, pp. 501–508.
- Yan, H.Y., & Popper, A.N., (1992) Auditory sensitivity of the cichlid fish *Astronotus ocellatus* (Cuvier). J. Comp. Physiol. A 171, pp. 105–109.
- Yoon, S. W., Crum, L. A., Prosperetti, A., and Lu, N. Q. (1991) An investigation of the collective oscillations of a bubble cloud. J. Acoust. Soc. Am. 89, pp. 700-706.
- Zeddies, D.G., Fay, R.R., Alderks, P.W., Shaub, K.S. and Sisneros, J.A. (2010) Sound source localization by the plainfin midshipman fish, *Porichthys notatus*. J. Acoust. Soc. Am. 127, pp. 3104-3113.

Zeddies, D.G., Fay, R.R., Gray, M.D., Alderks, P.W., Acob, A., & Sisneros, J.A. (2012) Local acoustic particle motion guides sound-source localization behavior in the Plainfin Midshipman fish, *Porichthys notatus*. *J. Exp. Biol.* 215: pp. 152–160.

Zhang, G., Wu, L., Li, H., Liu, M., Cheng, F., Murphy, B.R., & Xie, S. (2012) Preliminary evidence of delayed spawning and suppressed larval growth and condition of the major carps in the Yangtze River below the Three Gorges Dam. *Environ. Biol. Fishes.* 93, pp. 439–447.

Zielinski, D.P., & Sorensen, P.W. (2015) Field test of a bubble curtain deterrent system for common carp. *Fish. Manage. Ecol.* 22, pp 181–184;

Zielinski, D.P., & Sorensen, P.W. (2016) Bubble Curtain Deflection Screen Diverts the Movement of both Asian and Common Carp. *N. Am. J. Fish. Manage.* 36, pp 267–276.

Zielinski, D.P., & Sorensen, P.W. (2017) Silver, bighead, and common carp orient to acoustic particle motion when avoiding a complex sound. *PLoS ONE* 12(6)

Zielinski, D.P., Hondzo, M., & Voller, V.R. (2014a) Mathematical evaluation of behavioral deterrent systems to disrupt fish movement. *Ecol. Mod.* 272, pp. 150– 159

Zielinski, D.P., Voller, V.R., Svendsen, J.C., Hondzo, M., Mensinger, A.F., & Sorensen, P. (2014b). Laboratory experiments demonstrate that bubble curtains can effectively inhibit movement of common carp. *Ecol. Eng.* 67, pp 95–103

## **List of Appendices**

APPENDIX A:	Legislation
APPENDIX B:	Chapter 3 - GAM Models and Checks
APPENDIX C:	Examples of High Speed Frames used for Determination of Bubble Size Distribution
APPENDIX D:	Backscatter and Attenuation in the Presence of Bubbles
APPENDIX E:	Equations used for Determination of Extinction Cross-Sections
APPENDIX F:	Plots of Theoretical Extinction Coefficients
APPENDIX G:	Equations used for Calculating Mean Angle, Angular Dispersion, Straightness and Sinuosity
APPENDIX H:	Chapter 4 – GAM Models and Checks
APPENDIX I:	Chapter 5 – GAM Models and Checks



## APPENDIX A

### Legislation

In order to reduce environmental impacts of anthropogenic activities such as development and operation of hydropower dams, legislative frameworks have been put into place. Key drivers for this within the EU and UK include:

- Council Regulation (EC) No. 1100/2007 (The Eel Regulation): requires member states to prepare an Eel Management Plan for every eel river basin within its national territory. The objective of each Eel Management Plan is to: "*reduce anthropogenic mortalities so as to permit with high probability the escapement to the sea of at least 40% of the silver eel biomass relative to the best estimate of escapement that would have existed if no anthropogenic influences had impacted the stock.*"
- The Water Framework Directive 2000/60/EC (WFD): This directive requires EU member states to take steps to prevent any deterioration in the status of all bodies of surface water. The first management cycle ended in 2015, the deadline by which all surface water bodies should have achieved Good Ecological Status (GES) or Good Ecological Potential (GEP). The second management cycle is set to end in 2021, with a final cycle set for 2027.
- The Habitats Directive (92/43/EEC): is concerned with conservation of rare, threatened or endemic species by targeting specific habitat types for conservation. A total of over 1,000 species and 200 habitat types are listed in the directive's Annexes:
  - Annex II: core habitat regions of the species listed are designed as site of Community Importance;
  - Annex IV: species are strictly protected across their entire natural range;

- Annex V: Member States must ensure that exploitation of these species is compatible with retaining their favourable conservation status;
- Marine Strategy Framework Directive (MSFD): requires each Member State to develop a maritime strategy based on the ecosystem approach with the aim of achieving or maintaining 'good environmental status' in the marine environment by 2020. It harmonises existing directives such as the WFD and Habitats directive. Each Member State is required to set-up a monitoring programme for the ongoing assessment of targets for a total of 11 descriptors, the following of which are relevant to the present study; biodiversity, non-indigenous species, commercial fish and shellfish, food webs, energy including underwater noise. The process is cyclical and a second cycle is due to start in 2018.
- Council Regulation (EC) No. 1143/2014 (Invasive Alien Species Regulation): provides a set of measures to be taken across the EU in relation to invasive alien species included on the “List of Invasive Alien Species of Union concern.” The measures follow an agreed hierarchical approach and include; prevention, early detection and eradication, and management of species already established.
- Convention on Biological Diversity: provides a legal framework for biodiversity conservation by requesting that contracting Parties create and enforce national strategies and action plans. The most recent targets were set and outlined in the “Strategic Plan for Biodiversity 2011-2020” along with 20 “Aichi Targets”. The EU Biodiversity Strategy reflects the commitments taken by the EU in 2010, within the CBD, and aims to halt the loss of biodiversity and ecosystem services by 2020.
- Salmon and Freshwater Fisheries Act (SAFFA) 1975: Sections 14 and 15 set specific powers to screen intakes and outfalls for the ingress and egress of migratory salmonids.

- The Wildlife and Countryside Act 1981 (WCA): Is the principle mechanism for the legislative protection of wildlife in Great Britain. It is the means by which the Convention on the Conservation of European Wildlife and Natural Habitats (the 'Bern Convention'), the European Union Directives on the Conservation of Wild Birds (79/409/EEC) and Natural Habitats and Wild Fauna and Flora (92/43/FFC) are implemented in the UK. It is the principal legislation dealing with non-native species - Section 14(1) of the WCA making it illegal to release or allow to escape into the wild any such animal, or species listed in Schedule 9 to the Act.
  
- Water Resources Act (WRA) 1991:
  - Sections 24 and 25: require the fitting of a fish screen as a condition to adding new water abstraction facilities. Licence conditions under the EA may require not only the installation of screening systems at the owner's expense but also the installation of monitoring equipment and the carrying out of surveys. The WRA allows flexibility of regulatory approach, allowing placement of limits on timing of abstraction to avoid critical fish migration periods, flows, water levels and other operating conditions which are generally negotiated with the industry [Sheridan, 2014].
  
  - Section 105 (3): requires that due regard be given to the interests of fisheries when providing flood defence (Flood Defence – General).
  
- Land Drainage Act 1991: The appropriate authority is required to consider their general environmental duties in any land drainage application – including any conservation species included within the assessment. Furthermore, Land Drainage consent is required, such consent should not be issued if the structure would impede fish migration. Section 23 prohibits the obstruction or altering of flows on a watercourse without consent from the Environment Agency or Internal Drainage Board.



- United Kingdom Biodiversity Action Plan (UKBAP) and The Natural Environment and Rural Communities (NERC) Act (2006): Published in 1994, this was the UK Government's response to signing the CBD in 1992. The UK Biodiversity Steering Group has listed eels as a UK priority species and is included under Section 41 (S41) of the NERC Act which requires the Secretary of State to publish a list of habitats and species which are of principal importance for the conservation of biodiversity in England.
- The Eels (England and Wales) Regulations 2009 Statutory Instrument No. 3344 (The Eel SI): The eels regulation is essentially Council Regulation (EC) No. 1100/2007 transferred into British law.
  - Section 17: requires that since January 2015, an eel screen must have been placed within:
    - a. a diversion structure capable of abstracting at least 20 cubic metres of water through any one point in any 24-hour period;
    - b. any diversion structure returning water to a channel, bed or sea.
  - Section 18: a continuous bywash should be installed if an eel screen is not located at the entrance of the diversion structure. This should allow eels to return to the waters from which they entered the diversion structure.
  - Section 19: the eel screen or bywash should be maintained. Causing damage, interference or do anything to the eel screen or bywash that may render it less efficient is an offence.
- Marine and Coastal Access Act 2009 (The Marine Act): Part 7 (Fisheries), chapter 3 (Migratory and freshwater fish) of the act makes a number of amendments to a number allowing for the protection of fish at water intakes and outfalls:

- Section 223 of the Marine Act amends Section 41 of SAFFA (1975). It updates the definition of an eel to include any fish of the species *Anguilla anguilla*, including elvers and glass eels.
- Section 224 amends paragraph 6 of Schedule 25 to the WRA 1991, giving the EA the power to make byelaws for better protection, preservation and improvement of any “fisheries of fish to which this paragraph applies”.
- Section 230 amends Section 6 of the Environment Act 1995, making it a general duty of the EA to maintain, improve and develop fisheries of salmon, trout, eels, lampreys, smelt and freshwater fish.



## APPENDIX B -

### Chapter 3: GAM Models and Checks

#### Cullen and Frey graph

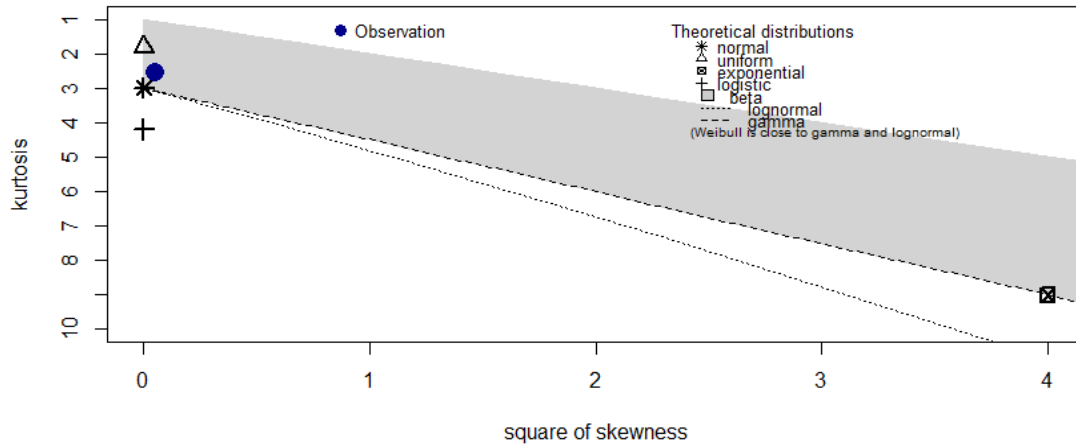


**Fig. AB 1** – Cullen and Frey graph for *Passes* dataset

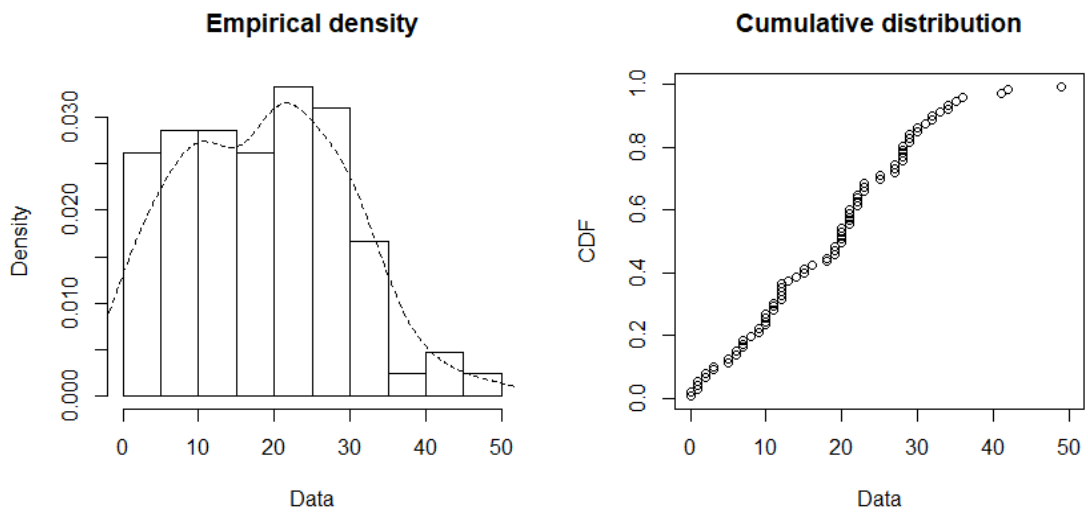


**Fig. AB 2** – Density and distribution plot for *Passes* dataset

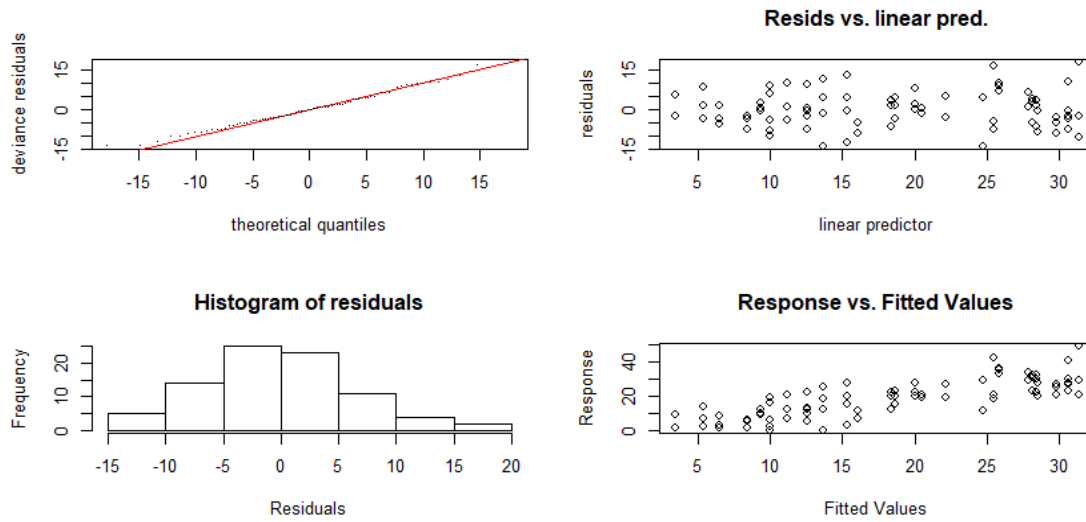


**Fig. AB 3** – GAM fitness check for Mimimum Adequate Model in *Passes* dataset

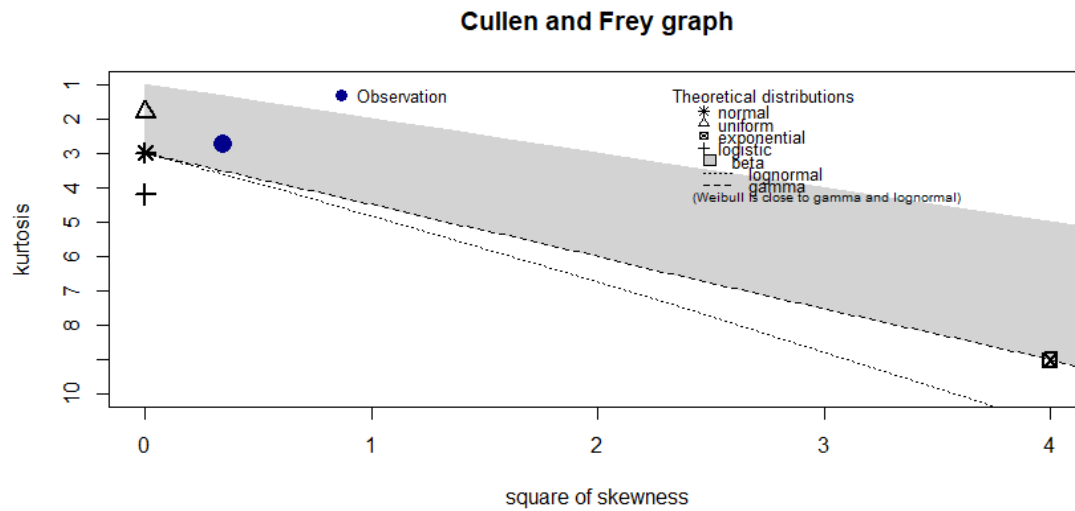


**Fig. AB 4** – Cullen and Frey graph for *Passes (excl. side passes)* dataset.

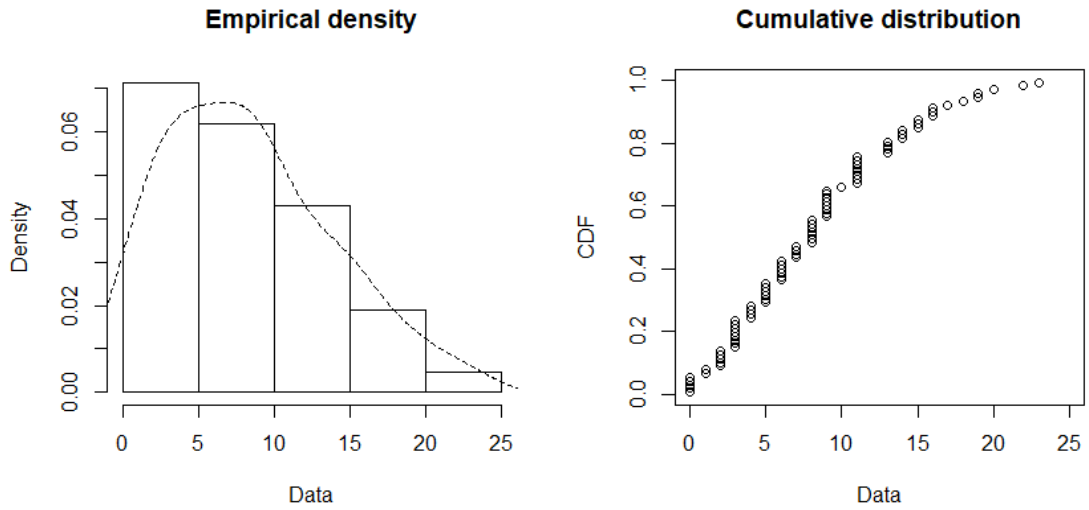


**Fig. AB 5** – Density and distribution plot for *Passes (excl. side passes)* dataset.

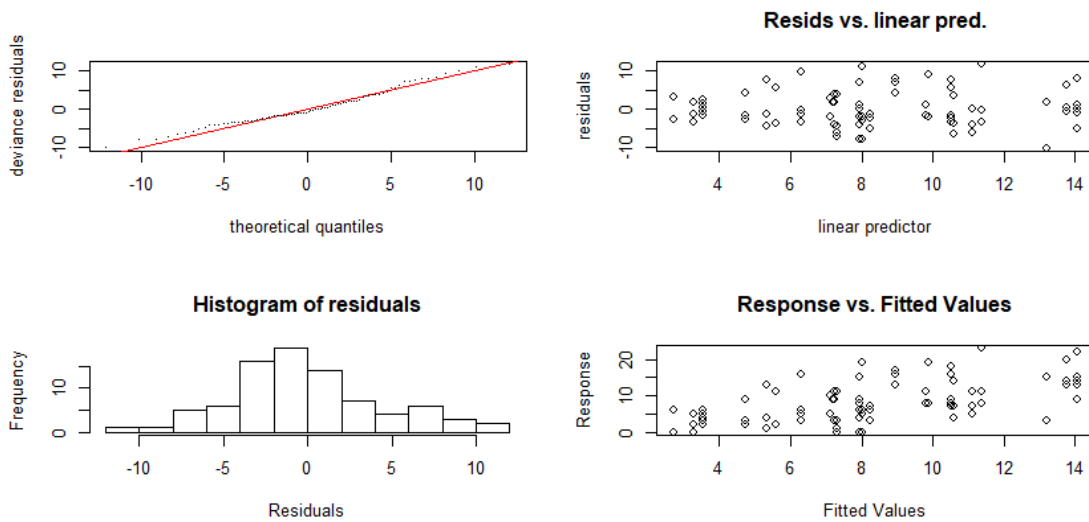


**Fig. AB 6** – GAM fitness check for Minimum Adequate Model in *Passes (excl. side passes)* dataset

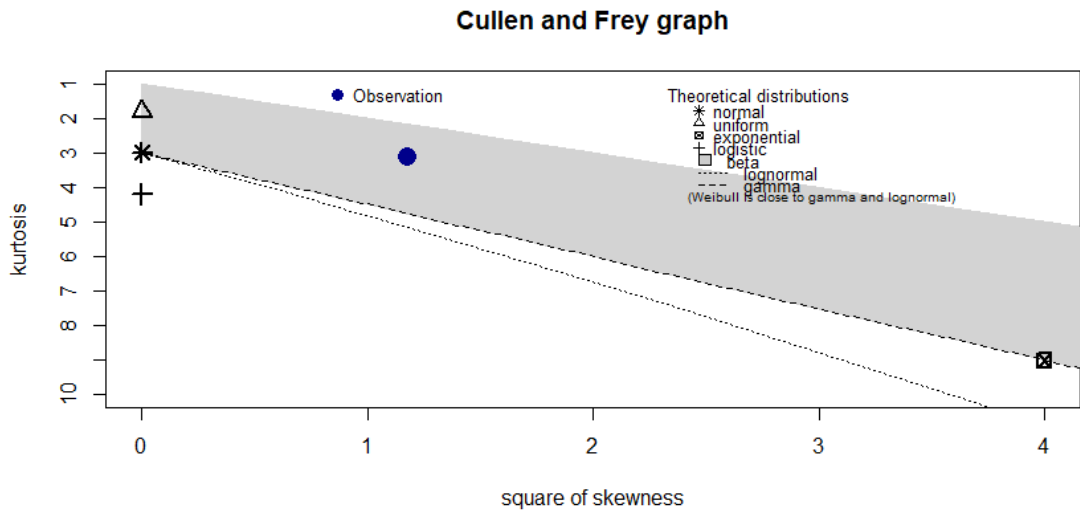


**Fig. AB 7** – Cullen and Frey graph for *Passage Efficiency* dataset.

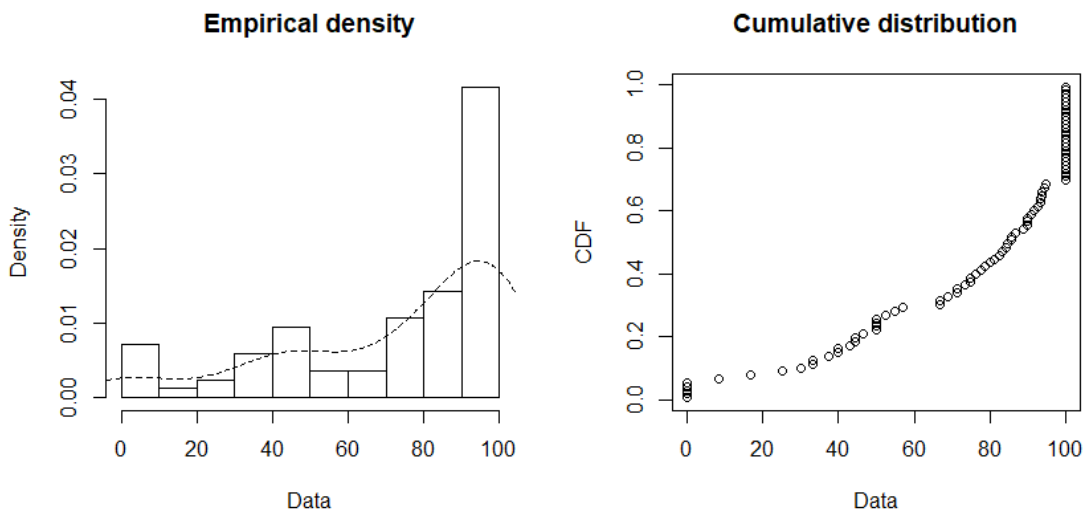


**Fig. AB 5** – Density and distribution plot for *Passage Efficiency* dataset.

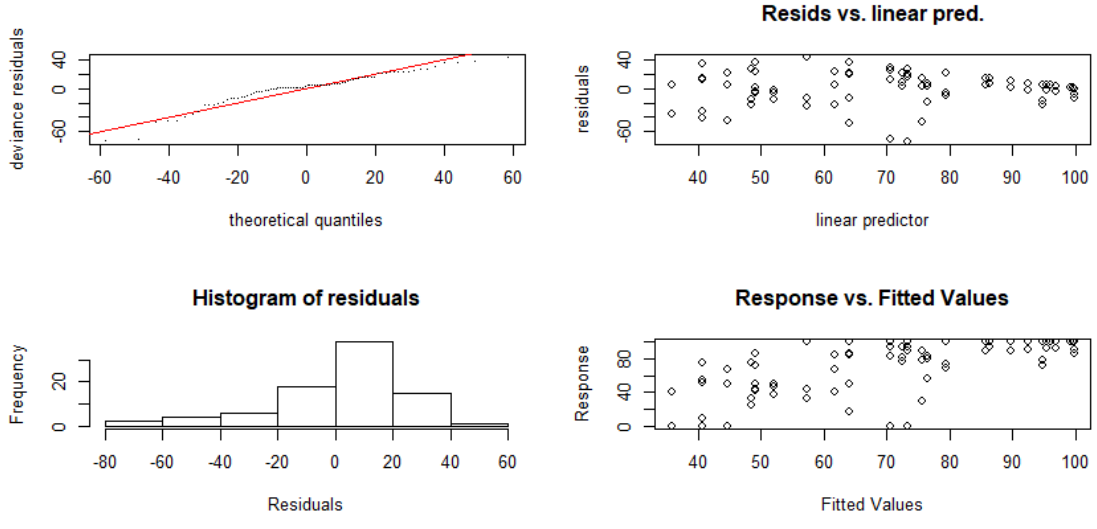


**Fig. AB 6** – GAM fitness check for Minimum Adequate Model in *Passage Efficiency* dataset





## APPENDIX C:

### Examples of High Speed Frames used for Determination of Bubble Size Distribution

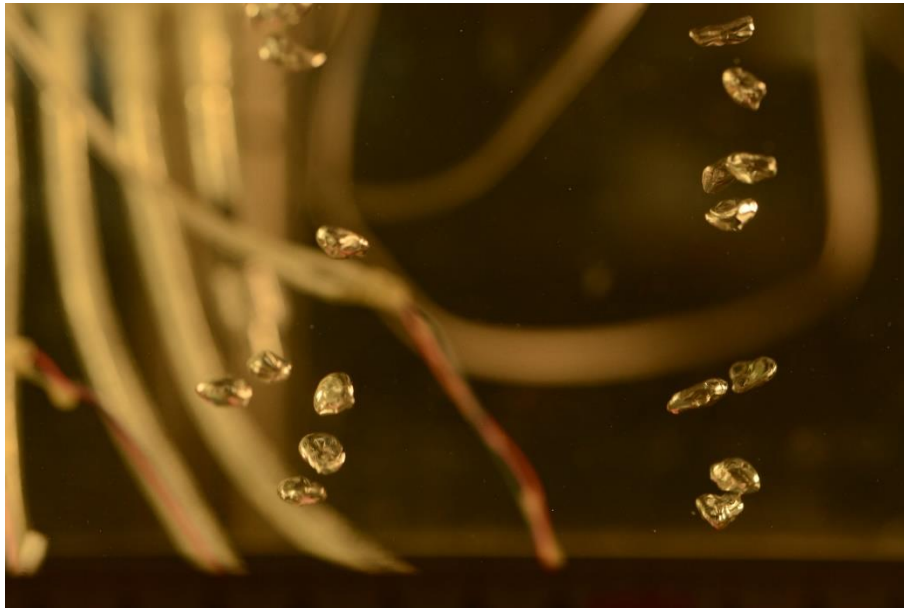


**Fig. AC 1:** Example of frame for air flow equivalent to  $10 \text{ L min}^{-1}$  ( $5 \text{ L min}^{-1} \text{ m}^{-1}$ ) at 2 bar, vibration 0V.



**Fig. AC 2:** Example of frame for air flow equivalent to  $10 \text{ L min}^{-1}$  ( $5 \text{ L min}^{-1} \text{ m}^{-1}$ ) at 2 bar, vibration 2.2V.

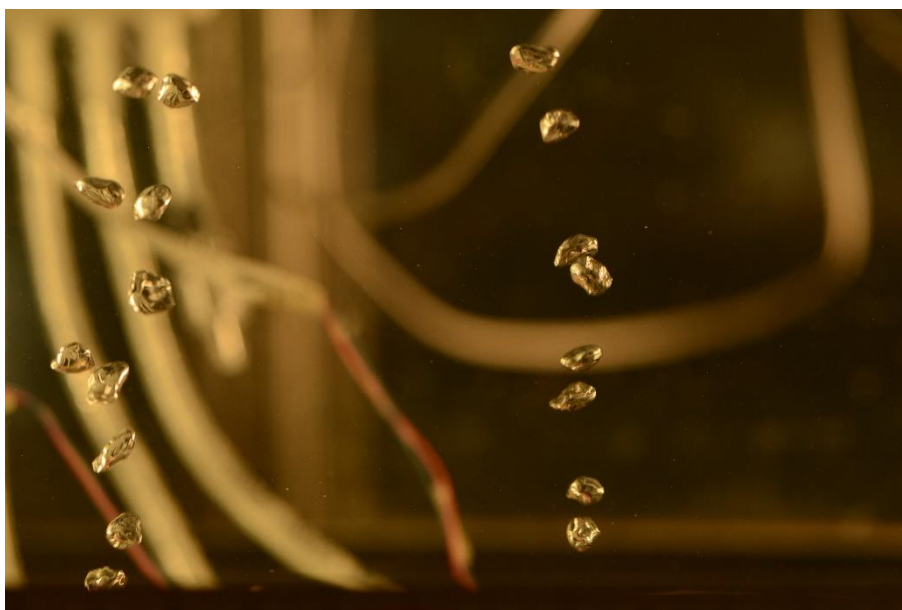


**Fig. AC 3:** Example of frame for air flow equivalent to  $6 \text{ L min}^{-1}$  ( $3 \text{ L min}^{-1} \text{ m}^{-1}$ ) at 2 bar, vibration 0V.

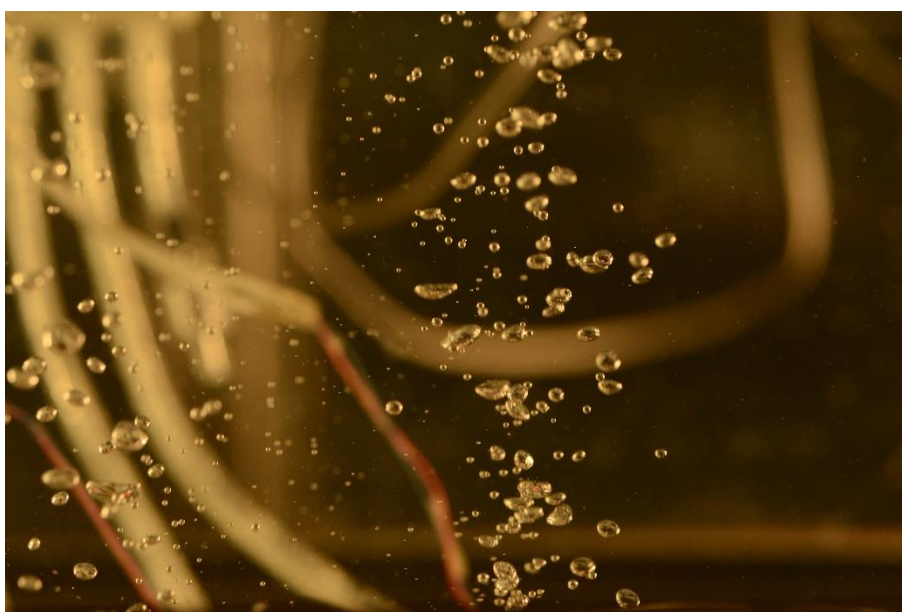


**Fig. AC 4:** Example of frame for air flow equivalent to  $6 \text{ L min}^{-1}$  ( $3 \text{ L min}^{-1} \text{ m}^{-1}$ ) at 2 bar, vibration 3V.

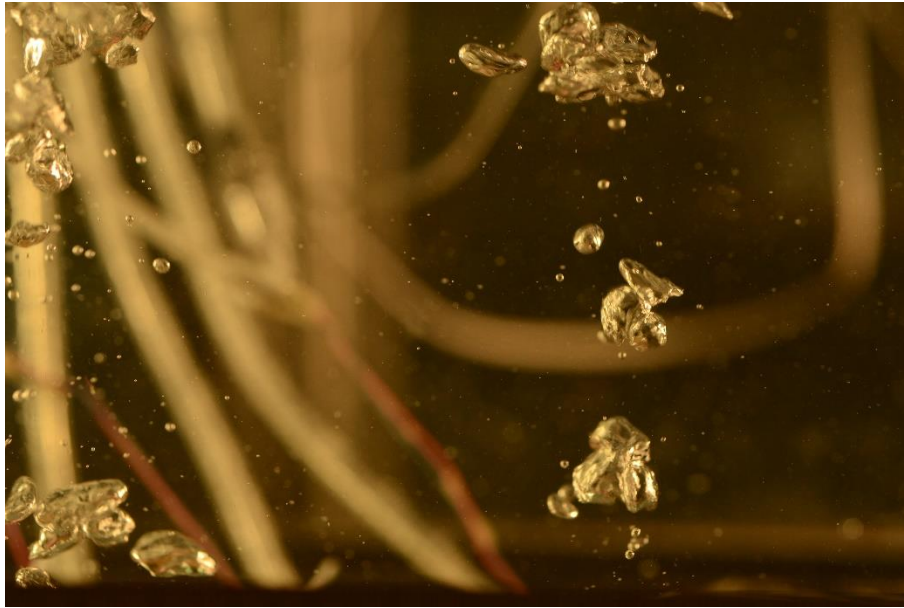


**Fig. AC 5:** Example of frame for air flow equivalent to  $60 \text{ L min}^{-1}$  ( $30 \text{ L min}^{-1} \text{ m}^{-1}$ ) at 1 bar, vibration 0V.

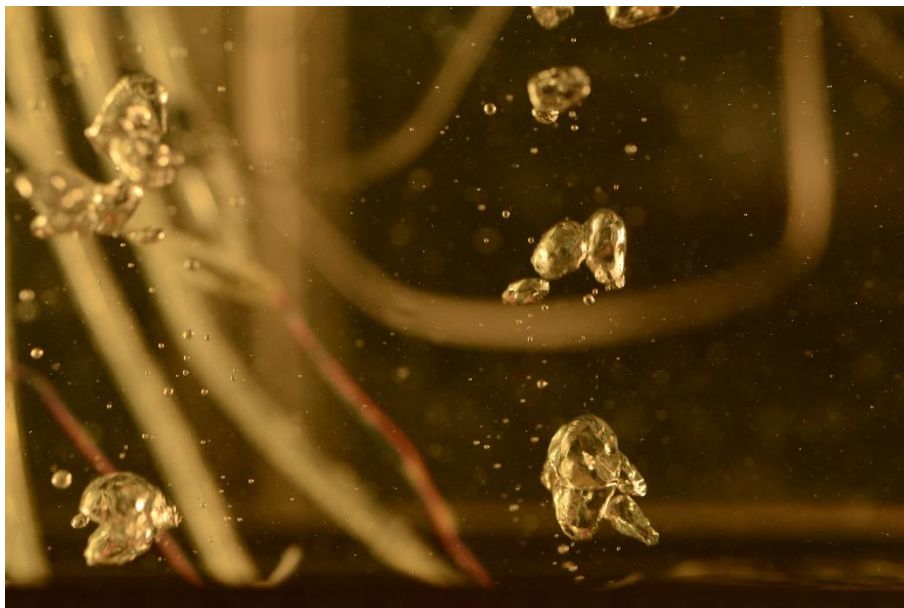


**Fig. AC 6:** Example of frame for air flow equivalent to  $60 \text{ L min}^{-1}$  ( $30 \text{ L min}^{-1} \text{ m}^{-1}$ ) at 1 bar, vibration 2V.

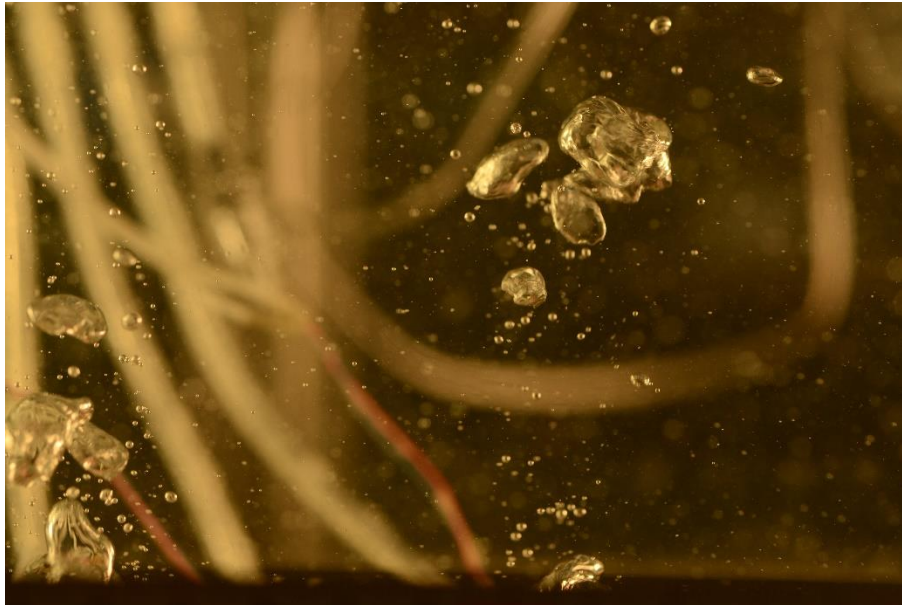


**Fig. AC 7:** Example of frame for air flow equivalent to  $60 \text{ L min}^{-1}$  ( $30 \text{ L min}^{-1} \text{ m}^{-1}$ ) at 1 bar, vibration 3V.

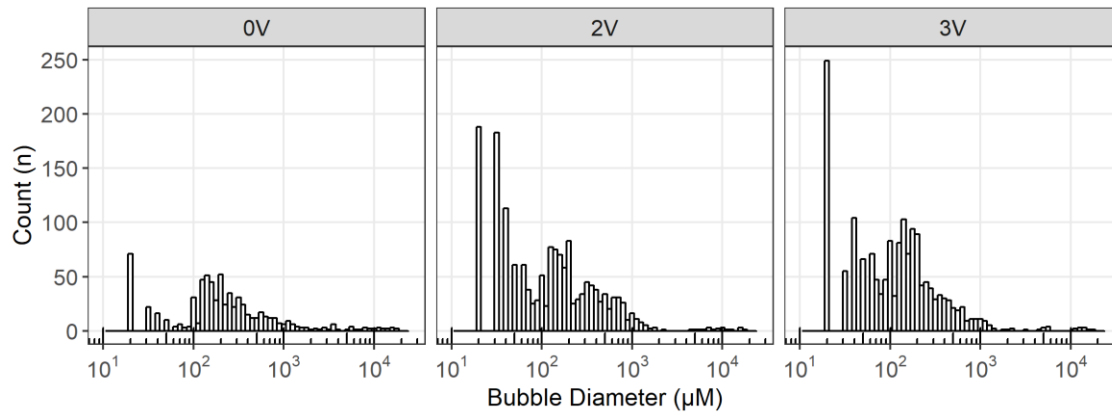


**Fig. AC 8:** Bubble size distributions for air flows equivalent to  $60 \text{ L min}^{-1}$  ( $30 \text{ L min}^{-1} \text{ m}^{-1}$ ) at 1 bar, and vibration levels of 0V, 2V, 3V.

## APPENDIX D:

### Backscatter and Attenuation in the Presence of Bubbles<sup>1</sup>

If sound is propagating through a medium containing a small bubble, that bubble will be forced into pulsation against thermal and viscous dissipative mechanisms. The energy required to overcome this dissipation will be absorbed from the incident acoustic wave. In addition, the pulsating bubble is itself a source of sound, so that as the driven bubble oscillates it will scatter acoustic energy from the incident wave. This loss of energy from an acoustic wave resulting from the presence of a bubble is usually expressed as the ratio of the time-averaged power loss per bubble,  $\langle \dot{W} \rangle$ , to the intensity of the incident acoustic beam,  $I$ . The quantity has the dimensions of area, and is called the *extinction cross-section*,  $\sigma_e^b$ , of the bubble so that [Andreae, 1986]:

$$\sigma_e^b = \frac{\langle \dot{W} \rangle}{I}$$

A plane wave of intensity  $I$ , travelling a distance  $\Delta z$ , through a population of  $n_b$  bubbles per unit volume, each having an extinction cross-section  $\sigma_e^b$ , has its intensity reduced by  $\Delta I = -n_b \sigma_e^b \Delta z$ . Integration gives:

$$I = I_0 \exp(-n_b \sigma_e^b z)$$

Where  $I_0$  is the intensity at  $z = 0$ . Since the intensity in plane waves is proportional to the square of the acoustic pressure,  $P$ , the latter varies as:

$$P \propto \exp(-n_b \sigma_e^b z/2)$$

It is often of interest to know specifically how much of the energy of an incident acoustic beam is scattered by the bubble, as opposed to being dissipated through thermal and viscous mechanisms. The ratio of time-averaged power loss per bubble that results from scattering alone, to the intensity of the incident acoustic beam is called the scattering cross section,  $\sigma_s^b$ , of the bubble.

---

<sup>1</sup> Leighton, T.G, (1994) "The Acoustic Bubble", Academic Press Ltd, pp 272 - 274

At resonance, the scattering and extinction cross-sections of an oceanic bubble are about three orders of magnitude greater than its geometrical cross-section, which can be considerable advantage when using acoustic spectroscopy, rather than optical techniques to measure bubble populations.

The cross-sections can still be formulated if there is a range of bubble sizes present by defining a function describing the number density size distribution of bubble in a cloud. The bubble density at a certain depth is given by  $n_b^{gr}(R_0)$  for increment [Charlson *et al.*, 1987]  $d(R_0)$  such that  $n_b^{gr}(R_0)d(R_0)$  is the number of bubbles per unit volume with radius between  $R_0$  and  $R_0 + dR_0$ . Thus the extinction cross-section for sound propagating through a bubble cloud with population described by  $n_b^{gr}(R_0)$  is simply:

$$\sigma_e^c = \int_{R_0=0}^{\infty} \sigma_e^b n_b^{gr}(R_0) d(R_0)$$

This parameter, which has units of [length<sup>-1</sup>], describes that component of attenuation of an acoustic beam propagating through a cloud which is due to the bubbles, since the intensity of the beam decays with distance of propagation  $z$  as:

$$I \propto e^{-\sigma_e^c z}$$

Knowing the cross-section for scatter from a bubble, the backscatter cross-section is simply  $\sigma_{b-s}^b = \frac{\sigma_s^b}{4\pi}$ , the solid angle ratio arising since the backscatter is omnidirectional. When insonating a bubble cloud one examines the backscattering cross-section per unit volume, that is  $\sigma_{b-s}^{cv}$ , the volume backscattering coefficient:

$$\sigma_{b-s}^{cv} = \frac{1}{4\pi} \int_{R_0=0}^{\infty} \sigma_s^b n_b^{gr}(R_0) d(R_0)$$

Thus, the backscatter and attenuation that results from the presence of bubbles, all of which have  $R_0 \ll \lambda$  can in principle be related to the bubble size spectrum of the bubble cloud [Medwin, 1980]

## Appendix E:

### Equations used for Determination of Extinction Cross-sections

When bubbles are driven into small amplitude pulsation by an acoustic field, energy is subtracted from the incident wave by the bubble. The ratio of the power lost from an incident plane wave, to the intensity of that incident plane wave, has dimensions of area, and is known as the extinction cross-section ( $\sigma_e$ ). Since this power loss is either scattered or absorbed, the power loss that the  $\sigma_e$  describes can be split into the sum of two other cross-sections, the absorption cross-section ( $\sigma_a$ ), and the scattering cross-section ( $\sigma_s$ ). These are in turn given by the ratio, to the intensity of a plane wave normally incident on the bubbles, of the rate at which energy is absorbed, and the power scattered by the bubble, respectively.

Despite these being long-established concepts, Ainslie and Leighton [2011] identified ambiguities and errors in the literature, dating back decades, so that great care must be used with historical formulations for them, particularly when there is the possibility that the size of the largest bubble present might not be much smaller than the shortest acoustic wavelength used [Ainslie & Leighton, 2009; Li *et al.*, 2020].

In this study the damping factors for  $Q_{rad}$  and  $Q_{th}$  from the scattering model proposed by Andreeva [1964] were used.

$$\frac{1}{Q_{rad}} = \frac{\omega_{res} R_0}{c} \quad \text{Equation E1}$$

$$\frac{1}{Q_{th}} = \frac{3(\gamma-1)}{R_0} \sqrt{\frac{D_p}{2\omega_{res}}} \quad \text{Equation E2}$$

Here,  $\omega_{res}$  is the angular frequency at resonance,  $R_0$  equilibrium bubble radius,  $c$  the speed of sound in water,  $\gamma$  is the specific heat ratio of gas, and  $D_p$  the gas diffusivity ( $D_p = k/(\rho_a c_p)$ ,  $k$  is the thermal conductivity of gas and  $c_p$  is the specific heat of gas at constant pressure).

Andreeva's model was intended for application to fish swimbladders approximated as a spherical gas bubble, assuming an infinite elastic medium with the



properties of fish flesh. Given that the medium used in the present study was water, the equation for the viscous damping factor,  $Q_{vis}$  was obtained by substituting  $\epsilon = 1$  into equation (2d) from Baik [2013]:

$$\beta_{vis} = \frac{2\eta_e}{\rho R_0^2}, \eta_e = \left(1 - \frac{1}{\epsilon^3}\right) \eta_{fs} + \frac{1}{\epsilon^3} \eta_{ws} \quad \text{Equation E3}$$

Here,  $\eta_{fs}$  and  $\eta_{ws}$  are the shear viscosities of the viscous shell and surrounding liquid, respectively. Given that  $\epsilon = 1$ , this gives:  $\eta_e = \eta_{ws}$ .

Andreeva's damping factor,  $Q_{vis}$ , is related to Baik's damping factor,  $\beta$ , by:

$$\beta = \frac{\omega_{res}}{2Q_{vis}} \quad \text{Equation E4}$$

Substituting Andreeva's equation for the viscous damping factor gives:

$$\beta_{vis} = \frac{\omega_{res}}{2Q_{vis}} = \frac{\omega_{res}}{2} \times \frac{4\mu_i}{\rho R_0^2 \omega_{res}^2} = \frac{2\mu_i}{\rho R_0^2 \omega_{res}} \quad \text{Equation E5}$$

In a viscoelastic material, the complex shear modulus,  $\mu^*$ , is represented as:

$$\mu^* = \mu - i\omega\eta \quad \text{Equation E6}$$

Here,  $\mu$  and  $\eta$  are the real value of the shear modulus and shear viscosity of the material, respectively, and  $\omega$  is the angular frequency of the incident sound field. The imaginary part of the complex shear modulus is therefore:  $\mu_i = -\omega\eta$ . When this is substituted into (Equation E4) as a magnitude, it becomes:

$$\beta_{vis} = \frac{2\mu_i}{\rho R_0^2 \omega_{res}} = \frac{2\omega_{res}\eta}{\rho R_0^2 \omega_{res}} = \frac{2\eta\omega}{\rho R_0^2 \omega_{res}} \quad \text{Equation E7}$$

Given equations (E4) and (E7),  $\frac{1}{Q_{vis}}$  becomes:

$$\frac{1}{Q_{vis}} = \frac{2\beta_{vis}}{\omega_{res}} = \frac{4\eta\omega}{\rho R_0^2 \omega_{res}^2} \quad \text{Equation E8}$$

The scattering cross section,  $\sigma_s$  is:  $\sigma_s = \frac{4\pi R_0^2}{\left(\frac{\omega_{res}^2}{\omega} - 1\right)^2 + \delta_{Weston}^2}$  Equation E9

Here,  $\delta_{Weston}$  is given by:

$$\delta_{Weston} = \frac{1}{Q_{rad}} \frac{\omega_{res}}{\omega} + \frac{1}{Q_{th}} \left(\frac{\omega_{res}}{\omega}\right)^{\frac{5}{2}} + \frac{1}{Q_{vis}} \left(\frac{\omega_{res}}{\omega}\right)^2 \quad \text{Equation E10}$$

The extinction cross-section,  $\sigma_e$  is:

$$\sigma_e = \sigma_s \left[ 1 + \frac{Q_{rad}}{Q_{th}} \left(\frac{\omega_{res}}{\omega}\right)^{\frac{7}{5}} + \frac{Q_{rad}}{Q_{vis}} \left(\frac{\omega_{res}}{\omega}\right)^3 \right] \quad \text{Equation E11}$$

## APPENDIX F:

### Plots of Theoretical Extinction Cross-Sections

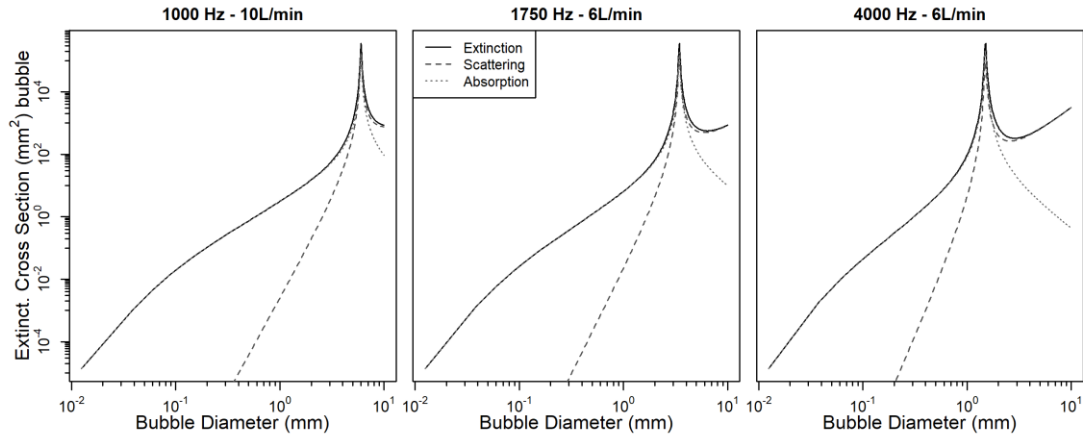


**Fig. AF 1** – Theoretical extinction, scattering, and absorption cross-sections for 1 bubble of each radius bin for the three frequencies used in Chapter 4.

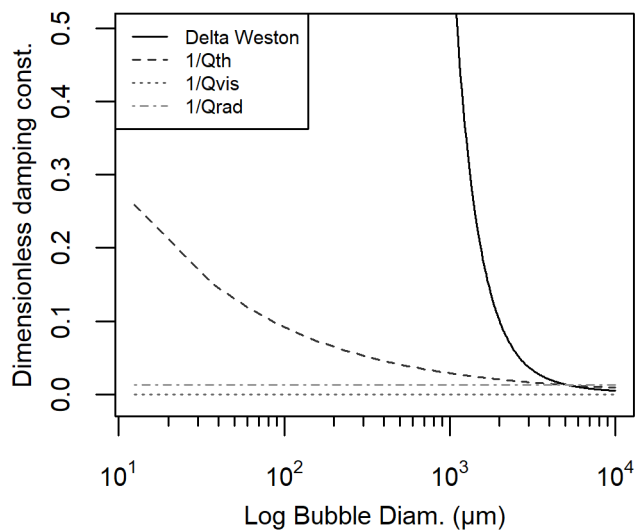


**Fig. AF 2** – Plot of dimensionless damping const. as calculated in Chapter 4.

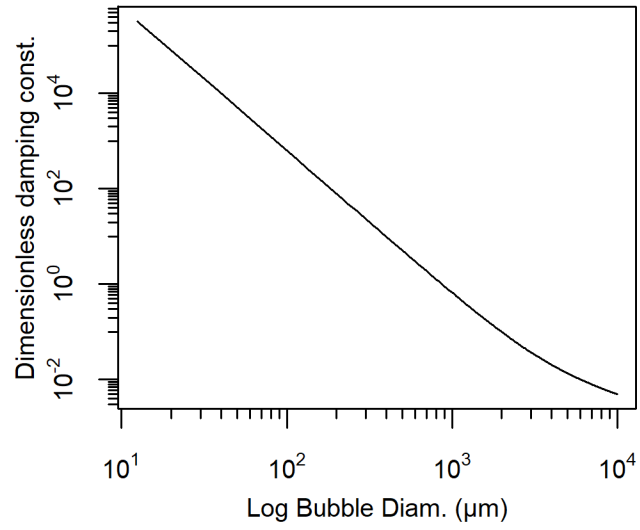


**Fig. AF 3** – Plot of values modelled for  $\delta_{Weston}$

## APPENDIX G:

### Equations used for Calculating Mean Angle, Angular Dispersion, Straightness and Sinuosity

The data collected were used to calculate indices of straightness and sinuosity and to investigate the relationship between turning angles, and swimming speed relative to distance from the bubble curtain. The Straightness index, ST [Batschelet, 1981], is the Euclidian distance,  $dE$ , between the start and the final point, divided by the total length of the movement,  $d$ :

$$ST = \frac{dE}{d}$$

The Sinuosity index, SNI [Bovet & Benhamou, 1988], is an estimate of tortuosity of a search path:

$$SNI = 2 \left[ p \left( \frac{1 - \bar{c}^2 - \bar{s}^2}{(1 - \bar{c}^2) + \bar{s}^2} + b^2 \right) \right]^{-0.5}$$

here:  $p$  = mean step length,  $\bar{c}$  = mean cosine of turning angles,  $\bar{s}$  = mean sine of turning angles,  $b$  = coefficient of variation of step length.

Relative turning angle data were first converted from degrees into radians, and binned at 5 cm intervals starting from the bubble curtain front. For each bin, the mean angle  $\theta_r$  was calculated using the following set of equations:

$$Y = \frac{\sum_{i=1}^n \sin \theta}{n} \quad X = \frac{\sum_{i=1}^n \cos \theta}{n}$$

$$r = \sqrt{X^2 + Y^2}$$

$$\cos \bar{\theta} = \frac{X}{r} \quad \sin \bar{\theta} = \frac{Y}{r}$$

$$\theta_r = \arctan\left(\frac{\sin \bar{\theta}}{\cos \bar{\theta}}\right)$$

here:  $\theta$  = the angle,  $X$  and  $Y$  = the rectangular coordinates of the mean, and  $r$  = the mean vector.

For each set of binned data, the Rayleigh  $z$  Test was performed,  $z = nr^2$ , where  $n$  is the sample size, and  $r$  is the mean vector a measure of angular dispersion, used in the mean angle calculation. Finally, for each binned data set, the circular standard deviation,  $v$ , was calculated:

$$v = \sqrt{-2\ln(r)}$$

APPENDIX H:

Chapter 4 – GAM Models and Checks

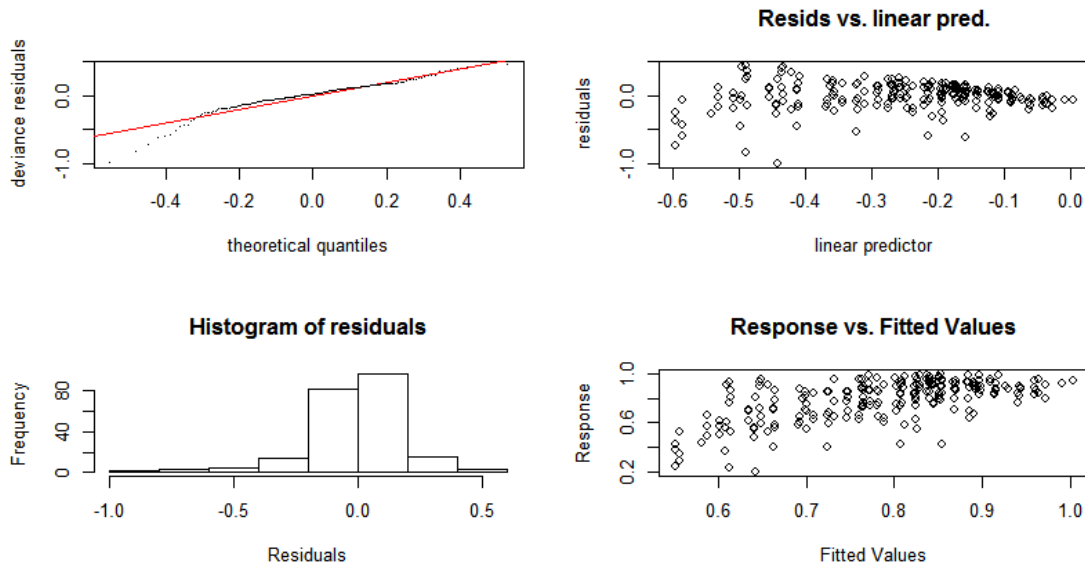


**Fig. AH 1** – GAM fitness check for modelled *Angular dispersion* for rejected attempts (Experiment 2 - model no. 8). Model terms =  $\text{gam}(r \sim s(\text{Bin}, \text{bs}="ps", k=18) + \text{DN} + \text{Direction} + \text{Phase}, \text{family} = \text{Gamma}(\text{link}=\text{log}, \text{method}="REML"))$ .

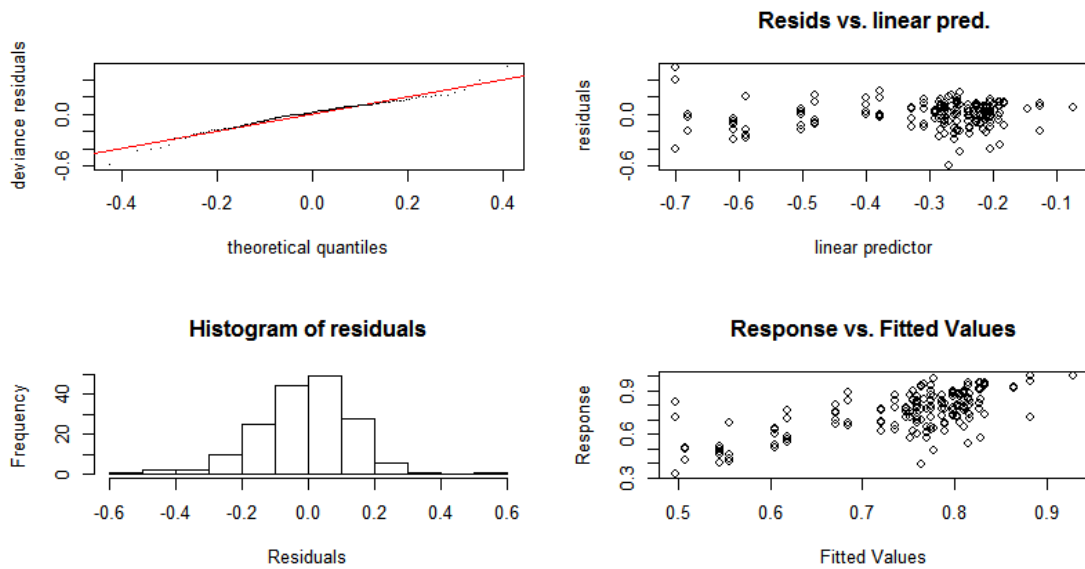


**Fig AH 2** – GAM fitness check for modelled *Angular dispersion* for rejected attempts (Experiment 3 – Model no. 8). Model terms =  $\text{gam}(r \sim s(\text{Bin}, \text{bs}="ps", k=10) + \text{Direction} + \text{Phase} + \text{Treatment}, \text{family} = \text{Gamma}(\text{link}=\text{log}, \text{method}="REML"))$ .

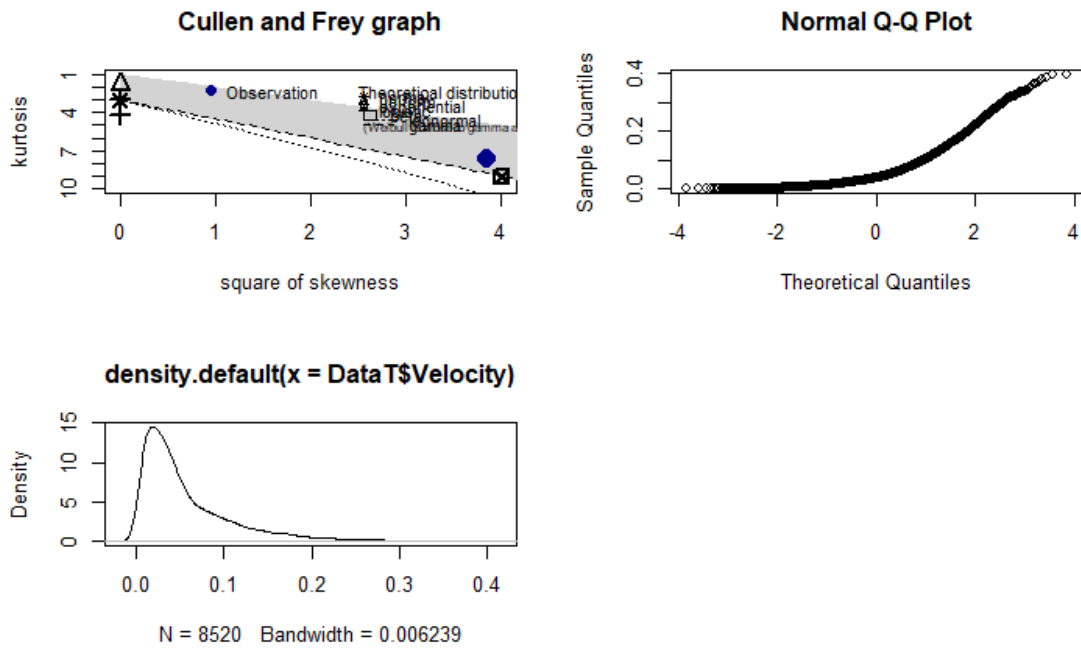


**Fig. AH 3** - Cullen and Frey graph, Q-Q, and density plot for *Swimming speed* for fish swimming towards the bubble curtain (Experiment 2)

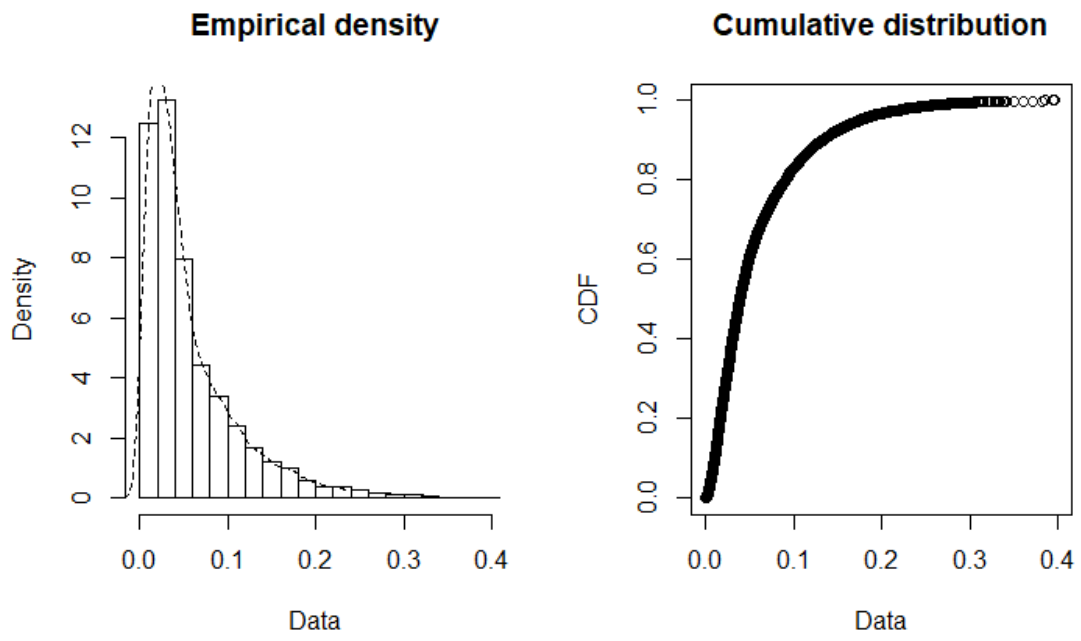


**Fig. AH 4** – Empirical density and cumulative distribution for *Swimming speed* for fish swimming towards the bubble curtain (Experiment 2).



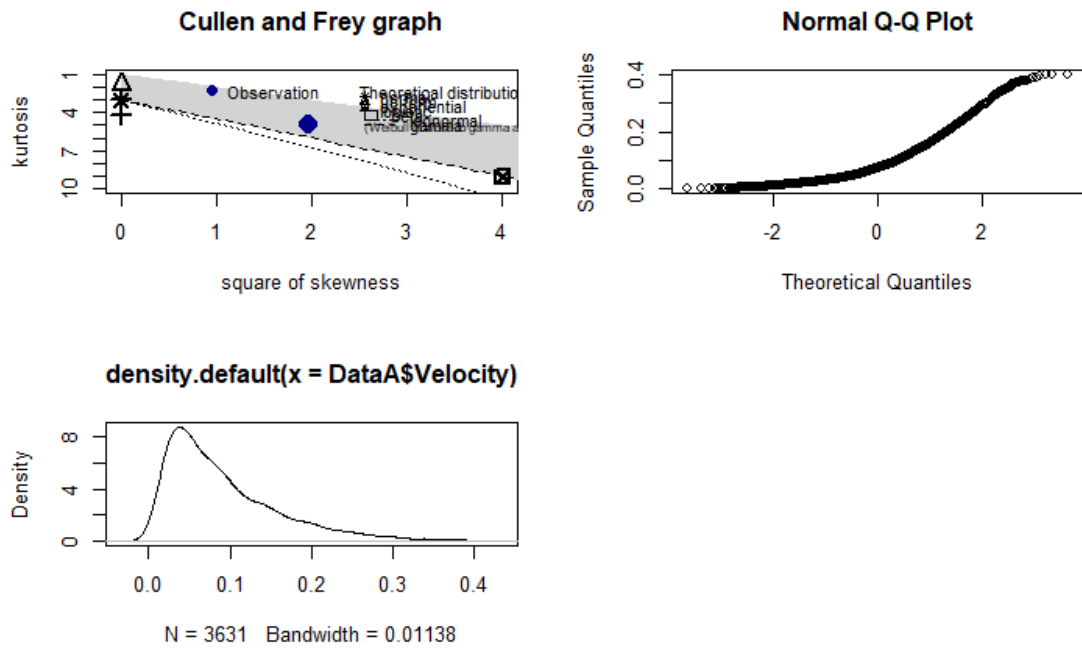


**Fig. AH 5** - Cullen and Frey graph, Q-Q, and density plot for *Swimming speed* for fish swimming away from the bubble curtain (Experiment 2)

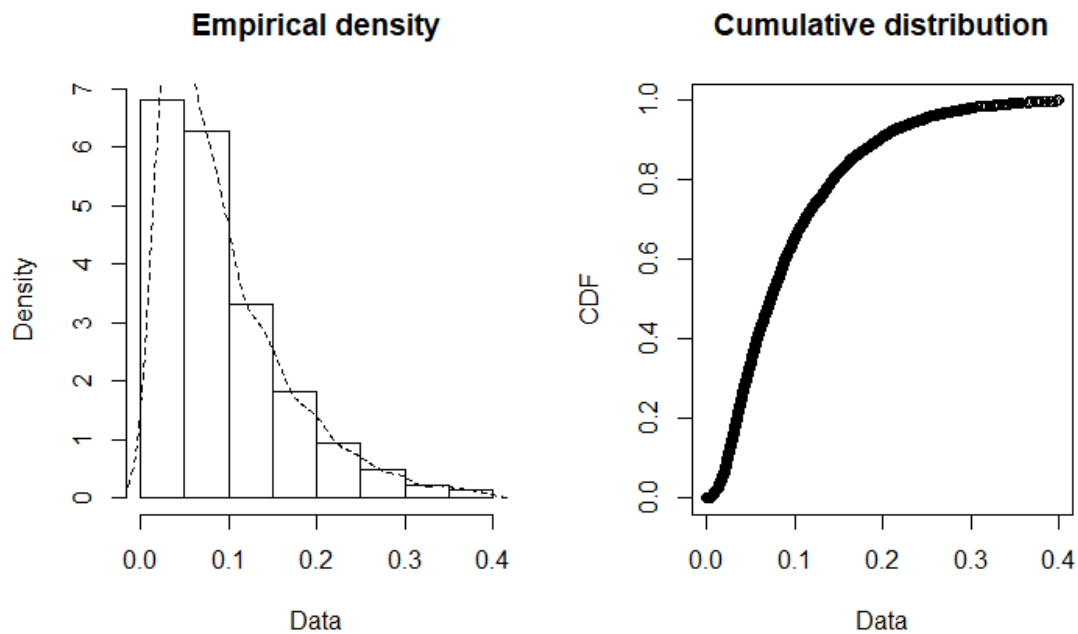


**Fig. AH 6** – Empirical density and cumulative distribution for *Swimming speed* for fish swimming towards the bubble curtain (Experiment 2).

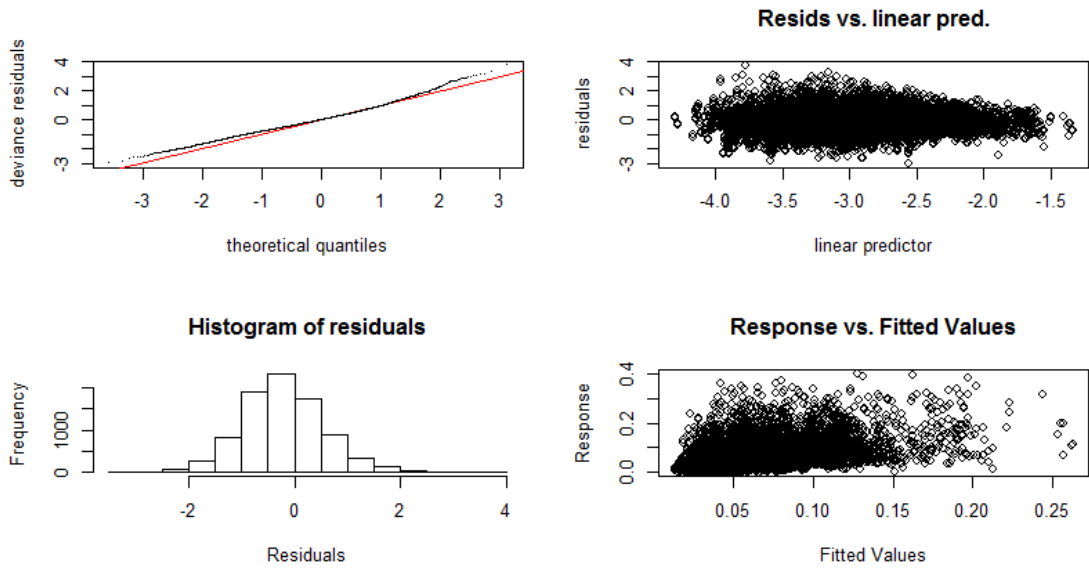


**Fig. AH 7** – GAM fitness check for saturated model of *Swimming velocity* for *Pass* data for fish swimming towards the bubble curtain (Experiment 2 – Model no. 7). Model terms =  $\text{gam}(\text{Velocity} \sim \text{s}(y, \text{bs}=\text{"ps"}, \text{k}=8) + \text{Phase} + \text{Treatment} + \text{DN}, \text{family} = \text{Gamma}(\text{link}=\text{log}), \text{method}=\text{"REML"})$ .

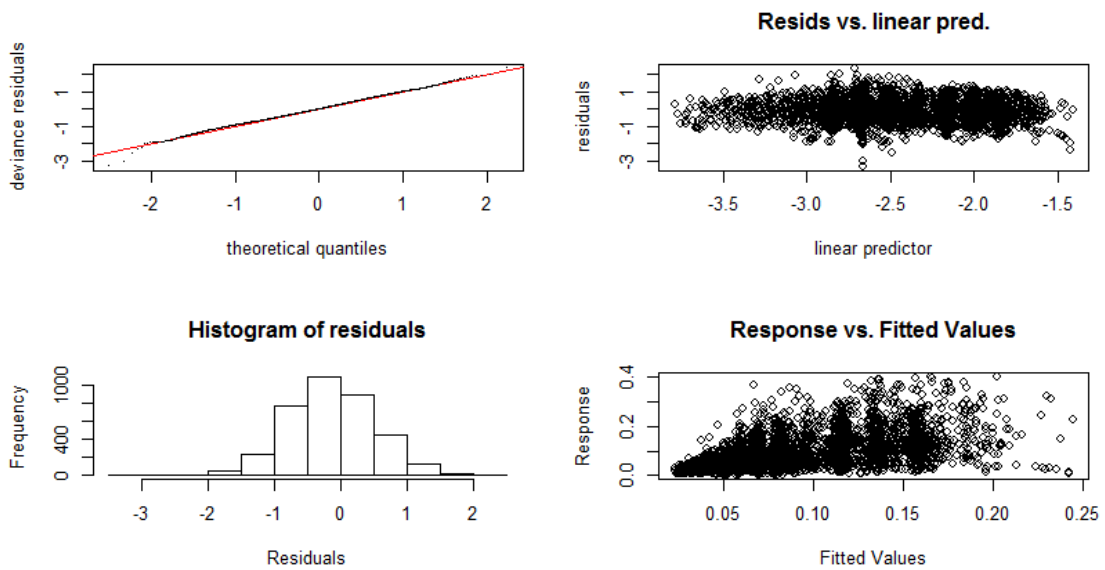


**Fig. AH 8** – GAM fitness check for saturated model of *Swimming velocity* for *Pass* data for fish swimming away from the bubble curtain (Experiment 2 – Model no. 7). Model terms =  $\text{gam}(\text{Velocity} \sim \text{s}(y, \text{bs}=\text{"ps"}, \text{k}=8) + \text{Phase} + \text{Treatment} + \text{DN}, \text{family} = \text{Gamma}(\text{link}=\text{log}), \text{method}=\text{"REML"})$ .

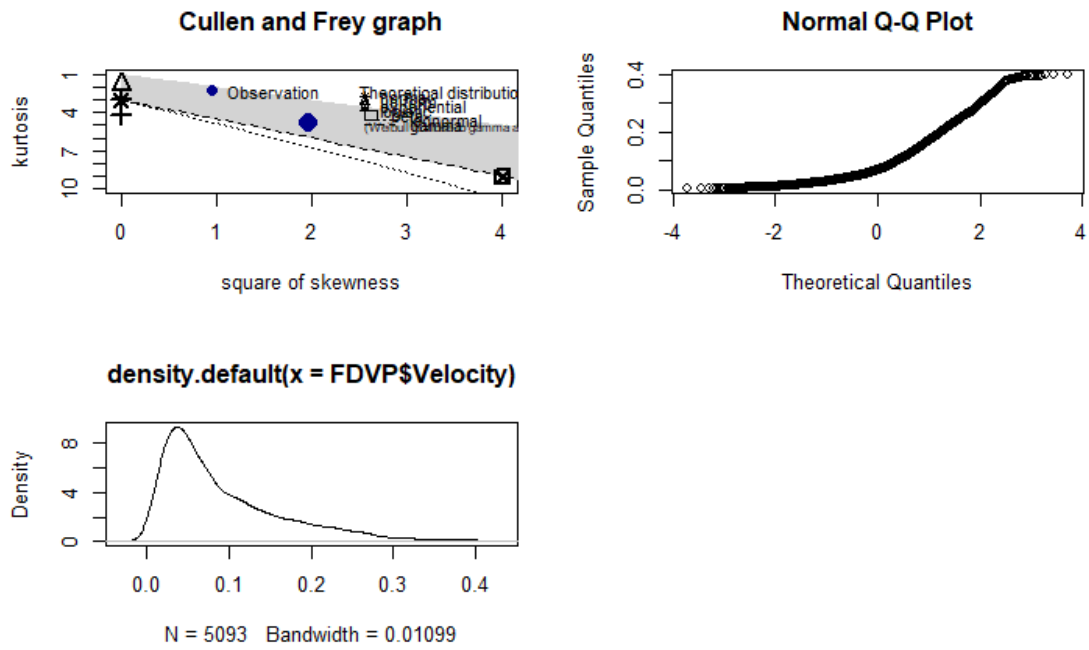


**Fig. AH 9** - Cullen and Frey graph, Q-Q, and density plot for *Swimming speed* for pass data (Experiment 3)

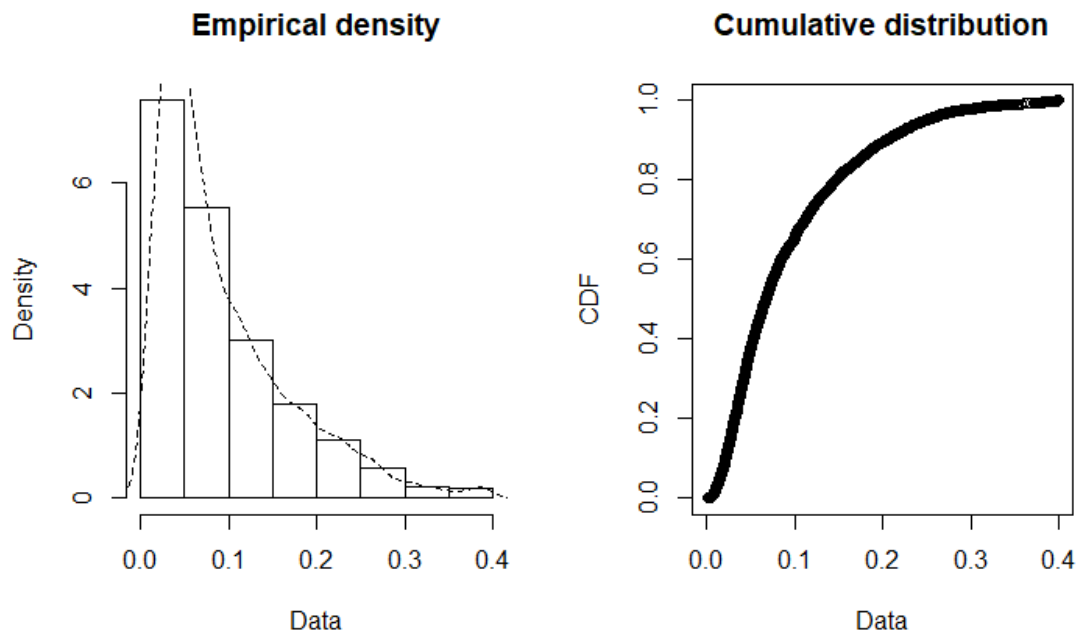


**Fig. AH 10** – Empirical density and cumulative distribution for *Swimming speed* for pass data (Experiment 3)

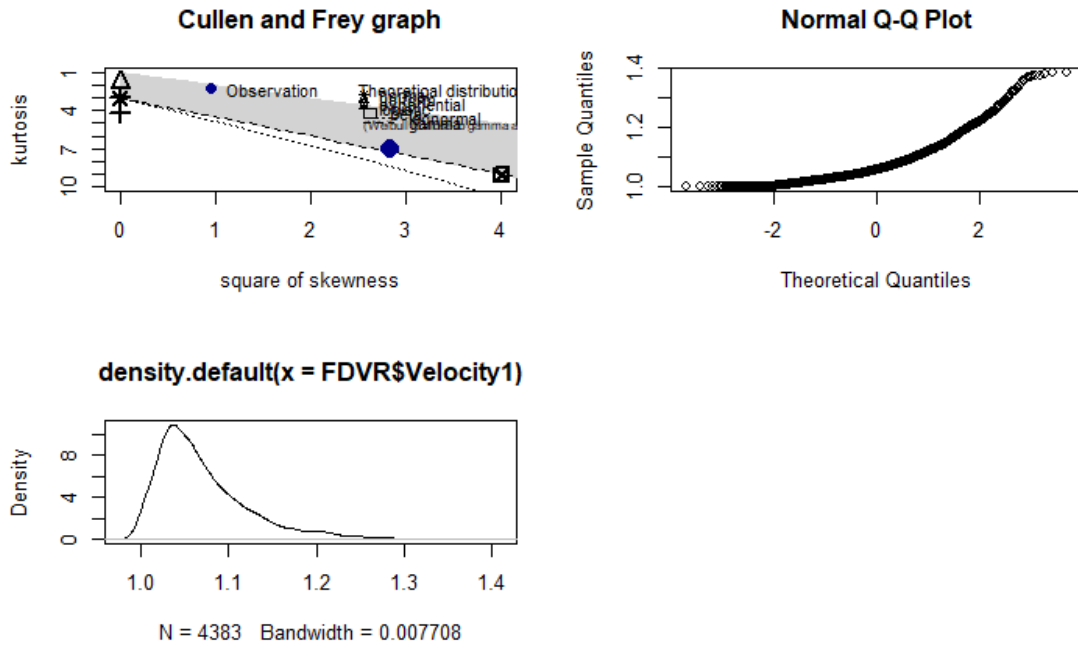


**Fig. AH 11** - Cullen and Frey graph, Q-Q, and density plot for *Swimming speed* for rejection data (Experiment 3)

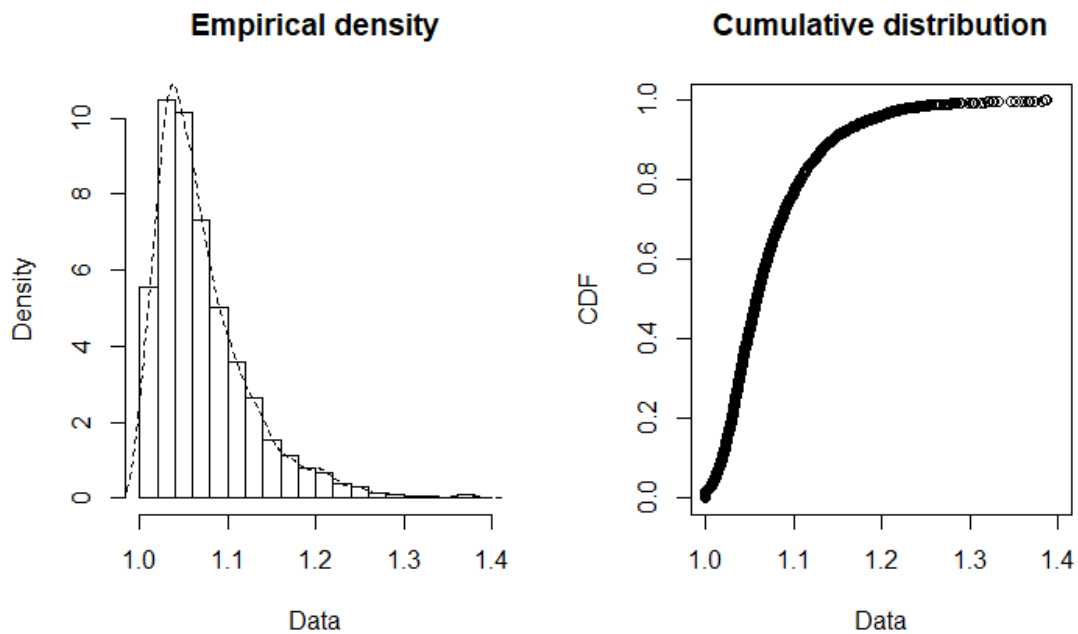


**Fig. AH 10** – Empirical density and cumulative distribution for *Swimming speed* for rejection data (Experiment 3)

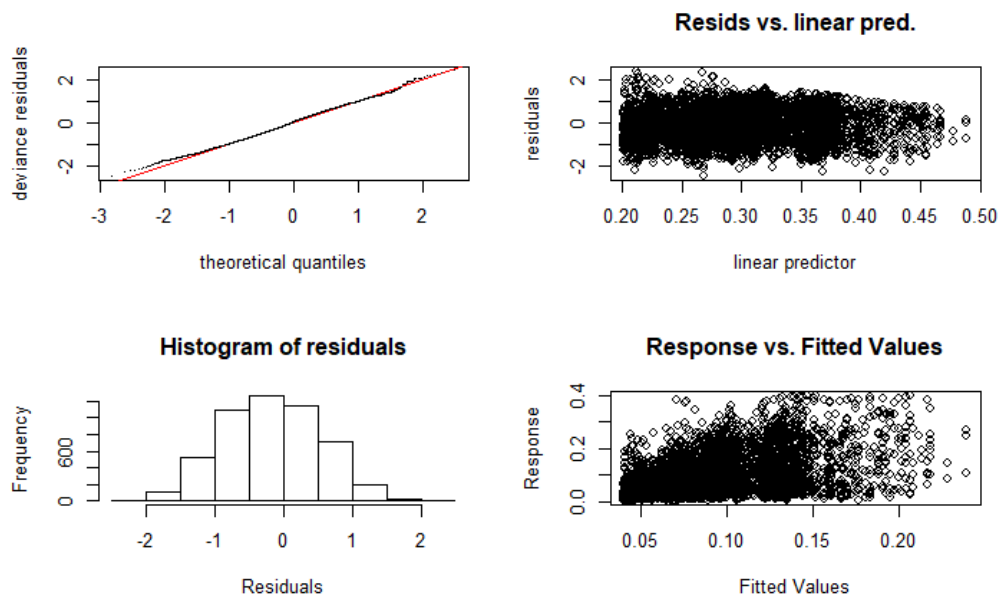


**Fig. AH 11** – GAM fitness check for minimum adequate model of *Swimming velocity* for *Pass* data (Experiment 3 – Model no. 13). Model terms =  $\text{gam}(\text{Velocity} \sim \text{Direction} + \text{Treatment} + \text{s}(\text{AbsY}, \text{bs}=\text{"ps"}, \text{k}=25), \text{family}=\text{Gamma}(\text{link}=\text{power}(0.5)), \text{method}=\text{"REML"})$ .

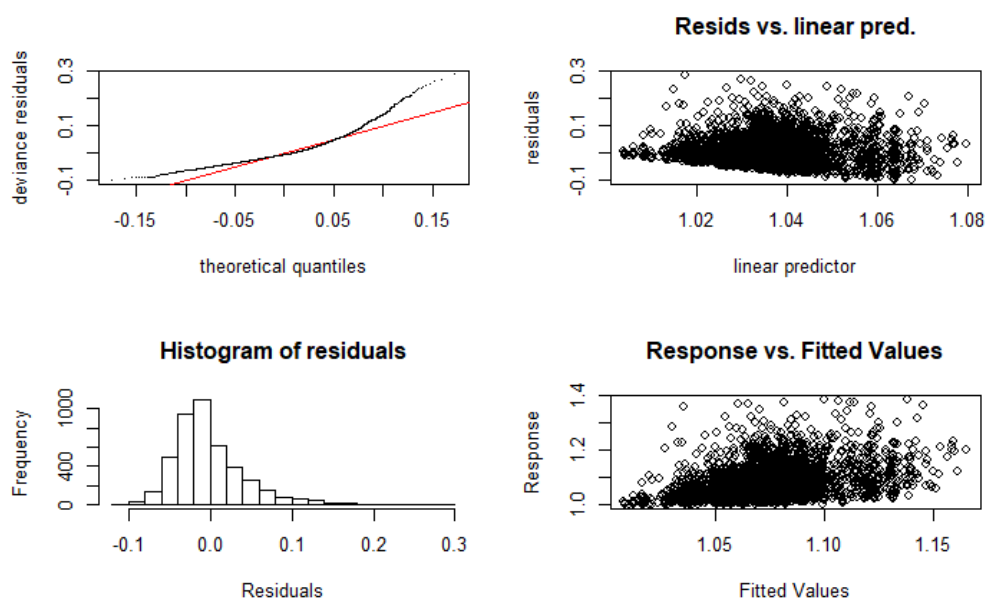


**Fig. AH 12** – GAM fitness check for modelled *Swimming velocity* for *Rejection* data (Experiment 3 – Model no. 6). Model terms =  $\text{Velocity} \sim \text{Treatment} + \text{HydroTreatment} + \text{s}(\text{AbsY}, \text{bs}=\text{"ps"}, \text{k}=25) + \text{s}(\text{SDFlow}, \text{bs}=\text{"ps"}, \text{k}=20) + \text{s}(\text{SPL}, \text{bs}=\text{"ps"}, \text{k}=20) + \text{s}(\text{PD}, \text{bs}=\text{"ps"}, \text{k}=20), \text{family}=\text{Gamma}(\text{power}(0.5)), \text{method}=\text{"REML"})$ .



# APPENDIX I:

## Chapter 5 – GAM Models and Checks

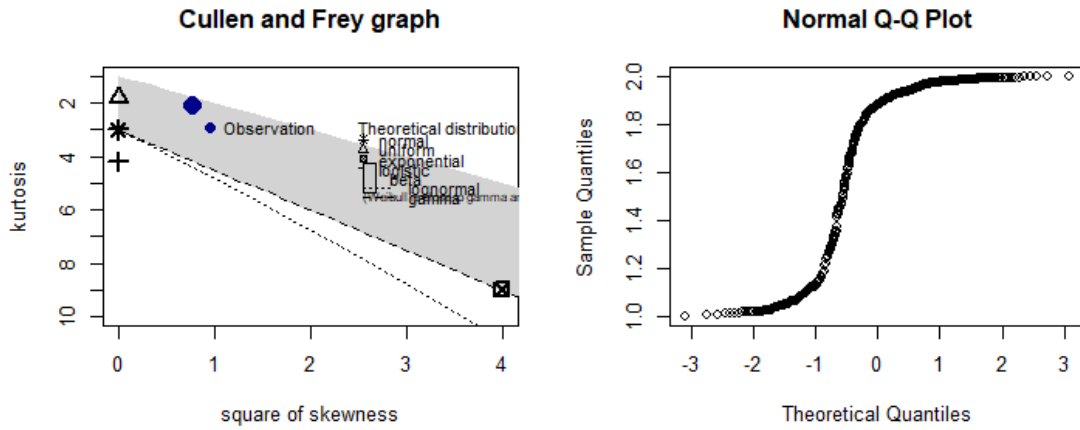


Fig. AI 1 – Cullen and Frey graph and Q-Q- plot for *Straightness index* data

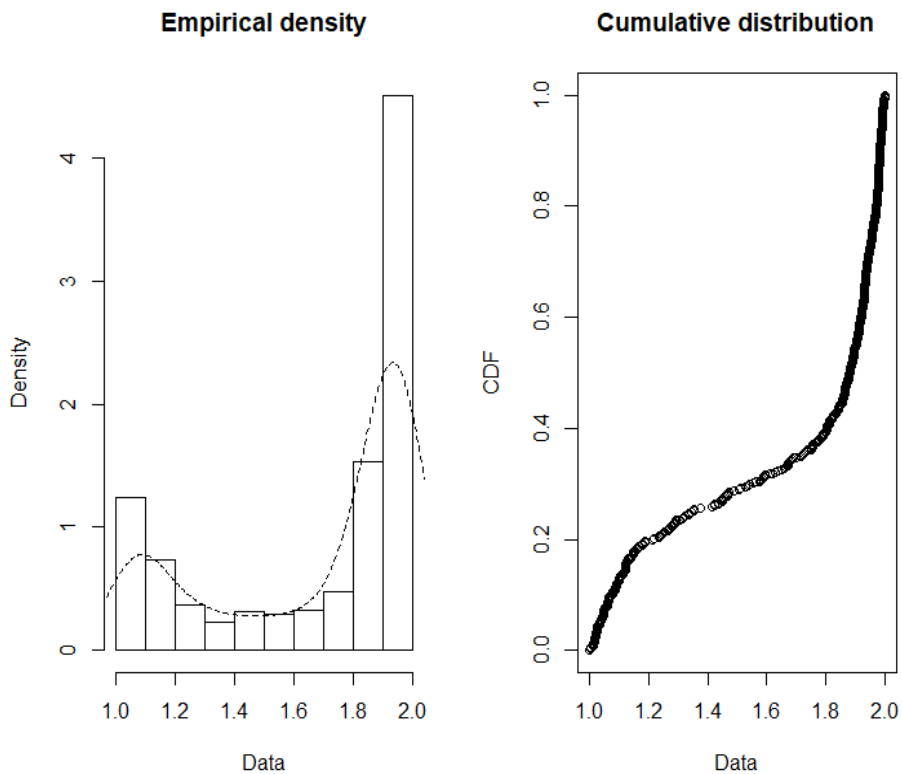
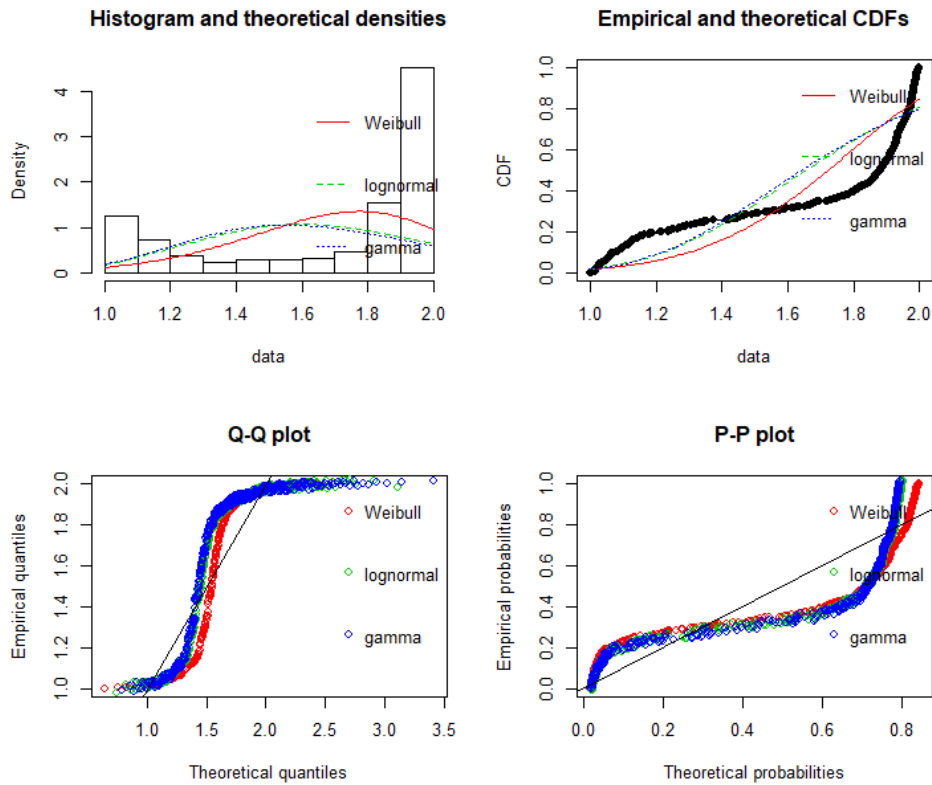
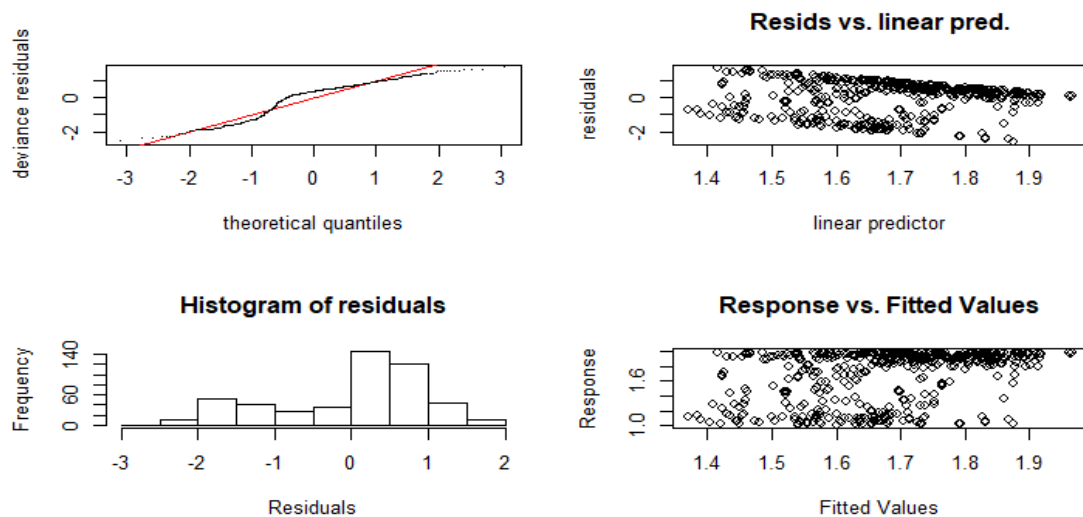


Fig. AI 2 – Empirical density and cumulative distribution plots for *Straightness index* data



**Fig. AI 3** – Distribution fitting plots for *Straightness index* data



**Fig. AI 4** – GAM fitness check for modelled *Straightness index* data (Model no. 3). Model terms =  $\text{gam}(\text{Str} \sim \text{s}(Y0.1, \text{bs}=\text{"ps"}, \text{k}=24) + \text{Treatment} * \text{Exp. Phase}, \text{family}=\text{scat}(\text{theta} = \text{NULL}, \text{link} = \text{"identity"}, \text{min.df}=3), \text{method}=\text{"REML"})$ .



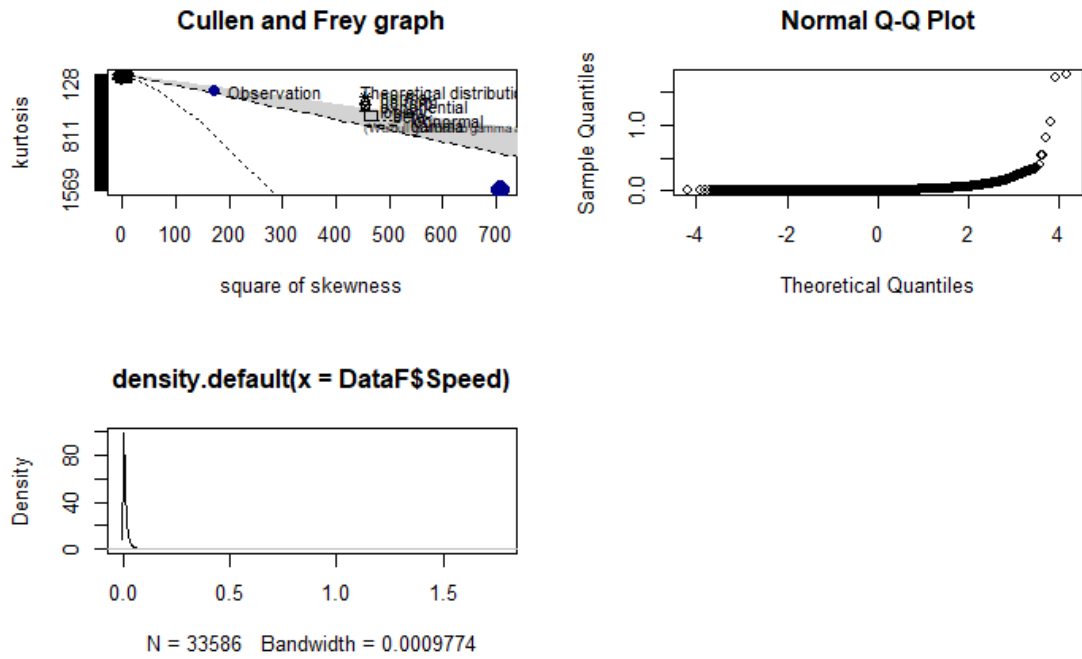


**Fig. AI 5** - Cullen and Frey graph, density, and Q-Q plots for *Swimming speed* data (no filter).

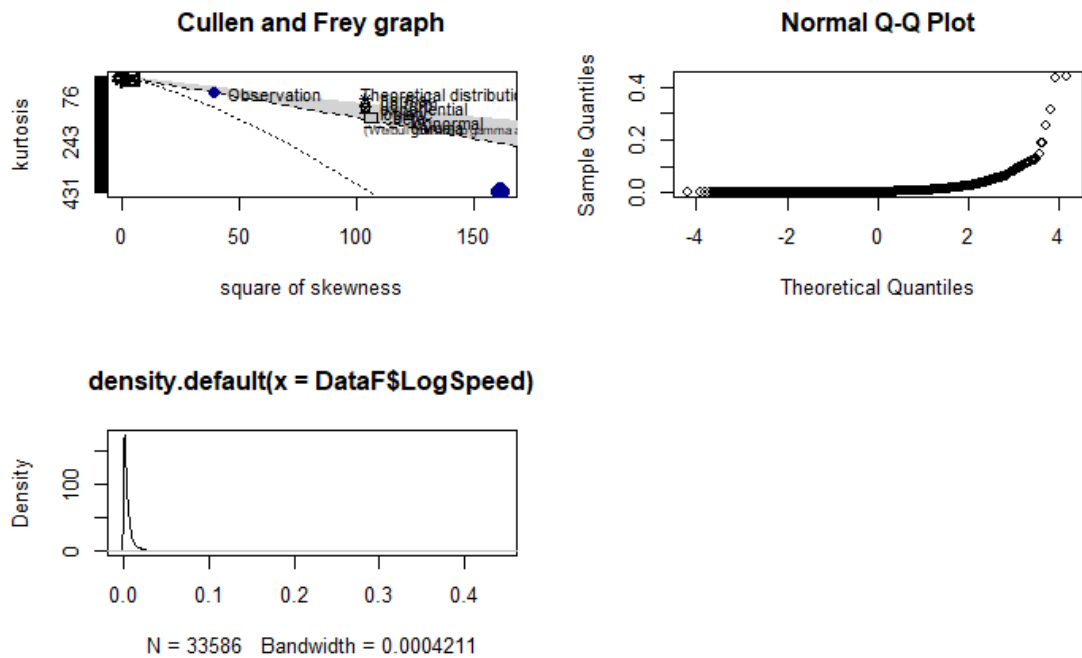


**Fig. AI 5** - Cullen and Frey graph, density and Q-Q plots for log *Swimming speed* data (no filter).

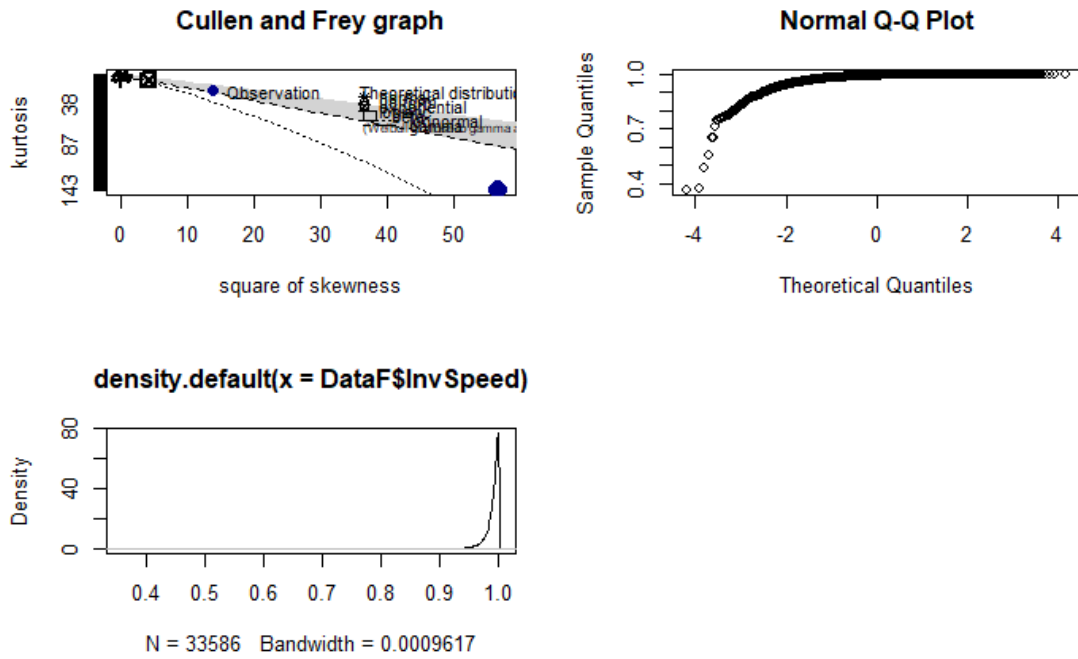


**Fig. AI 7** – Cullen and Frey graph, density, and Q-Q- plots for  $1/\text{Swimming speed}$  (no filter)

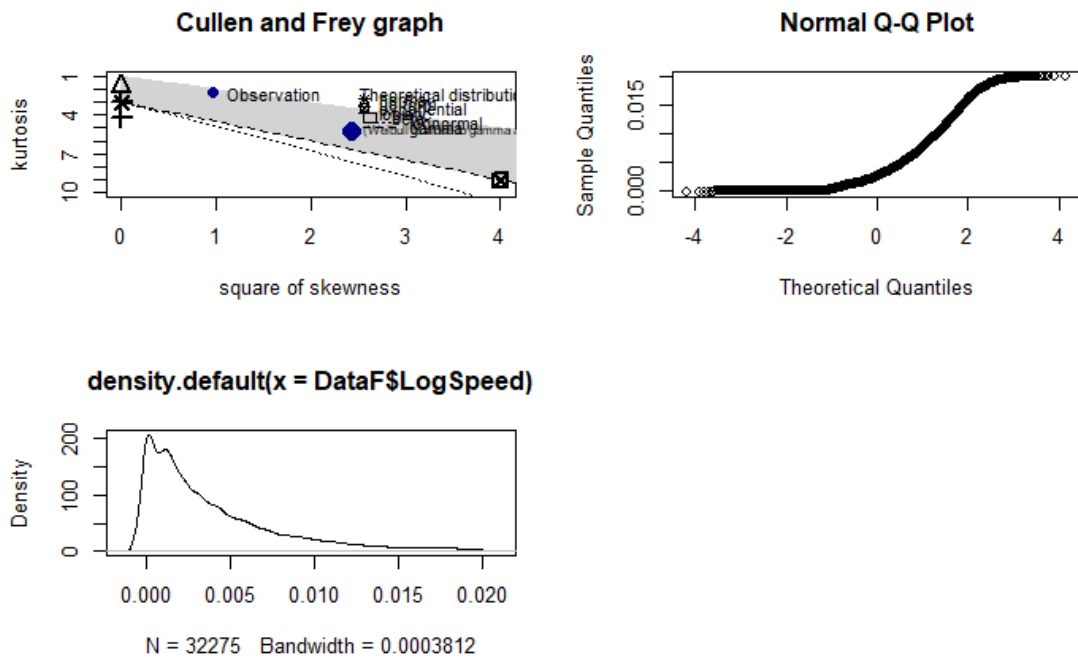


**Fig. AI 8** Cullen and Frey graph, density, and Q-Q- plots for  $\log \text{Swimming speed}$  data (filtered),

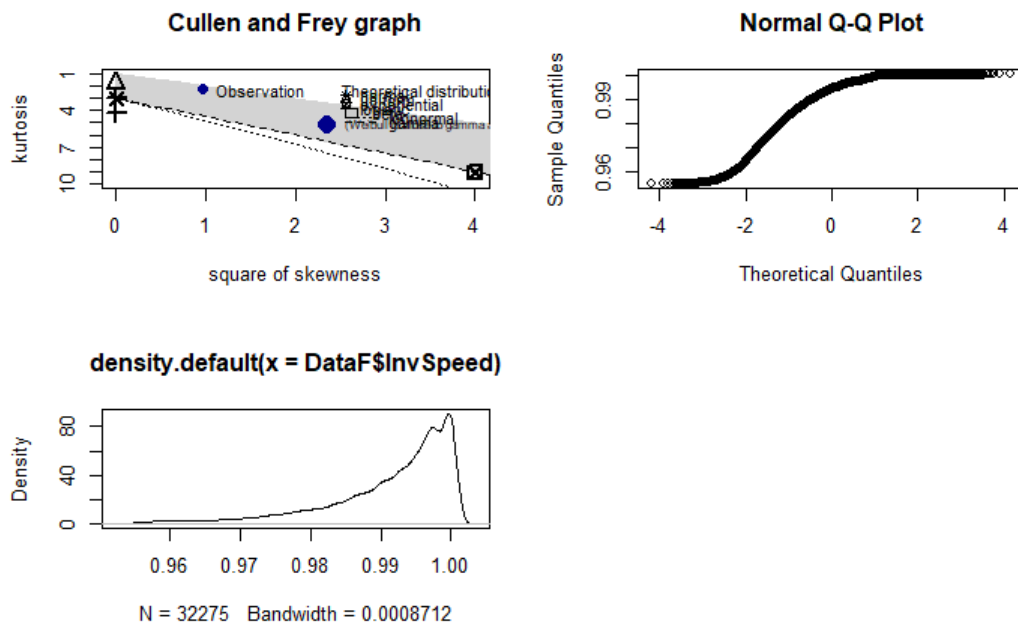


**Fig. AI 9** – Cullen and Frey graph, density, and Q-Q- plots for *1 / Swimming speed* data (filtered).

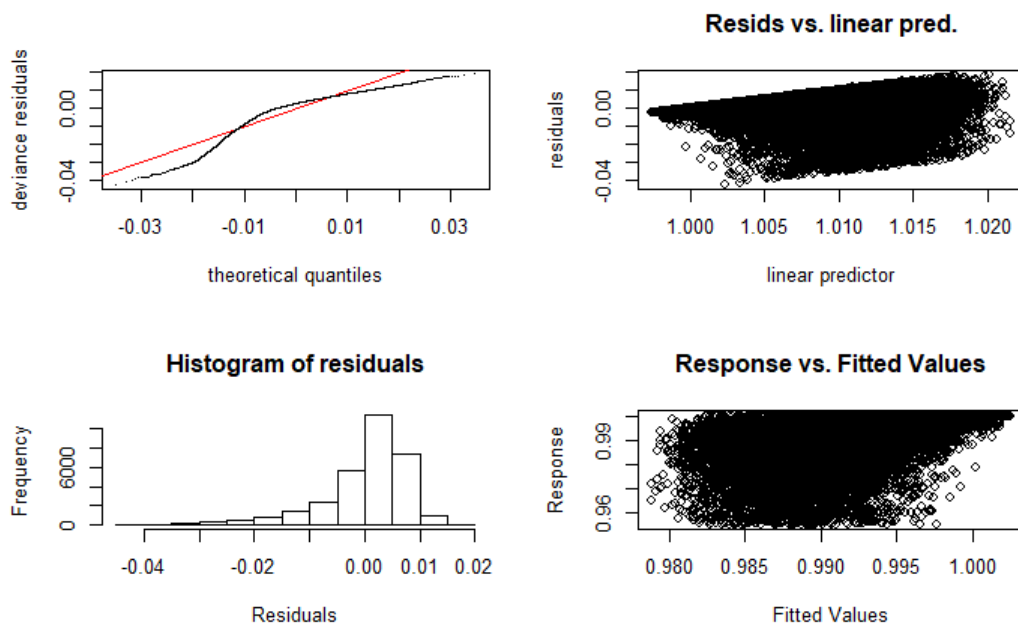


**Fig. AI 10** – GAM fitness check for modelled *1 / Swimming Speed* data. (Model no. 4). Model terms =  $\text{gam}(\text{InvSpeed} \sim s(\text{DistA}, k=50) + s(\text{DistB}, k=50) + s(\text{SPL}, k=20) + s(\text{PD}, k=20) + s(\text{SPLGrad}, k=20) + s(\text{X}, k=30) + s(\text{Y}, k=30) + s(\text{PDGrad}, k=20) + s(\text{Approach}, k=10) + s(\text{Time}, k=60) + s(\text{MeanLight}, k=20) + \text{Exp. Phase} * \text{Treatment}, \text{family}=\text{Gamma}(\text{link}=\text{"inverse"}), \text{method}=\text{"REML"})$ .

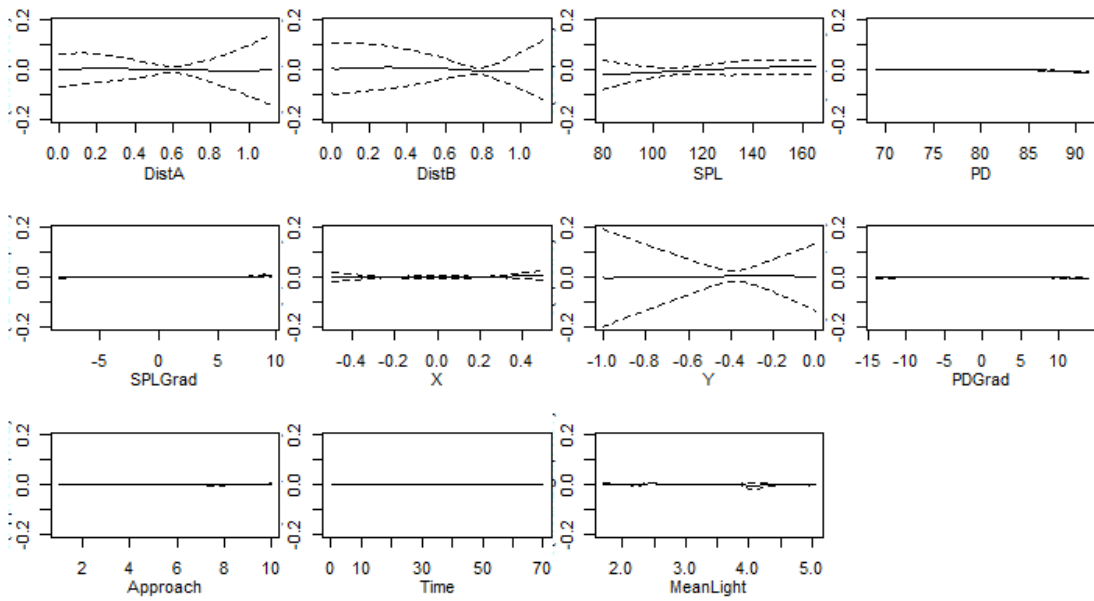


**Fig. AI 11** – GAM plot of  $1/\text{Swimming speed}$  against all candidate variables in Model no 4.

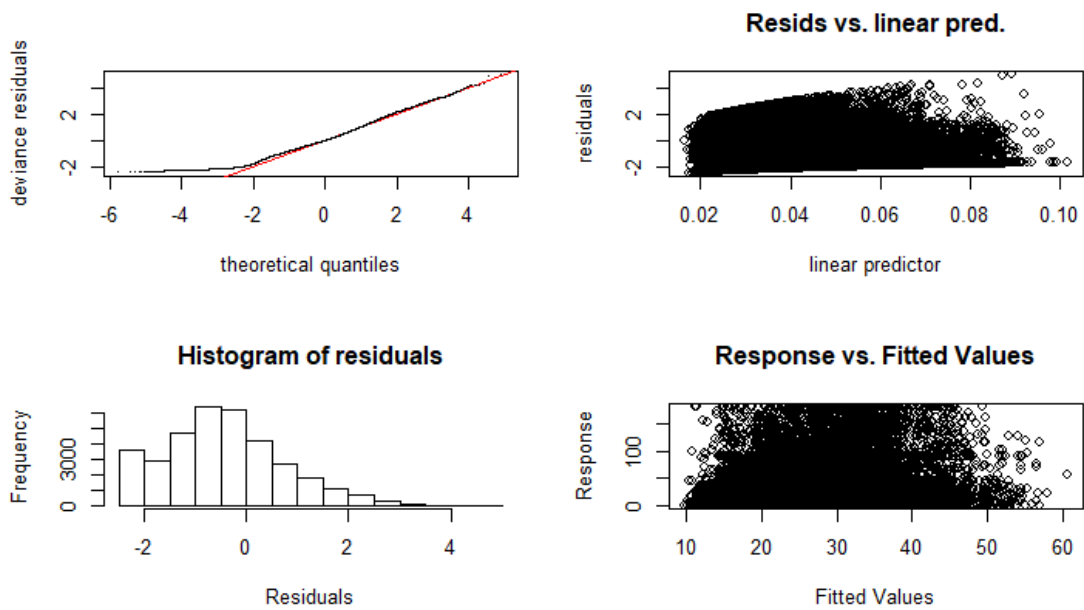


**Fig. AI 12** – GAM fitness check for modelled *Turning Angles* data [Not used for thesis].

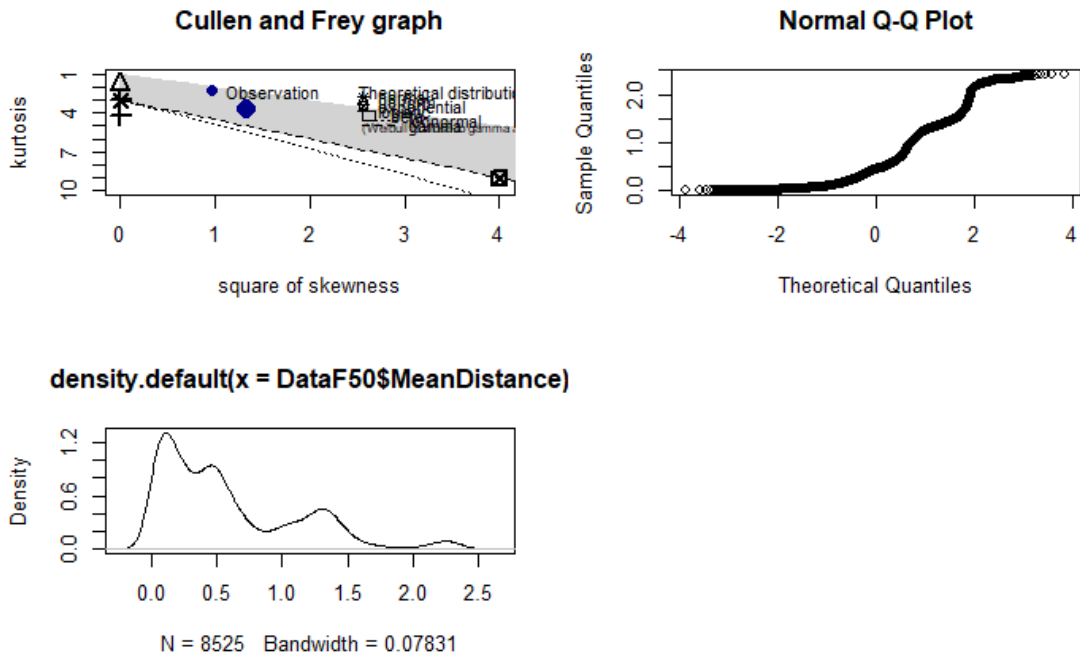


**Fig. AI 13** – Cullen and Frey graph, density, and Q-Q plots for *group distance data*.

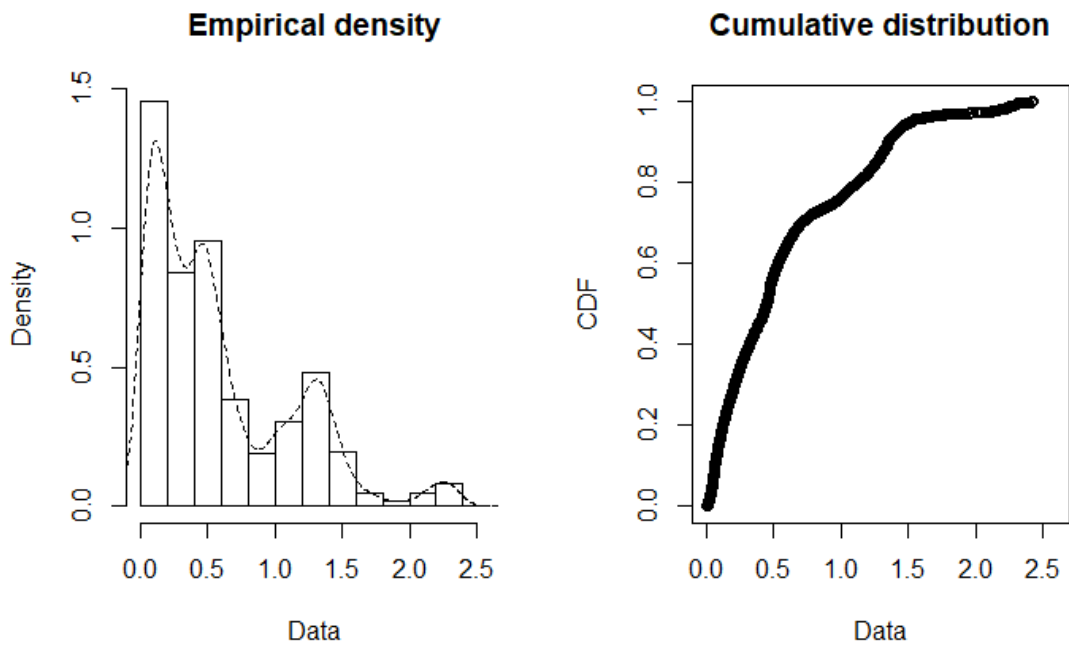


**Fig. AI 14** – Density and distribution plots for *Group Distance data*.

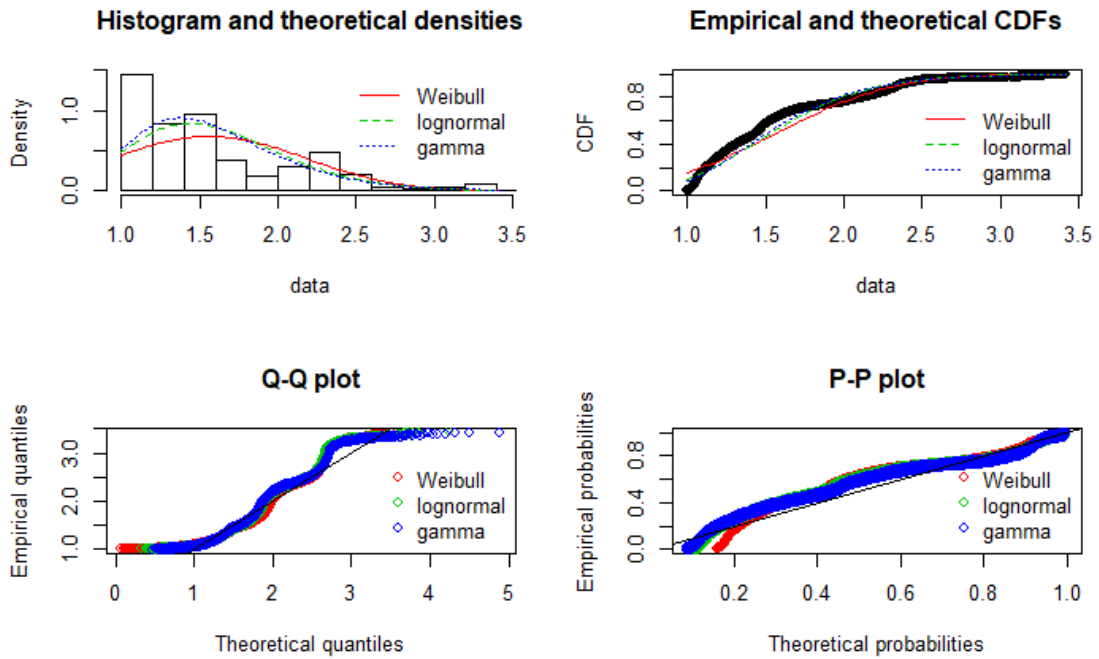


**Fig. AI 15** – Distribution fitting plots for *Group Distance* data

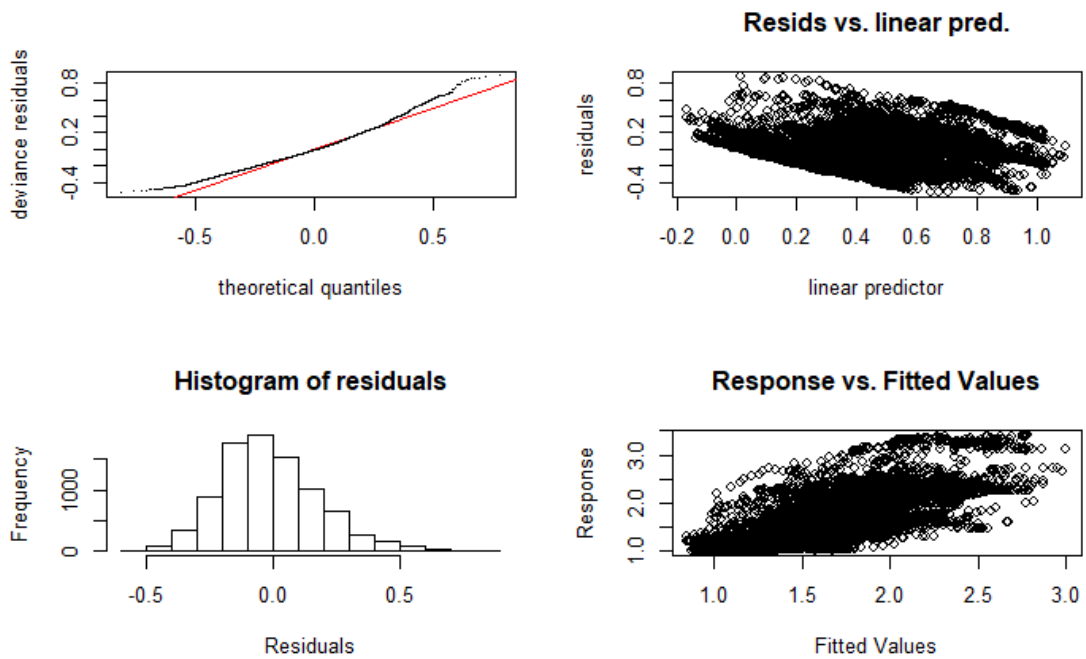


**Fig. AI 16** – GAM fitness check for modelled *Group Distance* data (Model no. 1). Model terms =  $\text{gam}(\text{Distance1} \sim \text{s}(\text{Time}, \text{bs}=\text{"ps"}, \text{k}=120) + \text{s}(\text{CentroidX}, \text{bs}=\text{"ps"}, \text{k}=100) + \text{s}(\text{CentroidY}, \text{bs}=\text{"ps"}, \text{k}=100) + \text{Treatment} * \text{Exp. Phase}, \text{family}=\text{Gamma}(\text{link}=\text{log}), \text{method}=\text{"REML"})$ .

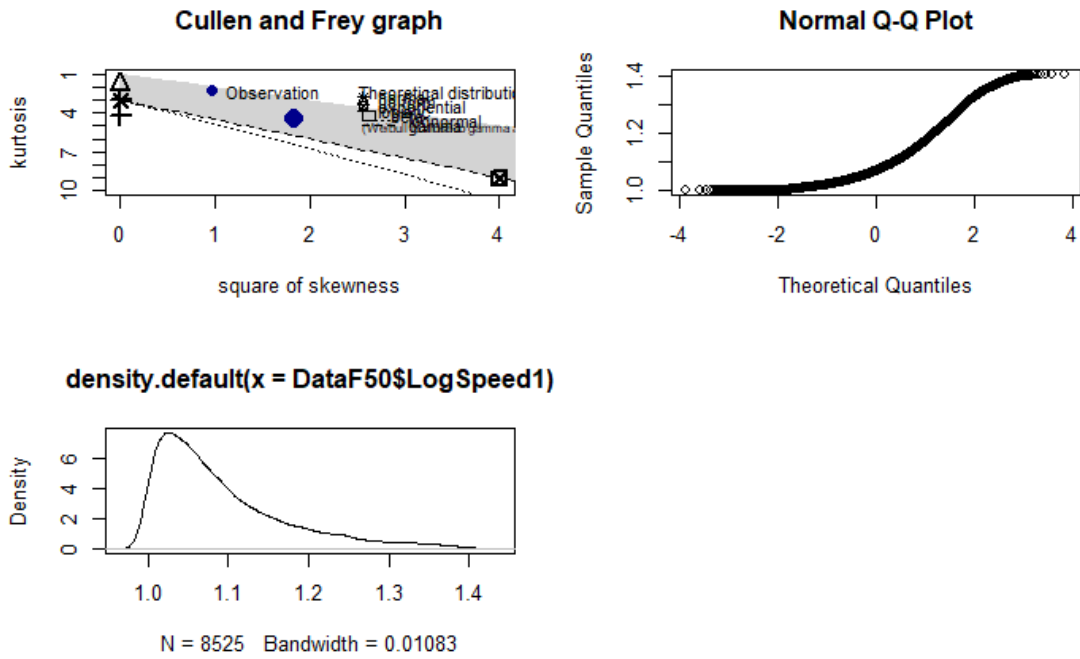


**Fig. AI 17** – Cullen and Frey graph, and Q-Q- plot for *Group Swimming Speed data*.

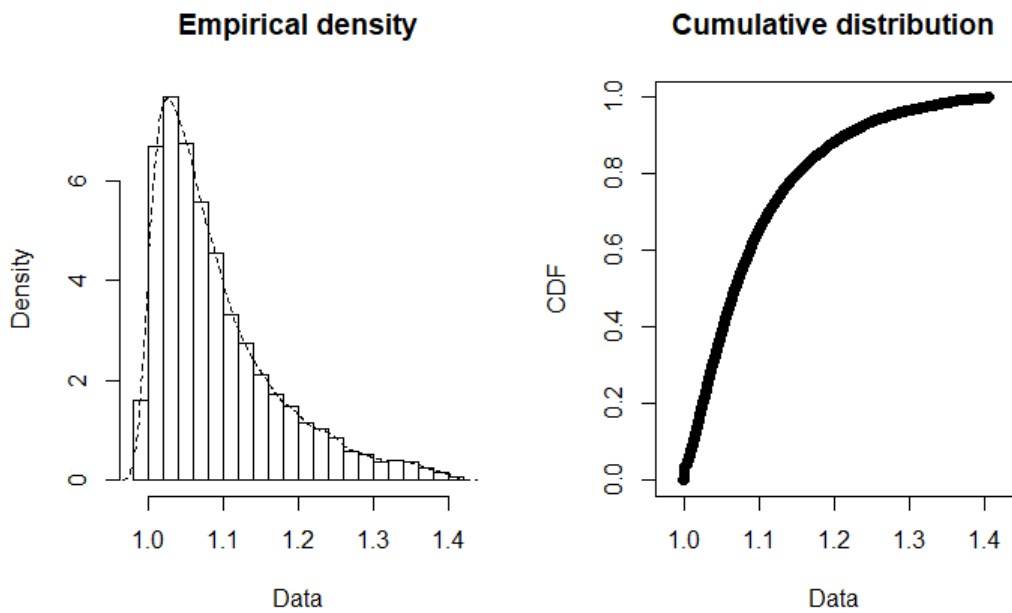


**Fig. AI 18** – Density and distribution plot for *Group Swimming Speed data*.

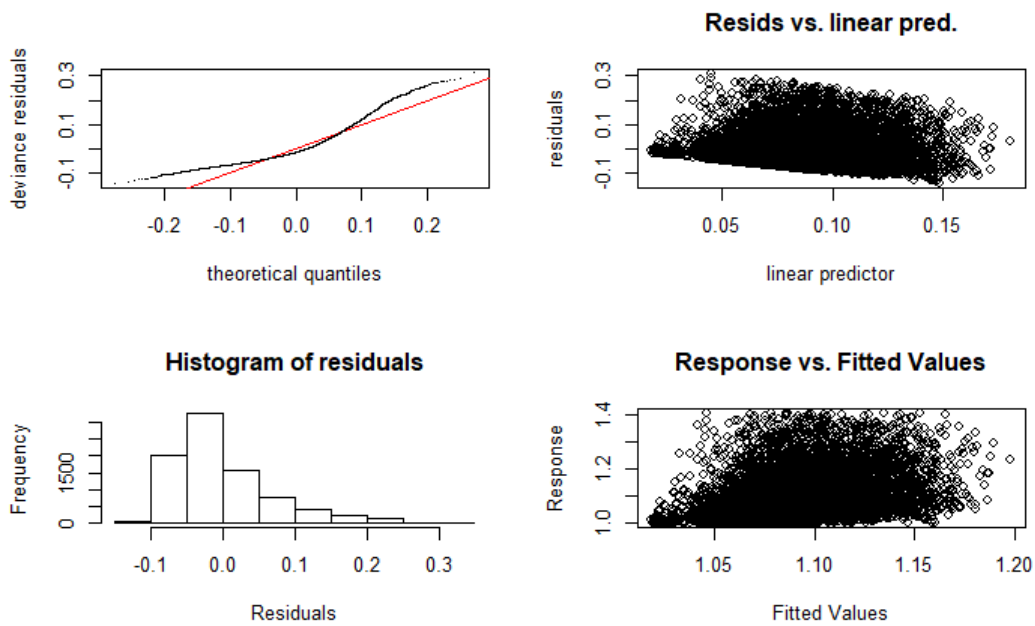


**Fig. AI 19** –GAM fitness check for modelled *Group Swimming Speed* data (Model no. 2). Model terms = gam(LogSpeed1 ~ s(Time, bs="ps", k=20) + s(CentroidX, bs="ps", k=20) + s(CentroidY, bs="ps", k=20) + Treatment + Phase, family=Gamma(link=log), method="REML").

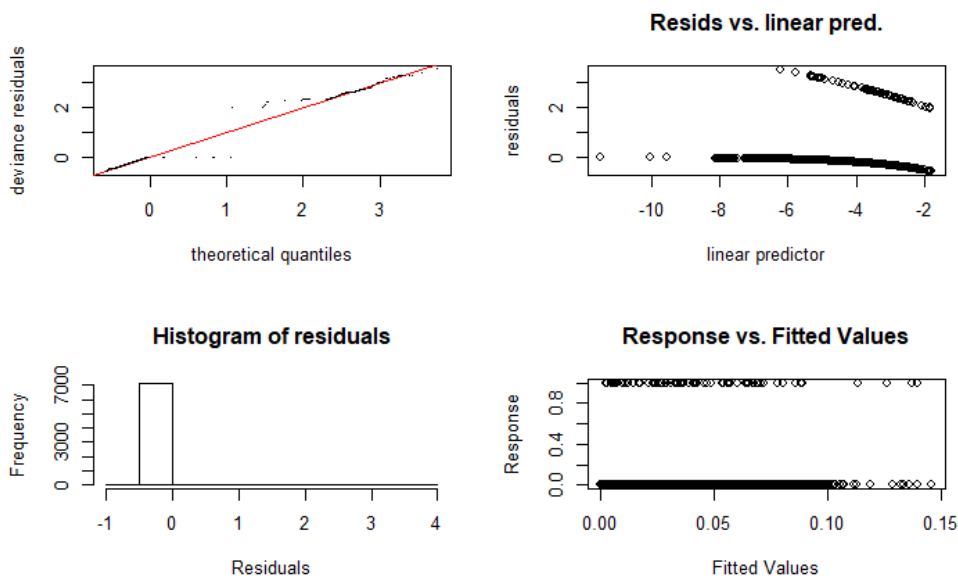


**Fig. AI 20** – GAM Check for Saturated Model for binary rejection data (Dataset (C) Model no. 1.2). Model terms = gam(Rej ~ s(MeanLight, k=12) + s(SPL, k=10) + s(PD, k=10) + s(SPLGrad, k=20) + s(PDGrad, k=20) + s(DistA, k=20) + s(Approach, k=10) +Treatment + Exp. Phase, family = binomial, method = "REML").



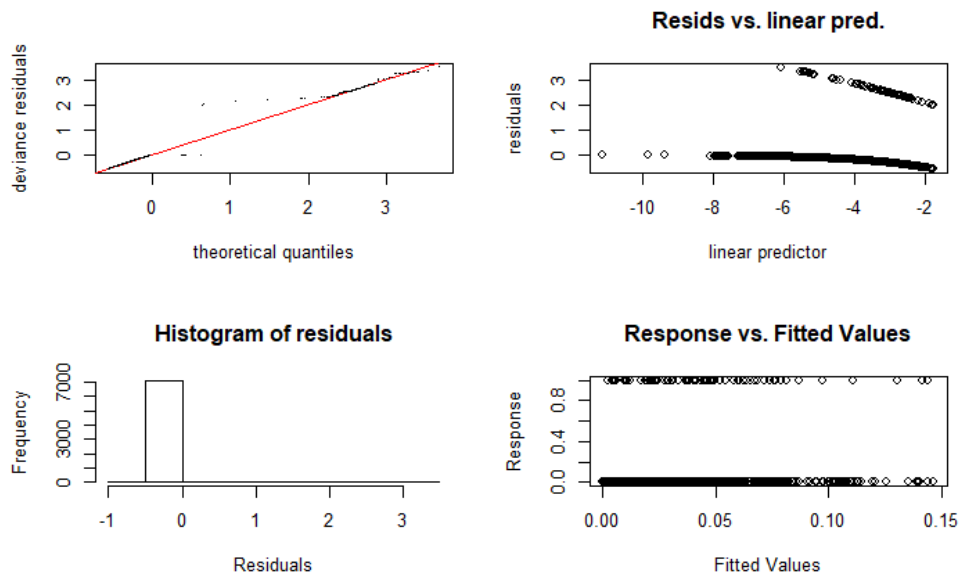


**Fig. AI 21** - M1.5 Minimum adequate model for binary rejection data (Dataset (C) Model no. 1.2). Model terms=  $\text{gam}(\text{Rej} \sim \text{s}(\text{MeanLight}, k=12) + \text{s}(\text{SPL}, k=10) + \text{s}(\text{PDGrad}, k=20) + \text{s}(\text{DistA}, k=20) + \text{s}(\text{Approach}, k=10) + \text{Exp. Phase}, \text{family} = \text{binomial}, \text{method} = \text{"REML"})$ .

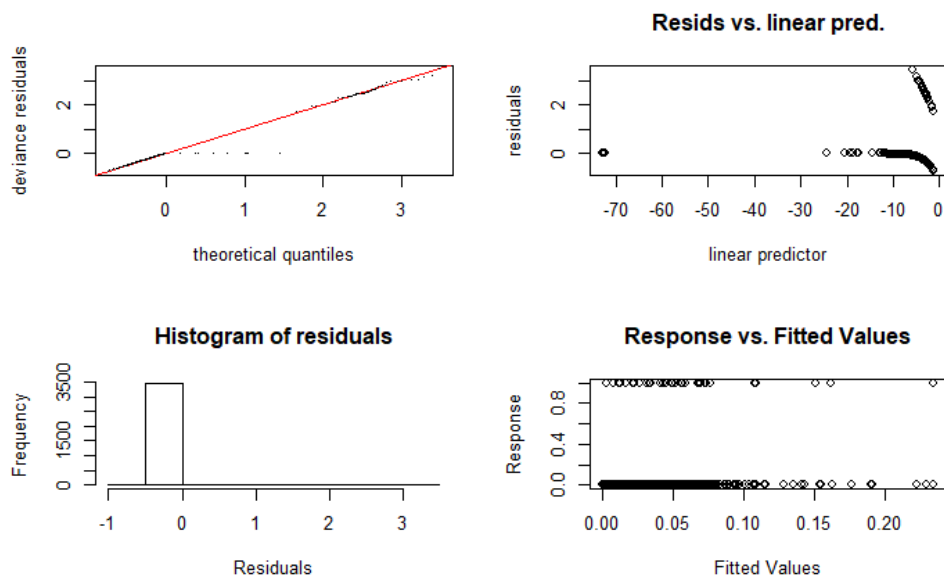


**Fig. AI 22** – Saturated model for binary rejection data (Dataset (D) Model no. 2.1). Model terms =  $\text{gam}(\text{Rej} \sim \text{s}(\text{MeanLight}, \text{bs}=\text{"ps"}, k=12) + \text{s}(\text{SPL}, \text{bs}=\text{"ps"}, k=10) + \text{s}(\text{PD}, \text{bs}=\text{"ps"}, k=10) + \text{s}(\text{SPLGrad}, \text{bs}=\text{"ps"}, k=20) + \text{s}(\text{PDGrad}, \text{bs}=\text{"ps"}, k=20) + \text{s}(\text{DistA}, \text{bs}=\text{"ps"}, k=20) + \text{Treatment*Exp. Phase}, \text{family} = \text{binomial}, \text{method} = \text{"REML"})$ .

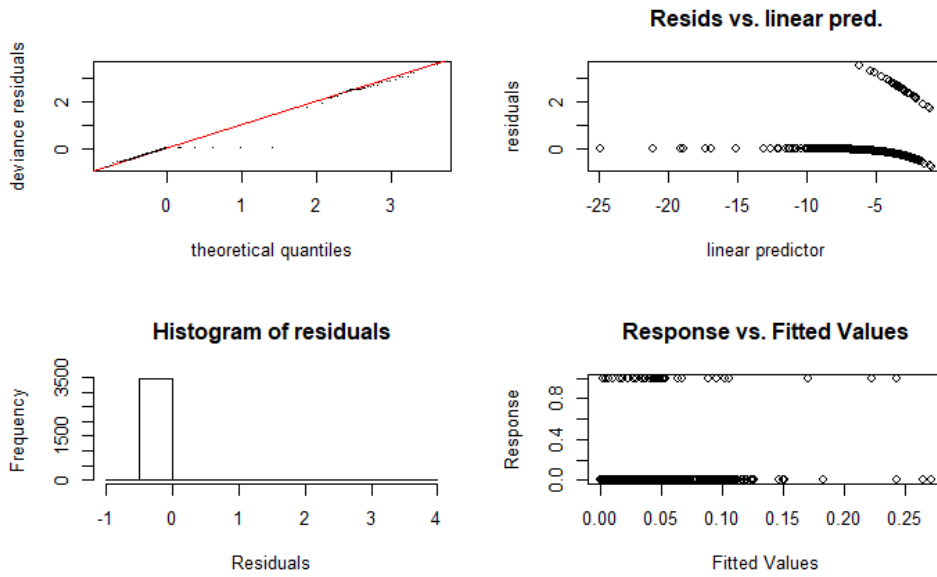


**Fig. AI 23** - Minimum adequate model for binary rejection data (Dataset (D) Model no. 2.3). Model terms =  $\text{gam}(\text{Rej} \sim \text{s}(\text{MeanLight}, \text{bs}="ps", \text{k}=12) + \text{s}(\text{SPL}, \text{bs}="ps", \text{k}=10) + \text{s}(\text{PD}, \text{bs}="ps", \text{k}=10) + \text{s}(\text{PDGrad}, \text{bs}="ps", \text{k}=20) + \text{s}(\text{DistA}, \text{bs}="ps", \text{k}=20) + \text{Treatment} + \text{Exp. Phase}, \text{family} = \text{binomial}, \text{method} = \text{"REML"})$ .

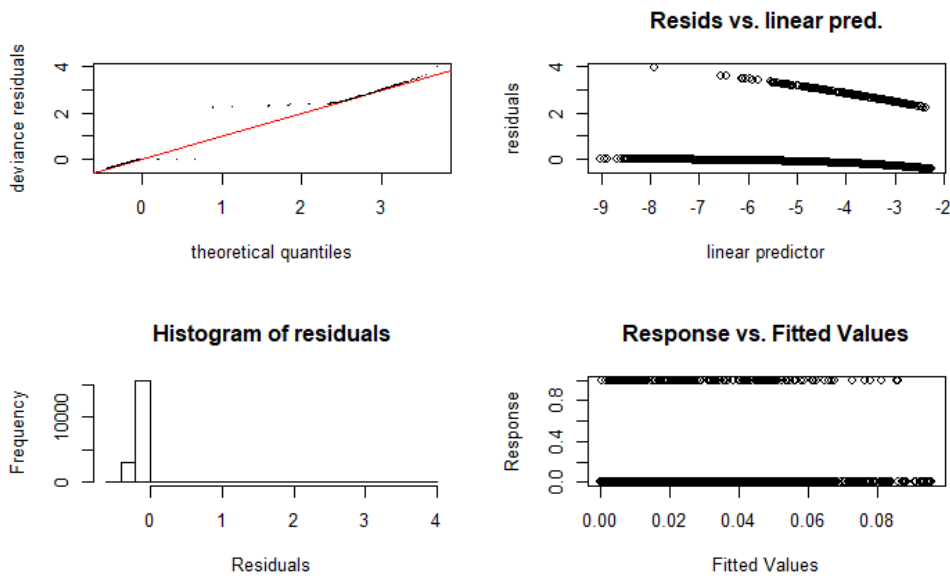


**Fig. AI 24** – Saturated and Minimum adequate model for binary rejection data (Dataset (A) Model no. 3.1). Model terms =  $\text{gam}(\text{Rej} \sim \text{s}(\text{MeanLight}, \text{bs}="ps", \text{k}=12) + \text{s}(\text{SPL}, \text{bs}="ps", \text{k}=10) + \text{s}(\text{PD}, \text{bs}="ps", \text{k}=10) + \text{s}(\text{SPLGrad}, \text{bs}="ps", \text{k}=20) + \text{s}(\text{PDGrad}, \text{bs}="ps", \text{k}=20) + \text{s}(\text{DistA}, \text{bs}="ps", \text{k}=20) + \text{s}(\text{DistB}, \text{bs}="ps", \text{k}=20) + \text{s}(\text{Approach}, \text{bs}="ps", \text{k}=10) + \text{Treatment} * \text{Exp. Phase}, \text{family} = \text{binomial}, \text{method} = \text{"REML"})$ .

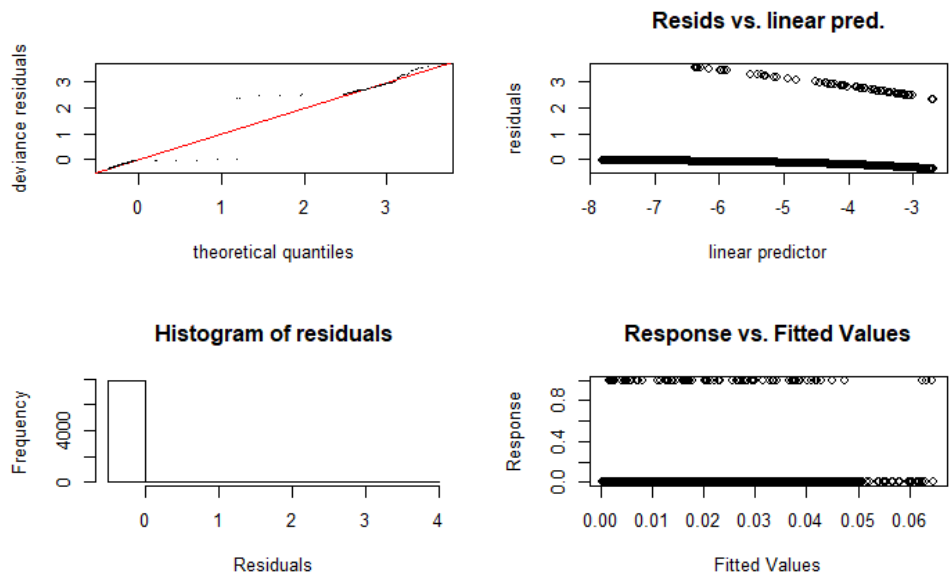


**Fig. AI 25** – Saturated model for binary rejection data (Dataset (B) Model no. 4.1). Model terms =  $\text{gam}(\text{Rej} \sim \text{s}(\text{MeanLight}, \text{bs}=\text{"ps"}, \text{k}=12) + \text{s}(\text{SPL}, \text{bs}=\text{"ps"}, \text{k}=10) + \text{s}(\text{PD}, \text{bs}=\text{"ps"}, \text{k}=10) + \text{s}(\text{SPLGrad}, \text{bs}=\text{"ps"}, \text{k}=20) + \text{s}(\text{PDGrad}, \text{bs}=\text{"ps"}, \text{k}=20) + \text{s}(\text{DistA}, \text{bs}=\text{"ps"}, \text{k}=20) + \text{s}(\text{DistB}, \text{bs}=\text{"ps"}, \text{k}=20) + \text{Treatment} * \text{Exp. Phase}, \text{family} = \text{binomial}, \text{method} = \text{"REML"})$ .

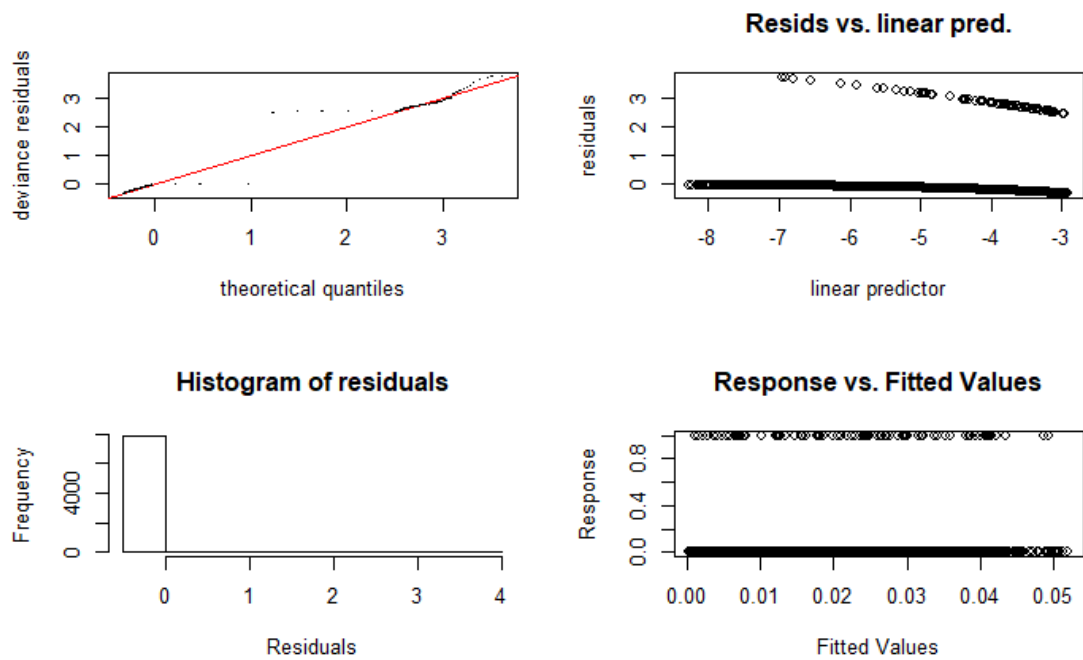


**Fig. AI 26** – Minimum adequate model for binary rejection data (Dataset (B) Model no. 4.6). Model terms =  $\text{gam}(\text{Rej} \sim \text{s}(\text{SPL}, \text{bs}=\text{"ps"}, \text{k}=10) + \text{s}(\text{SPLGrad}, \text{bs}=\text{"ps"}, \text{k}=20) + \text{s}(\text{DistA}, \text{bs}=\text{"ps"}, \text{k}=20) + \text{s}(\text{DistB}, \text{bs}=\text{"ps"}, \text{k}=20) + \text{Exp. Phase}, \text{family} = \text{binomial}, \text{method} = \text{"REML"})$ .